

THE UNIVERSITY OF HULL

The Oxidation Chemistry of the Xylenes and related Aromatic Hydrocarbons.

being a Thesis submitted for the Degree of

Doctor of Philosophy

in the University of Hull

by

Colin Ellis BSc.

(November 1999)

Contents.

	Page
Acknowledgements	i
Preface	ii
Abstract	iii
Chapter 1	1
Introduction to Hydrocarbon Oxidation.	
Chapter 2	47
Detailed Studies of Hydrocarbon Oxidation	
Chapter 3	85
Experimental Procedure	
Chapter 4	103
Results of the Kinetic Experiments for the Oxidation of the Xylenes	
Chapter 5	107
Results of the Analytical Experiments for the Oxidation of the Xylenes	
Chapter 6	112
The Decomposition of Neopentylbenzene in the Presence of Oxygen	
Chapter 7	143
Discussion of the Kinetic Experiments for the Oxidation of the Xylenes	
Chapter 8	165
Discussion of the Analytical Experiments for the Oxidation of the Xylenes	
Chapter 9	188
Summary and Conclusions	

Acknowledgements.

I would like to express my thanks to Prof. R.W. Walker for his guidance and supervision throughout the course of this project as well as provision of the facilities. Thanks are due to Dr. C. Morley and Shell Research, Thornton, Cheshire, for co-sponsoring this project and allowing me to obtain valuable industrial research experience. I would like to express my gratitude to Prof. R.R. Baldwin for his invaluable discussions and advice on the more detailed matters regarding the computation and background theory.

I would like to thank all of my family and friends especially Darren Starkey and Shahbaz Cheema for making the lab a happy and vibrant place working environment. I would also like to thank Dr. K.A. Holbrook, Dr. G.A. Oldershaw, Dr. T. Ingham and Dr. S.M. Kelly for their support and helpful discussions.

Finally I'd like to thank all of the cast and crew who are the School of Chemistry technicians, Mike Horne in stores, John Clannachan, Mike Dunn and Jamie Westaway in workshops, Martin Cawley and Dean Moore in analytical chemistry and Nigel 'Elvis' Parkin in electronics. Special thanks to Mike Bailey and Terry Aspinall in the glass blowing workshop for their excellent and speedy repair services. Last but by no means least thanks to *Sir* Barry Broady and Geoff Blake, the porters, for their ever efficient cylinder service.

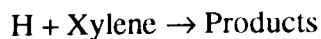
Preface.

All figures, equations and reactions are numbered with a prefix appropriate to the chapter except Chapter 7 where numbering corresponds to the conventions adopted in the computer program.

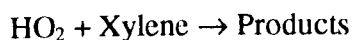
Abstract

The research was concerned with obtaining kinetic data and product information for the oxidation chemistry of the isomeric xylenes and benzyl radicals at 753K.

A trace amount (0.01% for kinetic study, 0.5% for product study) of each xylene was separately added to slowly reacting mixtures of H₂ + O₂ in aged boric-acid-coated Pyrex reaction vessels at 753K and 500 Torr total pressure. From measurements of the relative loss of H₂ and hydrocarbon rate constants for the reactions of the radicals H and HO₂ with each xylene were obtained.

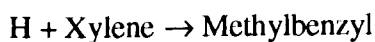


$$k=1.3 \cdot 10^9 \text{ l mol}^{-1} \text{ s}^{-1} \text{ (} p\text{-xylene)}, 1.4 \cdot 10^9 \text{ l mol}^{-1} \text{ s}^{-1} \text{ (} m\text{-xylene)}, 1.8 \cdot 10^9 \text{ l mol}^{-1} \text{ s}^{-1} \text{ (} o\text{-xylene)}.$$

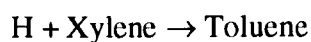


$$k=9.4 \cdot 10^4 \text{ l mol}^{-1} \text{ s}^{-1} \text{ (} p\text{-xylene)}, 1.03 \cdot 10^5 \text{ l mol}^{-1} \text{ s}^{-1} \text{ (} m\text{-xylene)}, 1.2 \cdot 10^5 \text{ l mol}^{-1} \text{ s}^{-1} \text{ (} o\text{-xylene)}.$$

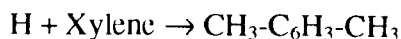
A detailed examination of the reaction products was carried out over a wide range of mixture composition. The major aromatic products from the oxidation of the xylenes were the isomeric tolualdehydes, toluene and *o*-xylylene oxide (from *o*-xylene). These were found to be similar to the products formed from the oxidation of toluene at 753K. From examination of the products available it was also possible to obtain more detailed rate constants for the attack of H radicals at each xylene giving specific products.



$$k=7.3 \cdot 10^8 \text{ l mol}^{-1} \text{ s}^{-1} \text{ (} p\text{-xylene)}, 8.3 \cdot 10^8 \text{ l mol}^{-1} \text{ s}^{-1} \text{ (} m\text{-xylene)}, 1.2 \cdot 10^9 \text{ l mol}^{-1} \text{ s}^{-1} \text{ (} o\text{-xylene)}.$$

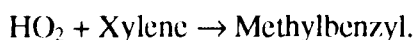


$$k=5.6 \cdot 10^8 \text{ l mol}^{-1} \text{ s}^{-1} \text{ (for all three xylenes)}.$$



$k=9.1 \cdot 10^6 \text{ l mol}^{-1} \text{ s}^{-1}$ (*p*-xylene), $8.4 \cdot 10^6 \text{ l mol}^{-1} \text{ s}^{-1}$ (*m*-xylene), $9 \cdot 10^5 \text{ l mol}^{-1} \text{ s}^{-1}$ (*o*-xylene).

In the case of $\text{HO}_2 + \text{RH}$, thermochemical considerations lead to the conclusion that both abstraction from and addition to the ring will be considerably less energetically favourable than the equivalent reaction of H atoms. Consequently $k_{(\text{HO}_2+\text{xylene})}$ should be taken to be the rate constant for



The decomposition of neopentylbenzene in the presence of oxygen and propene at 753K and a total pressure of 60Torr in an aged boric-acid-coated Pyrex reaction vessel was used to determine rate constants for the reactions between HO_2 and benzyl radicals.

The decomposition of neopentylbenzene at 753K produced *t*-butyl and benzyl radicals. The *t*-butyl radicals react with O_2 to produce HO_2 radicals. The presence of propene was used to determine the concentration of HO_2 radicals by monitoring the rate of production of propylene oxide. From measurements of the yields of benzaldehyde and toluene yields, and the rate of production of propylene oxide, rate constants for the reactions of HO_2 with benzyl radicals producing benzaldehyde and toluene were determined as $4.36 \cdot 10^9 \text{ l mol}^{-1} \text{ s}^{-1}$ and $8.44 \cdot 10^8 \text{ l mol}^{-1} \text{ s}^{-1}$ respectively at 753K.

A detailed examination of the products produced from the decomposition of neopentylbenzene in the presence of oxygen showed that the primary products were benzaldehyde, toluene, *i*-butene and 2-methyl-1-phenylprop-1-ene.

The key features highlighted in this research are the similarity in the oxidation chemistry between the xylenes and toluene and the importance of the reactions of the benzyl radical in the oxidation of methyl-substituted benzenes.

Chapter 1.

Introduction to Hydrocarbon Oxidation.

1.1. Importance and Impact of Combustion as an Energy Source.

Since the discovery of 'fossil fuels' centuries ago they have become one of the most widely used sources of energy. The understanding that fossil fuels are a non-renewable source of energy has been a major research point for scientists for the last 25 years. Other sources of energy have been invented and/or developed, such as nuclear power, wind, wave and solar power as well as hydroelectric power, but each has drawbacks in its application, efficiency or environmental effects. The consequence of this is that fossil fuels account currently for somewhere in the region of 95% of the world's energy production. With the increasing demands on energy in the modern world it is necessary to improve methods and efficiency by which fossil fuels are used. In recent years, the increase in energy demand cannot be compensated by the discovery of new sources of fossil fuels. Further new sources of fossil fuels tend to be of a lower grade than those previously used thus increasing the need to improve the efficiency by which they are used.

Fossil fuel combustion is the greatest contributor to man-made atmospheric pollution. This pollution takes the form of unburned hydrocarbons, partially oxidised hydrocarbons, polyaromatic hydrocarbons, nitrogen oxides, sulphur oxides and soot or particulates. A number of the compounds, particularly polyaromatic hydrocarbons (PAH) are

carcinogenic and others are lachrymatory for example peroxyacrylonitrile (PAN). Motor vehicle exhaust emissions generally include CO, CO₂, unburned hydrocarbons, particularly oxidised hydrocarbons, NO_x and soot, with power stations contributing with emissions of SO₂ and NO_x. All of the previous gases generate an increase in atmospheric pollution with major environmental implications on a global scale with significant effects being global warming (the greenhouse effect), due to the increase in CO₂, the formation of ozone in urban areas and the effects of acid rain^{1,2}. In built up areas the effect of atmospheric pollution can be visibly observed. Until recently this was noticed in Los Angeles USA where the air quality was so poor that the photochemical smog and general atmospheric pollution was visible almost every day; this affect is also becoming increasingly visible in London and other major built up areas. Since the introduction of the Clean Air Act in 1956³, which set guidelines to control visible pollution most noticeable in smogs, there have been many conferences which have introduced new guidelines to monitor and control automotive exhaust emissions. Consequently motor vehicle manufacturers are putting great emphasis on developing lean-burn engines and near-zero emission vehicles initially for use in highly polluted areas.

In recent years, the effects of lead from petrol on the environment and health, especially in built up areas, has created a push by environmental groups and governments for the use of lead-free petrol. The petrochemical and motor vehicle manufacturers have responded to this by increasing research and development on fuels and engine design such that lead-free fuels can be used as effectively and efficiently as leaded fuels. This lead to a search for a replacement to Et₄Pb as an antiknock agent and, as a second measure in reducing noxious emissions, the development of catalytic converters, for use with cars running on lead-free fuels, has been brought to the fore. Toluene has good

anti-knock properties, but its combustion particularly under rich conditions is likely to produce the carcinogenic PAH compounds. The use of highly-branched ethers such as methyltertiarybutylether (MTBE) appears to be offer much better prospects, particularly as MTBE can be produced relatively cheaply.

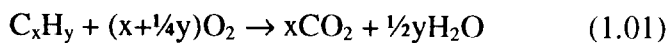
1.2. Preliminary View of the Computer Modelling Approach Applied to Combustion.

The concept of cost efficiency is paramount in the modern world. The petrochemical industry is very aware of this and as such uses computer simulations to simulate hydrocarbon oxidation processes reducing the need for expensive 'bench work.' In order for computer simulations to be reliable they need to be programmed with the mathematics of complex chemistry using three-dimensional differential equations for:

- Fluid mechanics to cope with flow patterns and turbulent mixing within the explosion or reaction chamber.
- Radiation and convective heat exchange, mass transport, momentum and energy functions.

Experimental workers have worked to improve the understanding of the physical processes involved such that the physics and mathematics of a computer model do not represent a real difficulty. However, problems begin to arise when an attempt is made to incorporate the chemistry for a hydrocarbon oxidation process into such a program. Further it is essential to validate models at regular intervals through carrying out appropriate practical experiments.

The overall stoichiometric equation for the *complete* oxidation of a hydrocarbon is:



This equation is limited to the extent that it refers only to the '*ideal*' complete oxidation of the hydrocarbon. Product and energy analysis of oxidation processes have illustrated that many intermediate steps and a very complex mechanism are involved. For a full analysis it is therefore necessary to include in a computer model the appropriate mechanistic steps involved in the oxidation process by including a series of elementary reactions. Computer programs also allow the efficiency and sensitivity in reaction conditions of a system to be assessed quickly and are used by the petrochemical industry to examine knock and particulate formation in petrol engines, spontaneous ignition in diesel engines and other potential safety hazards associated with autoignition of hydrocarbon vapours.

Computer models have been developed which attempt to deal fully with the oxidation of simple hydrocarbons such as HCHO^4 , CH_4^5 , C_2H_6^6 , C_2H_4^7 , C_3H_8^8 , and $\text{C}_4\text{H}_{10}^9$ and which are capable of reproducing experimentally-observed product yields and kinetic and physical characteristics. A complete model for the oxidation of higher hydrocarbons requires a far more extensive mechanism and an even larger database of rate constants than for example C_4H_{10} , the oxidation of which between 500 and 1200K was modelled with a mechanism containing over 500 elementary reactions. It is important to fully understand the oxidation process of the smaller hydrocarbons because they and their products are usually the observed intermediate products from the oxidation of the larger hydrocarbons. Further, the elementary reactions used for a small hydrocarbon, for

example C_2H_6 , can be incorporated directly as a sub-set into the mechanism for the oxidation of a larger species.

There are a number of problems still associated with the computer modelling of hydrocarbon oxidation despite over 50 years of study on these systems. Two major problems are:

1. The mechanisms for the oxidation of many hydrocarbons, especially for large alkanes and aromatic compounds, are still in doubt. The comment, of course, extends to many of the larger intermediates formed.
2. There is a lack of reliable rate constant data for many elementary reactions for large alkanes and aromatic compounds, which places several severe limitations on the application, accuracy and usefulness of computer modelling.

It is therefore still necessary for experimentalists to study the oxidation chemistry of compounds such as aromatic hydrocarbons in order to improve the database of kinetic information for use by modellers of combustion systems.

A consideration of the comprehensive mechanism containing over 500 elementary reactions used by Pitz and Westbrook⁹ to model the oxidation of butane, makes the task for kineticists appear highly daunting. However, widespread use of sensitivity analysis in order to evaluate the relative importance of individual elementary reactions in such a complicated mechanism has illustrated that typically only a few percent of the total reactions are important in determining combustion characteristics and pollution formation under any particular set of conditions. This invaluable technique assists in

identifying those key reactions which can become the focus of attention for kinetic determinations.

In order to make the best possible use of current available kinetic data in the literature, organisations such as CODATA and the EEC Data Evaluation Group have been formed. Their job is to carry out a critical evaluation of the kinetic data in the literature on specific types of elementary reactions in order to publish recommended values for rate constants and their variation with temperature and pressure for use by combustion modellers. This is no easy task and it is made more difficult by the existence of non-Arrhenius behaviour, as well as non-linear pressure dependencies associated with some elementary reactions. This means that it is important not to extrapolate to significant degree any rate data beyond the limits determined by experimental methods as this may lead to significantly incorrect estimates for rate constants.

By use of existing data for certain groups of elementary reactions and using Benson's bond and group additivity rules^{10,11} it is also possible to construct a database such that any patterns in the variation of rate constants can be identified. This enables, sometimes very accurate predictions for a rate constant to be made despite the lack of experimental data, although it is preferable to use experimentally determined rate constants where possible. Due to the sheer volume of unstudied reactions the development of such a database is a practical necessity, especially when modelling the oxidation processes for large hydrocarbons or complex mixed fuel systems.

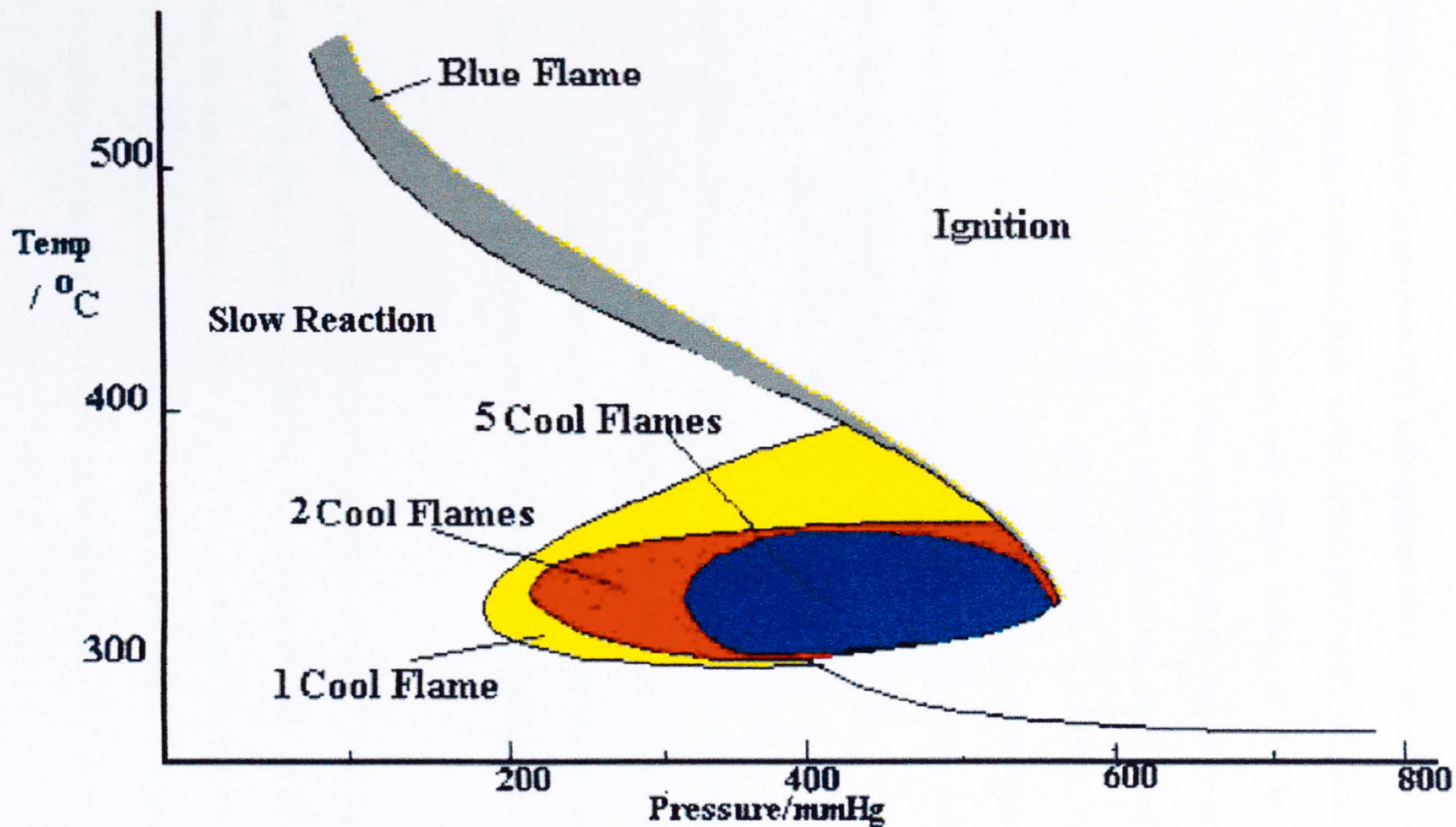
1.3. Characteristics of Hydrocarbon Oxidation.

The oxidation chemistry of a hydrocarbon is an extremely complicated process which exhibits various chemical and physical features which are associated with chain reactions, three of which are outlined below.

1. There is the existence of distinct pressure and temperature boundaries between slow reaction and explosion. These boundaries are usually sharp and are sensitive to the nature of the reaction vessel surface, the diameter of the reaction vessel, the addition of inert gas and the addition of traces of foreign material.
2. The reactions exhibit induction periods, a maximum reaction rate and the production of intermediate products. Explosions are often preceded by marked induction periods.
3. The observed orders in the equation for the reaction rates are typically non-integral in both oxygen and hydrocarbon.

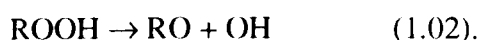
The early work of Newitt and Thornes¹² for the oxidation of a 1:1 mixture of propane and oxygen illustrates some of the above characteristics very well. Figure 1.1 clearly shows the change in the nature of this mixture in a classic static apparatus under different initial pressure and temperature conditions. The four main areas shown are slow reaction, cool flame, blue flame and true ignition. Each individual oxidation process is separated from the others by distinct boundaries which are sharply dependant upon the initial temperature and pressure. Although the form and features of Figure 1.1 are similar to those for many hydrocarbon + oxygen systems, such a diagram is highly specific to a particular system and indeed to the mixture composition.

Figure 1. 1: Pressure-temperature diagram for a 1:1 propane + oxygen mixture.



1.3.1. The Slow Reaction.

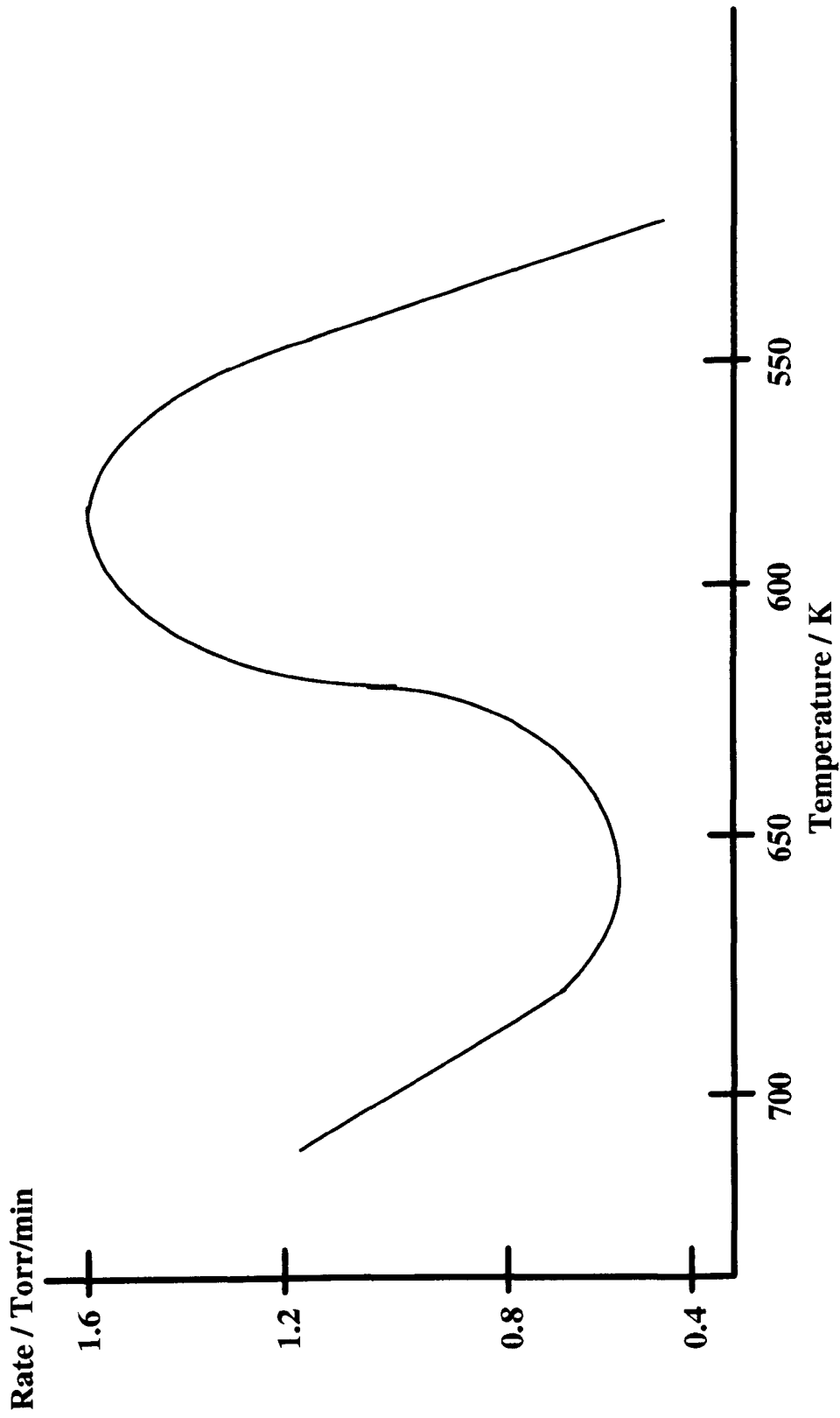
There is normally no visible emission observed in this region throughout the oxidation. After an induction period (a period where there is no apparent reaction which may vary from a few milliseconds to, in extreme cases, several hours,) the reaction rate increases auto-catalytically reaching a finite maximum rate before falling off due to the consumption of reactants. The length of the induction period and the magnitude of the maximum rate are often sensitive to the reaction vessel surface, the diameter of the reaction vessel, the addition of inert gas and the addition of traces of foreign material. All of these features are characteristic of complex chain reactions. The auto-catalysis has been attributed to the formation of reactive intermediate molecular compounds such as peroxides (ROOH) which undergo homolysis to give two radicals:



The slow reaction also usually exhibits a very peculiar feature referred to as the Negative Temperature Coefficient (N.T.C.). Over a temperature range the observed maximum rate of reaction falls as the initial temperature is increased above a value specific to the system in question. This is another feature characteristic of gas-phase oxidation reactions.

Seakins and Hinshelwood¹³ observed this feature in the oxidation of a 1:2 mixture of propane and oxygen (100 Torr propane + 200 Torr oxygen) (Figure 1.2). In this the maximum rate increased with temperature up to 330°C. Increasing the temperature above 330°C caused the maximum rate to begin to rapidly fall off until the temperature reached 375°C above which the maximum reaction rate increased again.

Figure 1. 2: Temperature maximum rate plot for 1:2 propane-oxygen.¹³



This behaviour is associated with the temperature dependence of competing reactions. The increase in temperature produces a change in the relative importance of such reactions in the mechanism in the N.T.C. region. A consequence of this change in the mechanism is the variation of the product distribution. The initial products generated in the lower temperature regions (typically $<330^{\circ}\text{C}$) are oxygenates such as alkylhydroperoxides (ROOH), carbonyls and alcohols. At higher temperatures (typically $>400^{\circ}\text{C}$) the initial products consist of the conjugate alkene, CH_4 , lower alkenes and O-heterocycles.

1.3.2. Cool Flames.

The occurrence of cool flames is associated with oxidations where the temperature is well below that for true ignition. They are identified as a pale blue glow generated from the production of electronically excited formaldehyde and generally last about one second. It is possible for up to 10 cool flames to occur one after another with time periods of about ten seconds; these generally occur as a pulsed sequence with each cool flame being accompanied by a temperature rise of $100\text{-}200^{\circ}\text{C}$. However, only a relatively small consumption of reactant is observed, in contrast to true ignition.

A cool flame occurs after an induction period, with the formation and subsequent decomposition of a branching agent. A typical branching agent is an alkylperoxide (ROOH), the formation of which is favoured at low temperatures prior to the N.T.C. region. The sharp temperature increase occurs because of the highly exothermic nature of the oxidation. This temperature rise moves the system into the N.T.C. region such that the source of branching agent (ROOH) is suppressed. Consequently the reaction is

rapidly quenched causing the temperature to fall quickly. A pulsed sequence occurs if the branching agent is produced again after the temperature decrease.

The findings of Burgess and Laughlin¹⁴ supported this explanation by use of measurements of the concentration of the branching agents prior to, during and after the passage of a cool flame. The fact that the cool flame/slow reaction boundary lies within the N.T.C. region suggests that both cool flames and the N.T.C. region stem from a common mechanism. True ignition is possible if the temperature rise generated by a cool flame is sufficient for another reaction product, such as HCHO or H₂O₂, to be produced as a branching agent.

1.4. Semenov Theory of Branched Chain Reactions.

Although the Semenov¹⁵ theory was developed in the 1930's, it is useful to review it here because it predicts the characteristics of both straight and branched chain processes. More importantly the theory illustrates the main principles of chain reactions.

Semenov subdivided the reactions occurring in a chain reaction into four types:-

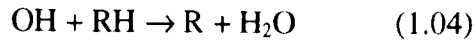
- **Initiation.**

Initiation is where chain centres are produced independently of the current radical concentration. A generally accepted primary initiation reaction for the oxidation of an alkane RH between 300-600°C is:



- **Propagation.**

In a propagation process one chain centre produces another chain centre keeping the number of chain centres constant. A typical reaction is:



- **Branching.**

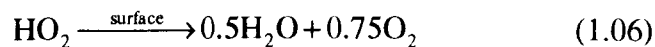
Branching reactions lead to an increase in the number of chain centres at a rate dependant on the concentration of chain centres. This may be of a linear (rate $\propto n$) or quadratic (rate $\propto n^2$) nature where n = concentration of radicals.



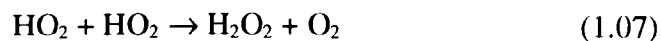
- **Termination.**

In termination, radicals are removed thus depleting the radical pool. Termination can be classified into three types:-

a Surface termination: Radicals are destroyed at the vessel surface:



b: Mutual termination in the gas phase: Chain centres are removed in pairs:



c: Homogeneous linear termination:



under conditions where HO_2 is unreactive.

Semenov developed a differential equation which clearly describes the build up of chain centres, n , with time, t , in terms of initiation, propagation, branching and termination reactions.

$$\frac{dn}{dt} = \theta + fn - gn - \gamma n + Fn^2 - \delta n^2 \quad (i)$$

θ = initiation coefficient, f = linear branching coefficient, g = homogenous termination coefficient, γ = surface termination coefficient, F = quadratic branching coefficient, δ = mutual termination coefficient. To obtain n at any time t , the differential equation (i) must be integrated.

Providing the chain length is reasonably long so that little reactant is removed in the initiation reaction the rate of reaction (ω) at any time t is given by equation (ii) where p is the propagation constant and n is the concentration of radicals.

$$\omega = pn \quad (ii)$$

The Semenov equation can be simplified to give equation (iii),

$$\frac{dn}{dt} = \theta + \phi n + Fn^2 - \delta n^2 \quad (iii)$$

where $\phi = f - g - \gamma$.

The majority of hydrocarbon oxidations are branched chain reactions, but it is interesting to consider a more simplified version of the Semenov equation where the effect of the vessel surface upon the rate of a straight chain process is considered, i.e. $f=F=0$. There is still the nature of the surface to consider; namely is it efficient or inefficient at

destroying chain centres. In either case the Semenov equation simplifies; thus if it is assumed that termination occurs solely at the surface, i.e. $g = \delta = 0$:

$$\frac{dn}{dt} = \theta - \gamma n \quad (\text{iv})$$

1.4.1. Efficient Surface Destruction of Chain Centres.

In the case where the surface of the reaction vessel is efficient at destroying chain centres ϵ , the efficiency, is greater than 10^{-2} and there is a non-uniform distribution of radicals over the reaction vessel with a maximum concentration at the centre of the vessel and zero concentration at the wall. The rate of termination is controlled by the rate of diffusion of the chain centres to the surface. Blackmore¹⁶, and Baldwin and Howarth¹⁷ have treated the case of efficient destruction and the more complicated situation where $10^{-4} < \epsilon < 10^{-2}$. For a cylindrical vessel with an efficient surface Semenov deduced that:

$$\gamma = \frac{32D}{d^2} \quad (\text{v})$$

D = diffusion coefficient and is inversely proportional to the total pressure and d = the diameter of the vessel. At the steady state $\frac{dn}{dt} = 0$, so that $n_s = \frac{\theta}{\gamma}$ and equation (vi) gives the steady rate:

$$\omega_s = \frac{p\theta}{\gamma} \quad (\text{vi})$$

Consequently, the rate of reaction is increased by the addition of inert gas and is proportional to the square of the vessel diameter.

1.4.2. Inefficient Surface Destruction of Chain Centres.

In the case of an inefficient surface for the destruction of chain centres ϵ is less than 10^{-4} and there is an even distribution of radicals across the reaction vessel. The rate of destruction of chain centres is given by $\frac{dn}{dt} = \theta - \gamma n$ where γ is given for a cylinder by equation (vii).

$$\gamma = \frac{\epsilon \bar{c}}{d} \quad (\text{vii})$$

\bar{c} is the mean velocity of the radicals and d is the vessel diameter.

Consequently the steady reaction rate is given by $\omega_s = \frac{p\theta d}{\epsilon \bar{c}}$. The rate of reaction is thus proportional to the vessel diameter, inversely proportional to the efficiency, ϵ , and is independent of added inert gas. The fact that the rate is dependant on the efficiency of the surface, which can vary from reaction to reaction and even during a particular reaction, can account for the lack of reproducibility so frequently observed

1.4.3. Branched Chain Reactions.

Generally, hydrocarbon oxidations are branched rather than linear chain reactions. The Semenov theory predicts the existence of regions of slow reaction and explosion together with sharp boundaries between the two.

In the case of a reaction with linear branching and linear termination:

$$\frac{dn}{dt} = \theta + \phi n \quad (\text{viii})$$

where $\phi = f - g - \gamma$.

Integration with the boundary conditions of $n = 0$ at $t = 0$ gives equation (ix) for the variation of n with t .

$$n = \frac{\theta}{\phi} (e^{\phi t} - 1) \quad (\text{ix})$$

ϕ is positive.

If ϕ is positive, the linear branching rate is greater than the sum of the termination rates, $f > (g + \gamma)$; therefore n increases exponentially and the reaction will become explosive (Figure 1.3).

The explosion is caused therefore by the kinetic features of the reaction and not the self-heating. However, as the reaction is exothermic, the explosion will be accompanied by a release of heat.

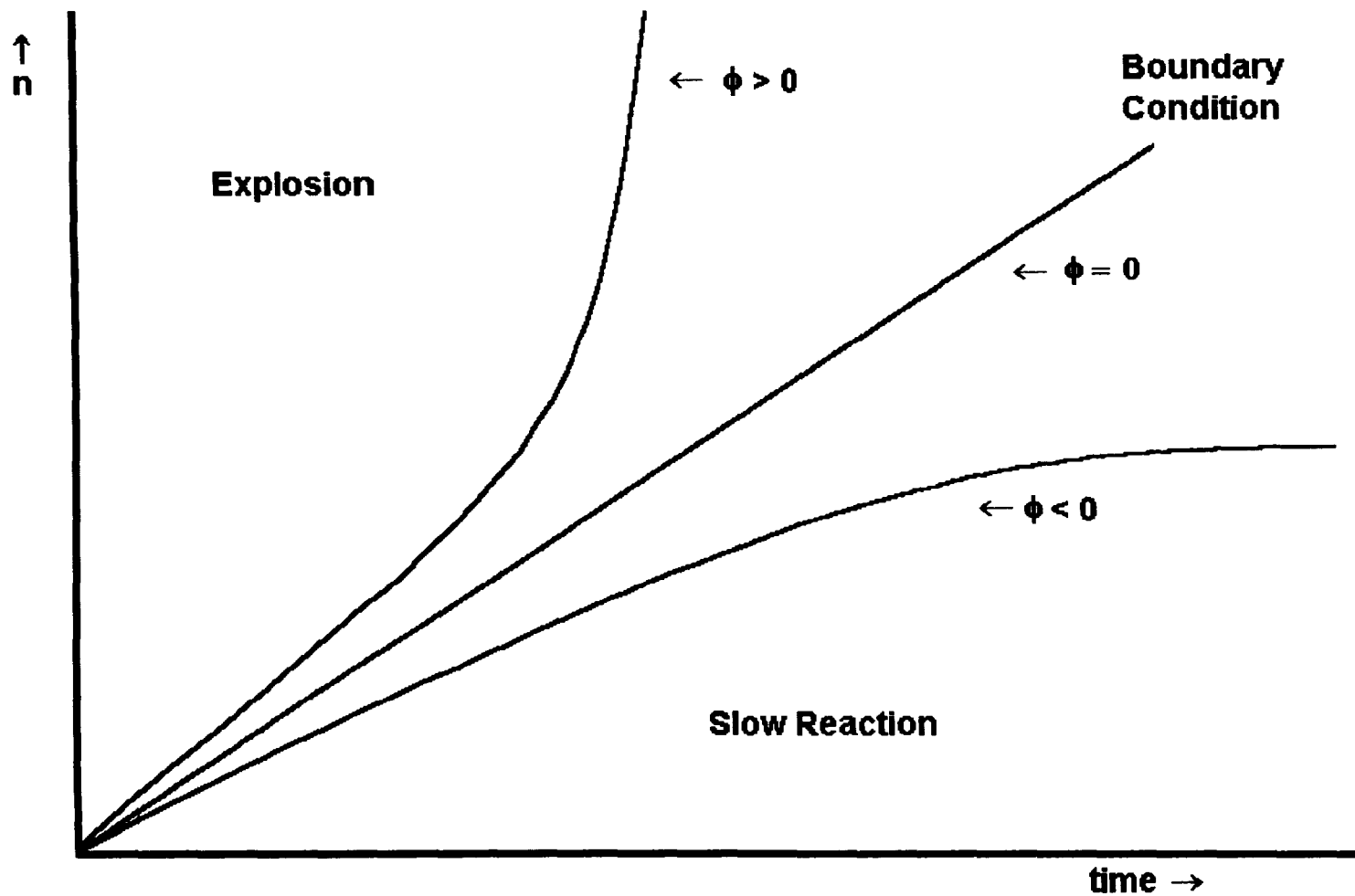
ϕ is negative.

When ϕ is negative, the sum of the linear termination reaction rates is greater than the linear branching reaction rate, $f < (g + \gamma)$. Equation (ix) may be re-written as (x).

$$n = \frac{\theta}{|\phi|} (1 - e^{-|\phi|t}) \quad (\text{x})$$

As time increases, $e^{-|\phi|t}$ approaches zero and a steady concentration $n_s = \frac{\theta}{|\phi|}$ of radicals is achieved. This steady concentration of radicals allows a finite rate of reaction to be achieved (Figure 1.3). Since a finite rate is reached, an explosion is not possible unless the exothermicity leads to a thermal runaway.

Figure 1. 3: Time variation of chain centres for positive, negative and zero ϕ for linear branching.



ϕ is zero.

For the case of $\phi = 0$, the rate of linear branching equals the sum of the linear termination rates, ($f = g + \gamma$). This is the boundary condition between slow reaction and explosion (Figure 1.3). It is important to note that the boundary is independent of the initiation rate θ . As a *small* increase in branching (f) will result in an explosion, ($\phi > 0$); or any increase in termination rates will result in the finite rate of reaction being obtained ($\phi < 0$), then it is clear that the explosion boundary will be very sensitive to traces of foreign material, to changes in vessel surface and diameter and to changes in mixture composition.

1.4.4. Treatment Involving Quadratic Terms.

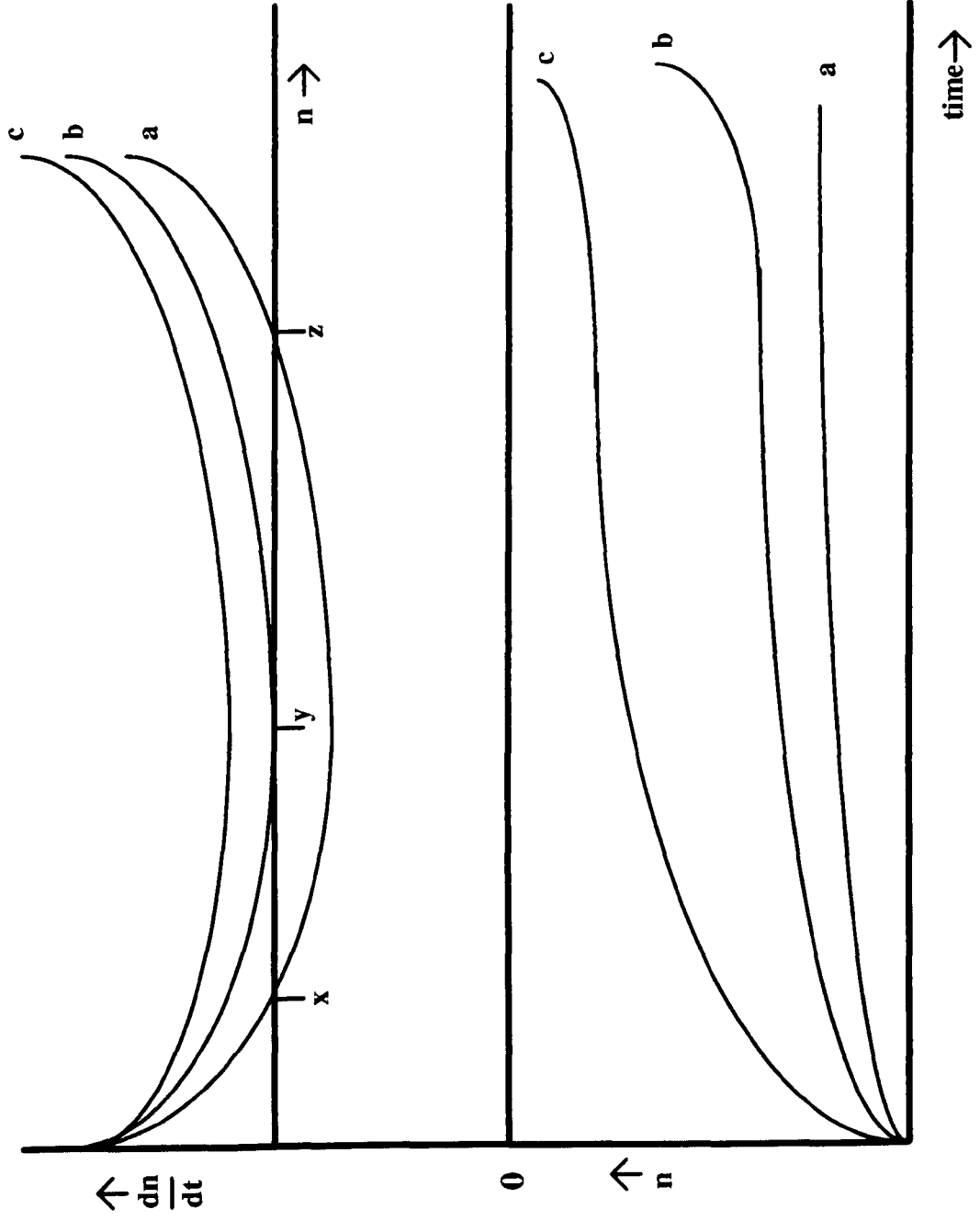
1.4.4.1. Linear Branching and Mutual Termination.

No isothermal explosion is possible for this case because the chain centre concentration must remain finite. If, however, there is excess self-heating, a thermal explosion could occur.

1.4.4.2. Linear Branching and Quadratic Branching.

These conditions permit the occurrence of an isothermal explosion even if $\phi < 0$ (Figure 1.4 lines c). In the upper part of Figure 1.4, line a shows the case where dn/dt becomes zero, so that a stationary state is reached with no isothermal explosion. However, there is a boundary condition between slow reaction and explosion (Figure 1.4 line b). Examination of the conditions using the Semenov theory gives $\phi^2 = 4\theta F$. Consequently here the initiation rate does affect the explosion boundary.

Figure 1. 4: Variation of n and dn/dt with t for positive (a), zero (b) and negative (c) quadratic branching ϕ .



1.5. The General Mechanism for Hydrocarbon Oxidation.

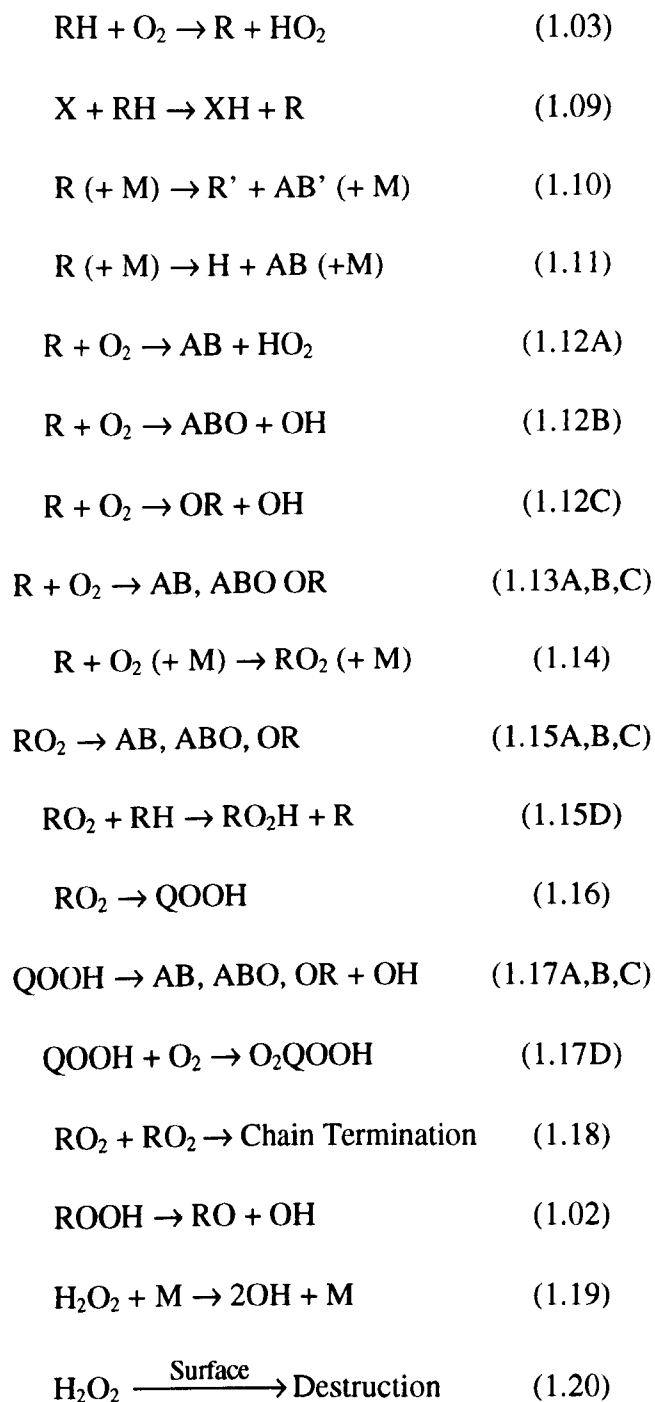
Although there were many studies of hydrocarbon oxidation during the first half of the 20th century, relatively little information was obtained on the detailed mechanism or the elementary reactions involved. The main experimental characteristics had been established by the 1940's which, together with the use of the Semenov theory, enabled the development of a reliable qualitative explanation of the processes involved. Before the 1960's it was very difficult to obtain accurate quantitative data in order to interpret hydrocarbon oxidations accurately for the following reasons.

1. Analytical techniques before the 1960's were not suitable or sensitive enough to analyse the oxidation products early in reaction and therefore the oxidation process had to be examined fairly late in reaction particularly if the minor products were kinetically important (>50% reaction). The consequence of this was that the intermediate or secondary products, produced from the reaction of the less stable primary products, tended to dominate.
2. The available kinetic data were very limited because techniques were often unavailable to study elementary reactions involving free radicals.

The development of sensitive gas chromatography enabled the detection and accurate measurement of primary products very early in reaction (<1% consumption) before secondary products could begin to dominate. Techniques such as the addition of trace amounts of a hydrocarbon to the hydrogen + oxygen slow reaction were developed¹⁸ to study the elementary reactions occurring. The combination of these and other absolute methods enabled rate data to be determined for the elementary reactions.

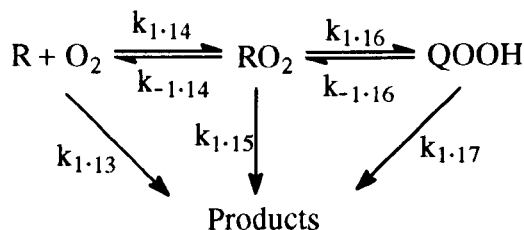
The generally accepted mechanism for oxidation reactions between 600 and 1000K is based upon the reactions given in Scheme 1.1.

Scheme 1.1.



AB = Alkene; ABO = Carbonyl; OR = Oxygenated Compound; X = Radical.

The general formation of products from $R + O_2$ is indicated by reactions such as (1.12A). There are different reaction pathways by which products could be formed, illustrated below:



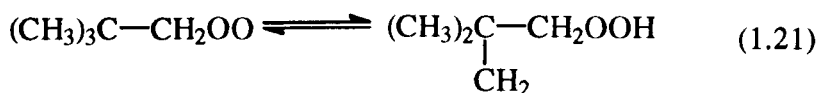
The overall rate constant $k_{1.12A}$ for the formation of product 'A' is given by:

$$\begin{aligned}
 k_{1.12A} = k_{1.13A} + & \left[\frac{k_{1.14} k_{1.15A} [X_A]}{k_{-1.14} + \sum k_{1.15} [X] + \left[k_{1.16} \sum k_{1.17} [X] / (k_{-1.16} + \sum k_{1.17} [X]) \right]} \right] \\
 + & \left[\frac{k_{1.14} k_{1.16} k_{1.17A} [X_A]}{(k_{-1.16} + \sum k_{1.17} [X]) \left\{ k_{-1.14} + \sum k_{1.15} [X] + \left[k_{1.16} \sum k_{1.17} [X] / (k_{-1.16} + \sum k_{1.17} [X]) \right] \right\}} \right] \quad \text{(xi)}
 \end{aligned}$$

where $\sum k_{1.15} [X]$ and $\sum k_{1.17} [X]$ are the summations of all of the reactions removing RO_2 and $QOOH$ by reactions of the type $RO_2 + X$ and $QOOH + X$ respectively. It is often assumed that $k_{1.15} = 0$ and that $k_{-1.16}$ is negligible in which case (xi) simplifies to (xii):

$$k_{1.12A} = k_{1.13A} + \frac{k_{1.14} k_{1.16} k_{1.17A} [X_A]}{(k_{-1.14} + k_{1.16}) + \sum k_{1.17} [X]} \quad \text{(xii)}.$$

The degree to which reaction (1.16) is reversible has been discussed recently, particularly in the case of the neopentylperoxy radicals¹⁹.



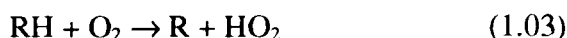
It is assumed that $k_{1.14} \gg k_{1.16}$, and considering the formation of one dominant product, such that $k_{1.17A}[X_A]/k_{1.17}[X] = 1$, (xii) approximates to:

$$k_{1.12A} = k_{1.13A} + K_{1.14}k_{1.16} \quad (\text{xiii})$$

The general mechanism comprises of a number of important reaction types.

1.5.1. Initiation.

The generally accepted normal primary initiation reaction occurring in the gas phase above 400°C is H abstraction from RH by O₂ yielding an alkyl radical (R) and HO₂.



This reaction was first suggested at least 50 years ago²⁰, although at low temperatures it almost certainly occurs at the surface unless very labile H atoms are involved such as in aldehydes.

This reaction is very endothermic and therefore rather slow and the nature of the H being abstracted alters the rate of reaction considerably. This is caused by the fact that a primary C-H bond is about 12 kJ mol⁻¹ stronger than a secondary C-H bond²¹. Consequently at above 400°C attack at a secondary hydrogen is a factor of about 10 faster than at the primary C-H position. Another effect of the slowness of this initiation reaction is that surface initiation, secondary branching or radical branching frequently masks the primary initiation even during the early stages of reaction. This is illustrated by examining the elementary reactions of methane²².

As illustrated in Table 1.1, assuming that $M = \text{O}_2 = 100\text{Torr}$, broadly over the temperature range 500-1000°C, only 10⁻²% of methane needs to be converted to HCHO

or $10^{-4}\%$ to H_2O_2 such that the rate of secondary initiation equals the primary initiation rate²³.

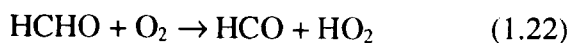


Table 1. 1: The Rates for primary and Secondary Initiation in Methane Oxidation.

Reaction	A / $1 \text{ mol}^{-1} \text{ s}^{-1}$	E_A / kJ mol^{-1}	$k_{(500\text{C})}$ / $1 \text{ mol}^{-1} \text{ s}^{-1}$	$k_{(1000\text{C})}$ / $1 \text{ mol}^{-1} \text{ s}^{-1}$
$\text{CH}_4 + \text{M} \rightarrow \text{CH}_3 + \text{H} + \text{M}$	$1.0 \cdot 10^{14}$	368	$1.3 \cdot 10^{-11}$	$7.9 \cdot 10^{-2}$
$\text{CH}_4 + \text{O}_2 \rightarrow \text{CH}_3 + \text{HO}_2$	$1.0 \cdot 10^{11}$	230	$2.8 \cdot 10^{-5}$	$3.6 \cdot 10^1$
$\text{H}_2\text{O}_2 + \text{M} \rightarrow 2\text{OH} + \text{M}$	$7.4 \cdot 10^{14}$	196	$3.8 \cdot 10^1$	$6.3 \cdot 10^6$
$\text{HCHO} + \text{O}_2 \rightarrow \text{HCO} + \text{HO}_2$	$1.0 \cdot 10^{11}$	167	$5.0 \cdot 10^{-1}$	$1.4 \cdot 10^4$

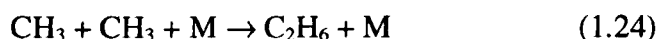
At temperatures less than 300°C the surface plays a major role in initiation reactions. Dixon et al.²⁴ examined the surface/volume effect on the initiation rate for acetaldehyde oxidation. Subsequent work by Walker²⁵ showed that the rate constant obtained was a factor of 10^{10} too high to be for a homogeneous gas phase initiation process and was thus attributed to surface initiation. As the temperature is increased the role of surface initiation becomes less important. Baldwin and Walker²³ have shown that between $200\text{-}400^\circ\text{C}$ there is a secondary initiation by the decomposition of ROOH (or RCO_3H for aldehydes). When the temperature is increased above 400°C the decomposition is superseded by reaction $\text{RCHO} + \text{O}_2$. Above 450°C the decomposition of H_2O_2 is the main secondary initiation process. Homolysis of alkane C-C bonds begins to become important at temperature above 750°C particularly at low O_2 concentrations although there are special cases such as those found with tetramethylbutane where strain energy makes C-C bond homolysis dominant even at 450°C .

1.5.2. Reactions of 'R' - Alkyl Radicals.

In the temperature region 400 to 800°C there are normally two reactions which alkyl radicals can undergo in an oxidation process.

1. React with O₂.
2. Decompose to form lower alkyl radicals and an alkene.

Radical-radical reactions tend to be unimportant except in special cases, for example:



The temperature affects which of these reactions will be the most dominant. Below about 250°C, the formation of RO₂ (reaction 1.14) is the general reaction.

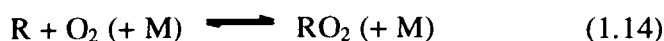
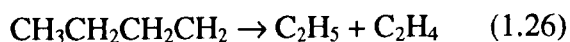
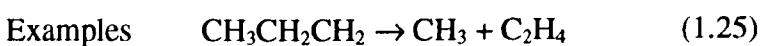


Table 1. 2: Temperature Variation for Equilibrium Constants for some R + O₂ → RO₂ Reactions.

Group	ΔH ₁₇ / kJ mol ⁻¹	log (K _{1.07} / atm ⁻¹)			Ceiling Temp / °C
		T = 300K	T = 500K	T = 700K	
H	196	30.4	16.4	10.6	1650
CH ₃	109	12.3	4.6	1.35	470
C ₂ H ₅	117	13.5	5.2	1.5	490
<i>i</i> -Pr	121	14.1	5.5	1.85	500
<i>t</i> -Bu	117	13.0	4.6	0.97	420

The position of this equilibrium plays a key role in the mechanism. Temperature has a dramatic effect on the position of the equilibrium (Table 1.2). Although not affecting the value of K (the equilibrium constant), third bodies (M) are usually required for small

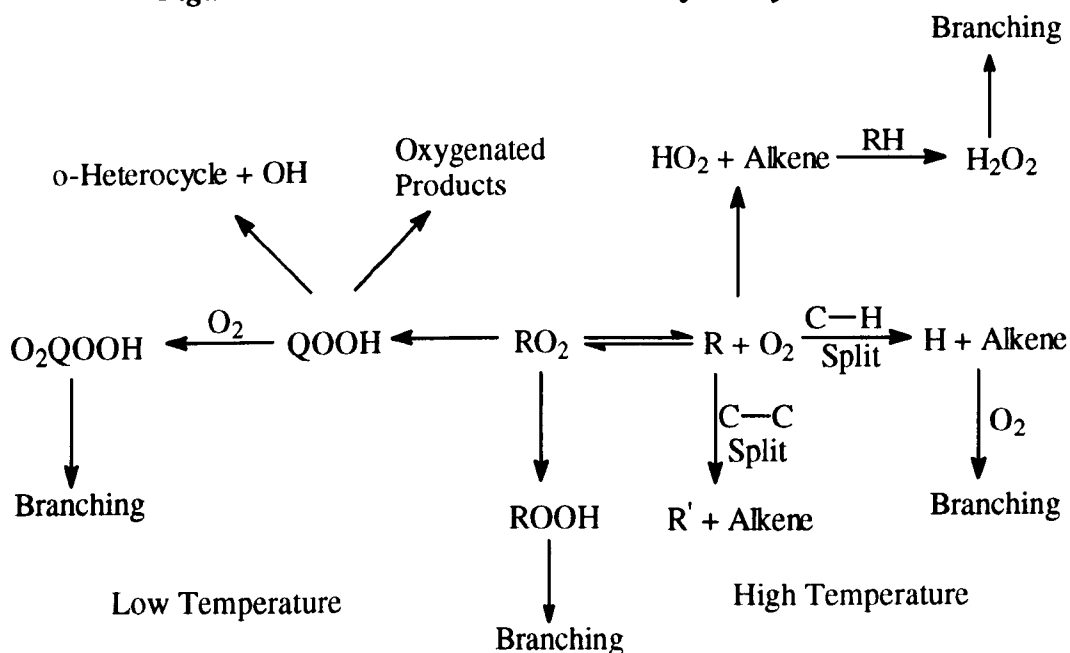
radicals such as methyl and ethyl. Larger alkyl radicals do not necessarily require a third body except at low pressures²⁶ and at high temperatures. In larger alkyl chains there are more internal degrees of freedom which can distribute the radicals energy during the reaction. The formation of the conjugate alkene is important at temperatures above 300°C due to reaction (1.13A) becoming important. Above 500°C smaller lower alkenes and smaller alkyl radicals such as methyl and ethyl are produced from the pyrolysis of the larger alkyl radicals^{27,28}.



1.5.3. The Reactions of the RO₂ Radical.

Figure 1.5 shows a general oxidation scheme for alkyl and RO₂ radicals.

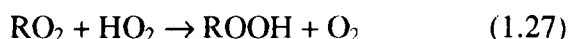
Figure 1. 5: General oxidation scheme for alkyl radicals.



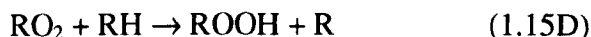
1.5.3.1. Intermolecular H-abstraction.

The nature of the reactions of the RO₂ radical with regard to H-atom abstraction change with temperature and pressure.

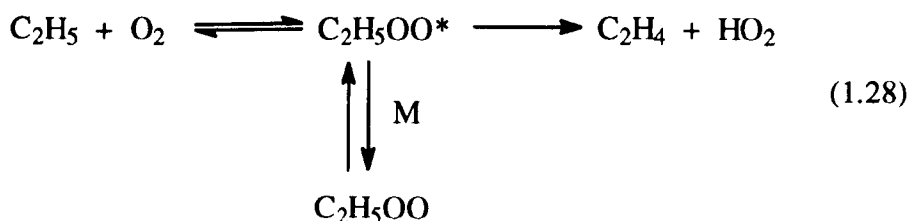
- At temperatures below 150°C and under *normal* oxygen concentrations the reaction sequence $R + O_2 \rightleftharpoons RO_2$ (1.14) lies well to the right with the major reaction of RO₂ being with HO₂ radicals or other RO₂ radicals (as described earlier).



- At higher temperatures, ca. 250°C for a tertiary C-H bond, RO₂ radicals tend to abstract hydrogen atoms from the parent hydrocarbon as a propagation reaction. The activation energy for this is dependant upon the carbon-hydrogen bond dissociation energy at the position of attack (typically E_A=42-86 kJ mol⁻¹ from RH = aldehyde to RH = C₂H₆).

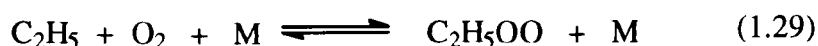


- Slagle et al²⁹ proposed that C₂H₄ formation from C₂H₅ radicals by a direct bimolecular abstraction route was inconsistent with a zero or slightly negative energy barrier and proposed a coupled reaction path between 300 and 1000K which would also account for the observed pressure effects involved in the reaction between C₂H₅ and O₂

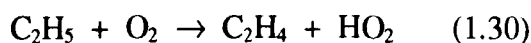


At low temperatures and high pressures, RO₂^{*} radicals are mainly stabilised by collision with M to form the product RO₂ (in real time). As pressure is lowered an

increasing proportion of the RO_2^* radicals will reform the reactants $\text{R} + \text{O}_2$ and the overall rate constant will fall as observed experimentally. However, Plumb and Ryan³⁰ concluded that the reaction between C_2H_5 and O_2 at 295K occurs in two uncoupled reactions, one pressure dependant and the other a direct bimolecular reaction independent of pressure.



Wallington et al³¹⁻³³ have shown that at 298K the yield of C_2H_4 decreases with increasing pressure from 12% of C_2H_5 consumed by O_2 at 1 Torr to 0.02 % at 600 Torr which corresponds to a “Pressure^{-0.8}” dependence. This leads to the conclusion that C_2H_4 is not produced at high pressures which validates the view that it is produced in the coupled set of reactions through an excited ethylperoxy intermediate rather than via a direct bimolecular reaction. McAdam and Walker³⁴ determined Arrhenius parameters for the reaction



from the oxidation of $\text{C}_2\text{H}_5\text{CHO}$ between 593 and 753K such that $E_{A(1.30)} = -6.3 \text{ kJ mol}^{-1}$ and $A_{1.30} = 10^{7.05} \text{ l mol}^{-1} \text{ s}^{-1}$. Later work by Gulati and Walker³⁵ gave a similar small negative activation energy for the analogous reaction of $i\text{-C}_3\text{H}_7 + \text{O}_2$.

Two important points are illustrated above for the reactions of the RO_2 radical.

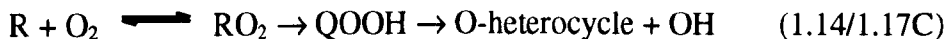
(i) At temperatures above 650K the reaction $C_2H_5 + O_2 \rightleftharpoons C_2H_5O_2$ is fully equilibrated such that the overall rate constant for the consumption of C_2H_5 is effectively independent of pressure and temperature.

(ii) The branching ratio is effectively zero above 650K (i.e. 100% C_2H_4), but, below this temperature the branching ratio is greatly effected by pressure. At low temperature and high pressure the branching ratio is high (reduced $[C_2H_4]$) because the $C_2H_5O_2^*$ radicals become increasingly stabilised by collisions.

1.5.3.2. Intramolecular H-abstraction.

In the oxidation of alkanes with carbon number greater than 4, significant yields of the conjugate o-heterocycle product are observed in the slow reaction and cool flame regions. Between the temperature range of 570-700K for the oxidation of n-butane, n-pentane, n-hexane and n-heptane, o-heterocycle yields of 8, 12, 43 and 56% respectively were observed³⁶.

Fish³⁷ introduced the Peroxy Radical Isomerisation and Decomposition (P.R.I.D.) theory to explain these observations and is summarised as follows:



The O-heterocycle formation proceeds via an internal hydrogen abstraction in the RO_2 radical to produce the $QOOH$ radical, which then undergoes a unimolecular decomposition. There is experimental evidence^{38,39} to suggest that the internal hydrogen abstraction process to generate $QOOH$ radicals is effectively irreversible for some systems. However, Pilling and Smith² maintain that this process will be reversible to some extent since the forward reaction is endothermic by about 30 kJ mol^{-1} hence the

reverse reaction back to RO_2 will have a lower potential barrier than the forward reaction.

The route for the formation of O-heterocycles is energetically favoured for higher alkanes since the activation energy for the reaction $\text{RO}_2 \rightarrow \text{QOOH}$ is determined by the bond dissociation energy for the hydrogen atom that is transferred and the strain energy involved in the formation of the cyclic transition state. The formation of O-heterocycles is most favourable when R-radicals can be formed by attack at a secondary or tertiary carbon-hydrogen bond followed by a low strain internal hydrogen atom transfer from either a secondary or tertiary carbon-hydrogen bond. The simplest hydrocarbon which generally meets the above criteria is $n\text{-C}_5\text{H}_{12}$. The yield of O-heterocycle is between 10-20% in this case⁴⁰. For lower alkanes or branched hydrocarbons the observed yield of O-heterocycle is usually much lower because of the formation of a strained transition state due to small ring size.

There are Arrhenius parameters available^{25,41} for many of the internal hydrogen transfers involved in the P.R.I.D. mechanism (Table 1.3).

Table 1. 3: Arrhenius Parameters for the RO₂ → QOOH Reaction.

H-atom Transfer	A/s⁻¹ (per C-H Bond)	E_A/kJ mol⁻¹
1,4p	1.4*10 ¹²	153
1,5p	1.75*10 ¹¹	123
1,6p	2.2*10 ¹⁰	105
1,7p	2.75*10 ⁹	90
1,3s	1.15*10 ¹³	176
1,4s	1.4*10 ¹²	133
1,5s	1.75*10 ¹¹	110
1,6s	2.2*10 ¹⁰	90
1,7s	2.75*10 ⁹	75
1,3t	1.15*10 ¹³	160
1,4t	1.4*10 ¹²	118
1,5t	1.75*10 ¹¹	93
1,6t	2.2*10 ¹⁰	75
1,7t	2.75*10 ⁹	62

The various transfers for 1,4, 1,5, 1,6 and 1,7 hydrogen atom transfers (Scheme (1.2)) allow for the formation of oxirans, oxetans, tetrahydrofurans and tetrahydropyrans respectively. Consequently it is possible to produce more than one O-heterocycle from a single alkylperoxy radical.

more oxygen. This was not found to be the case when neopentane was added to slowly reacting mixtures of hydrogen and oxygen between 650 and 790K⁴¹. Neopentane was chosen because the neopentyl radical is structurally unable to form a conjugate alkene so that consequently the chemistry of QOOH radicals is predominant. The results from this study gave firm evidence that QOOH radicals are sufficiently stable at these temperatures to undergo O₂ addition followed by decomposition to produce lower oxygenated compounds.

Further it has been suggested that some of the possible decomposition reactions of the O₂QOOH radical can lead to chain branching which may be of great importance in the autoignition region.

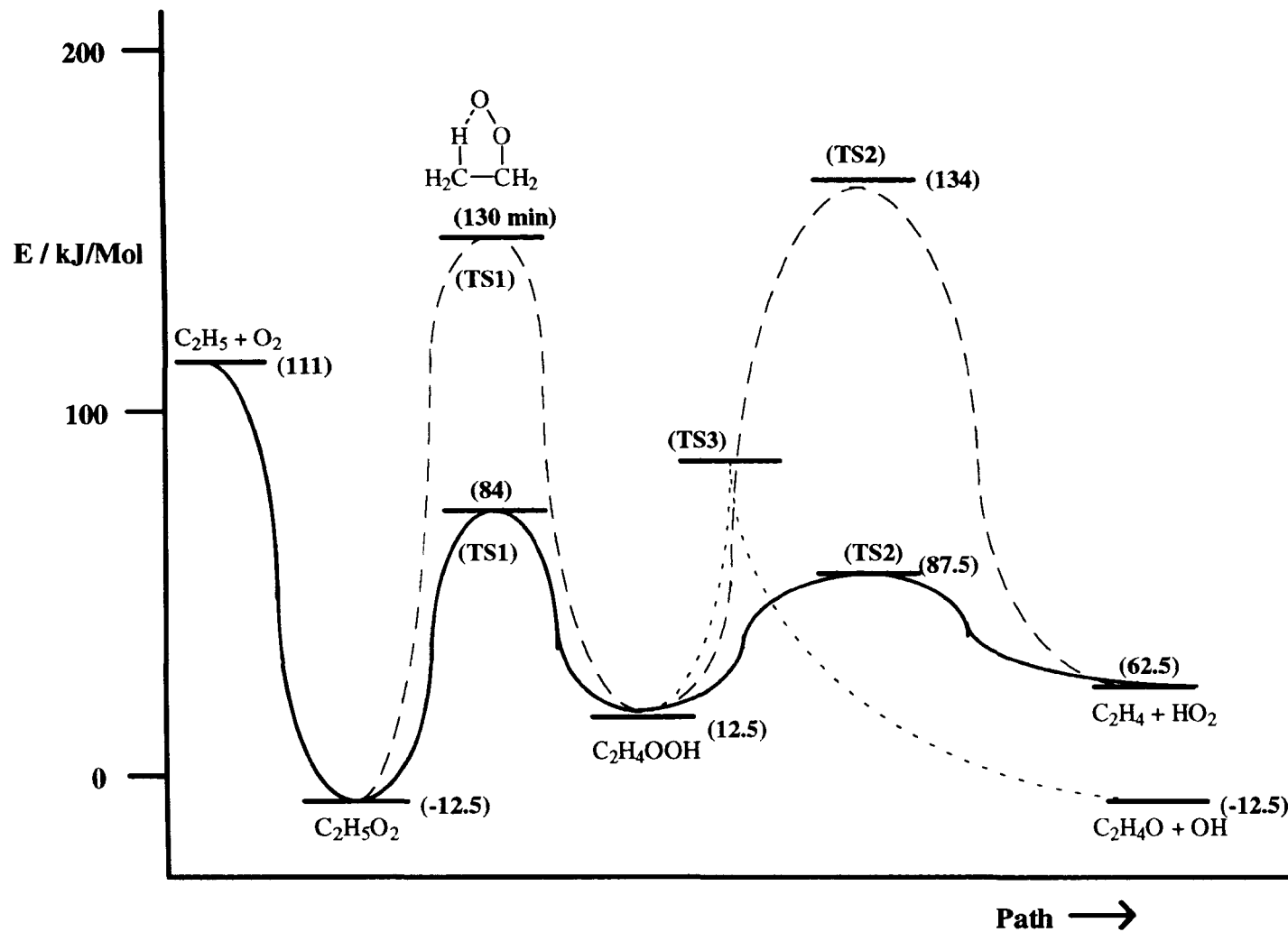
1.6. Mechanism of Conjugate Alkene Formation.

1.6.1. QOOH → Conjugate alkene + HO₂ reaction.

As indicated earlier, Slagle et al.²⁹ proposed a mechanism for the formation of the conjugate alkene from a process involving an internal hydrogen transfer in the RO₂* adduct to give transient species QOOH which can then decompose. Figure 1.6⁴⁵ shows the potential energy diagram for the reaction between C₂H₅ and O₂. Following the addition of O₂ to C₂H₅, the C₂H₅OO radical passes through a 5-centre cyclic transition state (TS1) which passes directly through the ethylhydroperoxide species C₂H₄OOH and the formation of C₂H₄ occurs via transition state (TS2). The full line shows the energy changes suggested by Slagle et al.^{29,45} As both TS1 and TS2 lie below the original level of C₂H₅ + O₂, then unless C₂H₅O₂* is stabilised, C₂H₄ formation is inevitable. Baldwin et al.⁴⁶, however, have questioned the viability of this mechanism and have determined

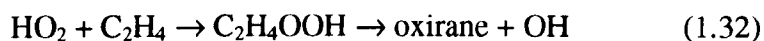
Figure 1. 6: Potential energy diagram for $C_2H_5 + O_2 \rightarrow C_2H_4 + HO_2$.

TS = transition state. Full line given by Wagner et al.⁴⁵, dotted line ammended by Baldwin et al.⁴⁶



extensive experimental evidence to support their argument that QOOH radicals decompose to produce oxirane and OH rather than the conjugate alkene and HO₂. Further, as shown by the dotted line in Figure 1.6, they consider that both TS1 and TS2 are at higher energy levels than the original value and in particular lie well above the C₂H₅ + O₂ energy asymptote.

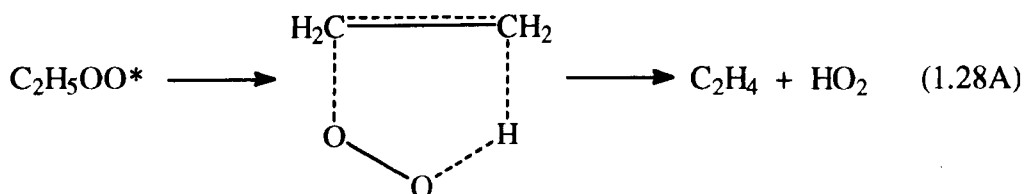
The use of the decomposition of tetramethylbutane (TMB) in the presence of O₂ as a source of HO₂ radicals between 650-790K⁴⁶ together with measurements of the appropriate oxirane permitted extremely reliable kinetic data to be obtained for the overall addition reaction between alkenes and HO₂ radicals. The overall reaction almost certainly occurs in two stages, firstly HO₂ addition followed by homolysis of the peroxide bond and cyclisation. However, Baldwin and co-workers⁴⁶ argued strongly that the first step was rate determining so that the experimentally determined activation energy referred to the addition step.



Three amendments were made by Baldwin et al.⁴⁶ to that proposed by Slagle et al.²⁹ for the potential energy diagram for C₂H₅ + O₂. First, the activation energy for the addition of HO₂ to C₂H₄ was taken as the experimental value of 72 kJ mol⁻¹ rather than 20-28 kJ mol⁻¹ given by Slagle et al.²⁹ Secondly, a second decomposition channel was needed for C₂H₄OOH leading to oxirane and OH; this was not originally considered by Slagle et al. The third amendment was that the potential energy barrier of 97 kJ mol⁻¹ given by Slagle for the transition C₂H₅OO to C₂H₄OOH, which is effectively an intramolecular H abstraction by peroxy species, is only slightly higher than the value of 86 kJ mol⁻¹ for an intermolecular abstraction at a primary C-H bond by HO₂ radicals^{47,48}. Allowing for ring

strain in the cyclic transition state, a barrier of at least 130 kJ mol^{-1} is likely for the transformation of $\text{C}_2\text{H}_5\text{OO}$ to $\text{C}_2\text{H}_4\text{OOH}$, consistent with values determined by Baldwin et al.⁴¹ This would indicate that the potential-energy barriers leading to C_2H_4 are considerable higher than the required energy back to the reactants C_2H_5 and O_2 ; also the formation of oxirane from $\text{C}_2\text{H}_4\text{OOH}$ radicals is more exothermic than the formation of C_2H_4 .

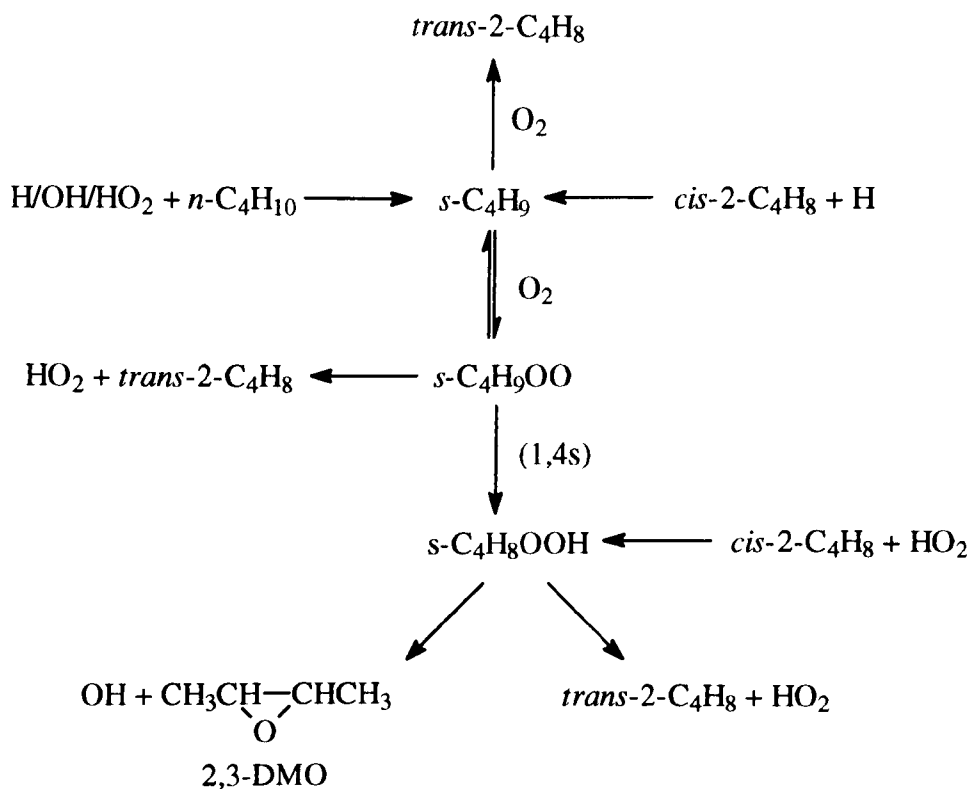
One possible solution put forward by Baldwin et al.⁴⁹ is that $\text{C}_2\text{H}_5\text{OO}^*$ is a precursor, but that C_2H_4 is formed directly in a concerted process without passing along the $\text{C}_2\text{H}_4\text{OOH}$ path.



If the barrier to the formation of the transition state is lower than that back to reactants, then the explanation given by Slagle et al. for the effect of temperature would still apply and the overall mechanism would also explain the observed effects of total pressure.

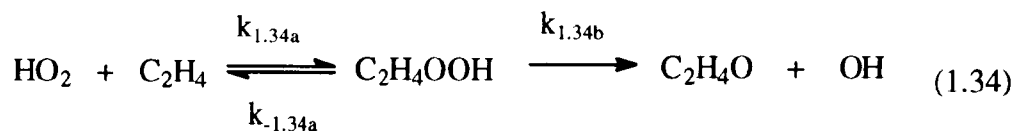
The following reaction scheme summarises the findings of Baker et al.³⁹ in the separate addition of *n*-butane and *cis*-but-2-ene to slowly reacting mixtures of hydrogen and oxygen at 480°C which are particularly relevant to the formation of alkenes from $\text{R} + \text{O}_2$. It should be emphasised that in the initial stages of reaction (where the measurements are made), the H, O, OH and HO_2 radical concentrations are essentially identical for both additives.

Scheme (1.4)



When the additive is *cis*-but-2-ene, the initial value for the ratio [2,3-DMO]/[*t*-2-C₄H₈] is 1.23; the value changes to 0.18 when *n*-butane is the additive. The formation of *s*-C₄H₈OOH will occur from both the isomerisation of *s*-C₄H₉OO radicals and the addition of HO₂ to *cis*-2-C₄H₈. For a case where *trans*-2-C₄H₈ is exclusively produced from the *s*-C₄H₈OOH radical then the value for the ratio [2,3-DMO]/[*t*-2-C₄H₈] would be the same for both additives. The explanation for the significantly higher value for the ratio when *cis*-but-2-ene is the additive is that *trans*-2-C₄H₈ is predominantly produced from a direct bimolecular reaction or via the decomposition of *s*-C₄H₉OO. The internal hydrogen transfer in *s*-C₄H₉OO to give *s*-C₄H₈OOH must be predominantly irreversible, otherwise the rapid equilibrium of *s*-C₄H₈OOH, *s*-C₄H₉OO and *s*-C₄H₉ would imply the same value for the ratio for both additives. Further, it is worth pointing out that the

al.⁴⁵ regarding the chemistry of QOOH for C₂H₄OOH. The mechanism for oxirane formation from HO₂ addition to C₂H₄ consists of two stages.



Waldwin et al.⁴⁶ suggested that $k_{1.34b} \gg k_{-1.34a}$ so that reaction (1.34a) is the rate determining step and $E_{A(1.34a)} = E_{A(\text{observed})} = 72 \text{ kJ mol}^{-1}$ where $E_{A(\text{observed})}$ = the activation energy for the formation of the oxirane. The view of Wagner et al.⁴⁵ is that C₂H₄OOH decomposes to give mainly C₂H₄ and HO₂, so that $k_{-1.34a} \gg k_{1.34b}$, so that the addition reaction is equilibrated and $E_{A(\text{observed})} = E_{A(1.34a)} + E_{A(1.34b)} - E_{A(-1.34a)}$. Assuming that $E_{A(-1.34a)} - E_{A(1.34b)} = 22 \text{ kJ mol}^{-1}$ (quoted above for isobutylhydroperoxyradicals) then with $E_{A(\text{observed})} = 72 \text{ kJ mol}^{-1}$ then $E_{A(1.34a)} = 94 \text{ kJ mol}^{-1}$, compared to a maximum value of about 25 kJ mol⁻¹ required by Wagner et al.⁴⁵ (Figure 1.6).

These conclusions indicate that the system may be more complicated than first suggested by Batt⁵⁰ and others. The abstraction of the peroxidic H in t-butylperoxide producing t-butylperoxy radicals may contribute to i-butene formation in the Batt work.

1.6.2. Radical-radical reactions.

The equilibrium for the reaction $\text{R} + \text{O}_2 \rightleftharpoons \text{RO}_2$ (1.14) lies well to the right at temperatures below 350°C for normal O₂ pressures and since the reaction between RO₂ and RH (reaction 1.15D) has a relatively high activation energy (Table 1.4 for HO₂ radicals) the concentration of RO₂ may reach a significant level.

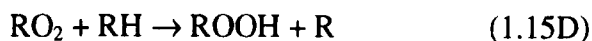
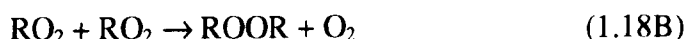


Table 1. 4: Arrhenius Parameters for Radical Attack at Specific C-H Bonds.

	O + RH		H + RH		OH + RH		HO ₂ + RH	
	A / s ⁻¹	E _A *	A / s ⁻¹	E _A *	A / s ⁻¹	E _A *	A / s ⁻¹	E _A *
1°	5.0*10 ⁹	24	2.2*10 ¹⁰	41	6.15*10 ⁸	7	2.8*10 ⁹	85.5
2°	1.3*10 ¹⁰	19	5.0*10 ¹⁰	35	1.41*10 ⁹	4	2.8*10 ⁹	74
3°	1.6*10 ¹⁰	14	8.7*10 ¹⁰	29	1.26*10 ⁹	-1	2.8*10 ⁹	67

* Units for E_A = kJ mol⁻¹

If this is the case, many reaction products will be produced from radical-radical reactions.



1.7. Propagation via H-atom abstraction by radicals.

In the temperature range 400-500°C, OH and HO₂ radicals are mainly responsible for the removal of the parent hydrocarbon. The importance of H-radical attack increases with increasing H₂ concentration in H₂ + O₂ mixtures. X in reaction (1.35) may also include H, O, RO₂ and CH₃ radicals. In general reactions of alkyl radicals (X) with RH (1.35) can not compete with their reaction with O₂.



Over the temperature range 200-2000K, rate constants for the reactions of OH + CH₄ and OH + C₂H₆ have been accurately determined using many reliable techniques. For other alkanes the data is a little less extensive; within the temperature range 300-800K reasonably accurate rate constants have been obtained for about 20 alkanes. For the

reaction $\text{HO}_2 + \text{RH}$ the number of kinetic data is limited because it is a fairly difficult reaction to study⁵¹ even by modern methods used to study elementary reactions because the reaction is relatively slow even at high temperatures.

The Arrhenius parameters⁵² for radical attack at primary, secondary and tertiary C-H bonds in RH by H, OH, and HO_2 are given in Table 1.4. It is possible to use these values to calculate overall rate constants for the removal of RH by a particular radical species by the use of group additivity rules¹¹ and to calculate the proportions of each species of alkyl radical produced. The additivity rules assume that the contribution, for primary (p), secondary (s) and tertiary (t) C-H bonds, per C-H bond is the same in any alkane such that:

$$k_{\text{overall}} = n_p A_p \exp(-E_p/RT) + n_s A_s \exp(-E_s/RT) + n_t A_t \exp(-E_t/RT).$$

n = Number of specific C-H bonds.

A = Arrhenius Constant per C-H bond.

E = Activation energy.

p = Primary C-H bond

s = Secondary C-H bond

t = Tertiary C-H bond.

A more detailed treatment has been developed in which it is possible to allow for the specific position of the C-H bond in the hydrocarbon and which takes into consideration the effect of near-neighbour groups⁵¹.

The selectivity of the OH radical regarding the position where it will attack is far lower than that for HO_2 , particularly at low temperatures. The relative selectivity of both radicals at the three possible C-H sites in an alkane at 400°C is compared in Table 1.5. However, the difference in bond selectivity becomes less noticeable as temperature is increased.

Table 1. 5: Relative Selectivity of OH and HO₂ at 400°C.

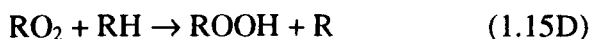
	k_s / k_p	k_t / k_p
OH	3.9	8.6
HO ₂	7.8	27.4

p= primary, s = secondary, t = tertiary.

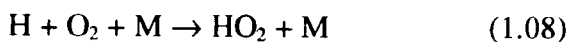
1.8. The Change of Mechanism with Temperature.

It is worth setting out in a focused way the change of the mechanism with temperature. In the slow reaction region of hydrocarbon oxidation there are a number of features which are associated with the transition from the so-called low temperature to the high temperature mechanism. The role played by the $R + O_2 \rightleftharpoons RO_2$ equilibrium can be used to explain the features of cool flames, the N.T.C region and the change in the product distribution, as illustrated earlier in this chapter. Great attention must be given to how the position of this equilibrium is altered with temperature as well as the activation energy for alternative reactions of R and RO₂.

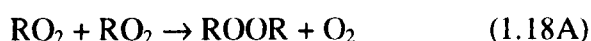
At temperatures below about 150°C, artificial initiators, sensitizers or irradiation are used to generate alkyl radicals and since the fastest reaction of these alkyl radicals is with oxygen, most R radicals produce RO₂. The propagation reaction (1.15D) has an activation energy between 42-86 kJ mol⁻¹ depending upon the nature of the C-H bond being attacked. The RO₂ radicals generally undergo mutual radical-radical reactions, or also react with HO₂ radicals if they were produced in the initiation process.



If the latter occurs the yield of alkylhydroperoxide is almost 100% and there is no significant chain reaction occurring.



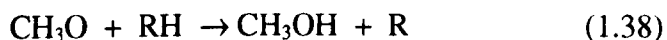
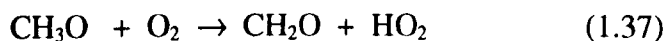
If the temperature is above about 150°C, following either surface or artificial initiation, a simple chain reaction may occur which involves reactions (1.14) and (1.15D). This chain may be terminated by either surface or mutual termination reactions of RO₂ (1.18A)



It is likely that the simple chain process would be complicated by a secondary initiation reaction created by the decomposition of ROOH (1.02).



The reaction will then become auto-catalytic reaching a maximum rate. The products are most likely to be carbonyls⁵³ and alcohols⁵⁴ associated with the reactions of the RO radical. Reactions (1.37) and (1.38) are shown for the CH₃O radical.



It would be expected that the rate of decomposition of ROOH would increase if the temperature is further increased which would increase the degree of branching leading towards an isothermal explosion; again products would be associated with those for peroxide decomposition.

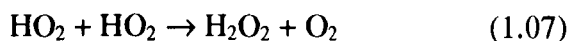
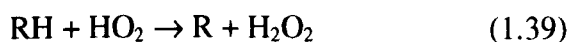
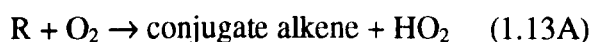
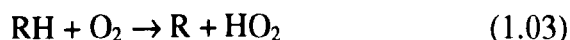
However, the experimentally determined product distribution between 300-400°C is different from the above predictions. The initial major product from alkane oxidation is

found to be the conjugate alkene, with larger alkanes also producing O-heterocycles. This is also inconsistent with the observations in the N.T.C. region in this temperature range. It can be concluded that alternative reactions of RO₂ with higher activation energies become dominant thus suppressing the formation of the ROOH branching agent at these temperatures.

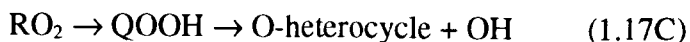
The dissociation reaction of RO₂ back to R and O₂ increases in importance as the temperature rises. In fact the reaction rate of reaction (-1.14) (depending upon $[RH]$ and the type of C-H bonds present) can become approximately equal to that of reaction (1.15D) at temperatures above 200°C. Consequently reaction (-1.14), due to its high activation energy, effectively competes with reaction (1.15D) and alternative reactions of R radicals increase in importance, the most significant being the overall reaction (1.13A).



It is thus possible for a virtually straight chain mechanism to develop which involves R and HO₂ as the chain centres which replaces the branched chain mechanism involving ROOH and hence the reaction rate is reduced.

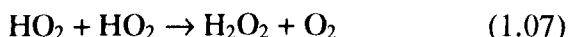


It is also possible for other propagation reactions involving the P.R.I.D. mechanism to lead to O-heterocycles.



The change in the position of the $\text{R} + \text{O}_2 \rightleftharpoons \text{RO}_2$ mechanism helps to explain the N.T.C. region and the occurrence of cool flames since both occur in the temperature range 300-400°C. As the temperature is increased in the N.T.C. region the equilibrium suppresses the branching reaction involving ROOH and hence straight chain reactions involving HO₂ increase in importance reducing the rate of reaction.

Since the reactivity of HO₂ is significantly lower than that for OH, the chain is not carried as rapidly since reaction (1.39) is in direct competition with termination reaction (1.07) although H abstraction by OH radicals will occur.



The reaction rate is also sensitive to the yield and stability of H₂O₂. At low temperatures the hydrogen peroxide is more stable than the ROOH and as such will not be a source of secondary initiation. However, as the temperature is increased the rate of decomposition of hydrogen peroxide increases sharply due to the high activation energy of 190 kJ mol⁻¹ for reaction (1.23).



There is therefore a turnover into a positive temperature coefficient as a result of reaction (1.23) at temperatures above 400°C.

1.9. References.

- ¹ Barnard J.A. and Bradley J.N., "*Flame and Combustion*", Chapman and Hill, London, (1985).
- ² Pilling M.J. and Smith I.W.M., "*Modern Gas Kinetics*", Blackwell, Oxford, (1987).
- ³ Unzelman G.H., *Oil Gas Journal*, Tulsa, vol **89**, iss 15, pp44, April (1991).
- ⁴ Dean A.M., Johnson R.L. and Steiner D., *Comb. Flame*, **37**, 41, (1980).
- ⁵ Olson D.B. and Gardiner W.C. Jr., *Comb. Flame*, **32**, 151, (1978).
- ⁶ Olson D.B., Tanzawa T. and Gardiner W.C. Jr., *Int. J. Chem. Kinet.*, **11**, 23, (1979).
- ⁷ Westbrook C.K., Dryer F.L. and Schug K.P., *19th Symp. (Int) on Combustion*, The Combustion Institute, Pittsburg, Pennsylvania, pp153, (1982).
- ⁸ Pitz W.J. and Westbrook C.K., *Combust Sci. Technol.*, **37**, 117, (1984).
- ⁹ Pitz W.J. and Westbrook C.K., *Combust Sci. Technol.*, **63**, 113, (1986).
- ¹⁰ Benson S.E. and Buss J.H., *J. Chem. Phys*, **29**, 546 (1958).
- ¹¹ Benson S.W., "*Thermochemical Kinetics*", Wiley, New York, (1976).
- ¹² Newitt D.M. and Thornes L.S., *J. Chem. Soc.*, 1656, (1937).
- ¹³ Seakins M. and Hinshelwood C.N., *Proc. Roy. Soc.*, **A261**, 281, (1961).
- ¹⁴ Burgess A.R. and Laughlin R.G.W., *Chem. Commun.*, 796, (1967).
- ¹⁵ Semenov N.N., *Some Problems of Chemical Kinetics and Reactivity*, Pergamon Press, London, (1958).
- ¹⁶ Blackmore D.R., *J. Chem. Soc. Faraday Trans. 1*, **74**, 765, (1978).
- ¹⁷ Baldwin R.R. and Howarth J. A., *J. Chem. Soc. Faraday Trans. 1*, **78**, 451, (1982).

- ¹⁸ Baldwin R.R., Hopkins D.E. and Walker R.W., *Trans. Faraday Soc.* **66**, 189 (1970).
- ¹⁹ Hughes K.L., Halford-Mow P.A., Lightfoot P.D., Turanyi T. And Pilling M.J., *Symp. Int. Combust. Proc.*, **24**, 645, (1992).
- ²⁰ Cullis C.F. and Hinshelwood Sir C.N., *Discuss. Faraday Soc.*, **2**, 117, (1947).
- ²¹ Gutman D., Niiranen J.T., Seakins P.W., Pilling M.J. and Krasnoperov L.N., *J. Phys. Chem.*, **75**, 9847, (1992).
- ²² Baker R.R., Baldwin R. R. and Walker R.W., *Symp. Int. Proc.*, **13**, 291, (1971).
- ²³ Baldwin R.R. and Walker R.W., *14th Symposium (International) on Combustion*, The Combustion Institute, Pittsburg, Pennsylvania, pp241, (1973).
- ²⁴ Dixon D.J., Skirrow G. and Tipper C.F.H., *Combustion Institute European Symposium*, Academic Press, (1974).
- ²⁵ Walker R.W., "Some Burning Problems in Combustion Chemistry," *Research In Chemical Kinetics, Volume 3*, pp1, Compton R.G. and Hancock G. (editors), © 1995 Elsevier Science B.V., Amsterdam.
- ²⁶ Hucknall, "*Chemistry of Hydrocarbon Combustion.*", Chapman and Hall, London, (1985), Chapter 5.
- ²⁷ Kerr J.K. and Trotman-Dickenson A.F., *Trans. Faraday Soc.*, **55**, 572, (1959).
- ²⁸ Kerr J.K. and Trotman-Dickenson A.F., *J. Chem. Soc.*, 1602, (1960).
- ²⁹ Slagle I.R., Feng Q. and Gutman D., *J. Phys. Chem.*, **88**, 3648, (1984).
- ³⁰ Plumb I.C. and Ryan K.R., *Int. J. Chem. Kinet.*, **13**, 1011, (1981).
- ³¹ Wallington T.J., Andino J.M., Kaiser E.W. and Japar S.M., *Int. J. Chem. Kinet.*, **21**, 1113, (1989).
- ³² Kaiser E.W., Rimai R. and Wallington T.J., *J. Phys. Chem.*, **93**, 4094, (1989).

- ³³ Kaiser E.W., Lorkovic I.M. and Wallington T.J., *J. Phys. Chem.*, **94**, 3352, (1990).
- ³⁴ McAdam K.G. and Walker R.W., *J. Chem. Soc. Faraday Trans. 2*, **83**, 1509, (1987).
- ³⁵ Gulati S.K. and Walker R.W., *J. Chem. Soc. Faraday Trans. 2*, **84**, 401, (1988).
- ³⁶ Barat P., Cullis C.F. and Pollard R.T., *13th Symposium (International) on Combustion*, The Combustion Institute, Pittsburg, Pennsylvania, pp179, (1971).
- ³⁷ Fish A., "*Organic Peroxides*", **vol 1**, Wiley, New York, Swern D. (editor), 141, (1970)
- ³⁸ Berry T., Cullis C.F. and Trimm D.T., *Proc. Roy. Soc., London*, **A316**, 377, (1970).
- ³⁹ Baker R.R., Baldwin R.R. and Walker R.W., *J. Chem. Soc. Faraday Trans. 1*, **71**, 756, (1975).
- ⁴⁰ Knox J.H. and Kinnear C.G., *13th Symposium (International) on Combustion*, The Combustion Institute, Pittsburg, Pennsylvania, pp217, (1971).
- ⁴¹ Baldwin R.R., Hisham M.W.M. and Walker R.W., *J. Chem. Soc. Faraday Trans 1*, **78**, 1615, (1982).
- ⁴² Benson S.W., *J. Amer. Chem. Soc.*, **87**, 972, (1965).
- ⁴³ Bawn C.E.H., *Chem. Soc. Spec. Publ. No. 9*, p. 65, (1957).
- ⁴⁴ Ivanov K., *Acta Physiochim., USSR.*, **9**, 421, (1938).
- ⁴⁵ Wagner A.F., Slagle I.R., Sarzynski D. and Gutman D., *J. Phys. Chem.*, **94**, 1853, (1990).
- ⁴⁶ Baldwin R.R., Dean C.E. and Walker R.W., *J. Chem. Soc. Faraday Trans. 2*, **82**, 1445, (1986).
- ⁴⁷ Baldwin R.R., Hisham M.W.M., Keen A. and Walker R.W., *J. Chem. Soc. Faraday Trans. 1*, **78**, 1165, (1982).

- ⁴⁸ Baldwin R.R., Dean C.E., Honeyman M.R. and Walker R.W., *J. Chem. Soc. Faraday Trans. 1*, **82**, 89, (1986).
- ⁴⁹ Baldwin R.R., Pickering I.A. and Walker R.W., *J. Chem. Soc. Faraday Trans. 1*, **76**, 1374, (1980).
- ⁵⁰ Batt L., The University of Aberdeen, (1992). [Written Communication]
- ⁵¹ Walker R.W., *Sci. Progress.*, Oxford, **74**, 163, (1990).
- ⁵² Walker R.W., *Int. J. Chem. Kinet.*, **17**, 573, (1985).
- ⁵³ Batt L., *Int. J. Chem. Kinet.*, **11**, 977, (1979).
- ⁵⁴ Gutman D., Sanders N. and Butler J.E., *J. Phys. Chem.*, **86**, 66, (1982).

Chapter 2.

Detailed Studies of Hydrocarbon Oxidation.

2.1. The Hydrogen + Oxygen Reaction.

Numerous studies have been made of the reaction between hydrogen and oxygen, and of the elementary reactions involved. The combined efforts have facilitated the elucidation of a mechanism. The considerable interest in the hydrogen + oxygen reaction was generated for many reasons. Fifty years ago, Hinshelwood indicated a number of characteristics found in the hydrogen + oxygen reaction as part of his Bakerian lecture to the Royal Society¹ in 1947.

- 1 It illustrates all of the features of a branched chain reaction.
- 2 The radicals involved, OH, H, HO₂ and O, are of general interest in combustion.
- 3 The chemistry of the slow reaction is in essence the same as the chemistry in a H₂ + O₂ flame.
- 4 A controllable source of radicals is generated. The relative proportion of each radical can be altered by varying the relative concentrations of H₂, O₂ and inert gas, as well as temperature.
- 5 The reaction between H₂ and O₂ is highly exothermic and hence a potential source of power. Due to the probable limited supply of fossil fuels, there is potential interest in using hydrogen as an alternative, generally pollution free, fuel.

Further, there is the existence of three explosion limits in the hydrogen + oxygen system as illustrated in Figure 2.1 for stoichiometric mixtures. A number of observations can be made by navigation along a selected isotherm on the diagram at a selected temperature, for example 500°C.

Below P_1 there is, in essence, very little reaction. The boundary at P_1 is sensitive to the vessel surface; an increase in the vessel diameter decreases the explosion limit. By adding inert gas a reduction in the explosion limit is sometimes observed, thus making the mixture more explosive.

At pressures just above P_1 , an explosion occurs in the form of a glow. The explosion becomes more intense the higher the pressure until P_2 , the second limit, is reached.

Above P_2 , the explosion is suppressed. P_2 is normally almost insensitive to the diameter and surface nature of the reaction vessel. Addition of inert gas has the ability to suppress the explosion which indicates that the termination reactions are occurring in the gas phase. There is virtually no fast reaction until the pressure approaches P_3 . At pressures near to one atmosphere a slow reaction is observed. Above P_3 , the third limit, the reaction becomes explosive again. The position of the third limit is affected significantly by the diameter and surface nature of the reaction vessel which is indicative of termination at the surface (HO_2 radicals in this case).

As the second limit is normally independent of the surface, the reaction at this point can be represented by elementary reactions (2.01-2.05) plus an initiation reaction.

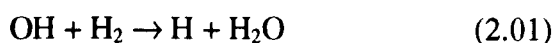
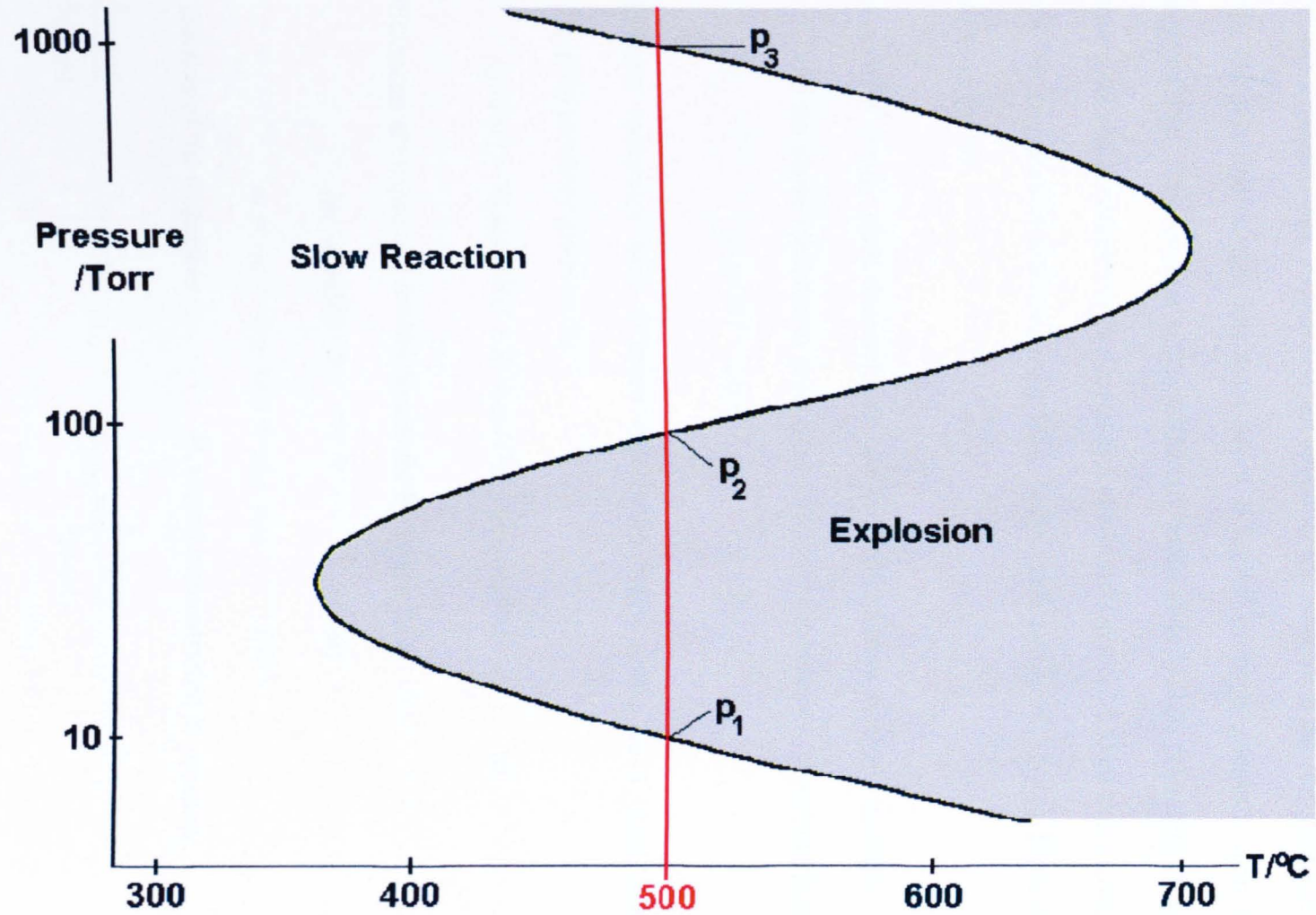
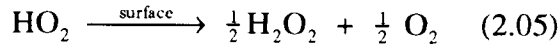
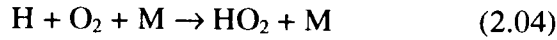


Figure 2. 1: Explosion Limits for the Hydrogen + Oxygen Reaction.





In order for homogeneous termination to suppress the explosion as the pressure is increased, the termination reaction must be of a higher order in pressure than the branching reaction. The reaction which fulfils this criterion is (2.04), providing HO_2 is considered inert and is completely destroyed in a reaction such as (2.05) so that (2.04) is effectively the termination reaction. Any third body, such as O_2 , H_2 , N_2 or H_2O , can represent M in (2.04).

Application of a steady state treatment or use of the Semenov theory², described in Chapter 1, with the above mechanism gives equation (i) for the value of the second limit.

$$k_{2.04}[\text{M}] = 2k_{2.02} \quad (\text{i}).$$

Since different molecules have different efficiencies when acting as a third body, $k_{2.04}[\text{M}]$ is more precisely given as (ii).

$$k_{2.04}[\text{M}] = k_{2.04(\text{H}_2)}[\text{H}_2] + k_{2.04(\text{O}_2)}[\text{O}_2] + k_{2.04(\text{N}_2)}[\text{N}_2] \quad (\text{ii}).$$

If the efficiencies are expressed relative to that for hydrogen then,

$$[\text{M}] = mM_t \quad (\text{iii})$$

$$\text{where} \quad m = x_{\text{H}_2} + a_{(\text{O}_2)} x_{(\text{O}_2)} + a_{(\text{N}_2)} x_{(\text{N}_2)} \quad (\text{iv})$$

x = mol fraction of the respective gas. M_t = total concentration or pressure.

$$a_{(\text{O}_2)} = \frac{k_{2.04(\text{O}_2)}}{k_{2.04(\text{H}_2)}}. \quad a_{(\text{N}_2)} = \frac{k_{2.04(\text{N}_2)}}{k_{2.04(\text{H}_2)}}.$$

A spectacular rise in the second limit as the oxygen mole fraction was decreased was noticed by Egerton and Warren³ as part of their study of the hydrogen + oxygen reaction in boric-acid-coated Pyrex vessels. An increase in the importance of quadratic branching

reactions was used to explain this effect at low oxygen concentration. Their experimental results closely fitted the empirical formula (v), where A and B are constants.

$$M = A + \frac{B}{[O_2]^{1/2}} \quad (v).$$

When the term $\frac{B}{[O_2]^{1/2}}$ is omitted, an expression similar to (i) is achieved and this represents the second limit in KCl-coated vessels where there is an absence of quadratic branching.

Egerton and Warren³ compared the results obtained in both KCl and boric-acid-coated vessels and deduced that the A term in (v) is due to linear branching and that the $\frac{B}{[O_2]^{1/2}}$ term arises from quadratic branching. This led to reaction (2.08) being suggested as the quadratic branching reaction at the second limit which is important because termination of HO_2 at the surface is inefficient in boric-acid-coated vessels.



Since HO_2 is generally inert above the second limit, one reactive chain centre, H , gives rise to two reactive chain centres but at a rate proportional to $[H][HO_2]$. Consequently, reaction (2.08) fulfils the definition for a quadratic branching reaction.

Application of the Semenov theory (described in Chapter 1) to a mechanism consisting of the quadratic branching reaction gives the boundary condition, $\phi^2 = 4\theta F$, between slow reaction and explosion. The implication of including reaction (2.08) in the mechanism is that the rate of initiation (θ) is important in determining the position of the second limit which is not the case for linear branching (equation (i)).

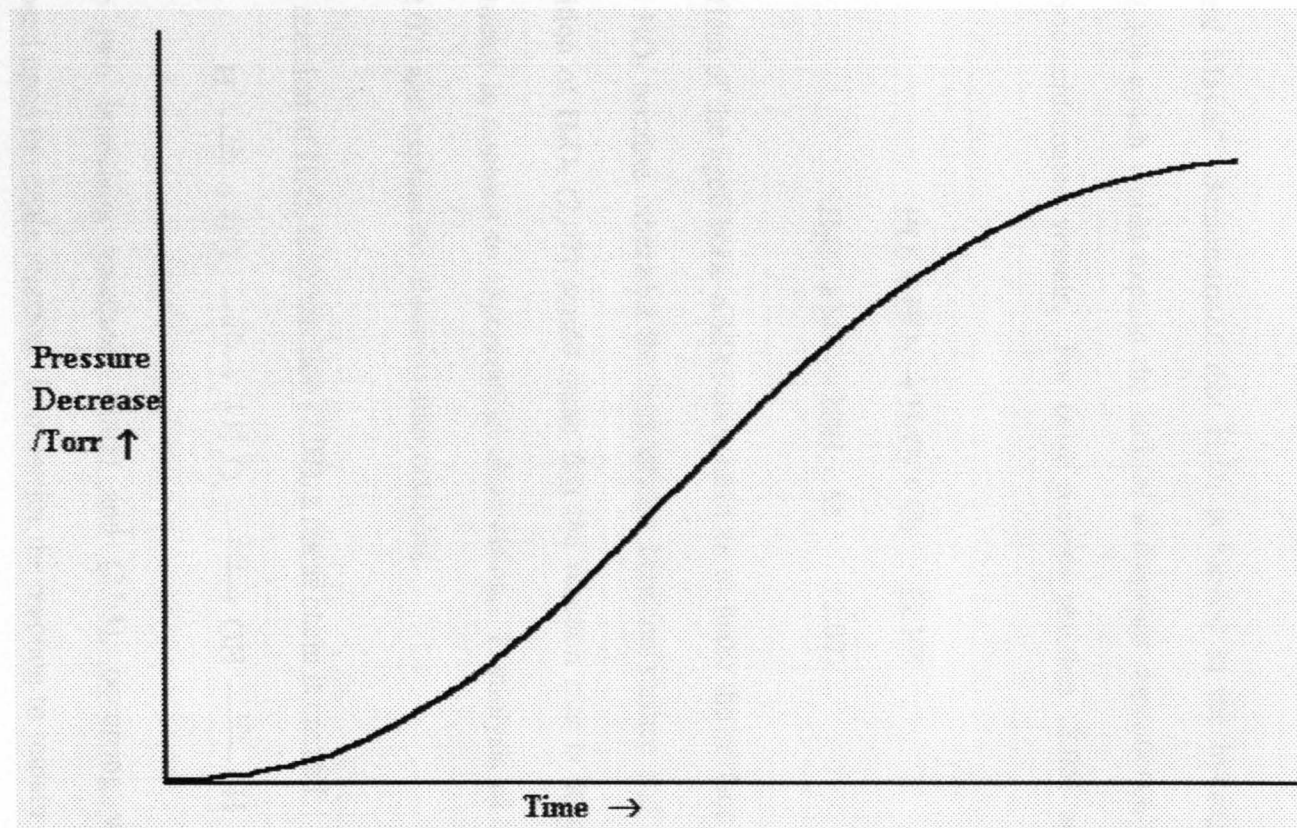
2.1.1. The Slow Reaction in Aged Boric-Acid-Coated Vessels.

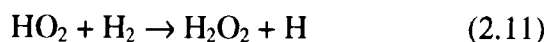
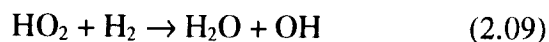
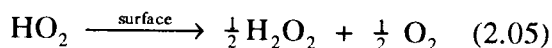
The discovery of the reproducible slow reaction in boric-acid-coated vessels by Baldwin and Mayor^{4,6} lead to controllable experiments and a detailed understanding of the mechanism.

At about 500°C and 500 Torr total pressure, the hydrogen + oxygen reaction in freshly boric-acid-coated vessels is very slow. However, after repeated second-limit explosions and slow reactions (approximately 200) with mixtures containing O₂/H₂ ratios of about 2, a rapid increase in the maximum rate is observed over a day (five of six runs) until a constant reproducible maximum rate is obtained. The vessel will normally remain in this *aged* condition for several months and in some extreme cases up to a year. A comparison of the maximum rates for different aged vessels gives the same value within experimental error at a fixed temperature and mixture composition. Allowing for dead volume effects, variation in the reaction vessel diameter between 14 and 55mm produced no change in the maximum rate for aged vessels. A typical reaction profile, illustrating the auto-catalytic nature of the reaction, is shown in Figure 2.2. The agreed explanation for the effect of the aged vessel surface on the maximum rate of the hydrogen + oxygen reaction is that the destruction of HO₂ and H₂O₂ at the surface has been reduced effectively to zero. This has the dual consequence of enhancing other reactions and effectively producing a vessel which is totally inert to the reaction species involved.

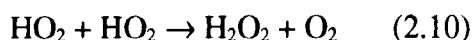
If the effect of an aged vessel is to reduce the importance of the removal of HO₂ at the surface, the competition between 2.09, 2.11 and 2.05, 2.06 would lead to a diameter dependence on the reaction rate. This is not the case. It would appear that HO₂ is either removed entirely in the gas phase or entirely at the surface.

Figure 2.2 : Plot of Autocatalysis of the Hydrogen + Oxygen Reaction in an Aged Boric-acid-coated vessel at 480°C.



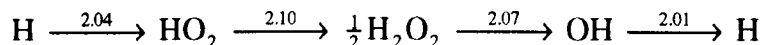


Baldwin and Mayor⁴ demonstrated that H_2O_2 is formed in the hydrogen + oxygen reaction (2.10) which would explain the lack of a diameter dependence at the second limit in boric-acid-coated vessels. For these reasons reaction (2.05) and (2.06) are excluded.



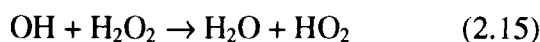
Another effect of the aged boric-acid-coating must be to make the surface inert to H_2O_2 as well as HO_2 because otherwise the competition between surface and homogeneous decomposition of H_2O_2 (2.07) would mean that the reaction rate is dependant on the vessel diameter in contrast to experimental observation. Homolysis of H_2O_2 through reaction (2.07) will explain the observed auto-catalysis.

If the sole reaction of H_2O_2 is by reaction (2.07), a linear chain is created.



There are two branching reactions, (2.02) and (2.03), occurring which can be superimposed upon the chain reaction. In order for the reaction to remain under control, termination reactions are required. The termination reactions must be in the gas phase due to the lack of surface effects.

It has been shown³⁻⁵ that reactions (2.14a) and (2.15) are the main termination processes. Simple use of the stationary state treatment shows why the observed activation energy for the reaction is approximately equal to $E_{A(2.07)}$.



With a mechanism of (2.01-2.05), (2.07) and (2.10) and (2.14a) the rate of water formation is given by equation (vii):

$$\frac{d[\text{H}_2\text{O}]}{dt} = \frac{2k_{2.02}k_{2.07}}{k_{2.14a}} [\text{O}_2] \text{I} \text{M}' \left(\frac{k_{2.04}[\text{M}] + k_{2.02}}{k_{2.04}[\text{M}] - k_{2.02}} \right) \quad (\text{vii})$$

With $k_{2.02}/k_{2.04}=0.05$ Torr ($M = \text{H}_2$) at 500°C , the term in brackets is approximately unity at 500 Torr of stoichiometric mixture so that equation (vii) is reduced to (viii).

$$\frac{d[\text{H}_2\text{O}]}{dt} \approx \frac{2k_{2.02}k_{2.07}}{k_{2.14a}} [\text{O}_2] \text{I} \text{M}' \quad (\text{viii})$$

With $E_{A(2.02)}=70 \text{ kJ mol}^{-1}$ ⁽⁷⁾, $E_{A(2.07)}=192 \text{ kJ mol}^{-1}$ ⁽⁸⁾ and $E_{A(2.14a)}=49 \text{ kJ mol}^{-1}$ ⁽⁸⁾, then $E_{A(\text{obs})}=213 \text{ kJ mol}^{-1}$ which is close to the observed value and to that of reaction (2.07)⁹, namely 192 kJ mol^{-1} . With $E_{A(2.02)}=70 \text{ kJ mol}^{-1}$ ⁽⁷⁾ and $E_{A(2.14a)}=49 \text{ kJ mol}^{-1}$ ⁽⁸⁾, then clearly the value of $E_{A(\text{obs})}$ for the rate of formation should be only slightly higher than $E_{A(2.07)}=192 \text{ kJ mol}^{-1}$. This prediction is borne out by the observed value of $245 \pm 10 \text{ kJ mol}^{-1}$ between 420 and 520°C ⁸ which is slightly higher than the true value due to self-heating at the higher temperatures.

When reaction (2.14a) is replaced with (2.15), a similar interpretation as above gives equation (ix)

$$\frac{d[H_2O]}{dt} = \frac{2k_{2.01}k_{2.02}k_{2.07}}{k_{2.15}k_{2.04}} [H_2][M'] \quad (\text{ix})$$

With $E_{A(2.01)}=13 \text{ kJ mol}^{-1(7)}$, $E_{A(2.02)}=70 \text{ kJ mol}^{-1(7)}$, $E_{A(2.04)}= -5 \text{ kJ mol}^{-1(8)}$, and $E_{A(2.15)}= 5 \text{ kJ mol}^{-1(7)}$ and $E_{A(2.07)}=192 \text{ kJ mol}^{-1(8)}$ then $E_{A(\text{obs})}\approx 270 \text{ kJ mol}^{-1}$.

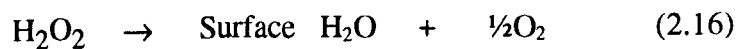
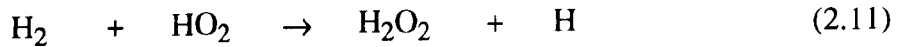
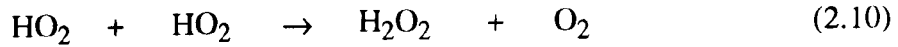
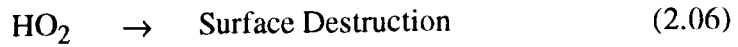
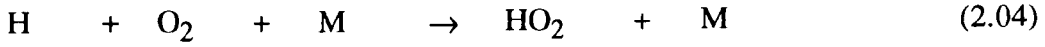
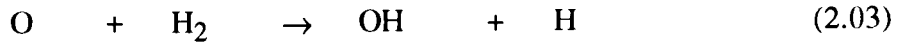
2.2. Use of the Hydrogen + Oxygen Reaction for Hydrocarbon Oxidation Studies.

With the mechanism for the hydrogen + oxygen reaction well defined in aged boric-acid-coated vessels (Table 2.1) and the rate constants for the elementary reactions now well known, it is possible to use the reaction as a controllable and reproducible source of H, OH and HO₂ radicals. Two types of information can be obtained from studies of the addition of traces of additive to slowly reacting mixtures of hydrogen and oxygen at above 500°C. Firstly, kinetic parameters for the attack of OH and H, or H and HO₂ on the additive can be made from measurements of the relative rate of consumption of the additive and hydrogen. Secondly, from studies of the products formed, information can be obtained on the reactions of the radicals formed from the additive in an oxygen environment.

2.2.1. The Kinetic Study.

When examining the kinetics for the attack of H, OH or HO₂ on an additive, less than 0.05% of the additive is added to the hydrogen + oxygen mixture in order not to perturb the radical concentrations. This can be checked by measuring the experimental maximum rate and induction period in the presence and absence of the additive. Any

Table 2. 1 : The General Mechanism for the Hydrogen + Oxygen Reaction. in boric-acid-coated vessels



variation of the radical pool by the additive would be indicated by a change in the induction period and/or maximum rate of the reaction. The hydrogen + oxygen system may be used across a wide range of mixture composition (Table 2.2) in order to achieve wide variation in the proportions of [H], [OH] and [HO₂]. A plot of ‘% Additive Consumed’ against ‘Pressure Change (ΔP)’ (Figure 2.3) enables ΔP₅₀, the pressure change at 50% consumption of the additive, to be obtained. A value for ΔP₅₀ for each mixture used is measured. Figure 2.3 shows a typical plot for p-xylene.

It is shown later that it is mainly the rate constant ratios $\frac{k_{2.21}}{k_{2.01}}$, $\frac{k_{2.22}}{k_{2.02}}$, $\frac{k_{2.23}}{k_{2.03}}$ and $\frac{k_{2.24}}{(k_{2.10})^{1/2}}$

rather than absolute values of the rate constants that determine ΔP₅₀ and hence the amount of additive consumed through radical attack by OH, H, O and HO₂ respectively.

It is possible to use a steady-state algebraic treatment in order to obtain approximate values of the rate constant ratios from the measured values of ΔP₅₀. However, this treatment of the results does not allow for features such as self-heating and pressure change due to the oxidation of the additive. Further, it is not possible to use the full mechanism of the H₂ + O₂ reaction. In practice, a full and comprehensive computer program is used. Nevertheless the algebraic treatment is of interest in elucidating the principles of the approach.

2.2.1.1. The Algebraic Treatment.

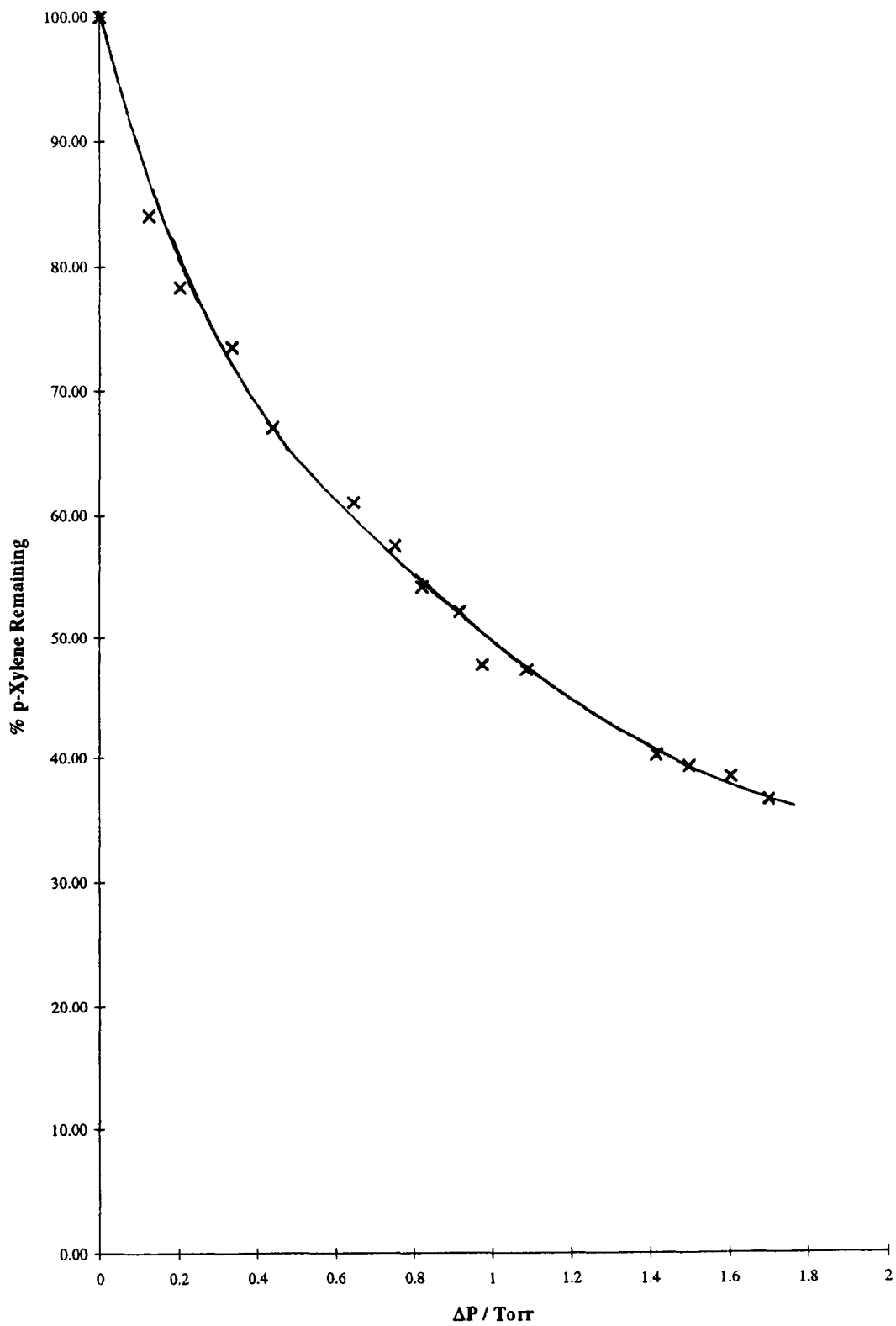
In order to apply the algebraic treatment for the addition of (say) a hydrocarbon to the hydrogen + oxygen reaction it is necessary to restrict the mechanism and make several assumptions in order to keep the equations manageable.

**Table 2. 2 : Reaction Mixtures used for the Xylene Kinetics Study -
0.05 Torr Xylene plus:**

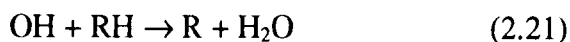
Pressure H₂ / Torr	Pressure O₂ / Torr	Pressure N₂ / Torr
140	360	0
140	270	90
140	210	150
140	140	220
140	70	290
140	35	325
430	70	0
270	70	160
210	70	220
70	70	360
35	70	395

Figure 2. 3 : Typical Decay Plot

Plot of % p-Xylene Remaining v.s. ΔP for
0.05 Torr p-Xylene + 70 Torr O₂ + 140 Torr H₂.



If a simplified mechanism consisting of reactions (2.01-2.04, 2.07, 2.10 and 2.14) is used and if it is assumed that the additive (**RH**) and H₂ are removed only by reactions (2.21) and (2.01) respectively,

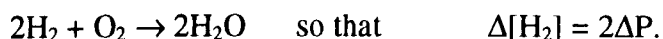


then:
$$\frac{d[\text{RH}]}{dt} = k_{2.21}[\text{OH}][\text{RH}] \quad (\text{xi})$$

and:
$$\frac{d[\text{H}_2]}{dt} = k_{2.01}[\text{OH}][\text{H}_2] \quad (\text{xii})$$

so that
$$\frac{d[\text{RH}]}{d[\text{H}_2]} = \frac{\Delta[\text{RH}]}{\Delta[\text{H}_2]} = \frac{k_{2.21}[\text{RH}]}{k_{2.01}[\text{H}_2]} \quad (\text{xiii})$$

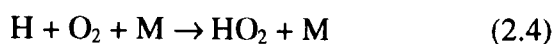
The relative rate of formation of RH and H₂ would be inversely proportional to [H₂]. In practice, orders of about 0.7 are observed with most additives used which indicates that OH attack is very important but does not remove all the RH. Δ[RH] can be obtained from gas chromatographic analysis of the reaction vessel mixture. Δ[H₂] can be obtained by measuring the pressure change due to the overall process



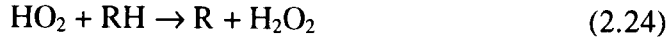
Alternatively if H atom attack on RH is considered as the only way RH is removed then the relative rate of RH and H₂ removal is given effectively by equation (xiv) at 500 Torr total pressure.



$$\frac{d[\text{RH}]}{d[\text{H}_2]} = \frac{k_{2.22}[\text{RH}]}{k_{2.04}[\text{O}_2][\text{M}]} \quad (\text{xiv})$$



Finally if RH is removed solely in reaction (2.24),



then the stationary state treatment gives,

$$\frac{d[\text{RH}]}{d[\text{H}_2]} = k_{2.24}[\text{RH}] \left(\frac{k_{2.14}}{4k_{2.02}k_{2.07}k_{2.10}[\text{O}_2][\text{M}']} \right)^{1/2} \quad (\text{xv})$$

Equations (xiii), (xiv) and (xv) assume that only OH or H or HO₂, respectively, remove RH. If it is assumed (as demonstrated experimentally) that the trace amount of RH does not perturb the radical concentrations in the H₂+O₂ system, then the relative rate of consumption of RH and H₂, when both H and OH remove RH, is given by equation (xvi).

$$\frac{d[\text{RH}]}{d[\text{H}_2]} = \frac{k_{2.21}[\text{RH}]}{k_{2.01}[\text{H}_2]} + \frac{k_{2.22}[\text{RH}]}{k_{2.04}[\text{O}_2][\text{M}]} \quad (\text{xvi}).$$

Integration of (xvi) under conditions where only a small amount of H₂ is consumed ([H₂] >>> [RH]), gives equation (xvii).

$$\ln \frac{[\text{RH}]_{\text{initial}}}{[\text{RH}]_{\text{final}}} = \frac{k_{2.21}\Delta\text{H}_2}{k_{2.01}[\text{H}_2]} + \frac{k_{2.22}\Delta\text{H}_2}{k_{2.04}[\text{O}_2][\text{M}]} \quad (\text{xvii})$$

At 50% consumption of RH, [RH]_{final} = 1/2[RH]_{initial} and ΔH₂ = (ΔH₂)₅₀ so that (xvii)

becomes (xviii).

$$\ln 2 = \frac{k_{2.21}(\Delta\text{H}_2)_{50}}{k_{2.01}[\text{H}_2]} + \frac{k_{2.22}(\Delta\text{H}_2)_{50}}{k_{2.04}[\text{O}_2][\text{M}]} \quad (\text{xviii})$$

Rearranging (xviii) gives:

$$\frac{[\text{O}_2][\text{M}]}{(\Delta\text{H}_2)_{50}} = \frac{k_{2.21}[\text{O}_2][\text{M}]}{0.693k_{2.01}[\text{H}_2]} + \frac{k_{2.22}K}{0.693k_{2.02}} \quad (\text{xix})$$

where $K = \frac{k_{2.02}}{k_{2.04}}$.

Since $\Delta[H_2] = 2\Delta P$, (xix) can be rewritten as (xx):

$$\frac{[O_2][M]}{(\Delta P)_{50}} = \frac{2k_{2.21}[O_2][M]}{0.693k_{2.01}[H_2]} + \frac{2k_{2.22}K}{0.693k_{2.02}} \quad (\text{xx})$$

When $\frac{[O_2][M]}{(\Delta P)_{50}}$ is plotted against $\frac{[O_2][M]}{0.693[H_2]}$, the gradient and intercept permit the

determination of $\frac{k_{2.21}}{k_{2.01}}$ and $\frac{k_{2.22}}{k_{2.02}}$. However, apart from other inaccuracies, this

treatment ignores both O and HO₂ attack on RH. Although O attack is usually relatively unimportant, HO₂ can become important particularly when the additive contains weak C-H bonds such as those in *iso*-butane or toluene.

As, to some degree, all of the radicals OH, H, O and HO₂ attack RH, the algebraic solutions become increasingly difficult. To account for all of the reactions in the hydrogen + oxygen mechanism, account for self heating and include the chemistry for the oxidation of the additive, RH, analysis through a comprehensive computer program⁸ has normally been carried out as this approach does not require a large number of approximations.

2.2.1.2. The Computer Treatment. Overview.

The analytical treatment, out of necessity, makes assumptions about radical attack, but also ignores the effect of self-heating of the reaction which naturally affects the measured value of ΔP . A computer treatment has been developed to account for these effects and other approximations, including a more detailed appraisal of the chemistry for the RH

additive, made in the analytical treatment. This will be discussed in more detail in Chapter 7 (Xylene Kinetics).

2.2.2. The Mechanistic Study.

The fate of the parent hydrocarbon and the radicals it produces during the oxidation process can be examined by product analysis. This can be accomplished by measuring the initial yields of the products over a wide range of mixture composition.

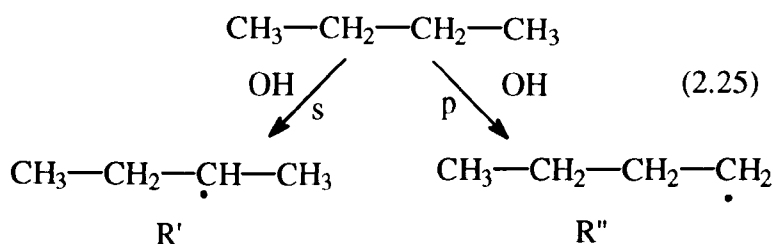
In many cases, the primary products are highly reactive and therefore require quantitative analysis during the early stages of reaction. This requirement for the early analysis of trace products clearly places stringent demands on the techniques used. In order to ameliorate this problem the concentration of the additive is typically increased from less than 0.05% used in the kinetic study to about 1%, although the increase in hydrocarbon concentration does perturb the radical pool of the hydrogen + oxygen reaction noticeably. (Fortunately, this does not significantly alter the determination of rate constant ratios for the formation of products since changes in the radical concentration are less important than in the kinetic study.) In order to differentiate between primary, secondary and tertiary products, the product yields are measured up to and above 50% consumption of the additive.

It is worth considering two important studies as examples of the power of the technique.

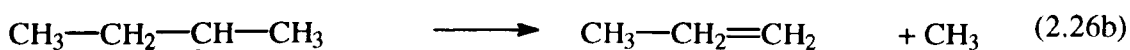
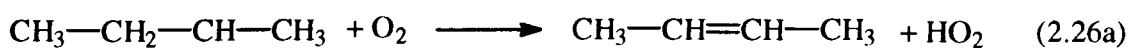
2.2.2.1. The Oxidation of Butane.

The oxidation of butane involves the formation of two butyl radicals (reaction 2.25) and was studied at 753K in great detail by Baldwin and co-workers¹⁰ who showed that the

primary products were the conjugate alkenes, o-heterocycles and homolysis compounds from the primary and secondary butyl radicals



The following analysis illustrates the elegance and simplicity of the relative rate study in an oxidation environment which is overall complex. Primary products produced uniquely from the *s*-butyl radical were found to be but-2-ene and propene, reactions (2.26a) and (2.26b) respectively.



The initial rate of formation of but-2-ene and propene is given by equation (xxi)

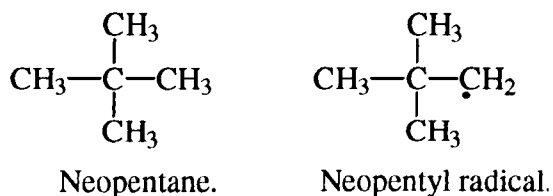
$$\frac{d[\text{But - 2 - ene}]}{d[\text{Propene}]} = \frac{k_{2.26a}[\text{O}_2]}{k_{2.26b}} \quad (\text{xxi}).$$

Consequently a plot of [But-2-ene]/[Propene] at different [O₂] should produce a straight line graph through the origin with an intercept equal to $k_{2.26a}/k_{2.26b}$. Baldwin and co-workers found this to be the case¹⁴ and since $k_{2.26b}$ was known from the literature¹¹⁻¹³, $k_{2.26a}$ for both isomers of but-2-ene was obtained for the first time^{10,14,15}.

This approach has been used in order to obtain rate constants for a range of reactions of alkyl radicals similar to reaction (2.26)¹⁶ for systems involving C₃H₈, i-C₄H₁₀, and n-C₅H₁₂ oxidation.

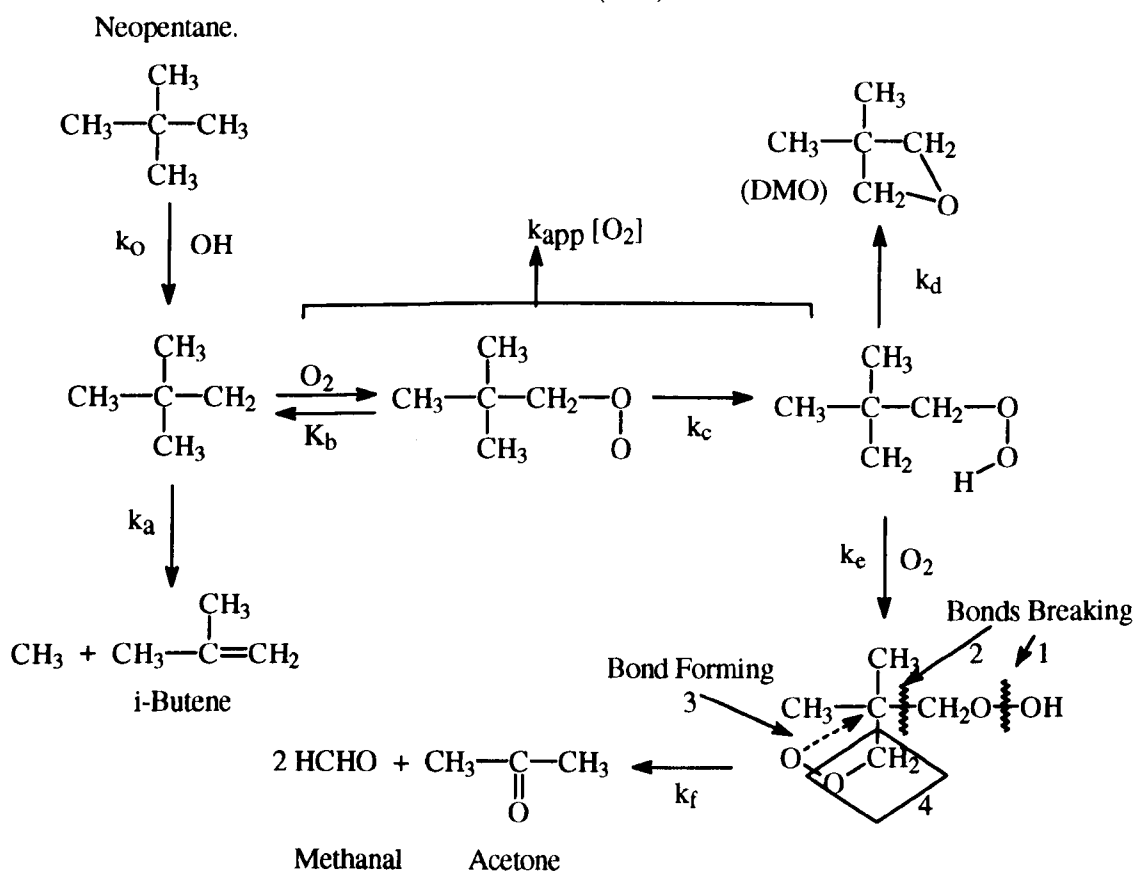
2.2.2.2. The Oxidation of Neopentane.

The oxidation chemistry of neopentane is very unique. It is a highly branched hydrocarbon with only primary hydrogens and forms only one species of neopentyl radical.



Formation of the conjugate alkene is not possible here and consequently types of products which would normally be of minor importance when produced from other alkanes are magnified in yield. The major products from neopentane oxidation at about 750K are *i*-butene, methane, methanal, acetone and 3,3-dimethyloxetane (DMO).

Overall Reaction (2.27)



Analysis of the initial products over a wide range of O₂ pressure¹⁷ indicated two important relationships.

$$\left(\frac{[\text{Acetone}] + [\text{DMO}]}{[\text{i-Butene}]} \right)_0 \propto [\text{O}_2] \text{ and } \left(\frac{[\text{Acetone}]}{[\text{DMO}]} \right)_0 \propto [\text{O}_2]$$

where the subscript 0 indicates the initial value of the ratios.

With the above scheme

$$\frac{d([\text{Acetone}] + [\text{DMO}])}{d[\text{i-Butene}]} = \frac{k_{app} [\text{O}_2]}{k_a} \quad (\text{xxii})$$

$$\frac{d[\text{Acetone}]}{d[\text{DMO}]} = \frac{k_e [\text{O}_2]}{k_d} \quad (\text{xxiii})$$

The occurrence of acetone and DMO in scheme (2.27) clearly illustrates the occurrence of the RO₂ → QOOH reaction, in this case through a 1,5p peroxy radical isomerisation and decomposition PRID transition. The degree of reaction proceeding via the RO₂ → QOOH reaction was determined by measuring ([Acetone]+[DMO])/[i-Butene] with the resulting reactions of the QOOH radical being determined by examining [Acetone]/[DMO] separately.

With R + O₂ \rightleftharpoons RO₂ equilibrated¹⁷, then k_{app} = K_bk_c. From a detailed analysis of the product yields, Baldwin et al.¹⁷ were able to determine Arrhenius parameters for the reactions shown in scheme (2.27) (summarised below).

Rate Constant	Arrhenius Parameters	k at 753K
k _a	4.45*10 ¹³ exp(-15340/T) s ⁻¹	6.36*10 ⁴ s ⁻¹
K _b ¹⁸	2.7*10 ⁻⁵ exp(+12640/T) l mol ⁻¹	528 l mol ⁻¹
k _c	1.2*10 ¹³ exp(-14430/T) s ⁻¹	5.68*10 ⁴ s ⁻¹
k _d	2*10 ¹¹ exp(-8780/T) s ⁻¹	1.73*10 ⁶ s ⁻¹
k _e	3.3*10 ⁷ exp(+962/T) l mol ⁻¹ s ⁻¹	1.18*10 ⁸ l mol ⁻¹ s ⁻¹
k _f	1.25*10 ¹² exp(-11610/T) s ⁻¹	2.53*10 ⁵ s ⁻¹

Here, as in the oxidation chemistry of butane, it is relatively easy to gain an understanding of which are likely to be the primary and secondary products as well as which product yields are sensitive to changes in the mixture composition, particularly $[O_2]$.

The rate constant k_c corresponds to a 1,5p H-atom transfer in neopentyl radicals. Hughes et al.¹⁹ confirmed the values of the $k_c K_b / k_a$ obtained by Baldwin et al.¹⁷ by direct measurement of $[OH]$. Further, Hughes's¹⁹ technique permitted the determination of K_b directly and the results show that the value of K_b calculated by Baldwin et al.¹⁷ from Benson's additivity rules is in error by a factor of about 10. As a result, k_c is lowered by the same factor.

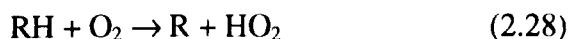
The direct determination of K_b and k_c by Hughes et al.¹⁹ was of great importance because the rate data are consistent with the series of 1,4, 1,5, 1,6 and 1,7 H-atom atom transfers (Table 1.2 in Chapter 1) in alkylperoxy radicals, determined by Baldwin et al.¹⁷, all based on calculated values of the equilibrium constant $R + O_2 \rightleftharpoons RO_2$ from Benson's additivity rules²⁰.

The work of Hughes et al.¹⁹ on the 1,5 H-atom transfer in neopentyl radicals effectively calibrated and validated the complete set of data obtained by Baldwin et al.¹⁷ which has been used extensively to model many practical combustion problems. Further it is important to emphasise that this system gives extensive evidence that the subsequent decomposition of QOOH radicals is sufficiently fast that the $RO_2 \rightarrow QOOH$ isomerisation is effectively irreversible^{17,19,21}.

2.3. The Generation of HO₂ Radicals.

Although kinetic data for the abstraction reactions of OH radicals, and to some extent H atoms, are well known, relatively few data are available for HO₂ radicals despite their great importance in combustion. Use of a system such as the hydrogen + oxygen reaction as a clean source of HO₂ radicals presents numerous problems, the most noticeable being the presence of OH which typically reacts with alkanes a factor of 10⁵ faster than HO₂ below about 600°C.

The primary initiation process for the oxidation of a hydrocarbon (RH) in the temperature range of 400-600°C is generally considered to proceed by reaction (2.28).

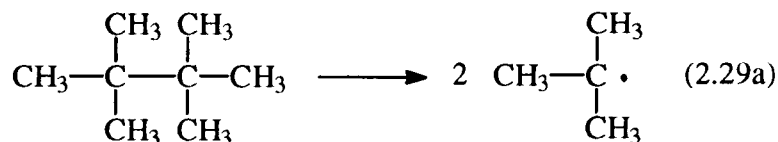


However if the compound RH contains a highly strained C-C bond it may be possible for a homolysis reaction (2.29) to occur at a much higher rate even at high O₂ pressures.



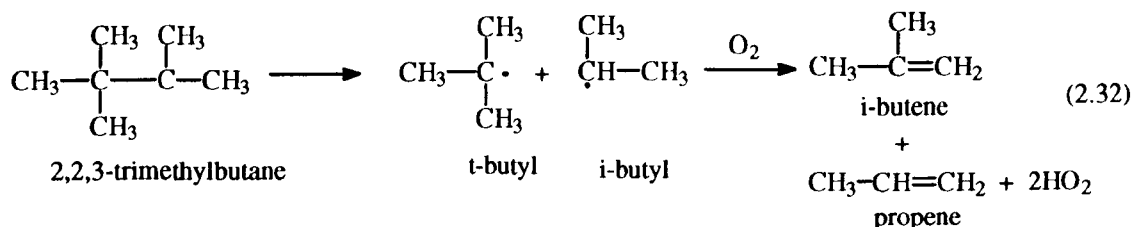
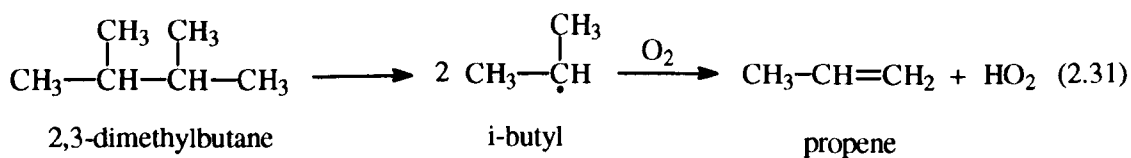
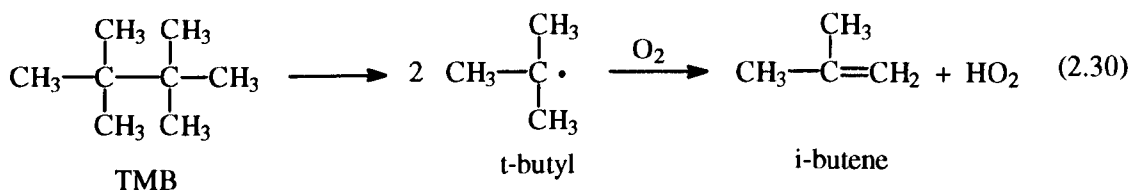
Walker and Tsang²² studied the thermal decomposition of tetramethylbutane (TMB) (*aka hexamethylethane*) into two t-butyl radicals in a flow system where rate data were determined from the competitive decomposition of TMB and cyclohexene between 700 and 900K. Tsang et al. obtained Arrhenius parameters $k_{\text{TMB}}^{(22)} = 2.51 \cdot 10^{17} e^{-299304/RT} \text{ s}^{-1}$, compared with $k_{\text{C}_2\text{H}_6}^{(23)} = 1.18 \cdot 10^{18} (T/298)^{-1.79} e^{-381063/RT} \text{ s}^{-1}$ for $\text{C}_2\text{H}_6 \rightarrow 2\text{CH}_3$ which give $k_{\text{TMB}}/k_{\text{C}_2\text{H}_6} \approx 5.5 \cdot 10^5$ at 750K and high pressures. At low pressure, the ratio will rise due to fall-off effects on the rate constant for C₂H₆ homolysis.

In the case of TMB, reaction (2.29) can be written as (2.29a):



Particularly if the subsequent reactions of the R' and R'' radicals result in small chain lengths, then it may be possible to study the reactions of R' and R'' with O₂. This approach has been used at Hull with a number of different strained hydrocarbons such as TMB (2.30)^{24,25,29}, 2,3-dimethylbutane(2.31)^{26,27} and 2,2,3-trimethylbutane(2.32)^{24,28}. More importantly the system, particularly for TMB homolysis, provides an excellent clean source of HO₂ radicals.


The homolysis rate data for TMB, 2,3-dimethylbutane and 2,2,3-trimethylbutane determined by the Hull group are summarised in Table 2.3.



Each of the above reactions has been used to determine kinetic information for the reactions of hydrocarbons with HO₂, the most widely used being the TMB + O₂ system

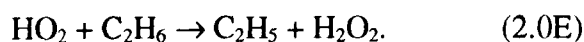
Table 2. 3 : Homolysis rate data for some strained and straight chain hydrocarbons. at 753K.

Reference	Hydrocarbon [•]	$E_A / \text{kJ mol}^{-1}$	A / s^{-1}	k_{753} / s^{-1}
29	$ \begin{array}{c} \text{CH}_3 \quad \text{CH}_3 \\ \quad \\ \text{CH}_3 - \text{C} - \text{C} - \text{CH}_3 \\ \quad \\ \text{CH}_3 \quad \text{CH}_3 \end{array} $ <p style="text-align: center;">TMB</p>	295	$1.04 \cdot 10^{17}$	$3.57 \cdot 10^{-4}$
26	$ \begin{array}{c} \text{CH}_3 \quad \text{CH}_3 \\ \quad \\ \text{CH}_3 - \text{CH} - \text{CH} - \text{CH}_3 \\ \quad \\ \text{CH}_3 \quad \text{CH}_3 \end{array} $ <p style="text-align: center;">2,3-dimethylbutane</p>	319	$2.63 \cdot 10^{16}$	$1.95 \cdot 10^{-6}$
28	$ \begin{array}{c} \text{CH}_3 \quad \text{CH}_3 \\ \quad \\ \text{CH}_3 - \text{C} - \text{CH} - \text{CH}_3 \\ \quad \\ \text{CH}_3 \quad \text{CH}_3 \end{array} $ <p style="text-align: center;">2,2,3-trimethylbutane</p>	305	$2.88 \cdot 10^{16}$	$2.00 \cdot 10^{-5}$

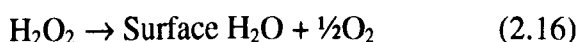
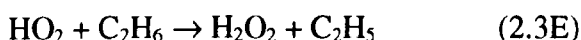
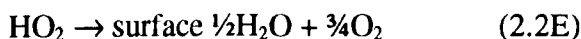
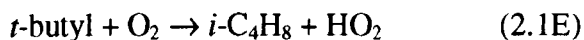
•  indicates the bond being broken.

because of the absence of tertiary C-H bonds in the alkane. As a consequence, TMB is consumed mostly by homolysis rather than by radical attack. As 99% of the *t*-butyl radicals react with O₂ under the conditions used, the system has been proved to be an extremely clean source of HO₂²⁹.

A good example of the use of the decomposition of TMB in the presence of O₂ to study HO₂ reactions is in the determination of the Arrhenius parameters for reaction 2.0E by Baldwin and co-workers³⁰. Studies were carried out in KCl and aged boric-acid-coated vessels.



For KCl-coated vessels a simple 'armchair' mechanism can be applied as shown below.



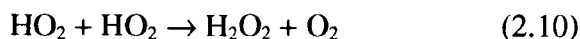
The rates of removal of TMB and C₂H₆ are given by,

$$-\frac{d[\text{TMB}]}{dt} = k_{2.29}[\text{TMB}] \quad \text{and} \quad -\frac{d[\text{C}_2\text{H}_6]}{dt} = k_{2.3\text{E}}[\text{HO}_2][\text{C}_2\text{H}_6],$$

As, at the stationary state, the rate of initiation = rate of termination, then it follows that $2k_{2.29}[\text{TMB}] = k_{2.2\text{E}}[\text{HO}_2]$. Consequently the relative rate of removal of TMB and C₂H₆ is given by equation (xxiv).

$$\frac{d[C_2H_6]}{d[TMB]} = \frac{k_{2.3E}[C_2H_6]}{k_{2.2E}} \quad (\text{xxiv})$$

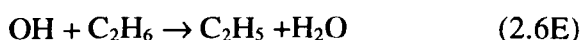
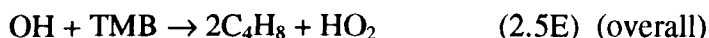
In boric-acid-coated vessels the HO₂ radicals are not destroyed at the surface, reaction (2.5E), but in the radical-radical process (2.10),



As $2k_{2.10}[HO_2]^2 = 2k_{2.29}[TMB]$ then $[HO_2] = \left(\frac{k_{2.29}[TMB]}{k_{2.10}} \right)^{1/2}$, and hence

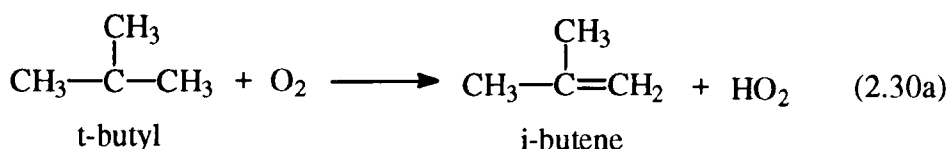
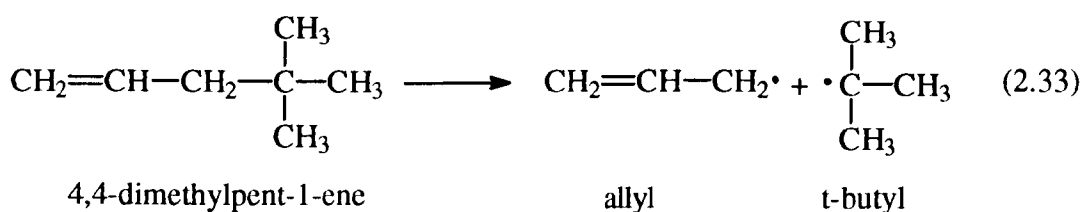
$$\frac{d[C_2H_6]}{d[TMB]} = \frac{k_{2.3}[C_2H_6]}{\{k_{2.29}k_{2.10}[TMB]\}^{1/2}} \quad (\text{xxv})$$

Allowances must also be made for the occurrence of an OH path as in reactions (2.07), (2.5E) and (2.6E)

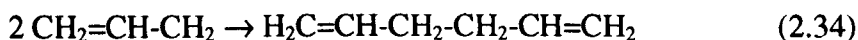


As H₂O₂ does not have a stationary concentration and the consumption of TMB and C₂H₆ is complicated by OH attack, a computer modelling approach is necessary. However, since $k_{2.29}$, $k_{2.07}$, $k_{2.6E}/k_{2.5E}$ and $[C_2H_6]$ are known, the only remaining unknown is $k_{2.3E}/(k_{2.10})^{1/2}$. This means that by measuring $\Delta[C_2H_6]/\Delta[TMB]$ at various times for a variety of mixtures the computer program can be used to determine $k_{2.3E}/(k_{2.10})^{1/2}$ with considerable accuracy. A rate constant of $3.0 \cdot 10^4 \text{ l mol}^{-1} \text{ s}^{-1}$ at 773K was obtained using this technique for reaction (2.3E) given that $k_{2.10}$ is known accurately and Baldwin et al.³¹ obtained an Arrhenius expression of $k_{2.03E} = 1.32 \cdot 10^{10} \exp(-85.6 \cdot 10^3/RT) \text{ l mol}^{-1} \text{ s}^{-1}$ between 713 and 813K.

More recently, rate data have been determined for HO₂ + radical reactions using the homolysis of a similar type of strained C-C bond structure. This was achieved in the decomposition of 4,4-dimethylpent-1-ene (2.33) where it was possible to determine the rate constants for several HO₂ + allyl radical paths of considerable importance in the oxidation of both alkanes and alkenes³²⁻³⁴.



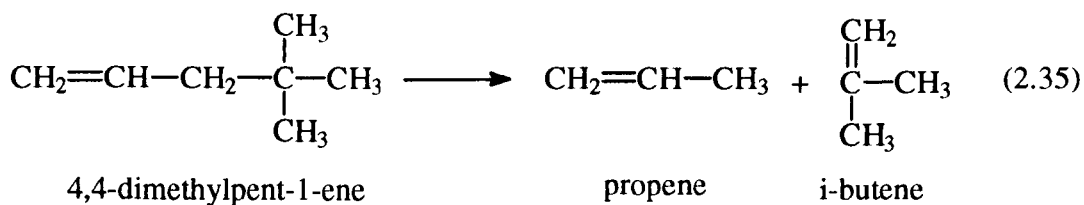
As with TMB decomposition, reaction (2.33) produces t-butyl radicals which will react with oxygen to produce i-butene and HO₂ radicals (reaction 2.30a). The electron-delocalised allyl radicals were found to undergo a number of different reactions. The presence of 1,5-hexadiene in large quantities confirmed the inertness of the allyl radical which can therefore readily undergo the recombination reaction (2.34) because of the high allyl radical concentration in the system.



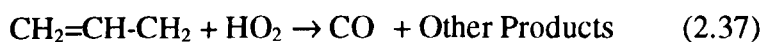
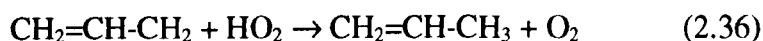
This is consistent with the work of Walker and Tsang²², and Rossi et al.³⁵ However, the work of Lohdi and Walker³² showed that reaction (2.34) occurred even in the presence of large amounts of O₂.

Lohdi and Walker³² also observed the formation of propene as a primary product. Although propene was produced in the molecular rearrangement reaction (2.35), this is

considered to be a minor pathway as the product ratio $[C_3H_6]/[i-C_4H_8]$ was about four in contrast to the expected maximum value of unity if reaction (2.35) is the only source of C_3H_6 and $i-C_4H_8$. It is clear that (2.35) is not the major source of propene.



The more important reaction route to propene was established as a radical-radical process between C_3H_5 and HO_2 , reaction (2.36), which competed with an alternative path (2.37) to give CO.



Lohdi and Walker³³ were able to obtain Arrhenius parameters for reactions (2.35), (2.36) and (2.37) such that $k_{2.35} = 1.71 \cdot 10^{12} \exp(-27393/T) \text{ s}^{-1}$, $k_{2.36} = 7.33 \cdot 10^9 \exp(-659K/T) \text{ l mol}^{-1} \text{ s}^{-1}$ and $k_{2.37} = 9.38 \cdot 10^9 \exp(-352K/T) \text{ l mol}^{-1} \text{ s}^{-1}$ therefore $k_{2.35} = 2.7 \cdot 10^{-4} \text{ s}^{-1}$, $k_{2.36} = 3.1 \cdot 10^9 \text{ l mol}^{-1} \text{ s}^{-1}$ and $k_{2.37} = 5.9 \cdot 10^9 \text{ l mol}^{-1} \text{ s}^{-1}$ at 753K.

This approach may be further extended to other systems where a study of radical + HO_2 radicals is specifically required, such as discussed in Chapter 6 of this thesis where the reactions of benzyl radicals with HO_2 are examined.

2.4. The Oxidation Chemistry of the Xylenes.

The simple alkylbenzenes such as toluene and xylene have been considered or used as anti-knock agents in gasoline, and over the last few years interest in the oxidation characteristics of these compounds has been intense. Although much is known about the

mechanism for the oxidation of small alkanes, there is relatively little detailed information on the mechanism for the oxidation of aromatic hydrocarbons and particularly on the rate constants for the elementary processes involved.

One of the first detailed studies of the oxidation chemistry of the xylenes was made in the early 1960's by Wright^{36,37} who also showed that o-xylene was the least able of the three isomers to suppress knock. However very little subsequent work was carried out until the early 1980's.

There are perhaps three key points to consider when examining the oxidation chemistry of the alkyl-substituted aromatic hydrocarbons.

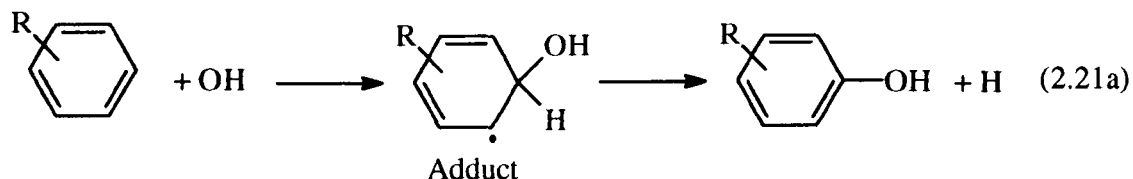
- 1) Both addition and abstraction reactions can occur, the latter from the ring or the side chain.
- 2) The role that electron delocalisation in radicals may play.
- 3) The change in the nature of attack on the aromatic compound with temperature.

Previous work^{36,37,39-43} indicates that there is a significant change in the mechanism for the reactions of OH with alkyl-substituted-aromatics as temperature increases. Addition to the aromatic ring, which dominates at room temperature, becomes of decreasing importance as the temperature is increased and abstraction of H from the ring, the side chain or substitution of one (or more) of the side chains increases in importance^{38,39}.

Compared to the relatively wide array of kinetic data available for reactions of the radicals O, H, OH and HO₂ with alkanes and alkenes, little is known regarding the reactions of these radicals with the alkyl-substituted benzenes/aromatics except for OH reactions at room temperature.

2.4.1. Reactions of OH radicals with Aromatics.

At temperatures around 298K, most of the simple alkyl-substituted aromatic compounds tend to undergo an electrophilic addition reaction with OH³⁹ (reaction 2.21a) whereby OH actually adds to the benzene ring to produce a *phenol*.



However, as the temperature increases above about 400K, H abstraction from the alkyl group occurs to form benzyl-type radicals. There are data available for the abstraction and addition reactions. Table 2.4 shows how the total rate constants for OH attack change between 300 and 1000K for benzene^{7,40,41}, toluene⁷ and the xylenes^{7,39}. However, there are currently no reliable data available for OH abstracting H from the ring of toluene, or the xylenes. On a per C-H bond basis, however, the rate constant is likely to be very similar to that for H atom abstraction in benzene.

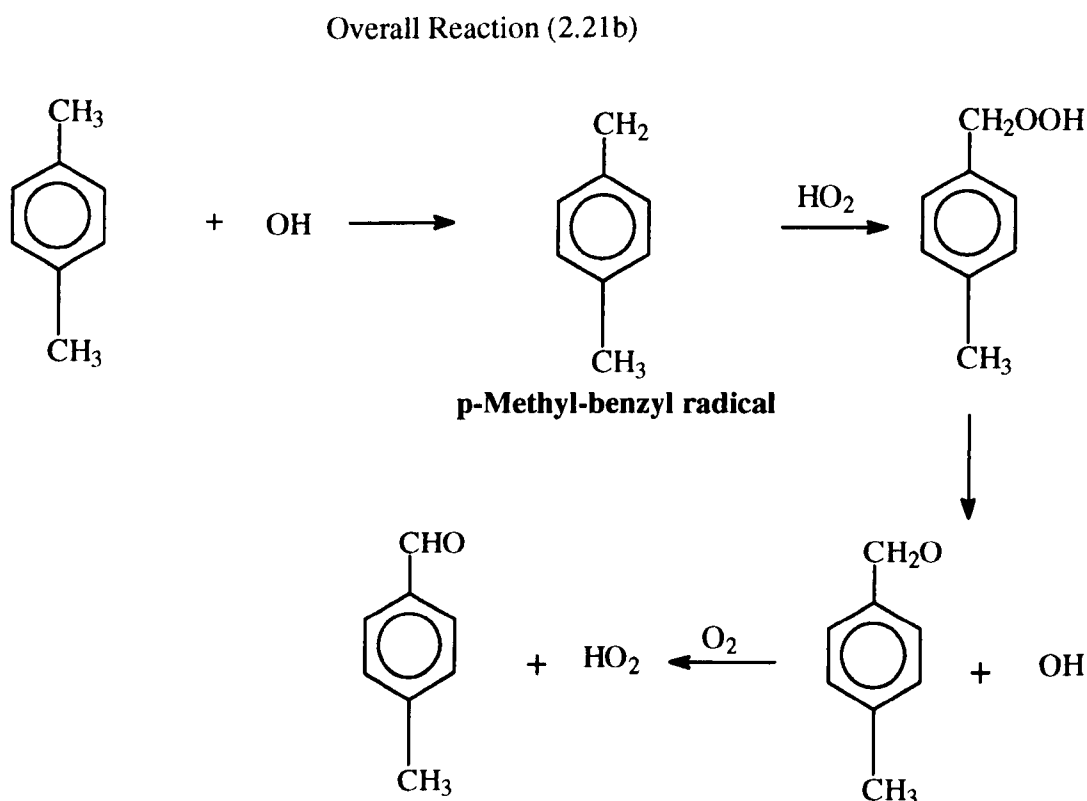
Emdee et al.⁴² examined the oxidation of the xylenes using a flow system between 820 and 926°C (using equivalence ratios from 0.47 to 1.7 of m- and p-xylene.), while Barnard and Sankey⁴³ used a conventional static system between 460 and 512°C using o-, m- and p-xylene individually. Nicovich et al.³⁹ studied the kinetics of the reaction of hydroxyl radicals with xylenes using the direct kinetic technique of flash photolysis-resonance fluorescence in the temperature range of 250-970K (Table 2.4).

Table 2. 4 : Summary of Rate Constants for the reactions between OH and some Aromatic Hydrocarbons.

Reaction	$T_l = 290 - 700 \text{ K}$	$T_h = 750 - 1000 \text{ K}$
	$k_l / \text{l mol}^{-1} \text{ s}^{-1}$	$k_h / \text{l mol}^{-1} \text{ s}^{-1}$
OH + Benzene \rightarrow Adduct ⁴⁰	$k_{296} = 7.83 \cdot 10^8$	
OH + Benzene \rightarrow Phenol + H ⁴¹		$k_{1000} = 6.49 \cdot 10^7$
OH + Benzene \rightarrow Phenyl + H ₂ O ⁷	$k_{400} = 1.30 \cdot 10^8$	$k_{1000} = 1.42 \cdot 10^9$
OH + Toluene \rightarrow Adduct ⁷	$k_{300} = 4.17 \cdot 10^9$	
OH + Toluene \rightarrow Benzyl + H ₂ O ⁷	$k_{300} = 3.60 \cdot 10^8$	$k_{1000} = 3.35 \cdot 10^9$
OH + p-Xylene \rightarrow Adduct ⁷	$k_{300} = 8.43 \cdot 10^9$	
OH + p-Xylene \rightarrow p-Methylbenzyl + H ₂ O ³⁹	$k_{500} = 1.94 \cdot 10^9$	$k_{970} = 7.03 \cdot 10^9$
OH + m-Xylene \rightarrow m-Methylbenzyl + H ₂ O ³⁹	$k_{500} = 1.72 \cdot 10^9$	$k_{970} = 6.61 \cdot 10^9$
OH + o-Xylene \rightarrow o-Methylbenzyl + H ₂ O ³⁹	$k_{500} = 2.01 \cdot 10^9$	$k_{970} = 7.57 \cdot 10^9$

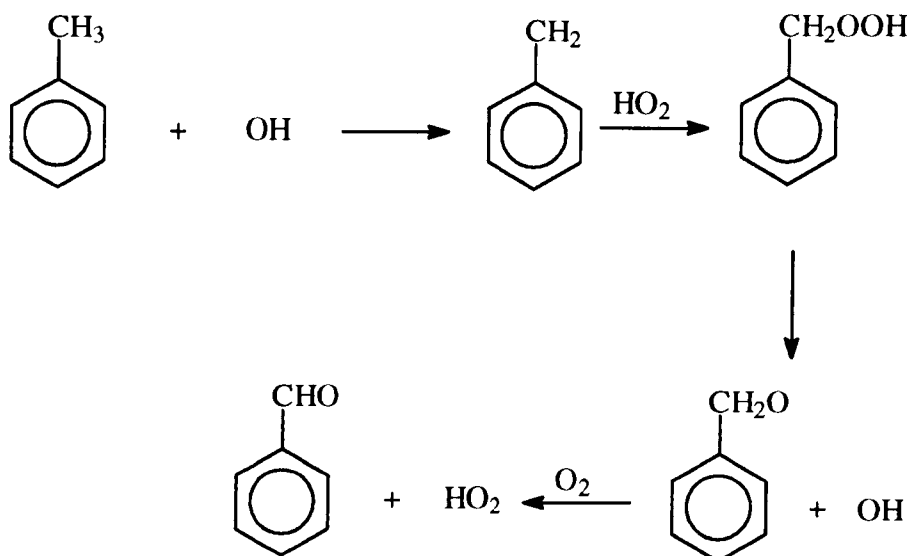
H abstraction from the side groups in the xylenes produces *methylbenzyl* radicals. The unpaired electron is delocalised into the ring with a stabilisation energy of about 50 kJ mol^{-1} , and hence the resulting radical is relatively inert towards O_2 so that it is consumed to a considerable degree through radical-radical reactions over a wide temperature range.

The reaction sequence below illustrates a major route for the removal of xylenes, (shown for p-xylene) at about 750K.



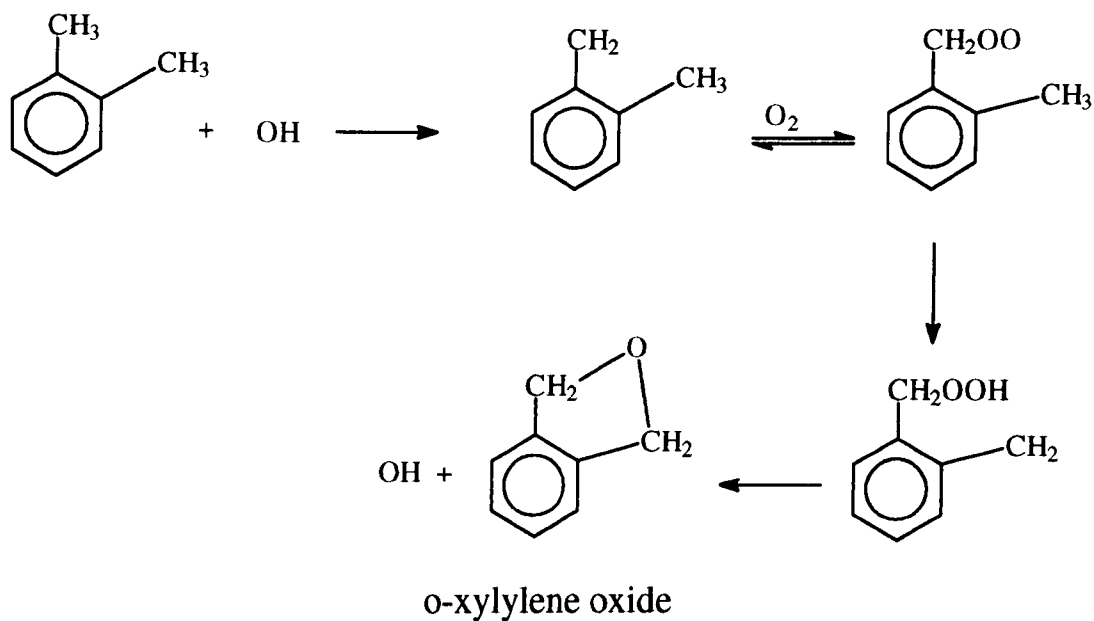
This mechanism is consistent with conclusions reached by Emdee et al.⁴², and by Baldwin, Scott and Walker⁴⁴ in the oxidation of toluene where benzaldehyde is a major initial product formed through the reaction sequence:

Overall Reaction (2.21c)

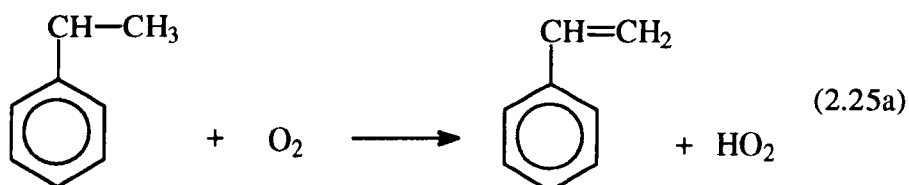


Another consideration is that it may be possible for xylene to react in a similar manner to that of propene where the *o*-heterocycle propylene oxide is produced⁴⁵. Barnard and Sankey⁴³ found this to be the case when examining the oxidation of *o*-xylene between 460 and 512°C, where *o*-xylylene oxide (phthalan) was found to be a major primary product. The scheme below indicates the likely mechanism for the formation of *o*-xylylene oxide from *o*-xylene. However, there has not been any evidence yet for the *m*- or *p*-xylylene oxides which are probably unstable due to ring strain.

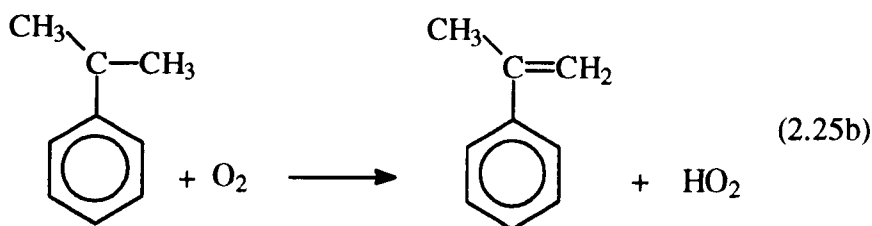
Overall Reaction (2.21d)



As might be expected, these mechanisms differ from those for ethylbenzene where large amounts of styrene are formed because the stabilised radical Ph-CH-CH_3 has a relatively easy reaction with O_2 ⁴⁶⁻⁴⁸:

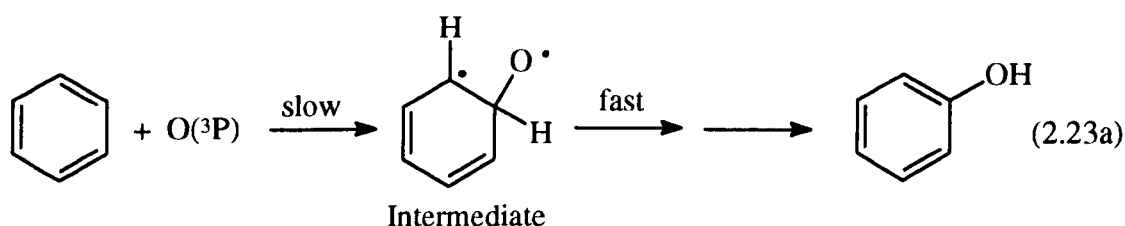


Similarly the $\text{Ph-C-(CH}_3)_2$ radical, formed from isopropylbenzene, reacts rapidly with O_2 ⁴⁹:



2.4.2. Reactions of O radicals with Aromatics.

Relatively little is known about the reactions of O radicals with aromatic hydrocarbons. Studies have been carried out at room temperature where detailed mechanistic information exists. However, only kinetic data are available at higher temperatures (above 400°C). At room temperature, it was observed that an electrophilic addition of an O radical occurs, which is similar to the reaction of OH with aromatics at low temperatures. The type of mechanism (2.23a) is related to a proposed^{50,51} mechanism for the reaction of O(³P) with alkenes and to one of tentative nature⁵² for O(³P) oxidation of benzene. The intermediate diradical is presumed to be in a *triplet state*. Collapse of the intermediate might occur via a simple intramolecular rearrangement to produce phenol.



The mechanism may be more complicated, as in the case of 1,2,3-trimethylbenzene + O(³P), when the major product is 2,6-dimethylphenol rather than 2,6-dimethylanisole, which is what might be expected if a simple 1,2-methyl shift occurred in the intermediate (reaction 2.23b)³⁸.

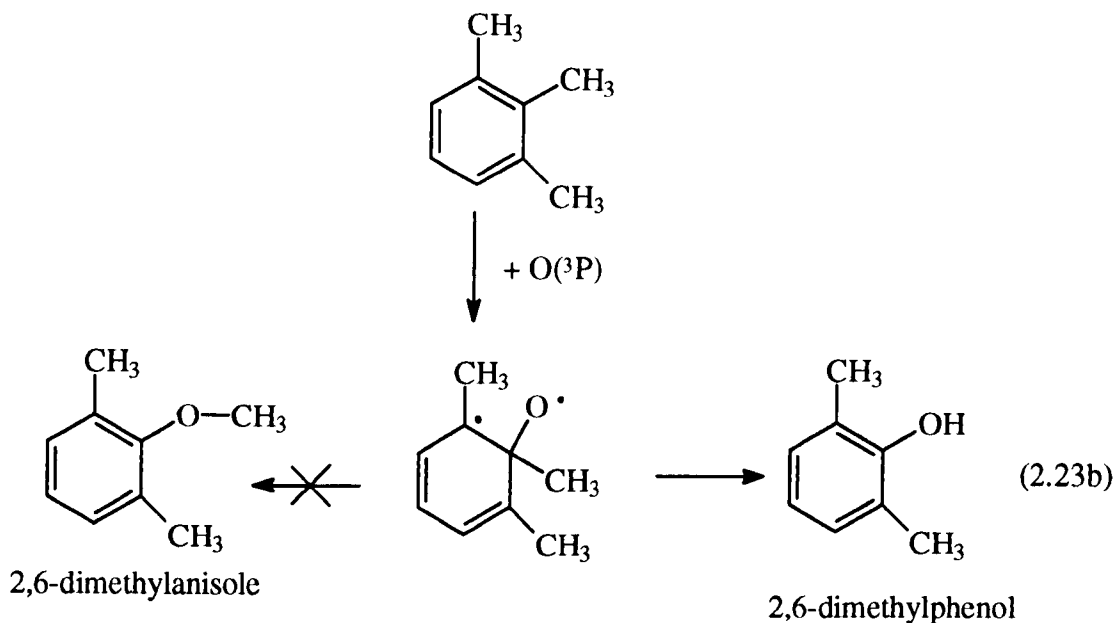
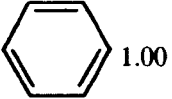
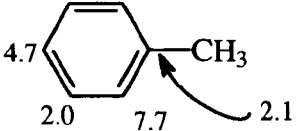
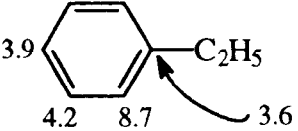
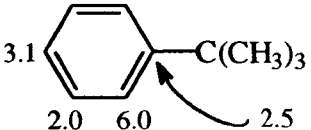
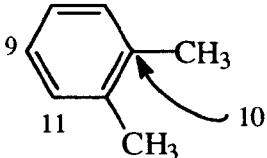
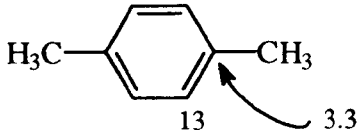
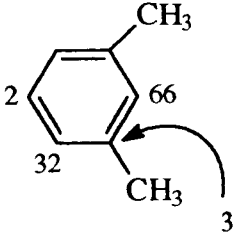
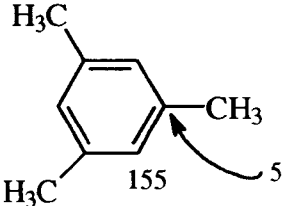
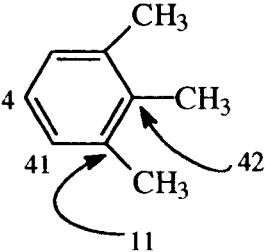
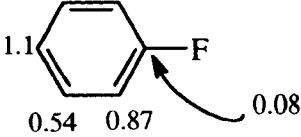
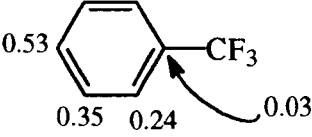
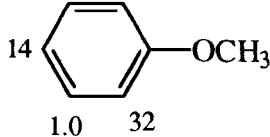


Table 2.5 illustrates the partial rate factors for the formation of phenols with atomic oxygen at 30°C³⁸ for a selection of aromatic hydrocarbons and how the degree of attack is affected by the position of the methyl groups. The degree of attack at a ring C-H bond will be determined by the different inductive/directive effects of the side chain substituents.

For the mono-substituted aromatics, the main position for substitution is *ortho* to the side chain which is in direct contrast to the effect of -CH₃ in electrophilic aromatic substitution reactions. The size of the side chain, ranging from -CH₃ to -C₂H₅ to -C(CH₃)₃, does not overly affect the relative proportion of attack at the ring.

It is the position of the side-chain substituents in the di- and tri- alkyl substituted benzenes that plays the important part in determining the relative degree of attack, and hence the relative proportion of the phenols formed. Since methyl groups are *ortho* directing it is clear to see why in the case of 1,3,5-trimethylbenzene the main position of attack will be between the methyl groups despite any steric hindrance.

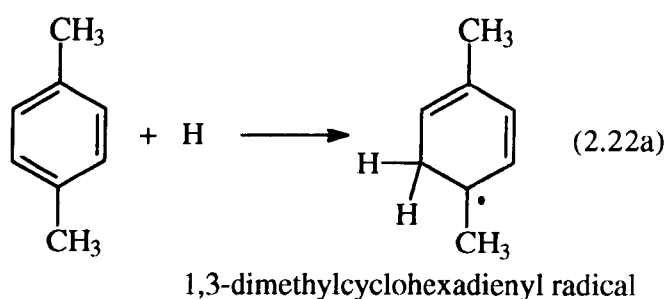
Table 2.5 : Partial Rate Factors for the Formation of Phenols with Atomic Oxygen at 30°C³⁸.

 <p>1.00</p>	 <p>4.7 2.0 7.7 2.1</p>	 <p>3.9 4.2 8.7 3.6</p>
 <p>3.1 2.0 6.0 2.5</p>	 <p>9 11 10 10</p>	 <p>13 13 3.3</p>
 <p>2 66 32 3 3</p>	 <p>155 5 5</p>	 <p>4 42 41 11 11</p>
 <p>1.1 0.54 0.87 0.08</p>	 <p>0.53 0.35 0.24 0.03</p>	 <p>14 1.0 32</p>

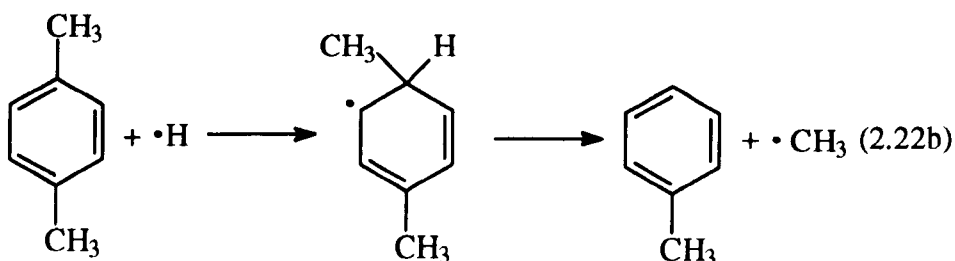
In the case where fluorine or a fluorinated alkyl group is the substituent, there is a noticeable alteration in the position of preference for addition in that the preferred product is likely to be the *para* product, in contrast to the situation for simple alkyl groups.

2.4.3. Reactions of H atoms with Aromatics.

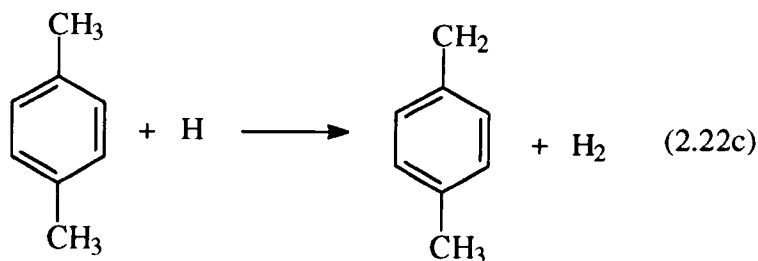
The reactions between H radicals and small aromatic hydrocarbons appear to show the same mechanistic features as observed with OH radicals. The mechanism at low temperatures (ca 298K) follows the addition of H to the aromatic ring⁵³ (Reaction 2.22a is one example)



Another possibility, which also occurs at high temperatures, is addition to a carbon atom attached to (say) a CH₃ group, which then becomes displaced, (Reaction 2.22b).



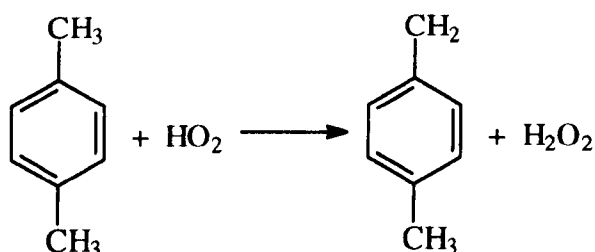
H abstraction from a side chain is likely to become increasingly predominant at higher temperatures (>400K) (Reaction 2.22c). Here a similar reaction to that for OH + xylene at high temperatures occurs.



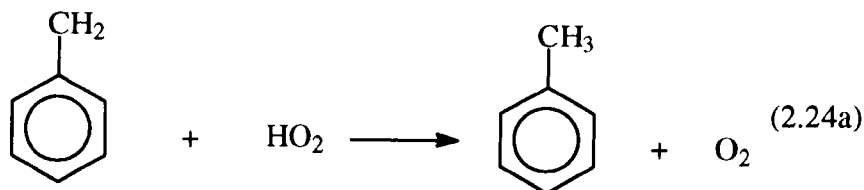
This reaction is facilitated by the weakness in the C-H bonds caused by electron delocalisation in the methylbenzyl radicals. At very high temperatures (>1000K) H atom abstraction from the ring will become noticeable.

2.4.4. Reactions of HO₂ with Aromatics.

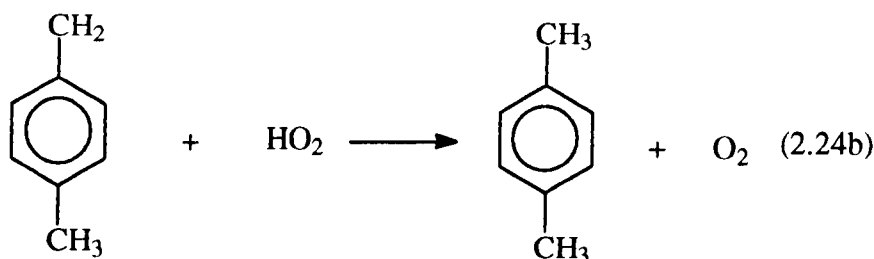
No data are available for the reactions between aromatic hydrocarbons and HO₂ radicals although at high temperatures H atom abstraction will become important.



The more common reactions involving HO₂ are those involving radical-radical processes; in the case of toluene this would be with *benzyl* radicals. With benzyl and methylbenzyl radicals, the lack of a fast reaction with O₂ is responsible for the different oxidation chemistry observed with toluene and the xylene when compared with other aromatics and alkanes. This has been illustrated earlier in the formation of aldehydes. Further, as termination reactions such as



and

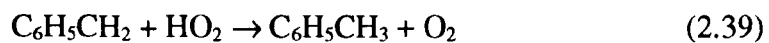
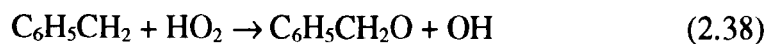


are also very important the chain length will tend to be low, thus reducing markedly the overall rate of reaction. The reaction where the *parent hydrocarbon* is regenerated as above will be considered in more detail in Chapter 6 (The decomposition of neopentylbenzene.)

2.5. The Oxidation Chemistry of Benzyl Radicals.

Benzyl and related radicals are important in the combustion chemistry of aromatics. As resonance-stabilised species they have a limited range of reactions so that radical-radical reactions increase in importance. This is particularly true for benzyl radicals which are the major initial species produced in the oxidation of toluene⁵⁴. Although rate data are available for benzyl reaction with O₂⁵⁵, only limited rate data are available for benzyl reactions with HO₂, all at relatively high temperatures^{54,56} of ca. 1000K and above. With more and more computer simulation of combustion processes, it is necessary to have rate data available for reactions across as wide a temperature range as possible.

An important consideration is the relative rate of propagation/branching (2.38) and termination (2.39) because this is important in determining the rate of oxidation of toluene.



There are no data currently available for the reactions of benzyl radicals with HO_2 in the 500°C temperature range. A more detailed appraisal of the oxidation chemistry of benzyl radicals will be given in Chapter 6.

2.6. References.

- ¹ Hinshelwood C.N., *Proc. Roy. Soc. A.*, **188**, 1, (1947).
- ² Semenov N.N., *Some Problems of Chemical Kinetics and Reactivity*, Pergamon Press, London, (1958).
- ³ Egerton A and Warren D.R., *Proc Roy. Soc. A.*, **204**, 465, (1951).
- ⁴ Baldwin R.R. and Mayor L., *Trans. Faraday Soc.*, **56**, 103, (1960).
- ⁵ Baldwin R.R. and Mayor L., *Trans. Faraday Soc.*, **56**, 80, (1960).
- ⁶ Baldwin R.R., Mayor L. and Doran P., *Trans. Faraday Soc.*, **56**, 93, (1960).
- ⁷ Baulch D.L., Cobos C.J., Cox R.A., Esser C., Frank P., Just Th., Kerr J.A., Pilling M.J., Troe J., Walker R.W. and Warnatz J., *J. Phys. Chem. Ref. Data.*, **21**, 411, (1992).
- ⁸ Baldwin R.R. Jackson D., Walker R.W. and Webster S.J., *Trans. Faraday Soc.*, **63**, 1676, (1967).
- ⁹ Baldwin R.R., Brattan D., *Eighth International Symposium on Combustion*, **8**, 110, (1962).
- ¹⁰ Baker R.R., Baldwin R.R., Fuller A.R. and Walker R.W. *J. Chem. Soc. Faraday Trans. 1*, **71**, 736 (1975).
- ¹¹ Gruver J.T. and Calvert J.C., *J. Am. Chem. Soc.*, **78**, 5208, (1956).
- ¹² Tsang W., *J. Am. Chem. Soc.*, **107**, 2872, (1985).
- ¹³ Dean A.A., *J. Phys. Chem.*, **89**, 4600, (1985).
- ¹⁴ Baker R.R., Baldwin R.R. and Walker R.W. *J. Chem. Soc. Chem. Comm.*, **23**, 1382, (1969).

- ¹⁵ Baker R.R., Baldwin R.R. and Walker R.W., *Symp. Int. Combust. Proc.*, **13**, 291, (1971).
- ¹⁶ Baldwin R.R. and Walker R. W., *J. Chem. Soc. Faraday Trans. 1*, **75**, 140, (1979).
- ¹⁷ Baldwin R.R., Hisham M.W.M. and Walker R.W., *J. Chem. Soc. Faraday Trans. 1*, **78**, 1615, (1982).
- ¹⁸ Benson S.W. and Shaw R., in *Organic Peroxides*, ed. Swern D. (Wiley, New York, 1970), vol. 1, p. 105.
- ¹⁹ Hughes K.J., Halford-Maw P.A., Pilling M.J. and Turanyi T., *Proc. Int. Symp. Combustion*, **24**, 645, (1992).
- ²⁰ Benson S.W., "*Thermochemical Kinetics*", Wiley, New York, (1976).
- ²¹ Baker R.R., Baldwin R.R. and Walker R.W., *J. Chem. Soc. Faraday Trans.*, **71**, 756, (1975).
- ²² Walker J.A. and Tsang W., *Int. J. Chem. Kinet.*, **11**, 867, (1979).
- ²³ Tsang, W. and Hampson, R.F., *J. Phys. Chem. Ref. Data.*, **15**, 1087, (1986).
- ²⁴ Atri G.M., Baldwin R.R., Evans G.A. and Walker R.W., *J. Chem. Soc. Faraday Trans I.*, **78**, 366 (1978).
- ²⁵ Evans G.A. and Walker R.W., *J. Chem. Soc. Faraday Trans I.*, **75**, 1458, (1979).
- ²⁶ Baldwin, R.R., Drewery G.G. and Walker R.W., *J. Chem. Soc. Faraday Trans. 1*, **80**, 2827, (1984).
- ²⁷ Baldwin, R.R., Cleugh C.J. and Walker R.W., *J. Chem. Soc. Faraday Trans. 1*, **72**, 1715, (1976).
- ²⁸ Baldwin, R.R., Walker R.W. and Walker R.W., *J. Chem. Soc. Faraday Trans. 1*, **76**, 825, (1980).

- ²⁹ Baldwin, R.R., Hisham M.W.M., Keen A. and Walker R.W., *J. Chem. Soc. Faraday Trans. 1*, **78**, 1165, (1982).
- ³⁰ Baldwin R.R., Fuller A.R., Longthorn D. and Walker R.W. *Combust. Inst. European Symp.*, Academic Press, London, **1**, 70, (1973).
- ³¹ Baldwin R.R., Dean C.E., Honeyman M.R. and Walker R.W., *J. Chem. Soc. Faraday Trans. 1*, **82**, 89, (1986).
- ³² Lodhi Z.H. and Walker R.W., *J. Chem. Soc Faraday Trans. 1*, **87**, 681, (1991).
- ³³ Lodhi Z.H. and Walker R.W., *J. Chem. Soc Faraday Trans. 1*, **87**, 2361, (1991).
- ³⁴ Baldwin, R.R., Lodhi Z.H., Stothard N. and Walker R.W., *Symp. Int. Combust. Proc.*, **23**, 123, (1991).
- ³⁵ Rossi M., King K.D. and Golden D.M., *J. Amer. Chem. Soc.*, **101**, 1223, (1979).
- ³⁶ Wright F.J., *J. Phys. Chem.*, **64**, 1944, (1960).
- ³⁷ Wright F.J., *J. Phys. Chem.*, **66**, 2023, (1962).
- ³⁸ Grovenstein E. Jr., and Mosher A.J., *J. Amer. Chem. Soc.*, **92**, 3810, (1970).
- ³⁹ Nicovich J.M., Thompson R.L. and Ravishankara A.R., *J. Phys. Chem.*, **85**, 2913, (1981).
- ⁴⁰ Wallington T.J., Neuman D.M. and Kurylo M.J., *Int. J. Chem. Kinet.*, **19**, 725, (1987).
- ⁴¹ He Y.Z., Mallard W.G. and Tsang, W., *J. Phys. Chem.*, **92**, 2196, (1988).
- ⁴² Emdee J.L., Brezinsky K., and Glassman I., *J. Phys. Chem.*, **95**, 1626, (1991).
- ⁴³ Barnard J.A., and Sankey B.M., *Comb. Flame.*, **12**, 345, (1968).
- ⁴⁴ Baldwin R.R., Scott M. and Walker R.W., *Twenty-first Symposium (International) on Combustion/The Combustion Institute*, 991, (1986).

- ⁴⁵ Baldwin R. R., Hisham M. W. M. and Walker R. W., *Symp. Int. Combust. Proc.*, **20**, 743, (1985).
- ⁴⁶ Venkat C., Brezinsky K. and Glassman I., *Symp. Int. Combust. Proc.*, **19**, 143, (1982).
- ⁴⁷ Newitt D.M. and Burgoyne J.H., *Proc. Roy. Soc. London A.*, **153**, 448, (1936).
- ⁴⁸ Burgoyne J.H., *Proc. Roy. Soc London A.*, **175**, 539, (1940).
- ⁴⁹ Shafikov N.Ya., Denisova L.N. and Dinsou E.T., *Kinet. Catal.*, **16**, 872, (1975).
- ⁵⁰ Cvetanovic R.J., *Advan. Photochem.*, **1**, 115, (1963).
- ⁵¹ Klein R. and Sheer M.D., *J. Phys. Chem.*, **73**, 1598, (1969).
- ⁵² Boocock G. and Cvetanovic R.J. *Can. J. Chem.*, **39**, 2436, (1961); Jones G.H.R. and Cvetanovic R.J. *ibid.*, **39**, 2444, (1961).
- ⁵³ Ackerman L., Hippler , Pagsburg P., Reihls C. and Tore J., *J. Phys. Chem.*, **94**, 5247, (1990).
- ⁵⁴ Brezinsky K., Litzinger T. A. and Glassman I., *Int. J. Chem. Kinet.*, **16**, 1053, (1984).
- ⁵⁵ Fenter F. F., Noziere B., Caralp F and Lezclaux R., *Int. J. Chem. Kinet.*, **26**, 171, (1994).
- ⁵⁶ Hippler H., Reihls C. and Troe J., *Symp. Int. Combust. Proc.*, **23**, 31, (1991).

Chapter 3.

Experimental Procedure.

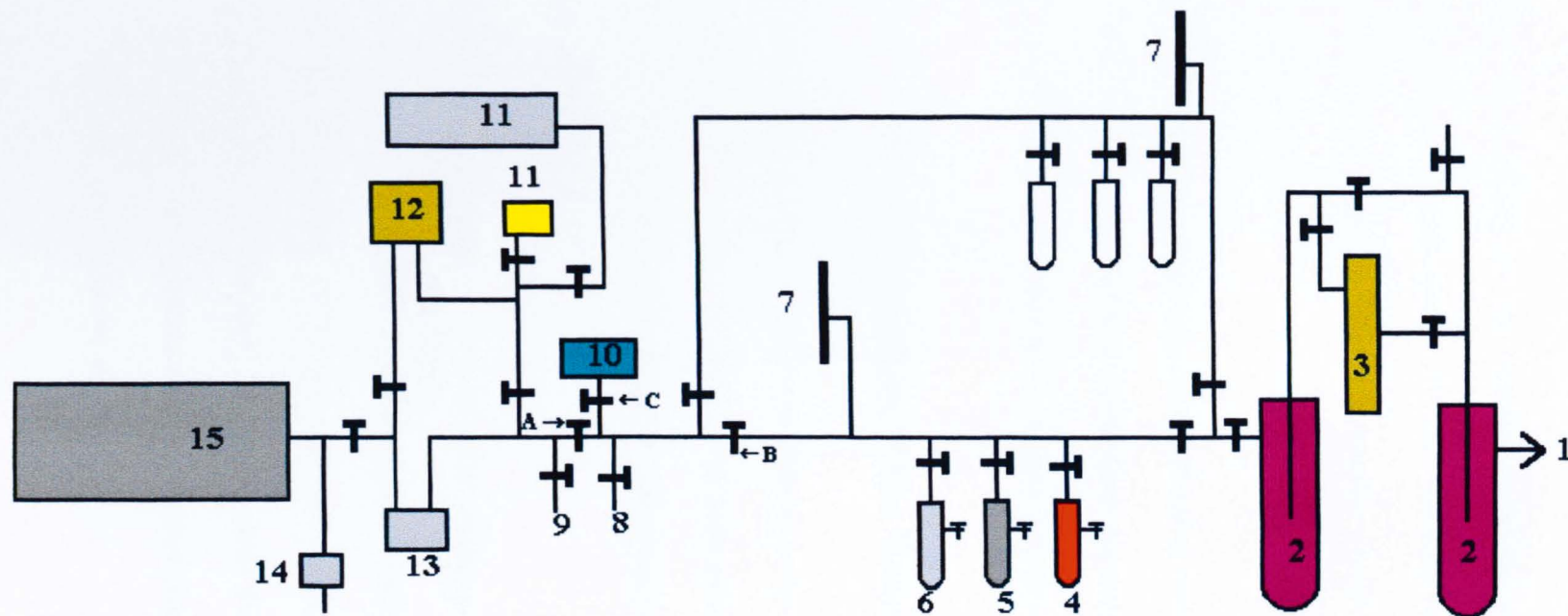
3.1. The Apparatus.

The work was carried out on a conventional static apparatus, as shown in Figure 3.1. The apparatus was constructed from Pyrex glass and fitted with greaseless P.T.F.E Young's taps to avoid the known problems of adsorption of organic compounds on tap grease. Reaction mixtures were prepared in the mixing bulb [MB] in order to achieve a homogeneous mixture before admission into the reaction vessel.

The system could be evacuated to better than 10^{-3} Torr in about 3 minutes using an Edwards Speedivac silicone-oil-vapour diffusion pump backed by an Edwards 2-stage rotary oil pump and assisted by liquid nitrogen cold traps to prevent any water or organic compounds contaminating the pumps or from being drawn back into the apparatus. The degree of evacuation was measured using an Edwards Pirani 14 gauge coupled to a Pirani G5C-2 head.

The main body of the apparatus consisted of two parallel sections of Pyrex tubing. The main line was constructed with outer diameter = 22mm, and internal diameter = 18 mm and the back line with outer diameter = 13mm, internal diameter = 9mm. The main line had inlets for hydrogen, nitrogen and oxygen gases and this design feature was aimed at zero contamination of these gases by any additives used. The back line contained three traps which could be used to hold liquid additive samples. However, in this work, the

Figure 3. 1 : Diagram Of The Combustion Vacuum Line.



- | | | |
|---------------------|------------------------------|----------------------------|
| 1... To oil pump | 6... Oxygen inlet | 11... Vacuum reservoirs |
| 2... Cold Traps | 7... Manometers | 12... Pressure transducer |
| 3... Diffusion pump | 8... Mixing bulb sample port | 13... Valve1 - V1 |
| 4... Hydrogen inlet | 9... Additive addition port | 14... Valve2 - V2 |
| 5... Nitrogen inlet | 10... Mixing bulb - MB | 15... Reaction vessel - RV |

back line was not used to any great extent due to the low vapour pressures of the hydrocarbons used; this will become clearer later in the thesis.

Admission and sampling of the reaction mixtures from the reaction vessel were controlled by two Edwards (model PVA5E) solenoid valves (V1 and V2). In order to minimise the *dead space* between the reaction vessel and the valves, 3mm internal diameter glass capillary tubing was used. The *dead volume* was measured as 9%.

Gas pressures in the apparatus were measured using one of two methods. For pressures greater than 50 Torr, conventional double-limb mercury manometers were used. For pressures less than 50 Torr a calibrated pressure transducer was used (see section 3.4).

3.2. Preparation of the Reaction Vessel.

The reaction vessel was made from Pyrex glass to a size of 250mm in length and 51mm internal diameter. The vessel was fitted with a glass greaseless tap in order to permit the admission and removal of gaseous reagents. The vessel was thoroughly cleaned prior to coating with boric acid.

The cleaning process consisted of sequential washings with distilled water, absolute ethanol, distilled water, tetrachloromethane (carbon tetrachloride), absolute ethanol and several washings with water. The vessel was then one-third filled with fuming nitric acid and heated gently for approximately 30 minutes until the nitric acid had become a pale yellow colour. Finally the vessel was washed several times with distilled water to ensure all traces of the nitric acid had been removed.

A saturated solution of Analar boric acid in 50:50 distilled water : absolute ethanol was made up and a volume of about 20-30cm³ was admitted to the vessel. The liquid was removed by heating and rotating the vessel under vacuum to facilitate the formation of an even coating of white boric acid on the surface of the vessel. The vessel was evacuated using a water pump to remove all visible traces of solvent before being attached to the main apparatus. The vessel was then evacuated for several hours to ensure all final traces of solvent had been removed. Once the vessel was placed in the furnace at 500°C the coating of boric acid became translucent.

The vessel was then 'aged' by repeatedly carrying out explosions and slow reactions with a mixture of 140 Torr hydrogen and 360 Torr oxygen in the reaction vessel. In order to age a newly-coated vessel between 200 and 300 reactions were generally required before reproducible maximum reaction rates were obtained of 13.5 Torr min⁻¹ at 500°C for the above mixture in agreement with the literature value¹. Once this rate had been reached the vessel gave absolutely reproducible results, and it was considered that the vessel surface was absolutely inert to the key species in the reaction, namely peroxy radicals and peroxides.

The lifetime of a vessel in the 'aged' state was generally several months at least. The condition of the vessel was checked every day before any new experimental runs were carried out by carrying out first a couple of second limit explosions using the above mixture and secondly two slow reactions.

3.3. The Reaction Furnace.

The furnace containing the reaction vessel consisted of a well insulated silica tube heated by three independent windings of electrical tape. The current to each winding was controlled by changing the setting on a **Variac** variable resistor. Six **Variac** resistors were used, connected as parallel pairs to the furnace (Figure 3.2). Each pair of resistors controlled the current to one of the three windings. The settings on each pair of resistors was such that there was about a 10% difference in current between the pair. The *background current* sets the lowest limit for the temperature for the windings. The *main current* sets the upper limit for the temperature of each winding. Switching between the resistors was controlled by a Foster Cambridge Ltd GTR210 temperature controller in conjunction with a number of thermocouples. The thermocouples connected directly to the temperature controller were mounted in the furnace such that it was possible to set the overall temperature of the furnace and allow switching between the **Variacs** to maintain a constant temperature during a day and an even temperature profile to be reached along the length of the reaction vessel (Figure 3.3). The absolute temperature was held constant to about $\pm 0.5^{\circ}\text{C}$ on any day with a maximum temperature variation of $\pm 2^{\circ}\text{C}$ along the length of the vessel.

The actual furnace temperature was monitored by two type k thermocouples connected to a ten-channel Comark Digital Thermometer. One thermocouple was fixed close to the centre of the reaction vessel while the second could be moved along the length of the furnace in order to monitor the temperature profile.

Figure 3. 2 : Diagram Of Furnace Temperature Control System.

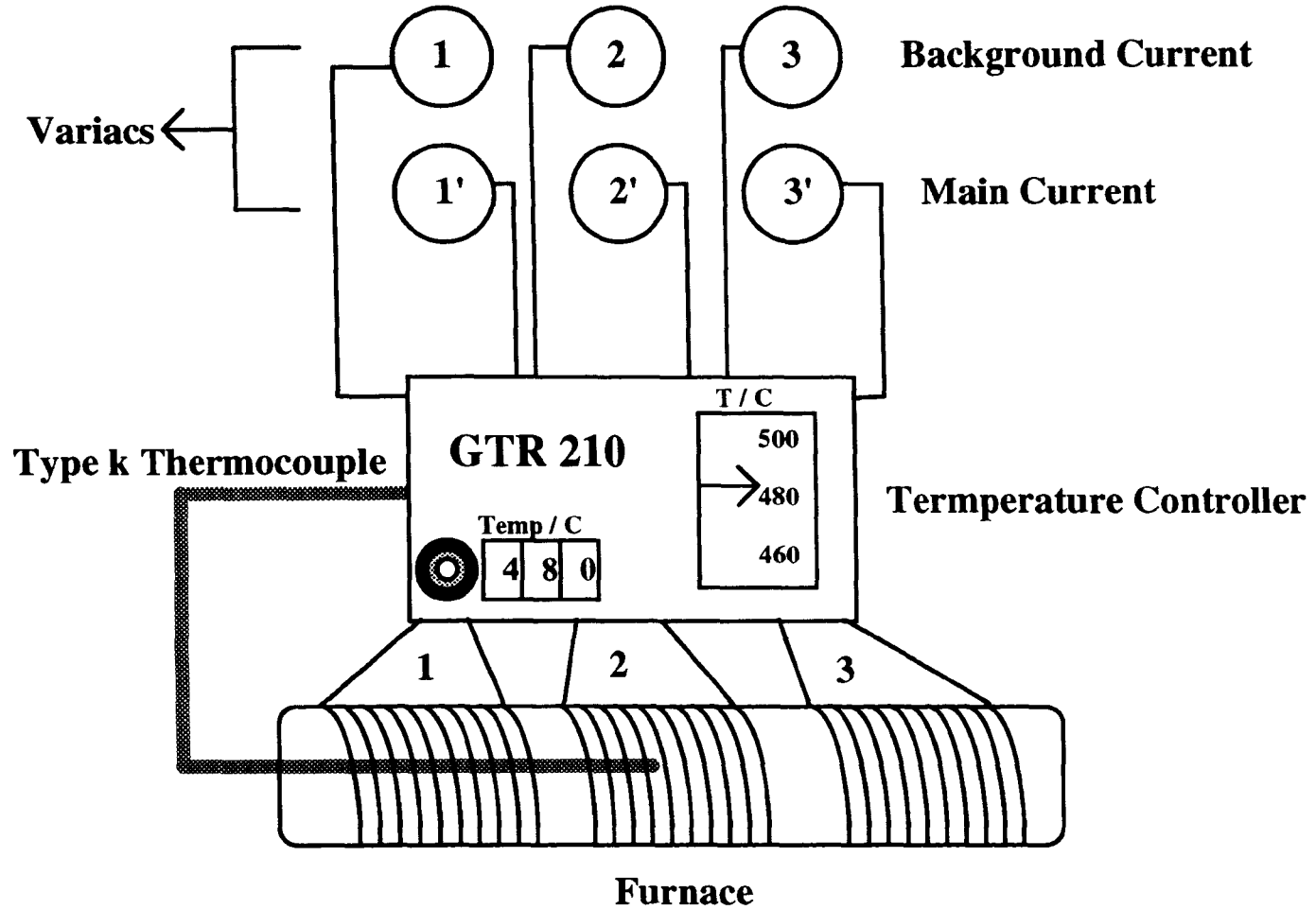
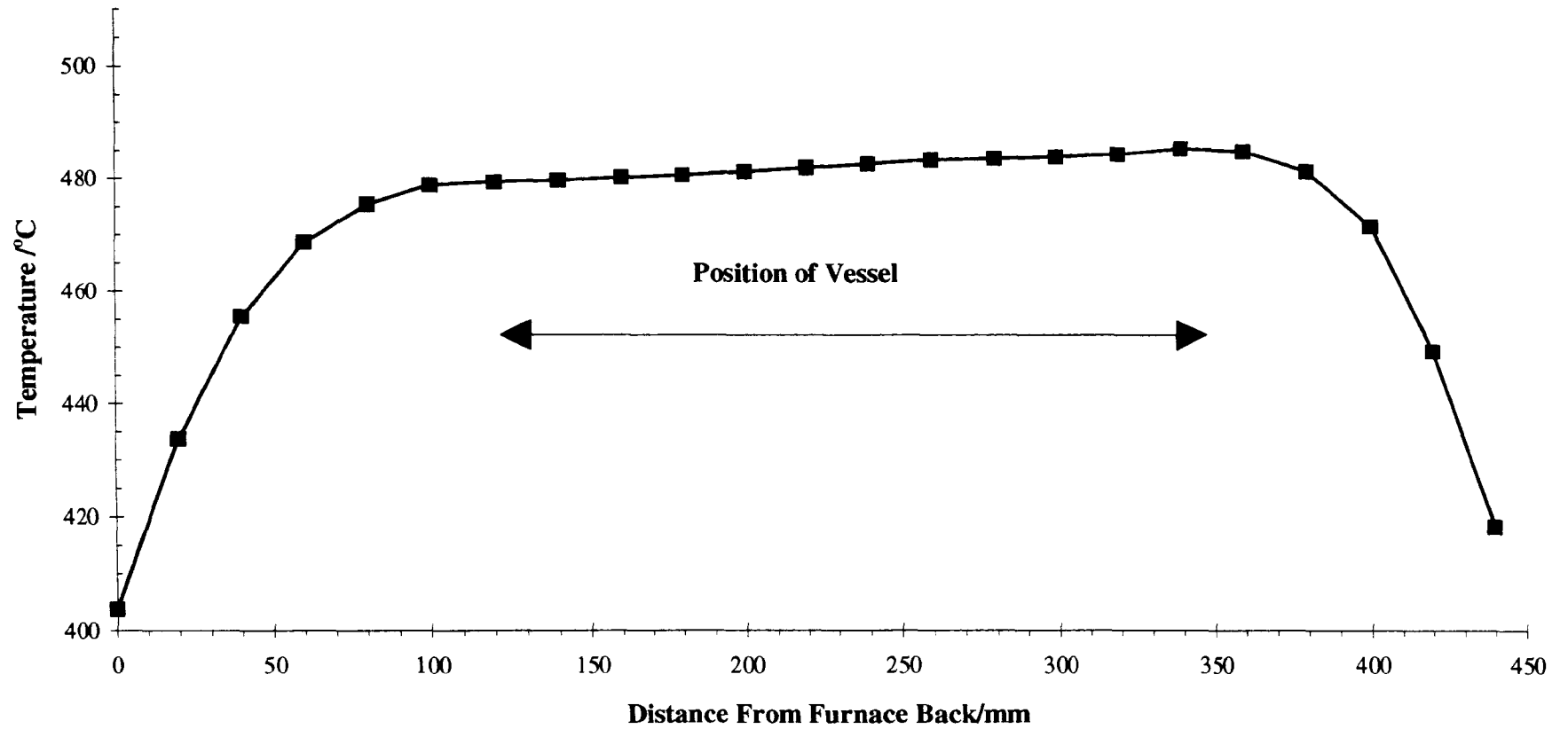


Figure 3.3

Furnace Temperature Profile



3.4. The Pressure Transducer.

A Southern Electronics SE1150 differential pressure transducer, and SE905 Transducer/Converter together with a Chessel chart recorder were used to measure out small pressures (<50 Torr) and to record pressure changes during reaction. The calibration was achieved by connecting a di-n-butyl phthalate manometer to one side of the transducer and leaving the other side open to atmospheric pressure. By application of a known pressure difference across the transducer, and recording the deflection of the chart recorder for the given attenuation and chart recorder settings it was possible to monitor pressures from about 2 to 160 Torr full-scale deflection (FSD) on the chart recorder. For FSD, the error even for 2 Torr does not exceed 1%. The full-scale deflection on the chart recorder for a given pressure in mm di-n-butyl phthalate could be converted to Torr using the simple equation below²

$$\text{FSD / Torr} = \frac{\Delta p / \text{mm Phthalate}}{\text{Deflection / divisions}} * 100 * \frac{\rho_{\text{Mercury}}}{\rho_{\text{Phthalate}}}$$

Δp is the pressure applied in mm of di-n-butyl phthalate and $\rho_{\text{Mercury}}/\rho_{\text{Phthalate}}$ is the relative density of mercury and di-n-butyl phthalate at the temperature at which the calibration was carried out (Figure 3.4). The calibration graphs are shown in Figures 3.5 - 3.11. The FSD was checked periodically and found to be reproducible to better than 1% over the whole period of the work. The results are summarised in Table 3.1. The attenuation number was the setting on the transducer converter and the mV values represent the full scale deflection setting on the chart recorder. In all cases an excellent linear response was observed.

Figure 3.4

Plot of Variation of Relative Density of Mercury to Di-n-butyl phthalate vs. Temperature

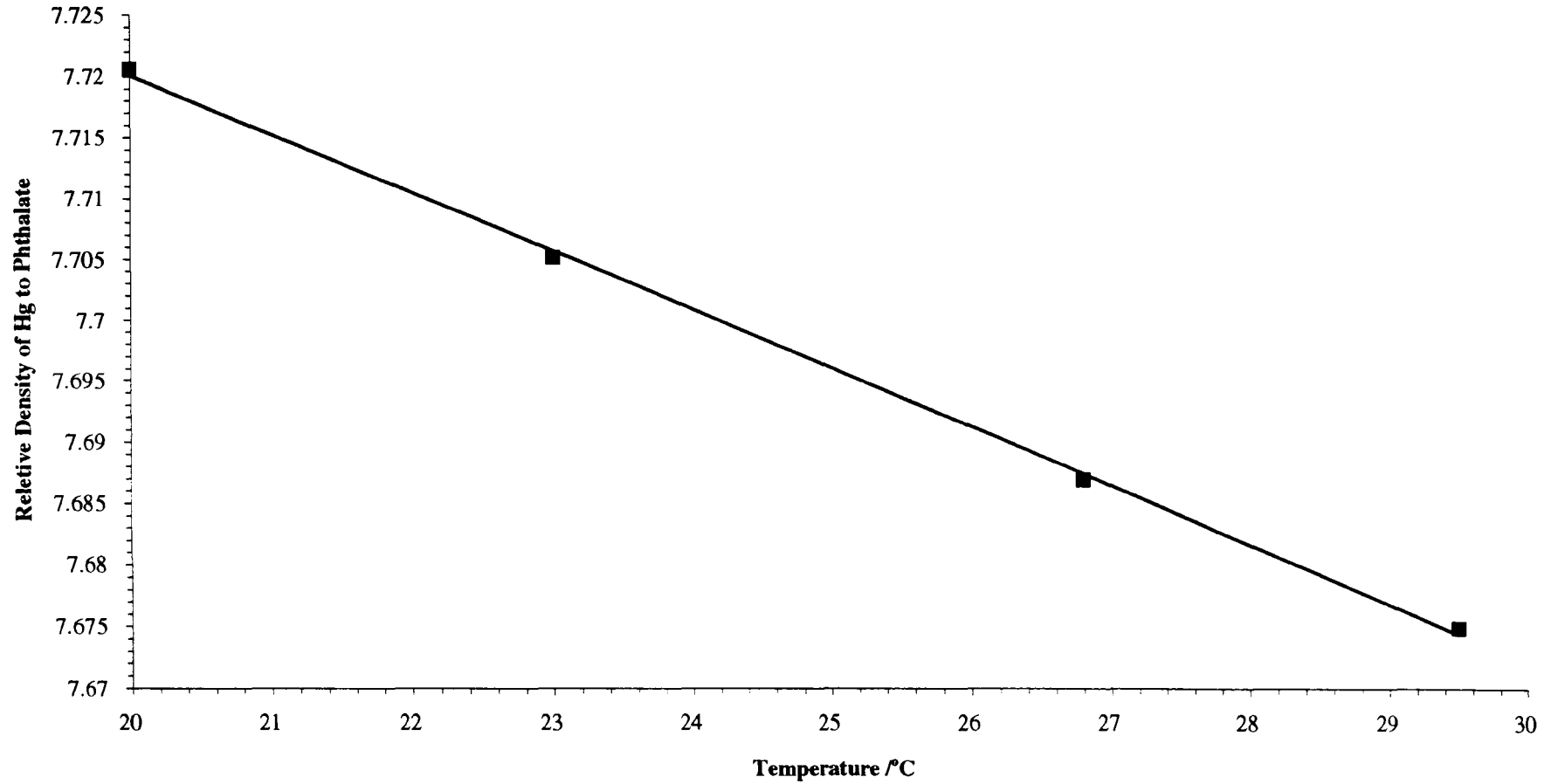


Figure 3.5[®]

Plot of Pressure of Di-n-butyl phthalate vs. Chart Recorder Deflection For Pressure Transducer Calibration

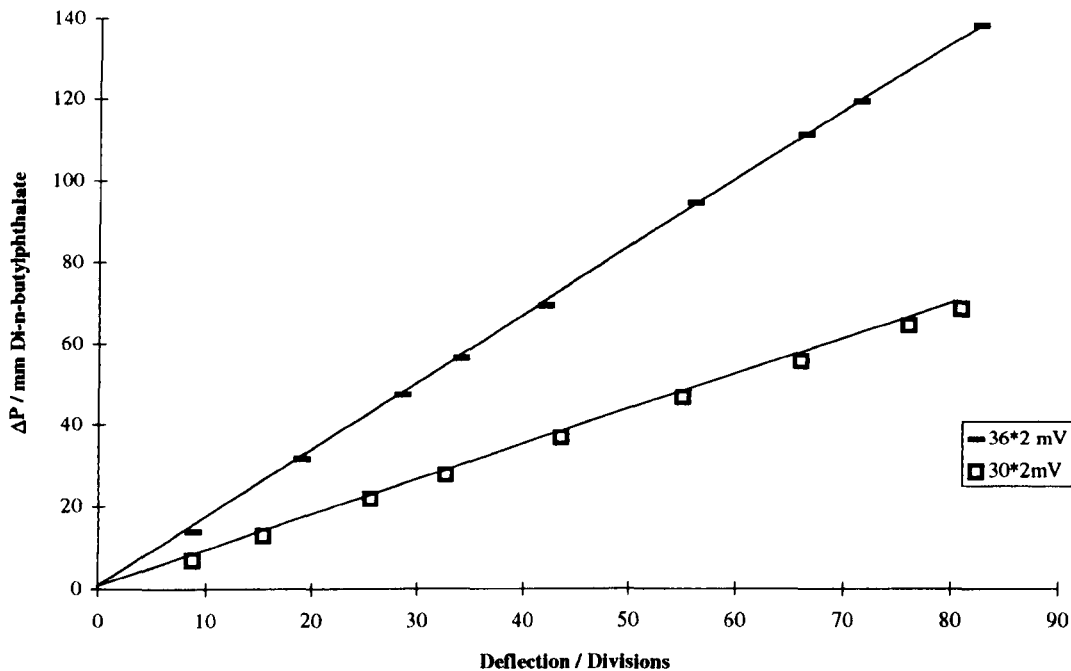
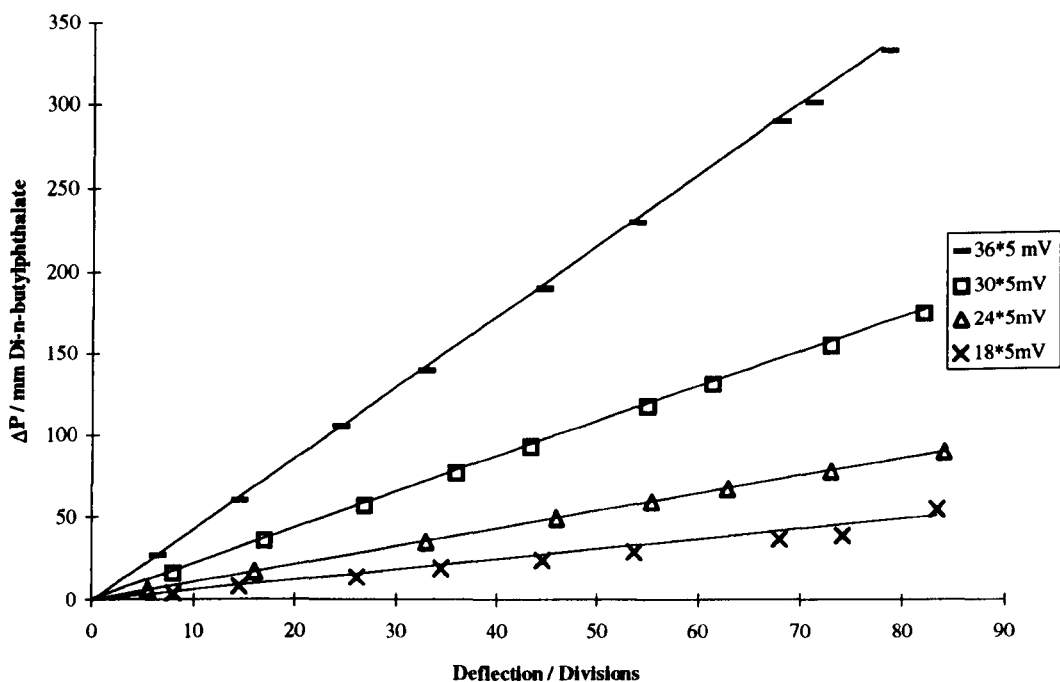


Figure 3.6

Plot of Pressure of Di-n-butyl phthalate vs. Chart Recorder Deflection For Pressure Transducer Calibration



[®] Legend corresponds to 'Transducer/Converter Setting' * 'Chart Recorder Setting'. See Table 3.1.

Figure 3. 7

Plot of Pressure of Di-n-butyl phthalate vs. Chart Recorder Deflection For Pressure Transducer Calibration

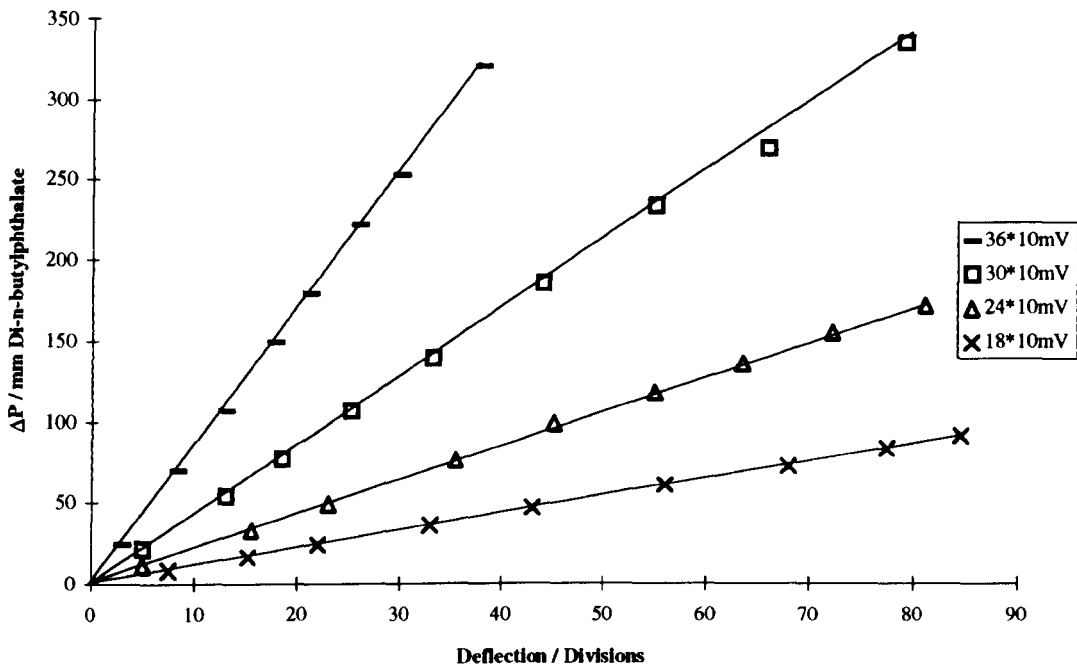


Figure 3. 8

Plot of Pressure of Di-n-butyl phthalate vs. Chart Recorder Deflection For Pressure Transducer Calibration

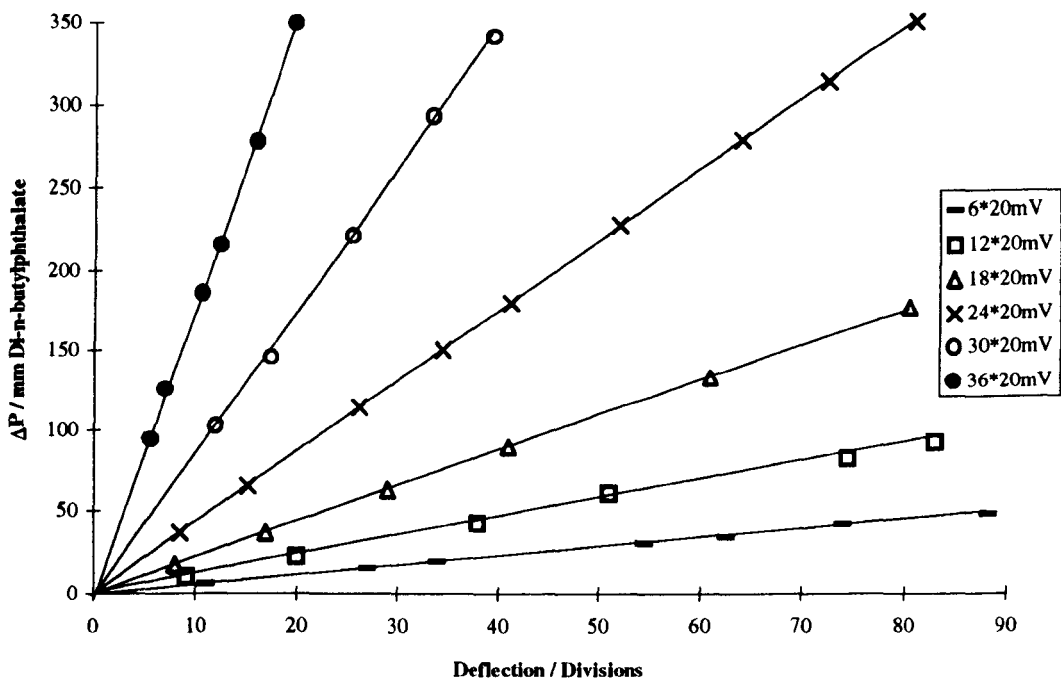


Figure 3. 9

Plot of Pressure of Di-n-butyl phthalate vs. Chart Recorder Deflection For Pressure Transducer Calibration

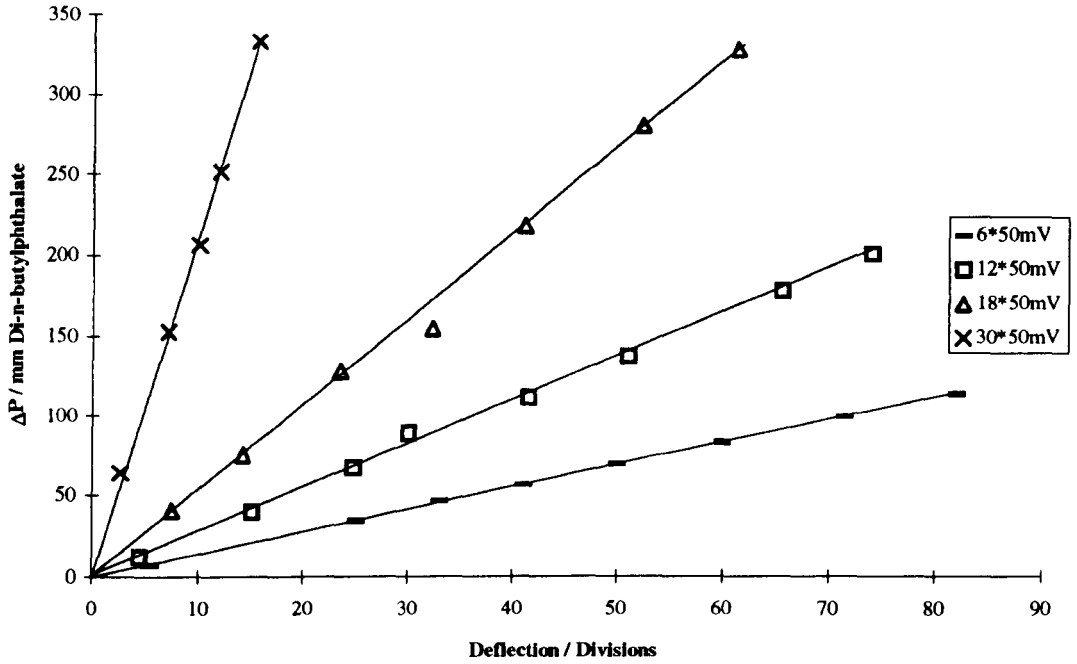


Figure 3. 10

Plot of Pressure of Di-n-butyl phthalate vs. Chart Recorder Deflection For Pressure Transducer Calibration

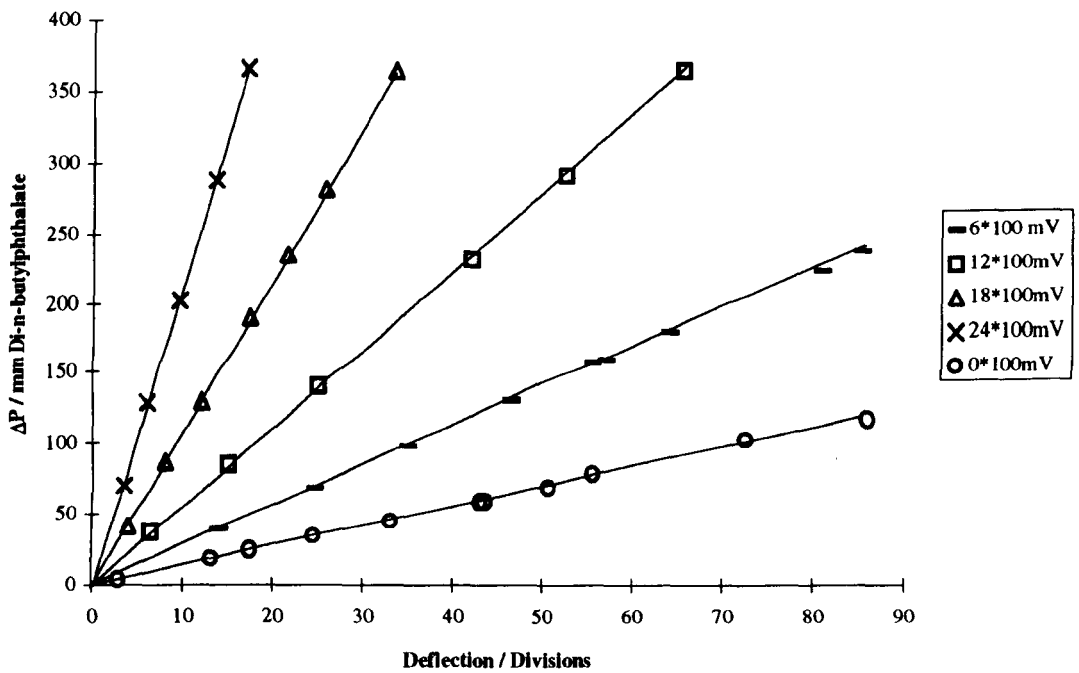


Figure 3.11

Plot of Pressure of Di-n-butyl phthalate vs. Chart Recorder Deflection For Pressure Transducer Calibration

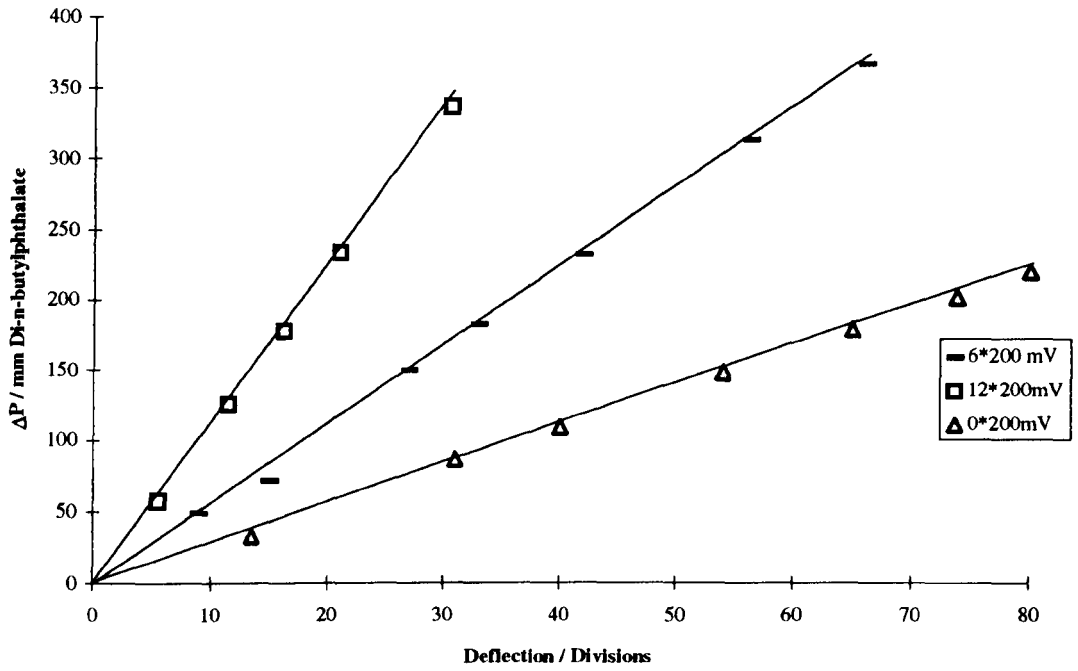


Table 3. 1 Summary of pressure transducer calibration showing the range in Torr for full scale (100 divisions) deflections.

Attenuation	2mV	5mV	10mV	20mV	50mV	100mV	200mV
0	-	-	-	-	-	10.57	21.30
6	-	-	2.13	4.26	10.79	21.62	43.09
12	-	2.10	4.24	8.60	20.85	43.11	85.35
18	-	4.17	8.26	16.58	41.70	84.01	-
24	-	8.22	16.64	33.22	79.77	164.95	-
30	6.58	16.38	32.72	65.77	162.94	-	-
36	12.98	32.55	65.11	134.89	-	-	-

The transducer could be used to measure either absolute or relative pressure changes. For absolute pressures, the reference side of the transducer was maintained under a vacuum of better than 10^{-3} Torr. When the transducer was used to monitor pressure changes occurring in reactions carried out at 500 Torr, the reference side of the transducer was connected to a 1 litre bulb, filled with 500 Torr of nitrogen, contained in a thermostated box in order to eliminate any temperature effects on the transducer measurements and to minimise the effect of any small leaks. Reactions carried out at different pressures used the same approach. When measuring absolute pressures the reference side of the transducer was connected to a fully evacuated 250cm^3 bulb to minimise the effects of small leaks.

3.5. Experimental Method.

Before commencing work each day the hydrogen, nitrogen and oxygen lines were flushed out to remove any air.

The *aged* condition of the reaction vessel was checked by measuring the slow reaction rate for the mixture containing 140 Torr hydrogen + 360 Torr oxygen at 500°C . Attainment of a maximum reaction rate of $13.5 \pm 0.3 \text{ Torr min}^{-1}$ confirmed the condition of the vessel¹.

3.5.1. Kinetic Study of the Xylenes.

The kinetic study for the determination of the rate constants $k(\text{OH}+\text{xylene})$, $k(\text{H}+\text{xylene})$ and $k(\text{HO}_2+\text{xylene})$ was carried out at a total pressure of 500 Torr at 480°C.

A total of eleven reaction mixtures were used with addition of 0.01% xylene (Table 3.2).

Generally 140 Torr of hydrogen ($\text{H}_2 + \text{N}_2$ for low hydrogen mixtures) were added directly to the reaction vessel. This ensured that when the gases from the mixing bulb were admitted into the reaction vessel the total pressure was above the second explosion limit pressure.

The xylene, oxygen and nitrogen (also H_2 for high hydrogen mixtures) were added to the mixing bulb to a total pressure of 590 Torr (see section 3.5.5). Upon expansion of the mixing bulb mixture into the reaction vessel a total pressure of 500 Torr was achieved. Once the required reaction time had been reached, the reaction was quenched by expansion of the reaction vessel contents into an evacuated 250cm³ bulb fitted with a Youngs P.T.F.E. tap by opening valve V2 (Figure 3.1). A sample from the mixing bulb was also taken ensuring that the sample bulb and section of glassware between the tap A and the main line were evacuated. Taps A and B were closed and tap C was opened expanding the mixing bulb contents into the sample bulb. This sample was used to determine the degree of consumption of the xylene as well as to calibrate the gas chromatograph for each run. For small errors in the quantity of additive present, the technique was thus self-compensating.

Table 3. 2 : Reaction Mixtures used for the Xylene Kinetics Study - 0.05 Torr Xylene plus:

Pressure H₂ / Torr	Pressure O₂ / Torr	Pressure N₂ / Torr
140.0	360.0	0.0
140.0	270.0	90.0
140.0	210.0	150.0
140.0	140.0	220.0
140.0	70.0	290.0
140.0	35.0	325.0
430.0	70.0	0.0
270.0	70.0	160.0
210.0	70.0	220.0
70.0	70.0	360.0
35.0	70.0	395.0

Table 3. 3 : Reaction Mixtures used for the Xylene Products Study - 2.5 Torr Xylene plus:

Pressure H₂ / Torr	Pressure O₂ / Torr	Pressure N₂ / Torr
140.0	357.5	0.0
140.0	70.0	287.5
427.5	70.0	0.0

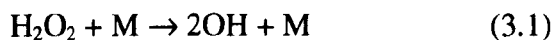
3.5.2. Product Study of the Xylenes.

The overall method for preparing the reaction mixtures was the same as for the kinetic study except that the amount of xylene was increased from 0.01% to 0.5% in order to facilitate the quantitative determination of the products produced in the early stages of reaction. Only three reaction mixtures were used (Table 3.3).

3.5.3. The Decomposition of Neopentylbenzene in the Presence of Oxygen.

The decomposition of neopentylbenzene (NPB) was carried out in the presence of oxygen and nitrogen at a total pressure of 60 Torr. For this study, all reaction mixtures were prepared in the mixing bulb and expanded into an evacuated reaction vessel.

The reaction mixture composition was 0.48 Torr (0.8%) NPB + 5, 10, 15, 30 or 59.5 Torr of oxygen, (with nitrogen to make up the total pressure to 60 Torr where required). The reactions were carried out at a maximum pressure of 60 Torr to reduce the decomposition of hydrogen peroxide³ due to the reaction



which generates the very reactive OH radicals.

Due to an unforeseen problem of adsorption of the neopentylbenzene on the solenoid valves they were replaced with Young's P.T.F.E. taps (section 3.5.4 and Chapter 6) which reduced the degree of absorption to less than 1% of NPB used.

3.5.4. The Adsorption of Hydrocarbons in the Apparatus.

Due to the low vapour pressure of each parent aromatic hydrocarbon it was necessary to see if absorption or adsorption occurred on any part of the apparatus. This was tested by carrying out a number of blank runs which involved making up a mixture of hydrocarbon and nitrogen in the mixing bulb, expanding it into the reaction vessel, and then sampling from the reaction vessel within a few seconds to reduce the possibility of pyrolysis. A second sample, taken from the mixing bulb, was also taken as a reference. Both samples were checked by gas chromatography. By comparing the peak areas it was possible to determine if any adsorption had occurred during the sampling processes.

Generally there was no problem with adsorption of the parent aromatic compounds apart from studies with neopentylbenzene where up to 30% of the compound was lost due to adsorption on the solenoid valves.

The valves were replaced with Young's P.T.F.E. taps and the test was repeated. This proved successful in reducing any adsorption effects to less than 1%.

3.5.5. Calibration of the Mixing Bulb.

In order to obtain a total pressure of either 500 Torr or 60 Torr in the reaction vessel via expansion from the mixing bulb the following procedure was used.

For a total pressure of 500 Torr (for the H₂ + O₂ work), the reference side of the pressure transducer was set to 500 Torr of nitrogen. 140 Torr of nitrogen was added to the evacuated reaction vessel. A trial and error method of adding a pressure (circa 600 Torr nitrogen) into the mixing bulb and then expanding the gas into the reaction vessel was then employed. When a pressure of 500 Torr was obtained in the reaction vessel the

differential pressure across the transducer was zero and this was established by reference to the null point on the chart recorder. The final pressure for the mixing bulb was found to be 590 Torr for runs at 480°C.

For a total pressure of 60 Torr in the reaction vessel (for the neopentylbenzene work), the reference side of the transducer was set to 60 Torr of nitrogen. The reaction vessel was evacuated and a pressure circa 75 Torr of nitrogen was added to the mixing bulb. Again by observing the null position of the chart recorder pointer it was possible to adjust the mixing bulb pressure until the the final pressure of 60 Torr was achieved. This was found to be 73.0 Torr for runs at 480°C.

In order to calculate the pressure of each reactant to be added to the mixing bulb in order to achieve the observed pressure in the reaction vessel, the following equation was used:

$$\text{MBP}_{(R)} = \frac{\text{RVP}_{(R)} * \text{MBP}_{(T)}}{\text{RVP}_{(T)} - \text{RVP}_{(P)}}$$

$\text{MBP}_{(R)}$ = Pressure of reagent required in the mixing bulb.

$\text{RVP}_{(R)}$ = Pressure of reagent required in the reaction vessel.

$\text{MBP}_{(T)}$ = Total pressure of all reagents in the mixing bulb.

$\text{RVP}_{(T)}$ = Total initial pressure of all reagents in the reaction vessel.

$\text{RVP}_{(P)}$ = Pressure in the reaction vessel before mixing bulb sample is added, usually

140 Torr in the H₂ + O₂ work and zero in the neopentylbenzene study.

3.6. Reagents

3.6.1. Hydrogen, Oxygen and Nitrogen Gases.

The hydrogen, nitrogen and oxygen gases used were supplied by Energas Ltd in 207 Bar cylinders. Hydrogen was connected to the apparatus by a single length of copper tubing. The nitrogen and oxygen cylinders were connected with single lengths of plastic tubing.

The hydrogen, oxygen and nitrogen gases were used directly from the cylinder without further purification. The purity of the gases was verified on gas chromatography by checking for traces of hydrocarbons and other organic compounds, and by measuring the maximum rate of the hydrogen + oxygen reaction and comparing the value with that from the literature. The maximum rate values measured were in excellent agreement with the literature value¹ and strongly supported the view was that no further purification was necessary.

3.6.2. Hydrocarbons.

The supplier of each reagent is given in Table 3.4.

All liquid samples were stored in small glass tubes fitted with Young's P.T.F.E. taps. Before using any of the liquid samples they were degassed after freezing the liquid by use of either liquid nitrogen or cardice/acetone, and pumping off any non-condensable material.

Table 3.4 : Table of Chemical Suppliers.

Compound	Supplier	Purity
o-Xylene	Hopkins and Williams	99 %
m-Xylene	Hopkins and Williams	99 %
p-Xylene	Koch-Light Laboratories	99 %
o-Tolualdehyde	Aldrich Chemical Co Ltd	99 %
m-Tolualdehyde	Avocado	99 %
p-Tolualdehyde	Janssen Chemica	99 %
o-Xylylene Oxide	Janssen Chemica	99 %
Benzaldehyde	May and Baker Ltd	99 %
Toluene	Koch-Light Laboratories	99 %
Benzene	Koch-Light Laboratories	99 %
Neopentylbenzene	Aldrich Chemical Co Ltd	99 %
2-Methyl-1-phenylprop-1-ene	Aldrich Chemical Co Ltd	99 %
Ethylbenzene	BDH	99 %
i-Butene Oxide	Lancaster	99 %
Propylene Oxide	Aldrich Chemical Co Ltd	99 %
i-Butene	Argo International Ltd	99 %
Propene	Matheson Co Ltd	99 %
Propane	Argo International Ltd	99 %
Ethane	Matheson Co Ltd	99 %
Ethene	Matheson Co Ltd	99 %
Methane	Argo International Ltd	99 %
Hydrogen	Engweld	99 %
Nitrogen	Engweld	99 %
Oxygen	Engweld	99 %
Compressed Air	Engweld	99 %

For most liquid samples, liquid nitrogen was the best cryogen for the freeze-thaw method. However, for liquids with very low vapour pressures (such as the tolualdehydes) cardice/acetone achieved a better purity of the sample. All of the liquid samples had their purity checked by gas chromatography.

Propene used in the neopentylbenzene study was stored in a clean 1 litre Pyrex bulb fitted with a Young's P.T.F.E. tap. Again the purity was checked by gas chromatography.

All standard reagents treated in the way described above gave a minimum purity of 99% by gas chromatography. No further purification was required for the work described in this thesis.

3.7. Analysis and Analytical Methods.

All of the quantitative and qualitative analyses were carry out by use of packed column gas chromatography equipment, fitted with dual flame ionisation detectors.

Two gas chromatographs were available for use, a Perkin Elmer CG8700 and a Perkin Elmer Sigma 1 analyser, coupled to a Sigma10 console. Both gas chromatographs were fitted with dual differential flame ionisation detectors with nitrogen carrier gas. Sample injection onto either gas chromatograph was achieved via a 10-port gas-sampling valve. Accurate pressures of gas (circa 100 Torr normally) could be loaded into the sample loop via the connection between the sampling valves and a small gas-handling apparatus, fitted with a double-limb mercury manometer (Figures 3.12 - 3.14). An accuracy of better than 0.5% was obtained for the pressure (100 Torr) injected.

Figure 3. 12 : Diagram Of Vacuum Line Used For Gas Chromatography Analysis..

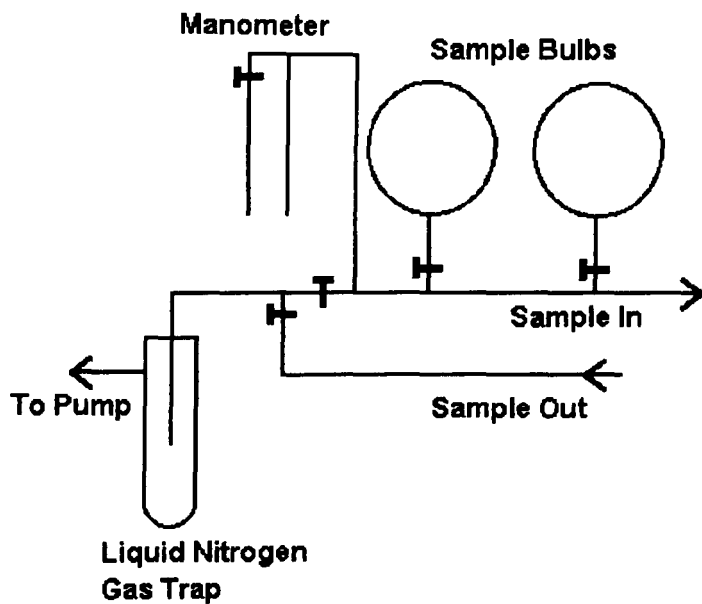


Figure 3. 13 : Gas Sampling Valve In Load Position.

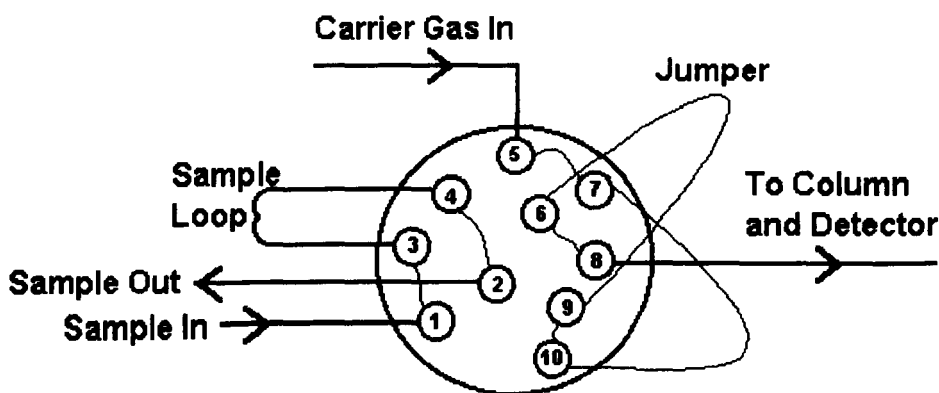
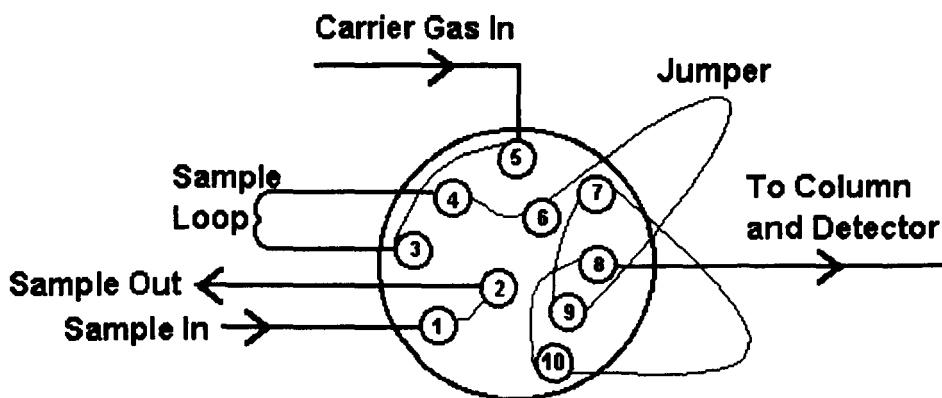


Figure 3. 14 : Gas Sampling Valve In Inject Position.



3.7.1. Calibration of Gas Chromatography.

When all of the oxidation products for each study had been successfully identified, it was necessary to calibrate the gas chromatograph detectors in order to obtain a quantitative analysis.

Where possible the parent compound was used as the reference to obtain relative sensitivities. In this way, complete calibration of the gas chromatograph could be obtained for every run by injection of the sample from the mixing bulb. However, if the parent compound exhibited excessive tailing another compound was chosen. Although toluene was not the parent compound it was used as the reference for all of the aromatic compounds because it gave a linear response and reproducible detection. At least two relative sensitivities were determined in a single day; in some cases it was possible to determine up to four. In order to ensure the greatest degree of accuracy the same reference compound stock sample was used over as many days as possible. However, fresh calibration standards were made up daily.

As indicated, a relative sensitivity technique was used whereby all compounds are calibrated relative to a common standard. This allowed for the possibility of a single calibration for each set of products, eliminating the necessity for daily calibrations for each product due to detector fluctuations from day to day. To obtain the sensitivity of a product relative to that of the starting material the following method was adopted. The sensitivity of each compound was measured across an appropriate concentration range.

$$\text{Sensitivity} = \frac{\text{Peak Area} / 100 \text{ Torr}}{\% \text{ Concentration}}$$

The response for all compounds was found to be linear for the calibration over the range of pressure used, and therefore, the relative sensitivity is clearly:

$$\text{Relative Sensitivity} = \frac{\text{Sensitivity of Compound}}{\text{Sensitivity of Reference}}$$

Tables 3.5-3.10 summarise the relative sensitivity factors for the detectable hydrocarbons for each study. Figures 3.15-3.38 are the calibration graphs for the detectable compounds from the appropriate column, all showing an excellent linear response over the chosen concentration range.

The percentage concentration of a compound in the reaction vessel was calculated for the xylene study from the following equation:

$$\% \text{ Xylene in RV bulb} = \frac{\text{Peak Area}_{\text{RV}}}{\text{Peak Area}_{\text{MB}} * \text{R}}$$

where *Peak Area*_{RV} and *Peak Area*_{MB} are the peak areas corresponding to a pressure of 100 Torr injected onto the column from the **RV** and **MB** sample bulbs, respectively, and **R** is a dilution constant which arises from expanding the mixing bulb sample into the reaction vessel already containing gas.

$$\text{R} = \frac{\text{Initial Percentage of Xylene in RV}}{\text{Initial Percentage of Xylene in MB}}$$

For the neopentylbenzene study the percentage of NPB in the **RV** after reaction was calculated by use of the equation below:

$$\% \text{ NPB in RV} = \frac{\text{Peak Area}_{\text{RV}} * \text{D}_{\text{RV}}}{\text{Peak Area}_{\text{MB}} * \text{D}_{\text{MB}}}$$

where *Peak Area*_{RV} and *Peak Area*_{MB} are the peak areas corresponding to a pressure of 100 Torr injected onto the column from the **RV** and **MB** sample bulbs respectively, and

Relative Sensitivities for the Products detected for the Xylene Product Study

Column = 1 metre packed 5% Alltech AT-1200 + 1.5% Bentone 34 on Chromosorb W-AW, 100/120 mesh..

Table 3. 5

		RF[⊗] = (Toluene / CPD[Ⓟ])		
Reference:		o-Xylene	m-Xylene	p-Xylene
Toluene		0.73	0.80	0.78

Table 3. 6

		RF = (Toluene / CPD)					
Reference:	O-Xylylene Oxide	o-Tolualdehyde	m-Tolualdehyde	p-Tolualdehyde	Benzaldehyde	Benzene	Methane

[⊗] RF = Response Factor.

[Ⓟ] CPD = Compound of Choice.

Table 3. 7 : Summary of Response Factors for Xylene Oxidation.

Compound	RF (CPD/PX)		RF (CPD/OX)		RF (CPD/MX)
Methane	0.12		0.11		0.12
Benzene	0.68		0.63		0.69
Toluene	0.78		0.73		0.80
Benzaldehyde	0.52		0.48		0.53
p/o/m - Tolualdehyde	0.24		0.24		0.29
o-Xylylene Oxide			0.15		

Relative Sensitivities for the Products detected for the Neopentylbenzene + Oxygen Product Study

Column for Aromatics = 1 metre packed 5% Alltech AT-1200 + 1.5% Bentone 34 on Chromosorb W-AW, 100/120 mesh.

Table 3. 8

		RF = (CPD/NPB)				
Reference:	2-Methyl-1-phenylprop-1-ene	Benzaldehyde	Toluene	Ethylbenzene	Benzene	i-Butene
Neopentylbenzene	0.48	0.30	0.46	0.54	0.38	0.23

Column for Hydrocarbons = 0.5 metre Porapak Q, 80/100 mesh.

Table 3. 9

		RF = (CPD / i-Butene)		
Reference	Methane	Ethane	Propene	
i-Butene	0.27	0.52	0.89	

Relative Sensitivities for the Products detected for the Neopentylbenzene + Propene + Oxygen Product Study.

Column for Aromatics = as above

Column for Hydrocarbons = 1.7 metre Chromosorb 102, 80/100 mesh.

Table 3. 10

	RF = (CPD / Propene)					
Reference	Methane	Ethene	Ethane	Propane	i-Butene	Propylene Oxide
Propene	0.35	0.69	0.71	1.06	1.28	0.48

Calibration Graphs for 1M Bentone 34 on Chromosorb W/AW

Figure 3. 15

Calibration Plot of Peak Area per 100Torr vs. Percentage for p-Xylene

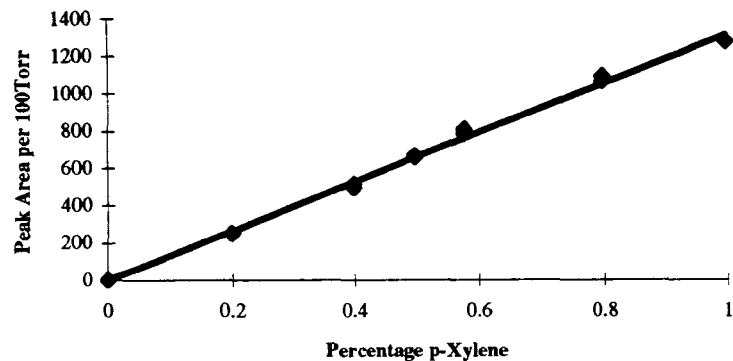


Figure 3. 17

Calibration Plot of Percentage vs. Peak Area per 100Torr for o-Xylene

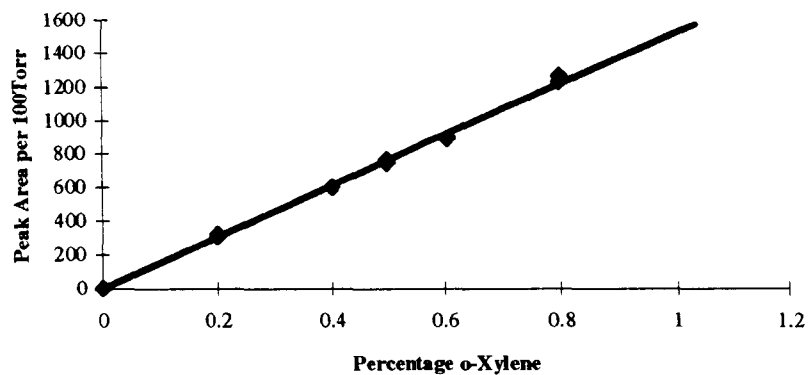


Figure 3. 16

Calibration Plot of Peak Area per 100Torr vs. Percentage for m-Xylene

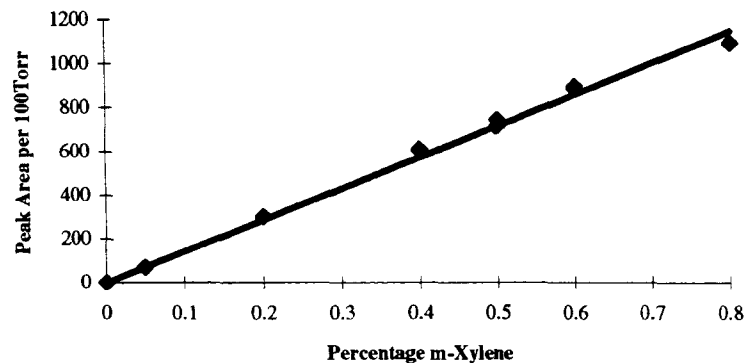


Figure 3. 18

Calibration Plot of Peak Area per 100Torr vs. Percentage for Toluene

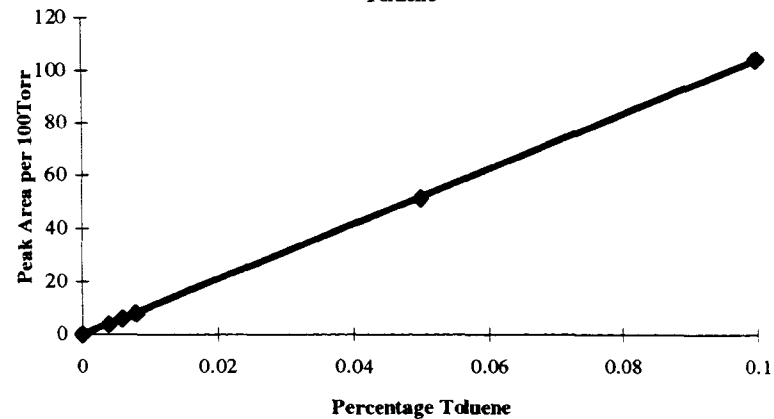


Figure 3. 19

Calibration Plot of Peak Area per 100Torr vs. Percentage for p-Tolualdehyde

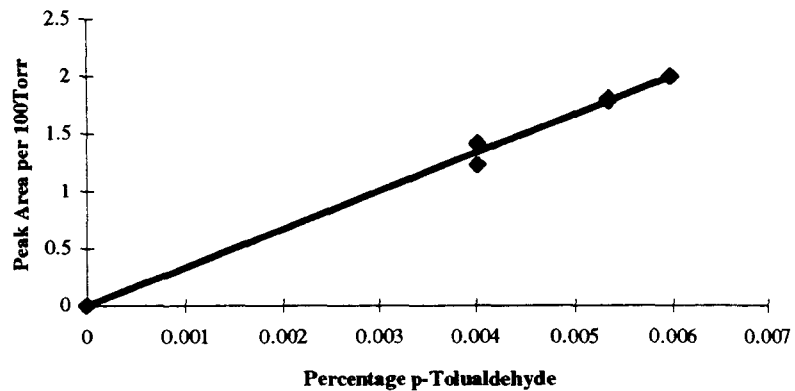


Figure 3. 20

Calibration Plot of Peak Area per 100Torr vs. Percentage for m-Tolualdehyde

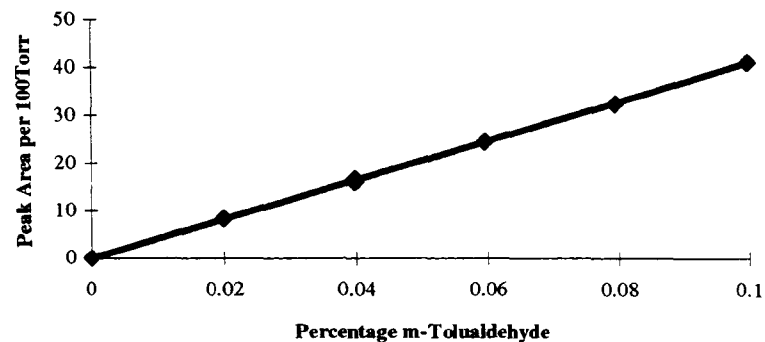


Figure 3. 21

Calibration Plot of Peak Area per 100Torr vs. Percentage for o-Tolualdehyde

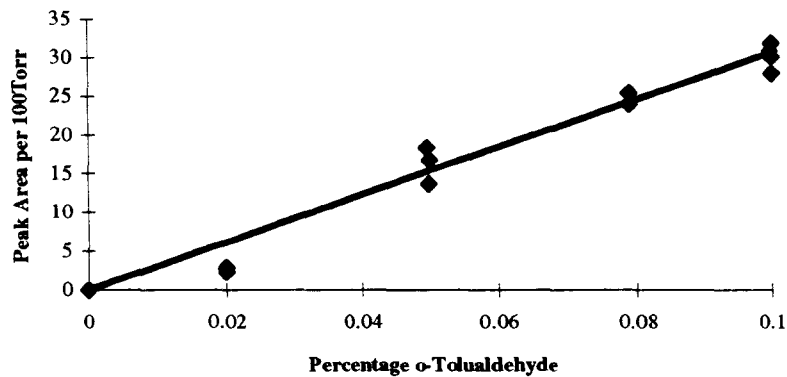


Figure 3. 22

Calibration Plot of Peak Area per 100Torr vs. Percentage for o-Xylylene oxide

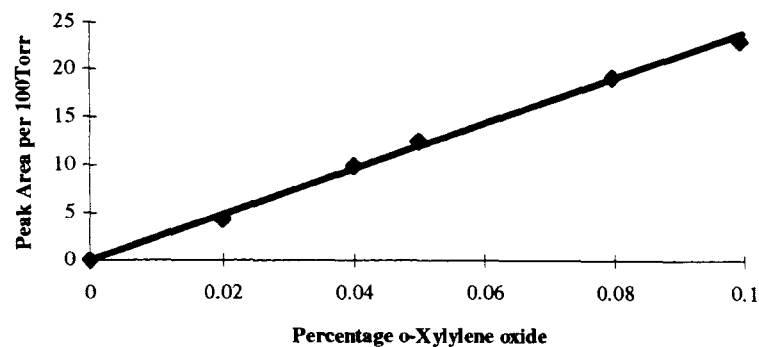


Figure 3. 23

Calibration Plot of Peak Area per 100Torr vs. Percentage for Benzaldehyde

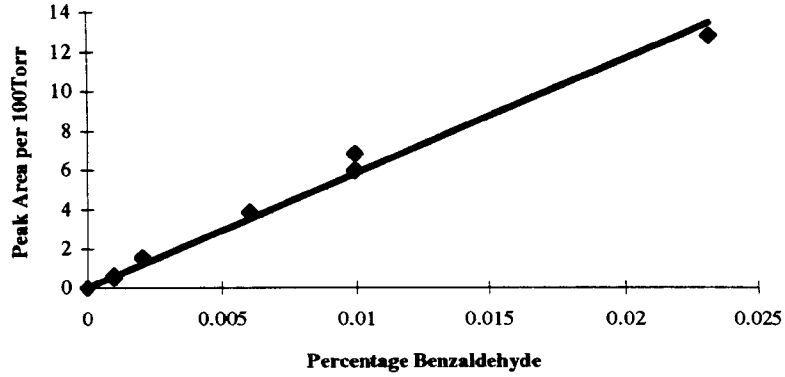


Figure 3. 24

Calibration Plot of Peak Area per 100Torr vs. Percentage for Benzene

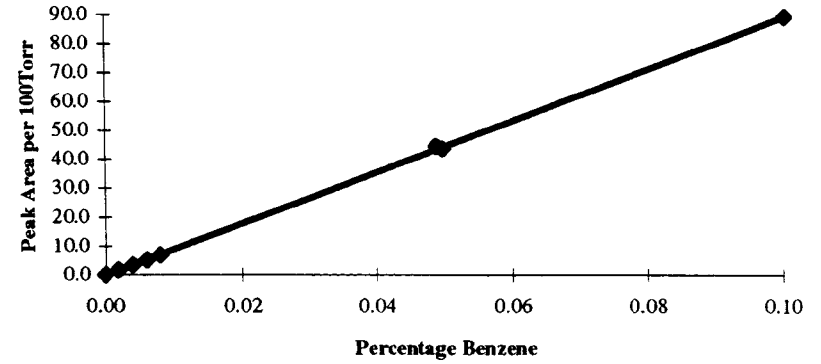


Figure 3. 25

Calibration Plot of Peak Area per 100Torr vs. Percentage for Methane

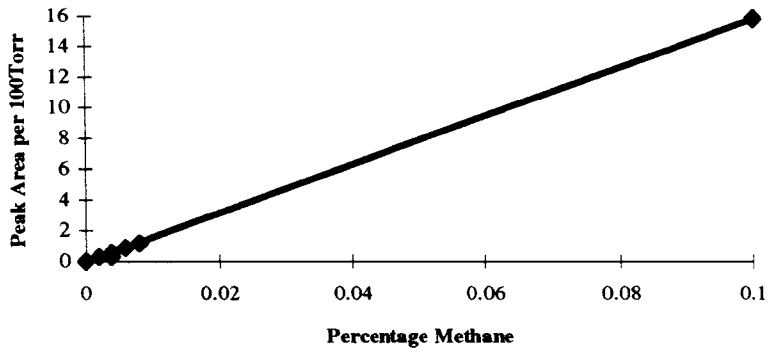


Figure 3. 26

Calibration Plot of Peak Area per 100Torr vs. Percentage for i-Butene

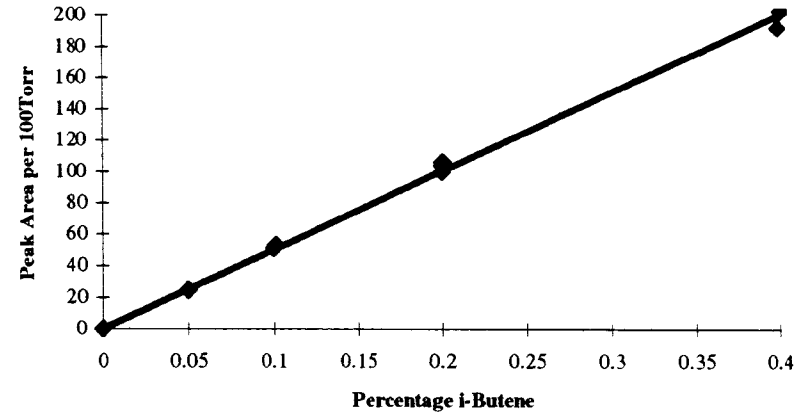


Figure 3. 27

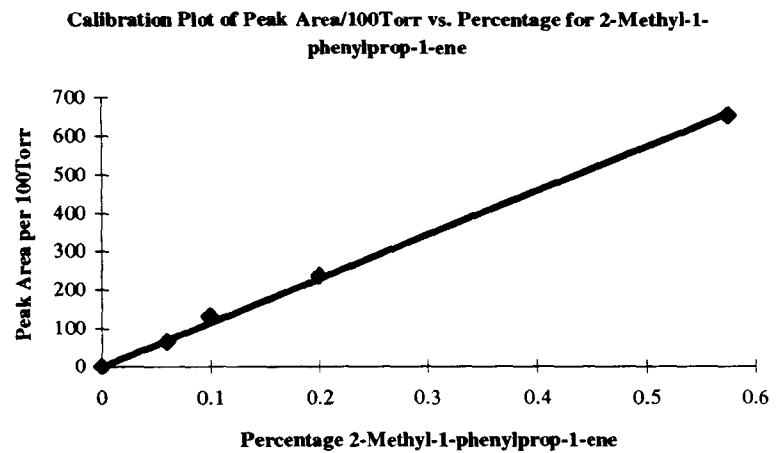
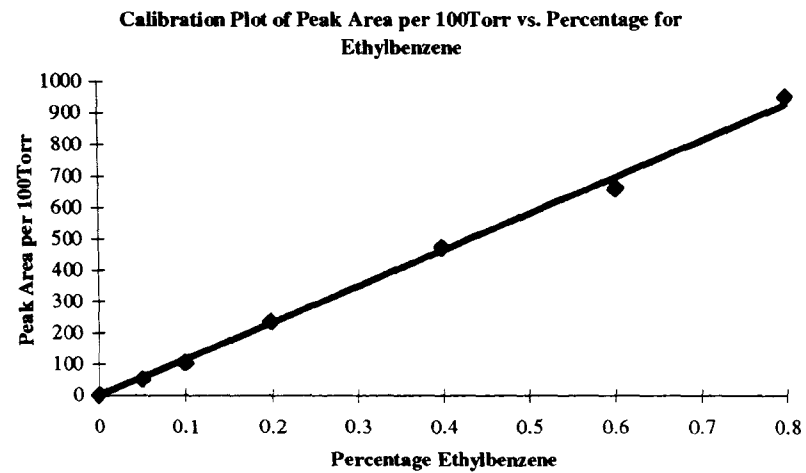


Figure 3. 28



Calibration Graphs for 0.5M Porapak Q

Figure 3. 29

Calibration Plot of Peak Area per 100Torr vs. Percentage for Methane

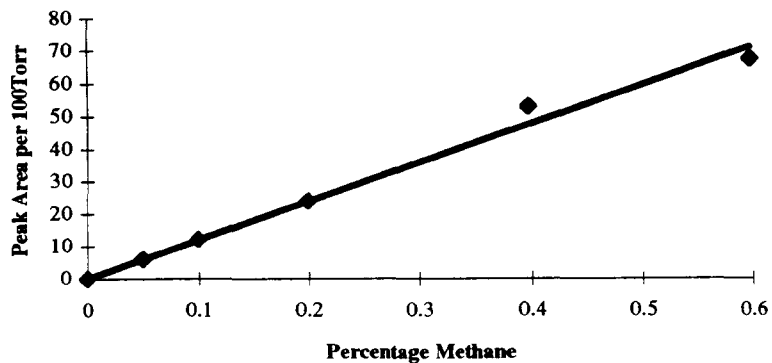


Figure 3. 30

Calibration Plot of Peak Area per 100Torr vs. Percentage for i-Butene

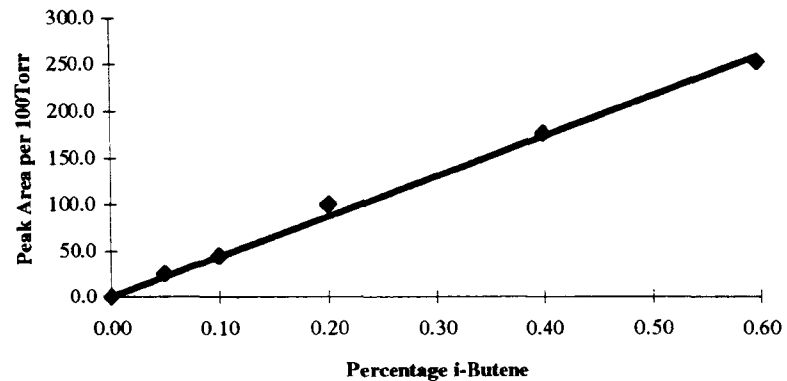


Figure 3. 31

Calibration Plot of Peak Area per 100Torr vs. Percentage for Ethane

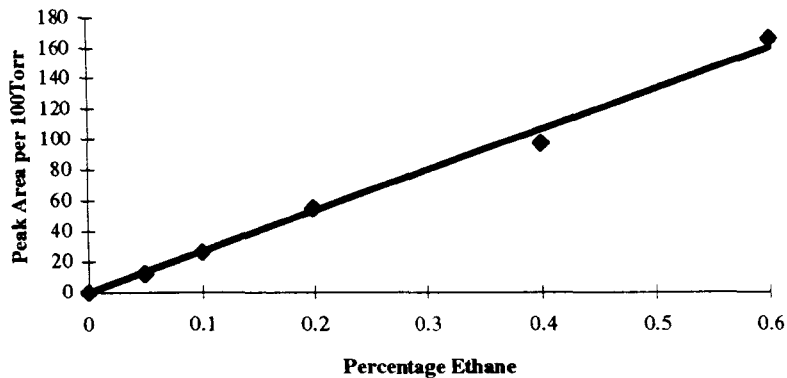
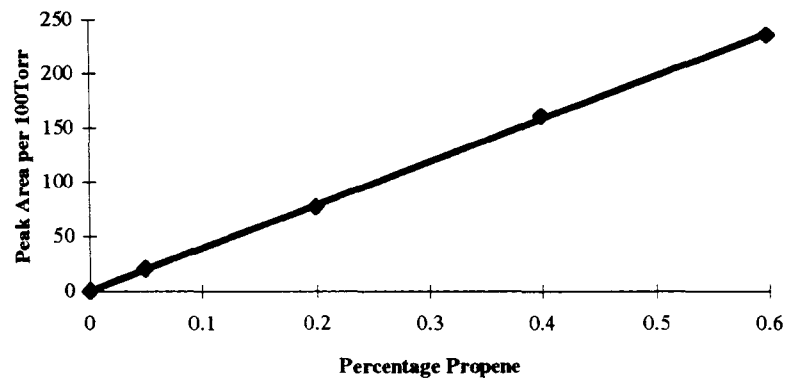


Figure 3. 32

Calibration Plot of Peak Area per 100Torr vs. Percentage for Propene



Calibration Graphs for 1.7M Chromosorb 102

Figure 3. 33

Calibration Plot of Peak Area per 100Torr vs. Percentage for Propene

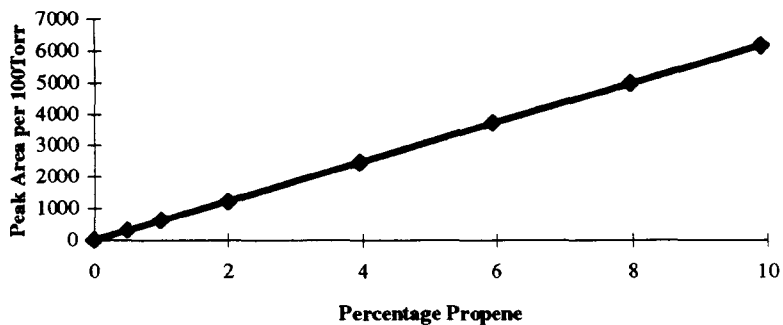


Figure 3. 35

Calibration Plot of Peak Area per 100Torr vs. Percentage for Ethene

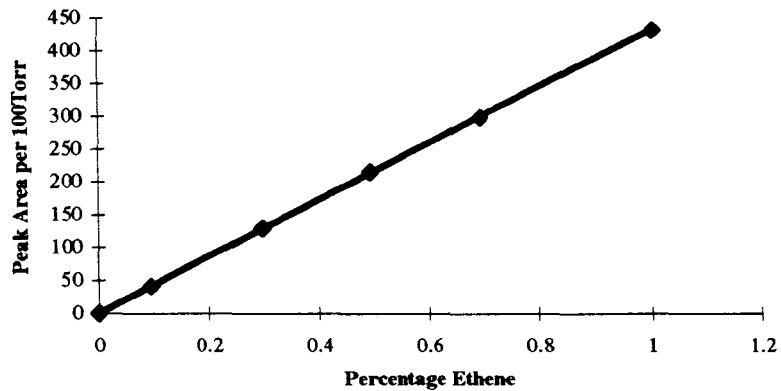


Figure 3. 34

Calibration Plot of Peak Area/100Torr vs. Percentage for Methane

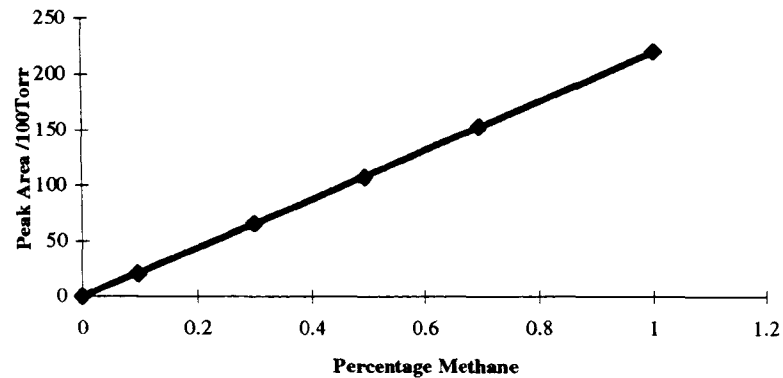


Figure 3. 36

Calibration Plot of Peak Area per 100Torr vs. Percentage for Ethane

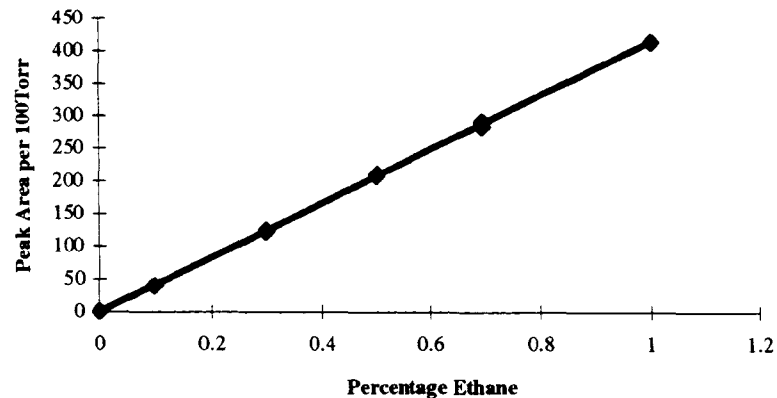


Figure 3. 37

Calibration Plot of Peak Area per 100Torr vs. Percentage for i-Butene

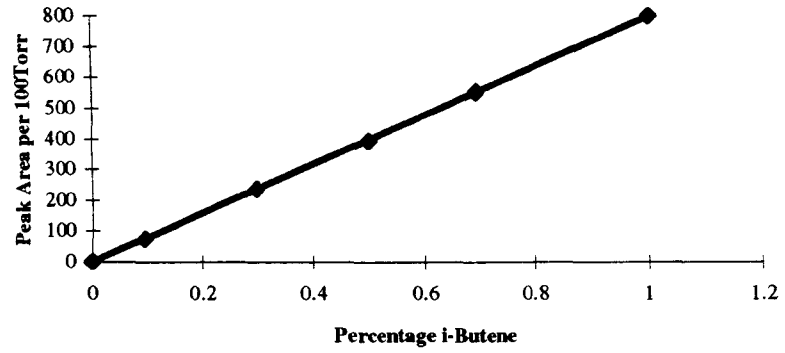
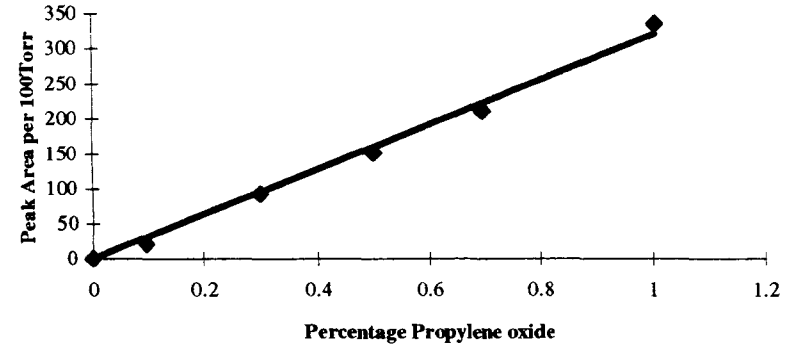


Figure 3. 38

Calibration Plot of Peak Area per 100Torr vs. Percentage for Propylene oxide



$D_{RV:MB}$ is the dilution ratio due to adding nitrogen into the sample bulbs prior to gas chromatography analysis, calculated using the equation below.

$$D = \frac{\text{Final pressure of nitrogen + sample in sample bulb}}{\text{Initial pressure of sample inside sample bulb}}$$

3.7.2. Columns and Conditions

Due to the nature of the compounds used, a different set of GC columns and conditions was required for each study. Numerous column packings (Porapak P-T and Chromosorbs) and column lengths (0.5 - 2.5m) were used to test for resolution, identification of products and the possibility of overlapping or masked product peaks. The best columns and the conditions used are given below.

3.7.3. Oxidation of Xylenes.

3.7.3.1. Xylene Kinetic Study.

1. 1.9 metre, packed column, containing 5% Alltech AT-1200 + 1.5% Bentone 34 on Chromosorb W-AW, 100/120 mesh; 120°C; carrier gas N₂, 20 cm³ min⁻¹, 8 minutes, isothermal.

These conditions were sufficient to obtain a sharp well resolved peak for the xylene being studied. The concentration of other compounds were not required and therefore not measured.

3.7.3.2. Xylene Product Study.

One column successfully separated all of the important compounds detected from methane to tolualdehyde. However, it was necessary to be run the column at two

different isothermal temperatures in order to ensure effective resolution of early peaks and detection of the peaks with long retention times.

1. 1 metre packed column containing 5% Alltech AT-1200 + 1.5% Bentone 34 on Chromosorb W-AW, 100/120 mesh; 100°C; carrier gas N₂, 20 cm³ min⁻¹, 40 minutes, isothermal.
2. As above, but run for 20 minutes at 120°C, isothermal.

3.7.4. The Decomposition of Neopentylbenzene.

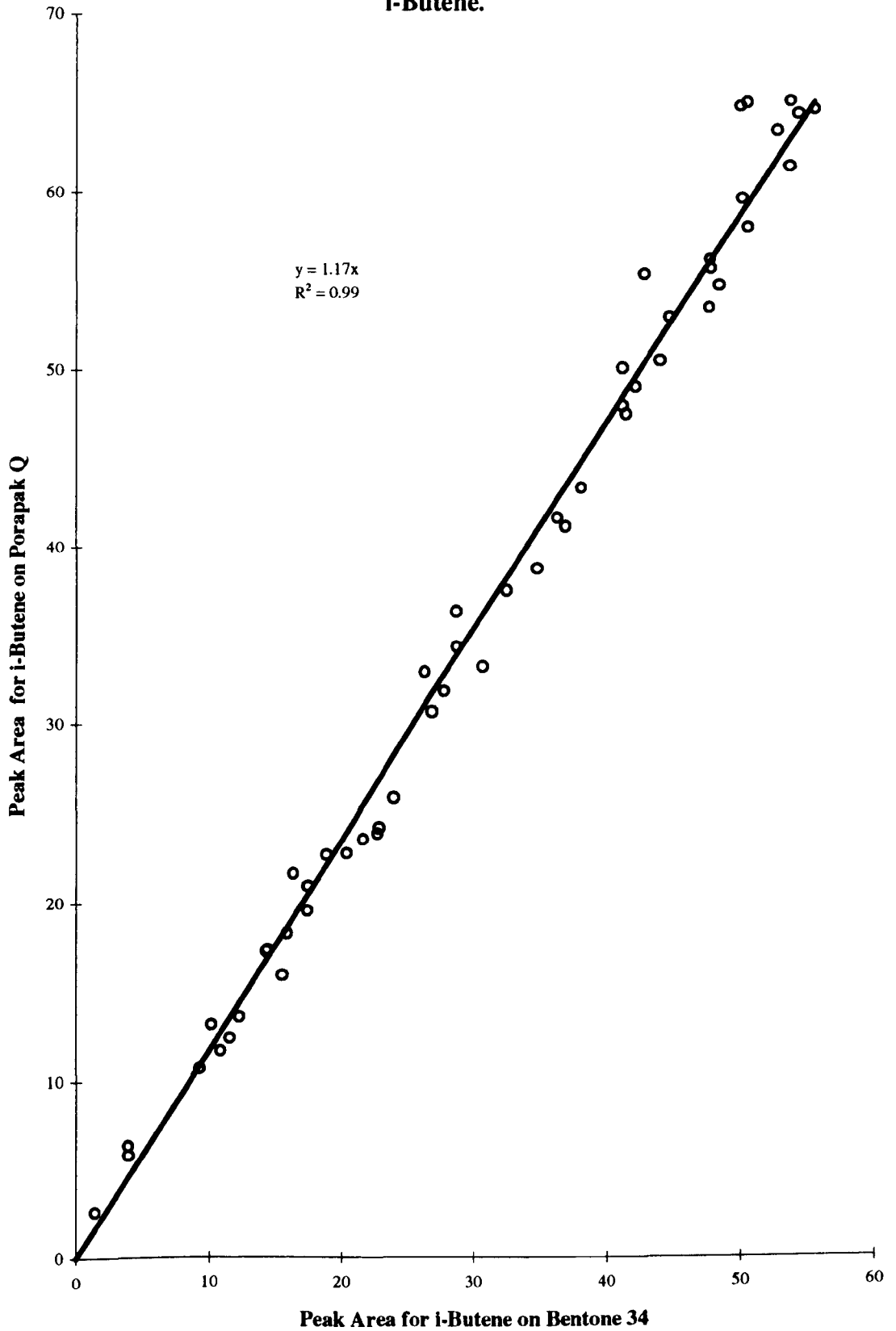
Two columns were required in order to obtain suitable resolution of the products.

1. 1 metre packed column containing 5% Alltech AT-1200 + 1.5% Bentone 34 on Chromosorb W-AW, 100/120 mesh; 85°C; carrier gas N₂, 20 cm³ min⁻¹, 45 minutes, isothermal.
2. 0.5 metre packed column containing Porapak Q, 80/100 mesh; 120°C; carrier gas N₂, 22 cm³ min⁻¹, 25 minutes, isothermal.

The Bentone 34 column resolved all of the aromatic products observed; benzene, toluene, NPB, benzaldehyde and 2-methyl-1-phenylprop-1-ene (MPP) as well as i-butene. The Porapak Q column resolved the important aliphatic products; methane to i-butene. The peak area for i-butene obtained using the Bentone 34 column displayed a linear correlation with the peak area for i-butene obtained on the Porapak Q column by a factor of $PA_{\text{Porapak Q}} : PA_{\text{Bentone 34}} = 1.17 \pm 0.04$ for the same pressure injected (Figure 3.39). Hence it was possible to use the quantity of i-butene obtained from the bentone 34

Figure 3. 39

Correlation between Porapak Q to Bentone 34 Peak Areas for
i-Butene.



column as the reference in order to accurately quantify the compounds measured on the Porapak Q column.

3.7.5. The Co-oxidation of Neopentylbenzene and Propene.

Again two columns were required.

1. 1 metre packed column containing 5% Alltech AT-1200 + 1.5% Bentone 34 on Chromosorb W-AW, 100/120 mesh; 85°C; carrier gas N₂ 20 cm³min⁻¹, 45 minutes, isothermal.
2. 1.7 metre packed column containing Chromosorb 102, 80/100 mesh; 70°C; carrier gas N₂, 40.5 cm³min⁻¹, 65 minutes, isothermal.

The Bentone 34 column successfully separated all aromatic products observed from toluene to MPP. However, the amount of benzene was not measured because the peak was not resolved from the products from the propene oxidation. Comparing the approximate peak area for benzene from this study to the accurate value from the *clean* oxidation of NPB it was clear to see that benzene is not a major product, (discussed in Chapter 6). The Chromosorb 102 column successfully resolved the aliphatic hydrocarbons and small oxygenates.

3.8. References.

¹ Doran P., *Ph.D. Thesis, University of Hull*, 1961, Ch.6.

² Hopkins D.E., *Ph.D. Thesis, University of Hull*, 1967.

³ Baldwin R. R., Hisham M. W. M., Keen A. and Walker R. W., *J. Chem. Soc. Faraday Trans. 1*, **78**, 1165-1176, (1982).

Chapter 4.

Results of the Kinetic Experiments for the Oxidation of the Xylenes.

Kinetic experiments were carried out on each isomer of xylene, (p-, m- and o-xylene respectively) using the addition of a trace amount of each to slowly reacting mixtures of hydrogen and oxygen as discussed in Chapter 2. The experiments were carried out at 753K and 500 Torr total pressure using the procedure detailed in Chapter 3. A detailed discussion of the results will be given in a later chapter.

4.1. Kinetic Experiments.

The kinetics of each xylene were studied individually. Trace amounts (0.01%) of one of the isomers were added to a wide range of hydrogen + oxygen mixtures. The mixture composition was varied from 360 to 35 Torr of oxygen with a fixed pressure of hydrogen of 140 Torr and from 430 to 35 Torr of hydrogen with a fixed pressure of oxygen of 70 Torr, using nitrogen to keep the total pressure at 500 Torr. The mixture compositions used are summarised in Table 4.1.

As indicated in Chapter 2, it is important to minimise the perturbation of the radical environment generated by the hydrogen + oxygen reaction when the xylene is added. The addition of trace amounts of a hydrocarbon to the hydrogen + oxygen reaction has been carried out for a range of compounds^{1,2}. It has been shown that the separate addition of less than 0.1% of an alkane to the hydrogen + oxygen reaction mixture

Table 4. 1: Summary of Reaction Mixtures Used for the Kinetic Study.

Pressure / Torr			
Hydrogen	Oxygen	Nitrogen	Xylene
140	360	0	0.0500
140	280	20	0.0500
140	210	150	0.0500
140	140	220	0.0500
140	70	290	0.0500
140	35	325	0.0500
430	70	0	0.0500
280	70	150	0.0500
210	70	220	0.0500
70	70	360	0.0500
35	70	395	0.0500

Table 4. 2 : Variation of the maximum rate of the hydrogen + oxygen reaction for the addition of different amounts of p-xylene at 773K.

Pressure / Torr				Maximum Rate at 773K/ Torr min ⁻¹
Hydrogen	Oxygen	Nitrogen	p-Xylene	
140	70	290	0	4.04
140	70	290	0.05	4.08
140	70	290	0.50	4.10

usually has no effect on either the induction period or maximum rate (Table 4.2), which implies that the radical concentrations are effectively unchanged.

The addition of 0.01% xylene was found to have no effect on the maximum rate (Table 4.2). Further, 0.01% was sufficiently high for very accurate detection by gas chromatography. The possibility of adding more than one xylene at a time to the reaction mixture and monitoring the consumption of each simultaneously was discounted. Arising from the similar nature of the isomers it was extremely difficult to accurately quantitatively resolve one isomer from another completely and so ensure very accurate measurements from the gas chromatograph.

No significant pyrolysis or molecular decomposition of the xylenes was observed over a time scale considerably larger than those used in this work. This was checked by adding a mixture of xylene in nitrogen into the reaction vessel followed by sampling at times up to five minutes and analysing the results by gas chromatography.

All of the figures show plots of 'Percentage Xylene Remaining' vs. ' ΔP '.

Figures 4.1 - 4.11 are for p-xylene,

Figures 4.12 - 4.22 are for m-xylene,

Figures 4.23 - 4.33 are for o-xylene.

As indicated in Chapter 2, ΔP is a measure of the hydrogen consumed in the overall reaction $2\text{H}_2 + \text{O}_2 \rightarrow 2\text{H}_2\text{O}$ so that $\Delta\text{H}_2 = 2\Delta P$. ΔP_{50} is the value of ΔP when 50% of the additive has been consumed and hence gives a measure of the relative rate of consumption of additive and hydrogen.

Consumption Plots for p-Xylene Kinetics

Figures for 0.05 Torr p-Xylene + 140 Torr Hydrogen with variable Oxygen.

Figure 4. 1

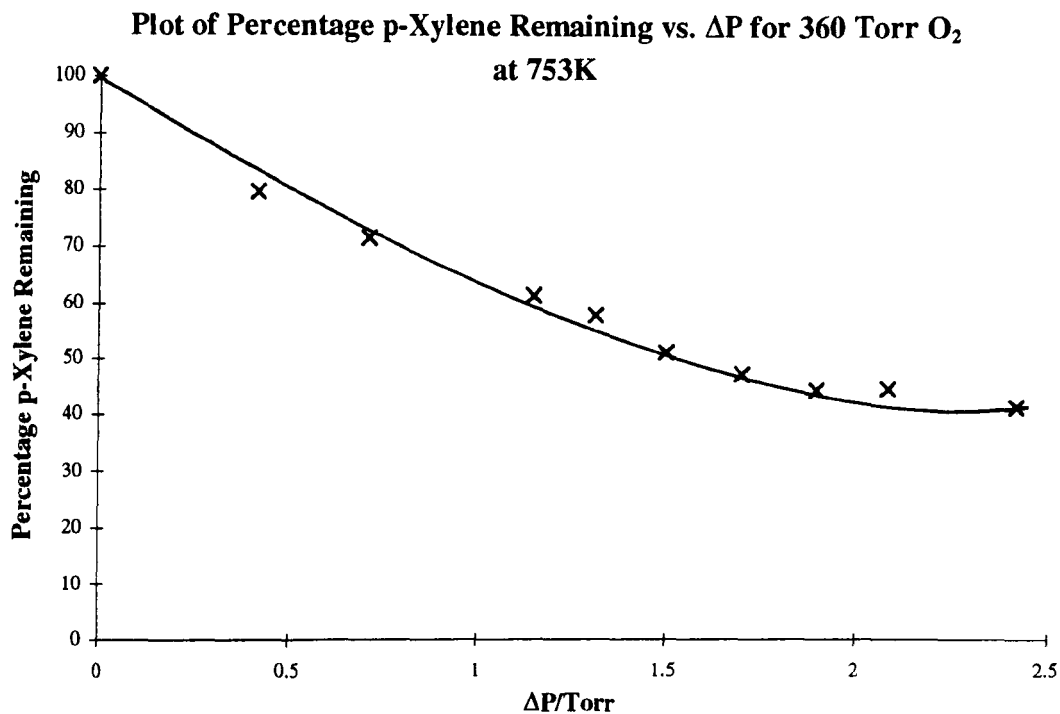


Figure 4. 2

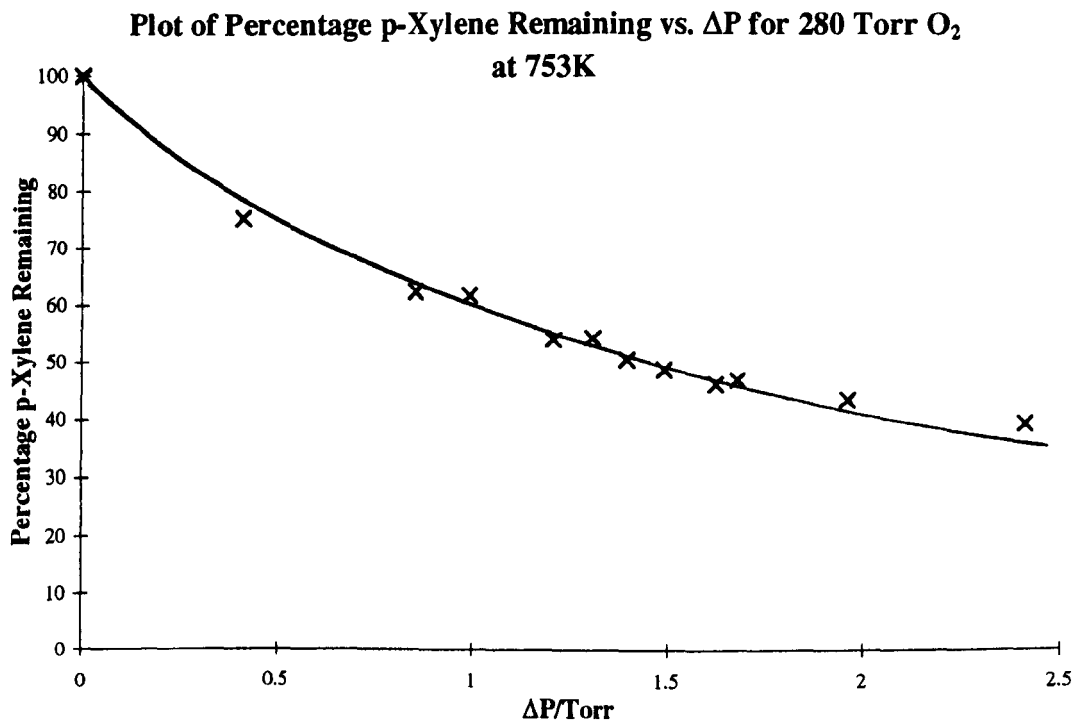


Figure 4. 3

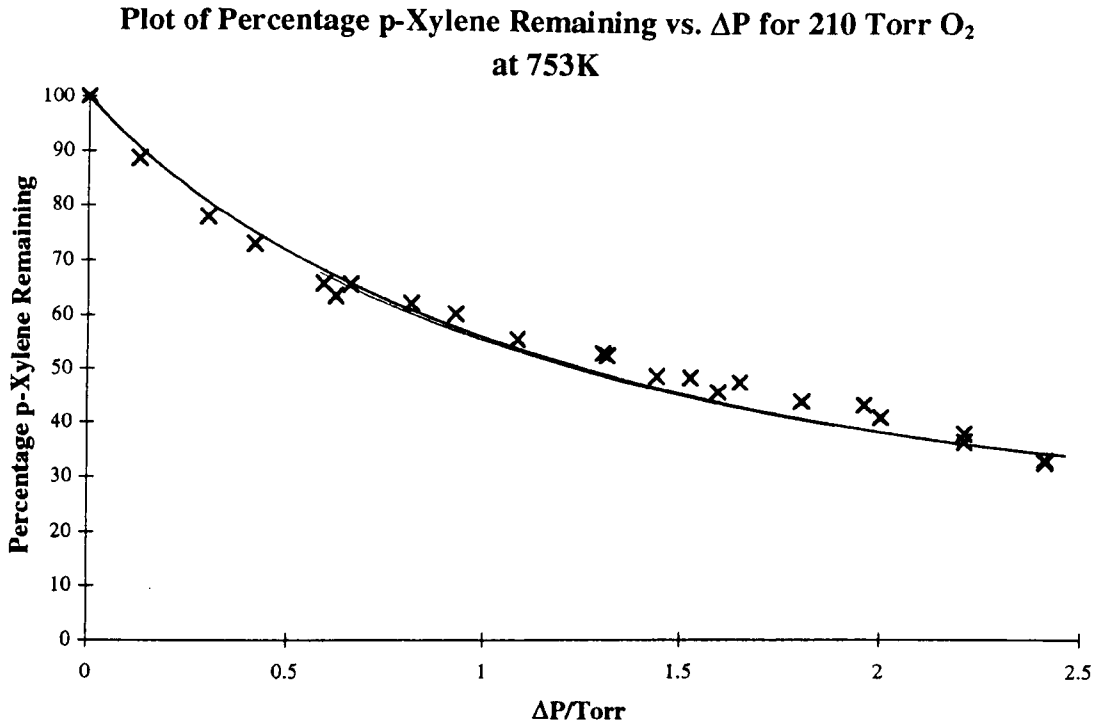


Figure 4. 4

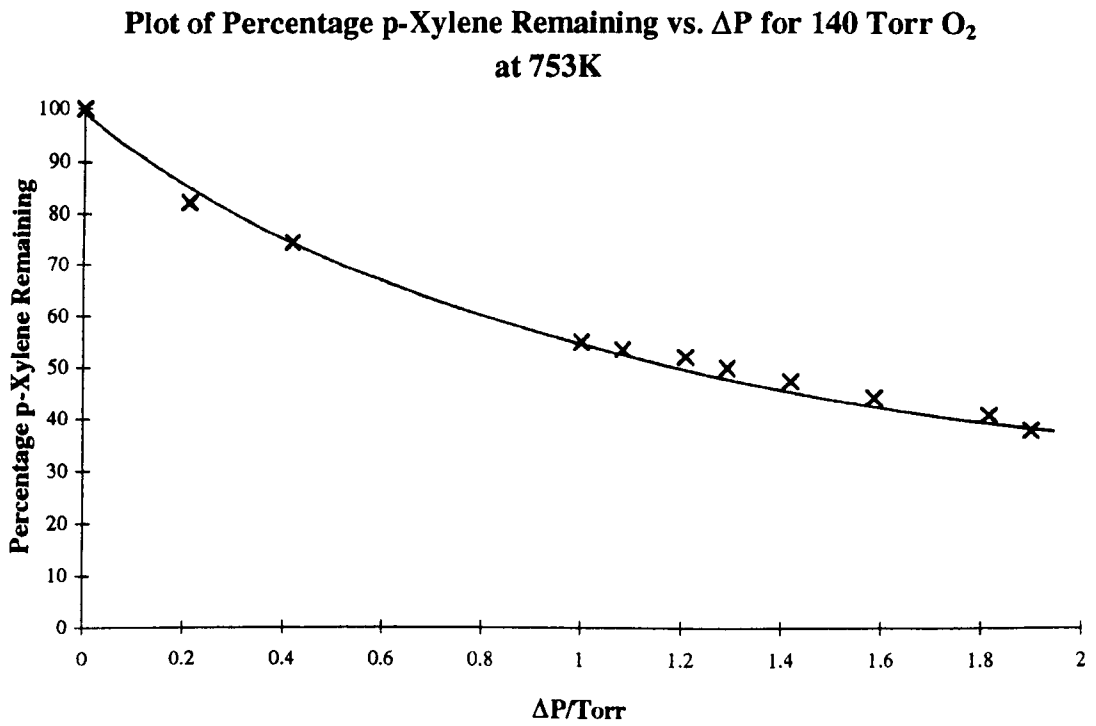


Figure 4. 5

Plot of Percentage p-Xylene Remaining vs. ΔP for 70 Torr O_2 at 753K

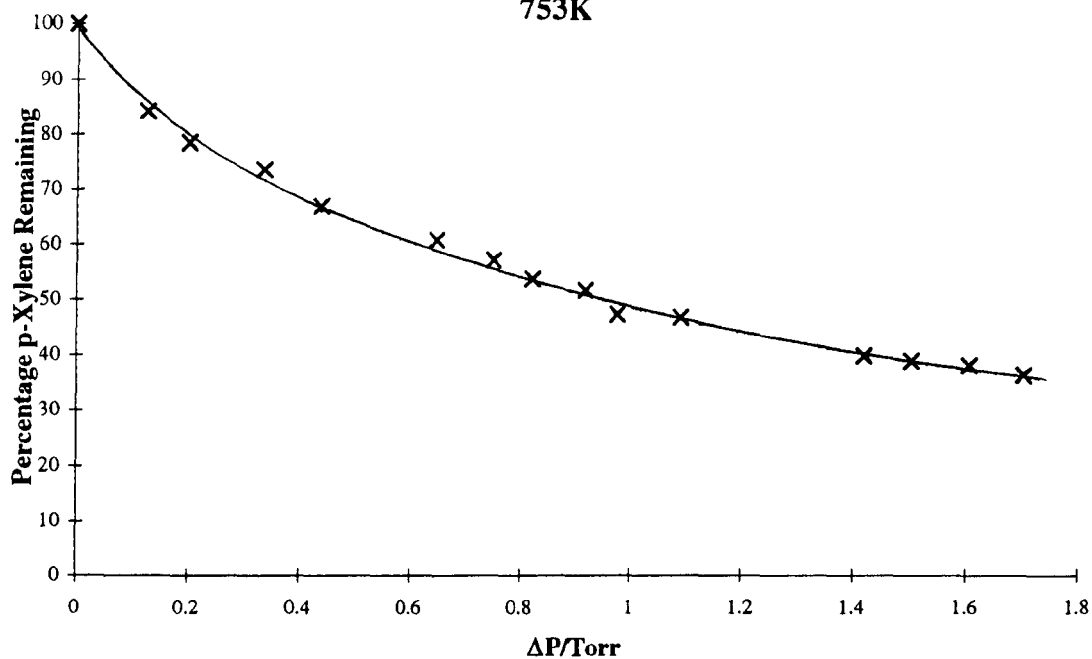
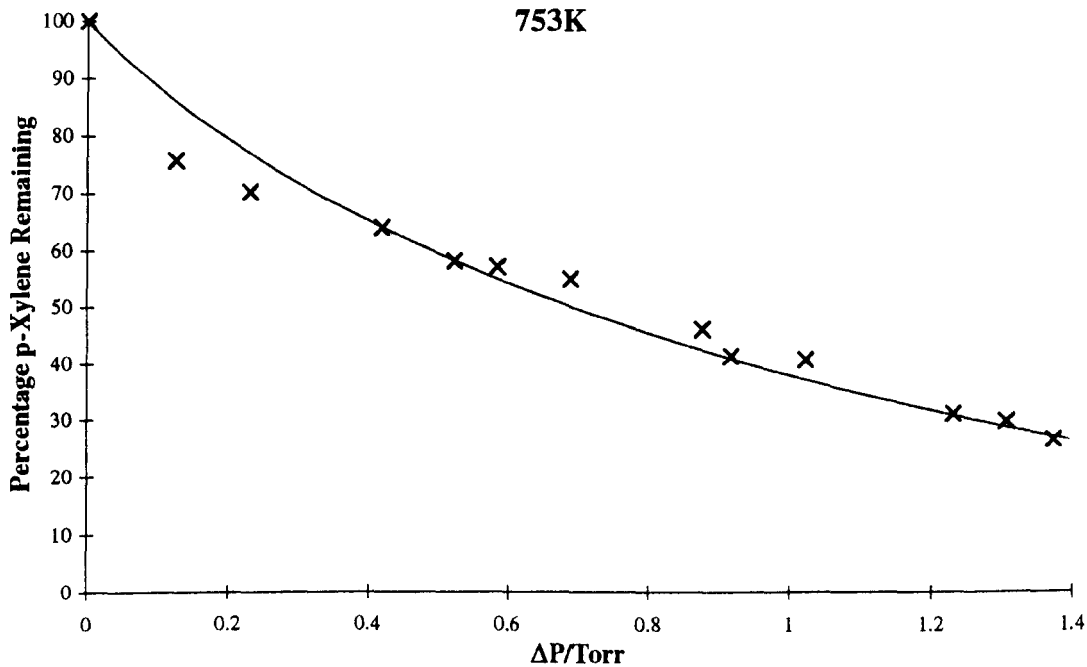


Figure 4. 6

Plot of Percentage p-Xylene Remaining vs. ΔP for 35 Torr O_2 at 753K



Figures for 0.05 Torr p-Xylene + 70 Torr Oxygen with variable Hydrogen.

Figure 4. 7

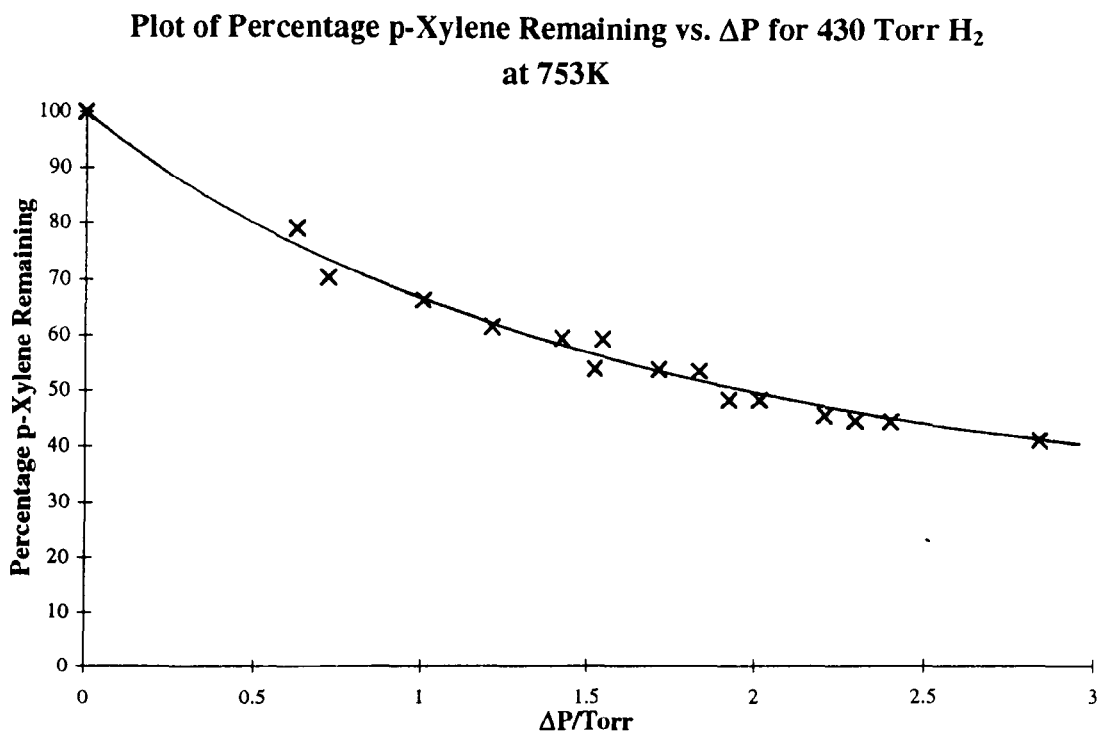


Figure 4. 8

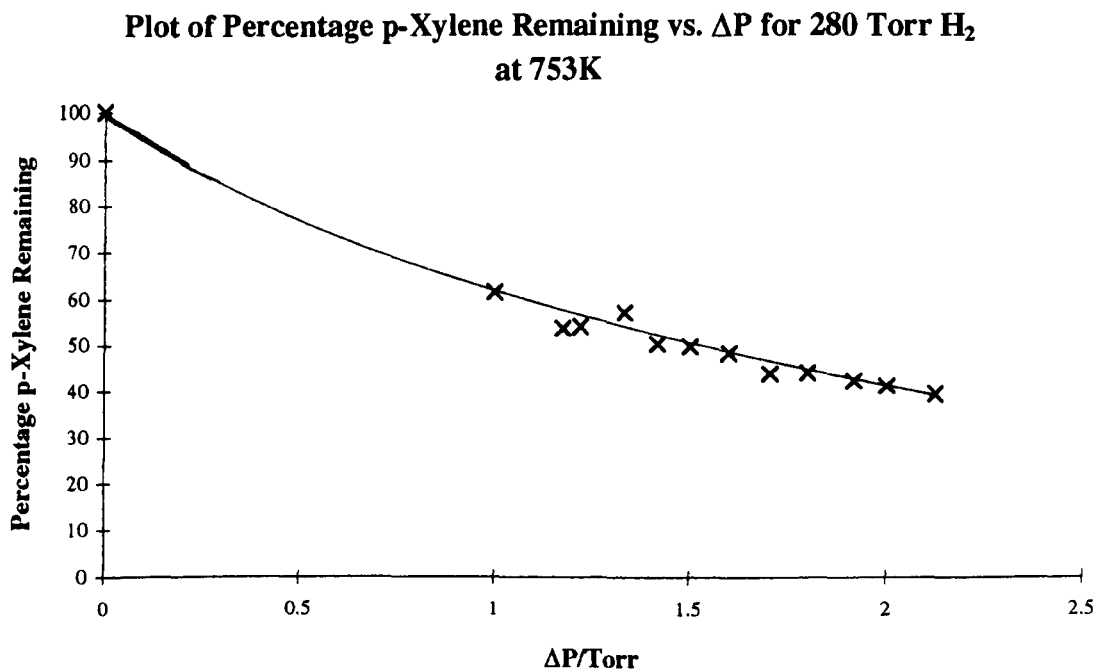


Figure 4. 9

Plot of Percentage p-Xylene Remaining vs. ΔP for 210 Torr H_2 at 753K

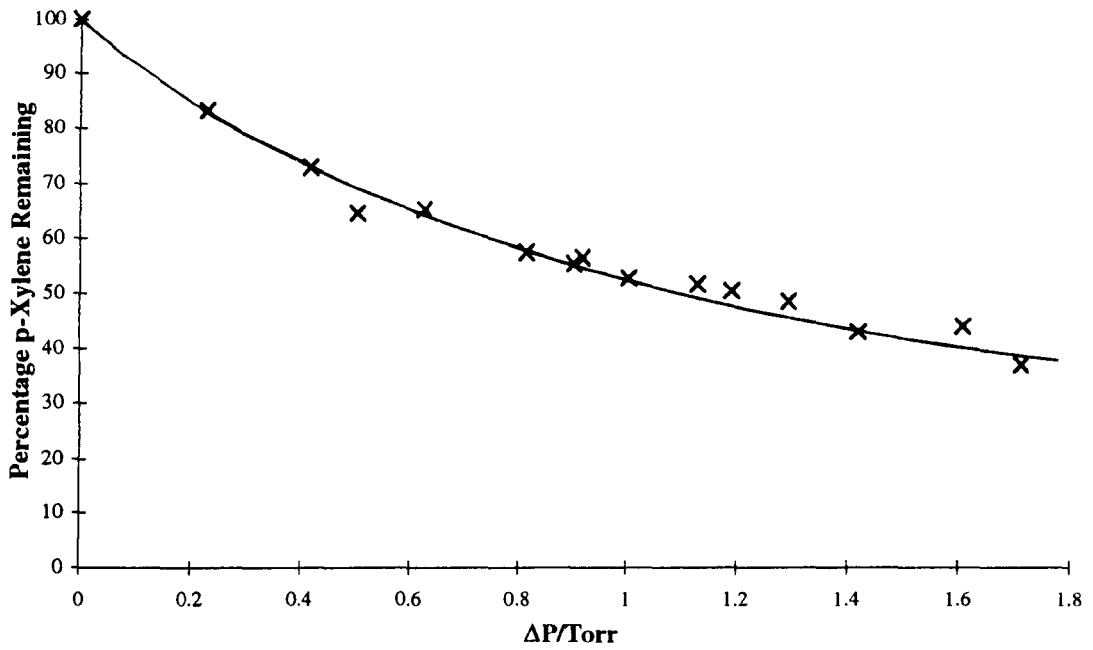


Figure 4. 10

Plot of Percentage p-Xylene Remaining vs. ΔP for 70 Torr H_2 at 753K

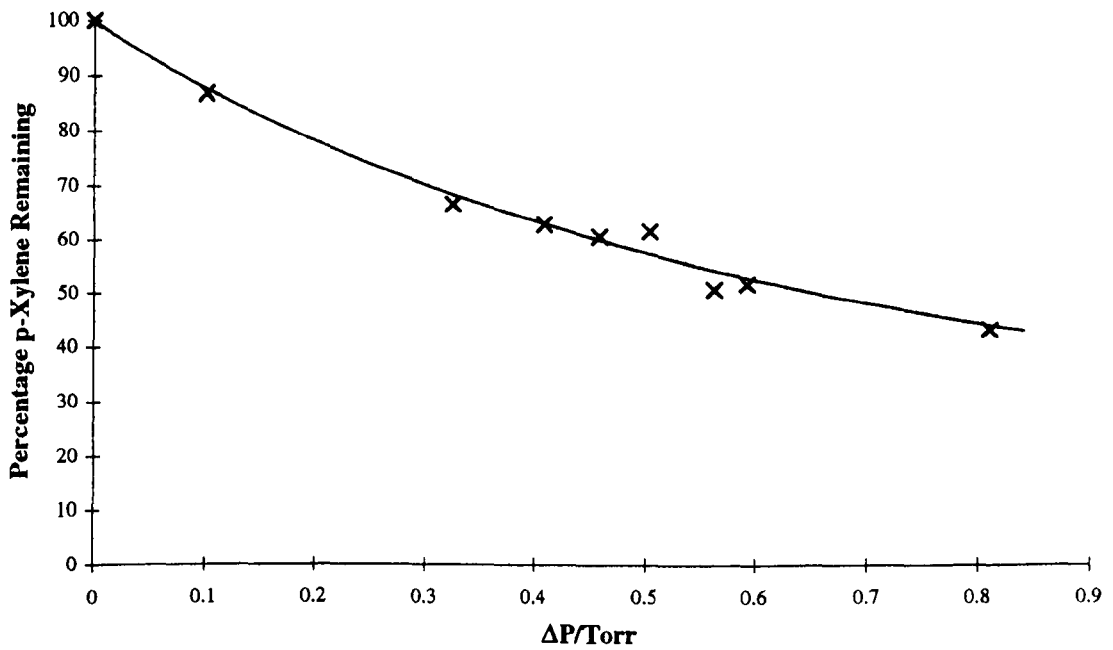
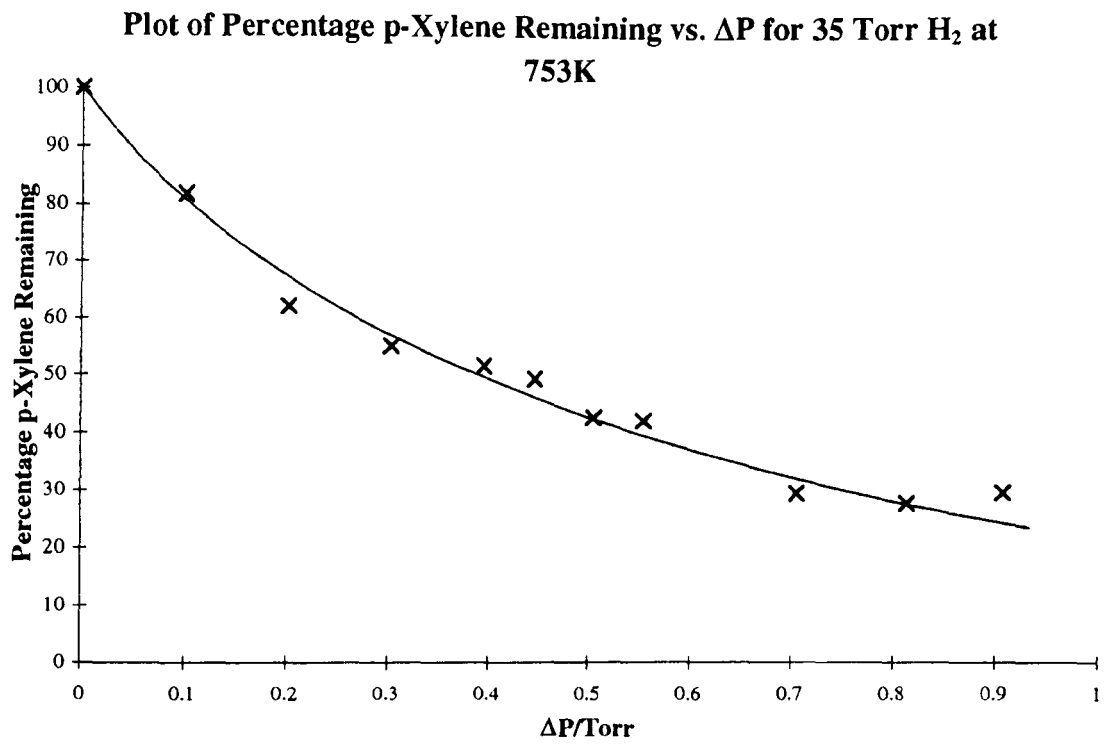


Figure 4. 11



Consumption Plots for *m*-Xylene Kinetics

Figures for 0.05 Torr *m*-Xylene + 140 Torr Hydrogen with variable Oxygen.

Figure 4. 12

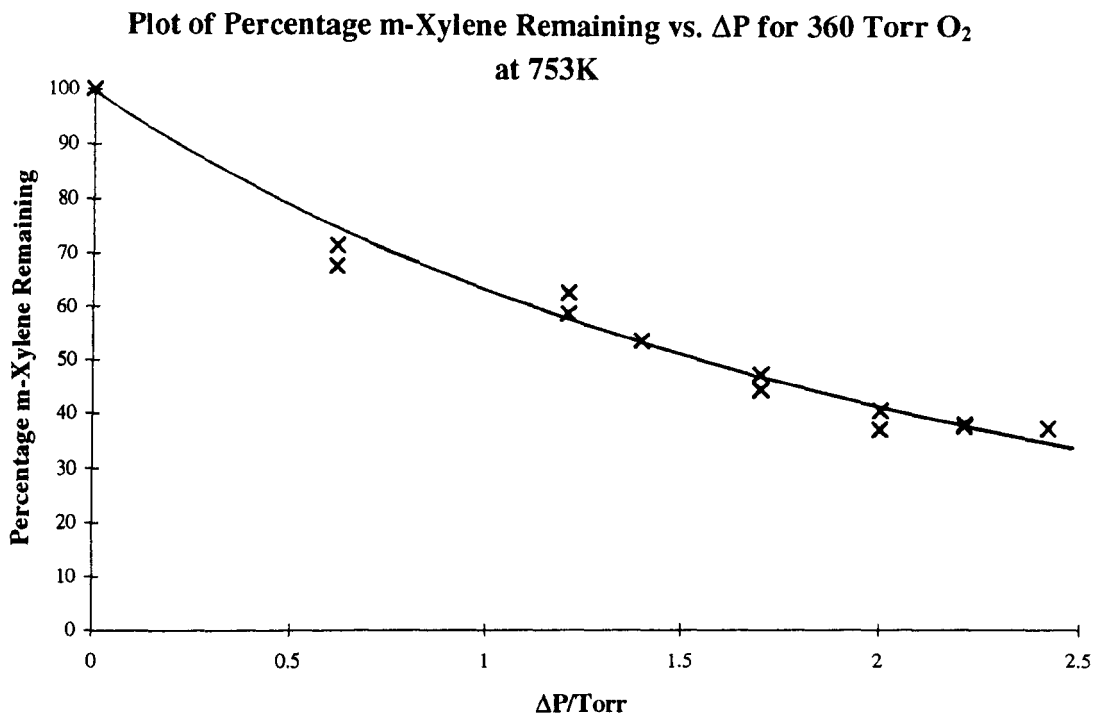


Figure 4. 13

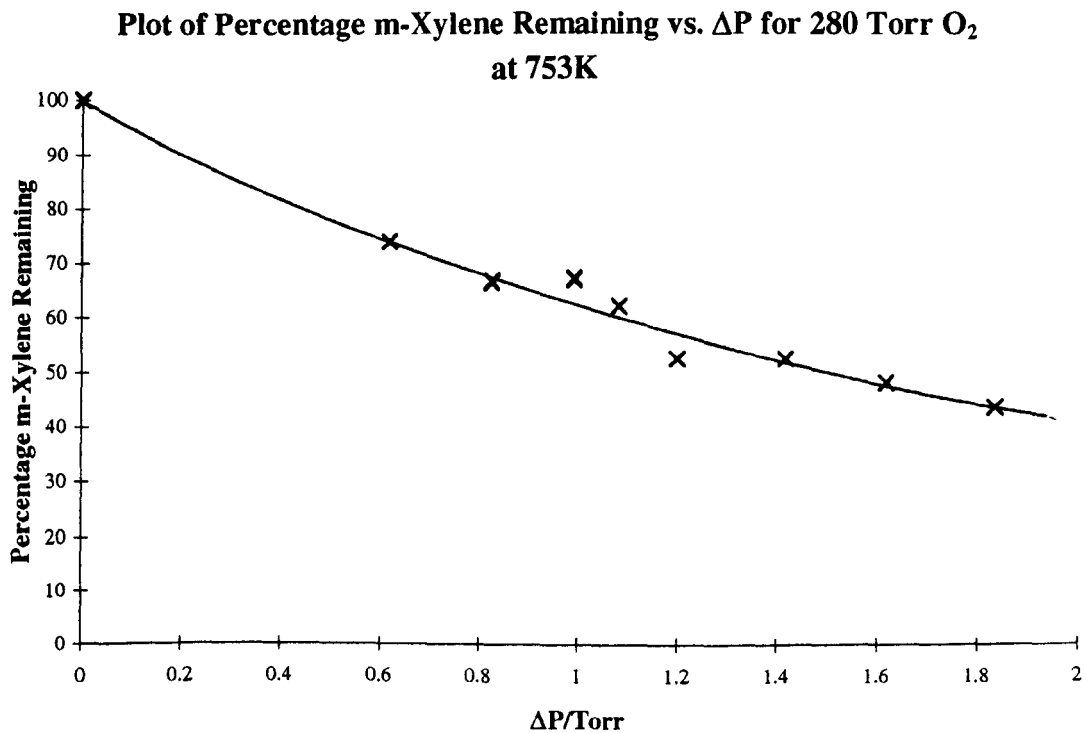


Figure 4. 14

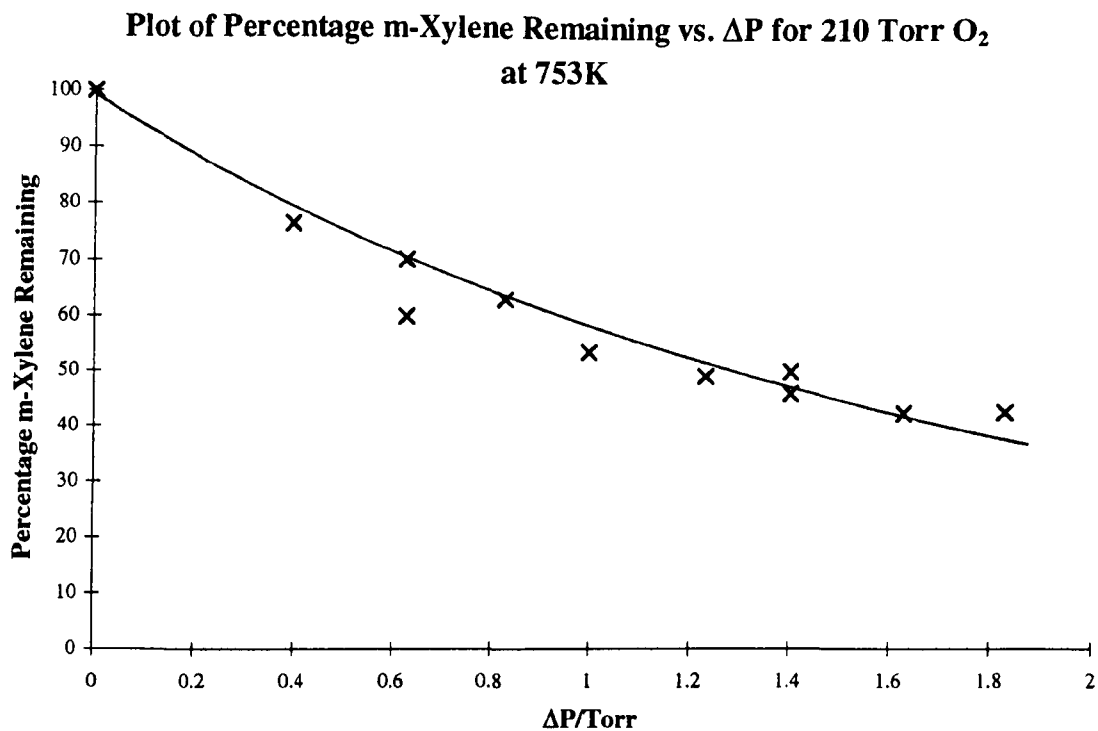


Figure 4. 15

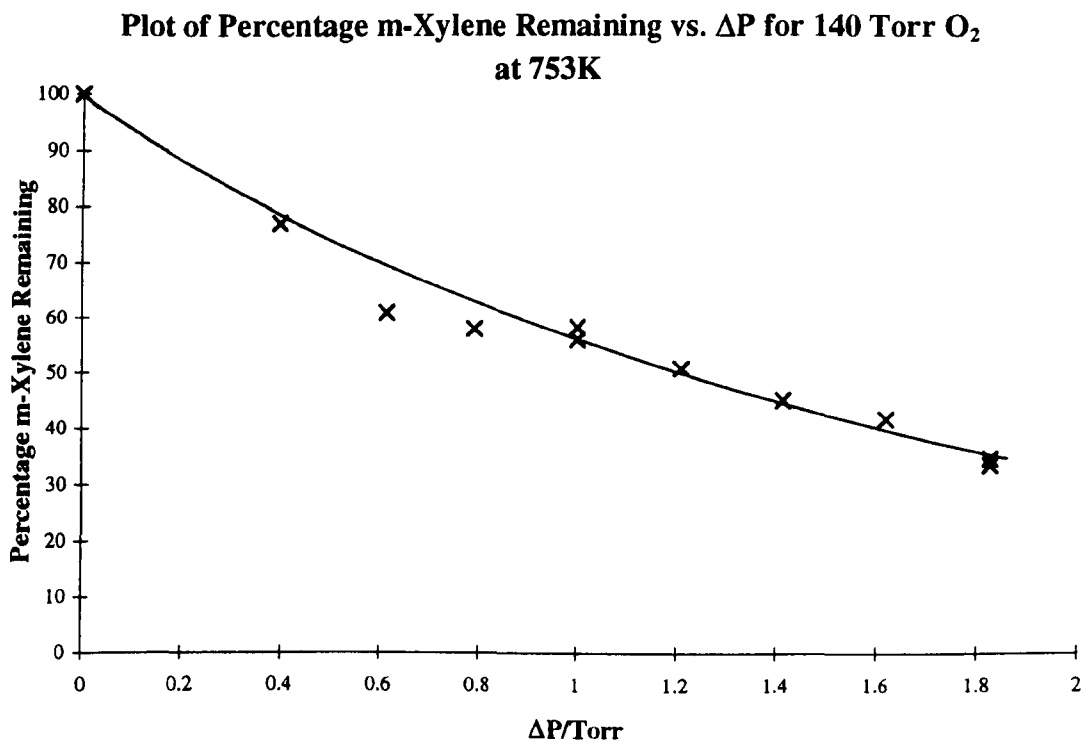


Figure 4. 16

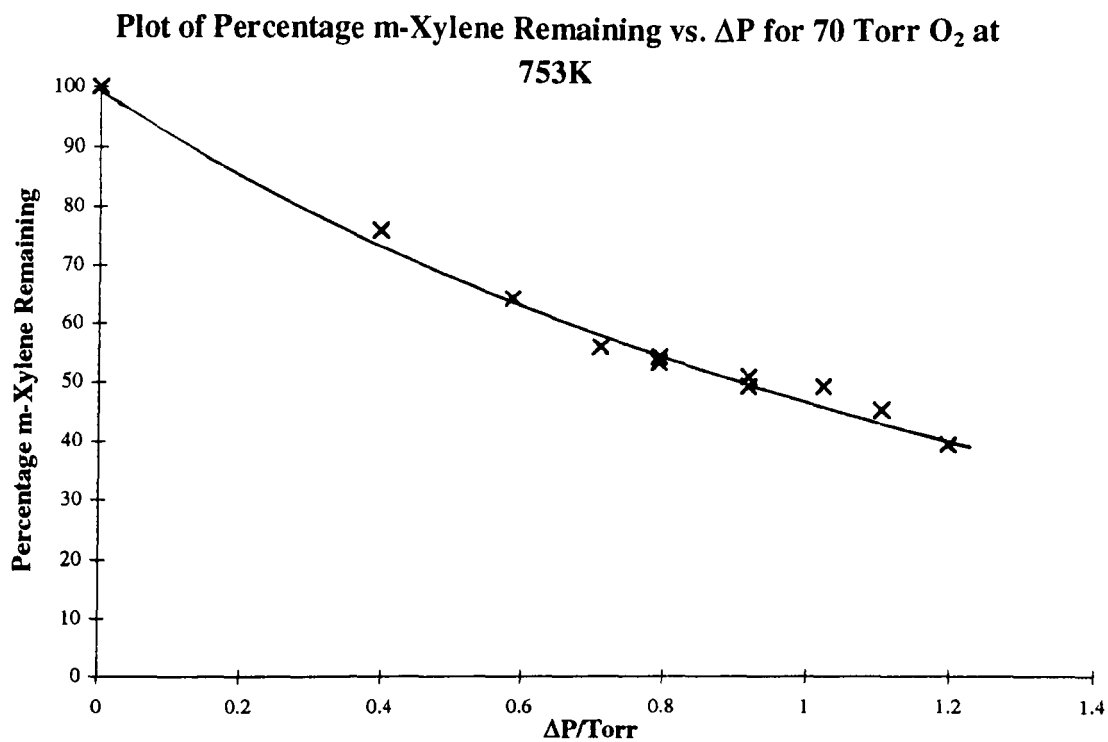
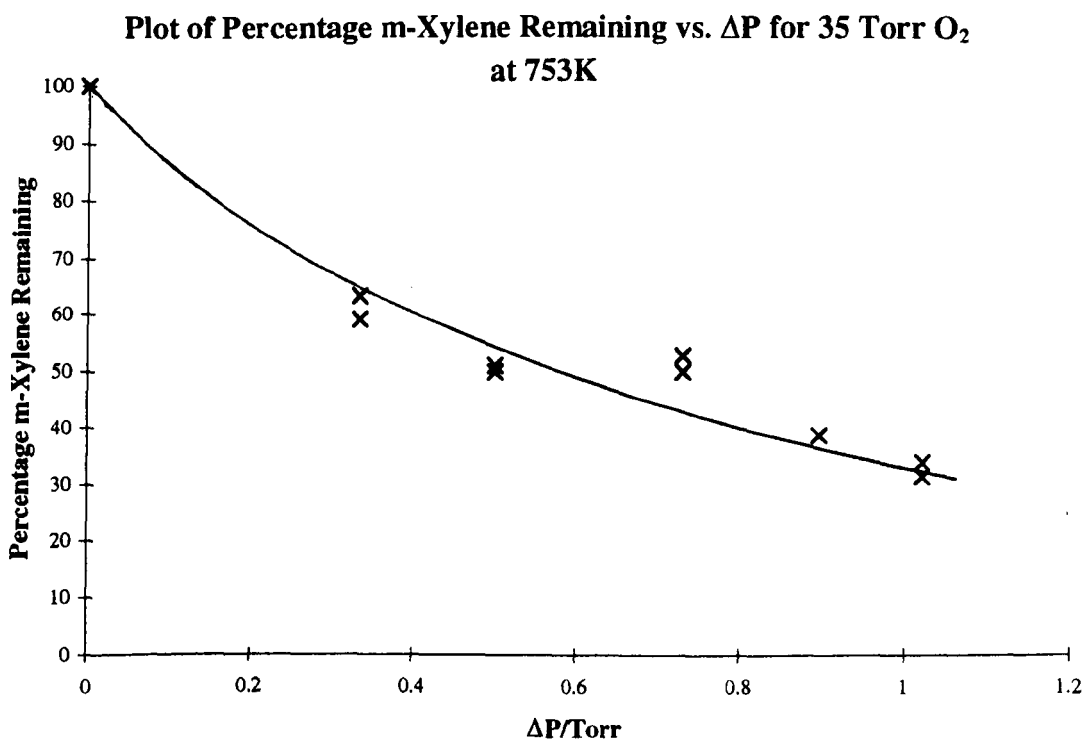


Figure 4. 17



Figures for 0.05 Torr m-Xylene + 70 Torr Oxygen with variable Hydrogen.

Figure 4. 18

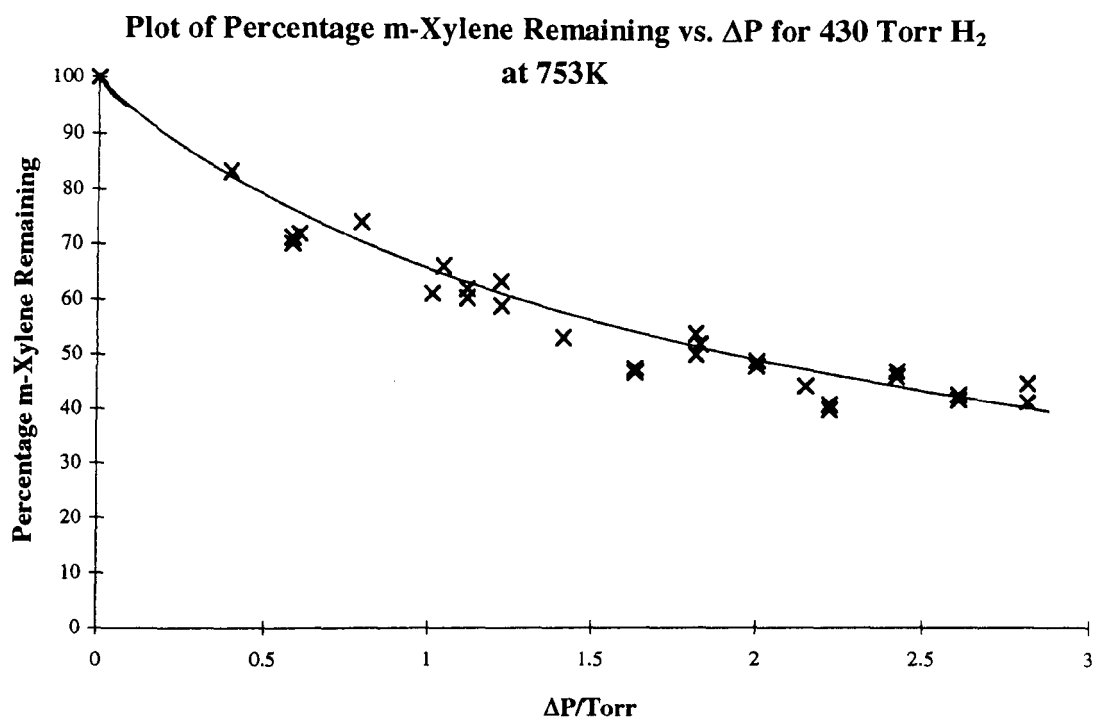


Figure 4. 19

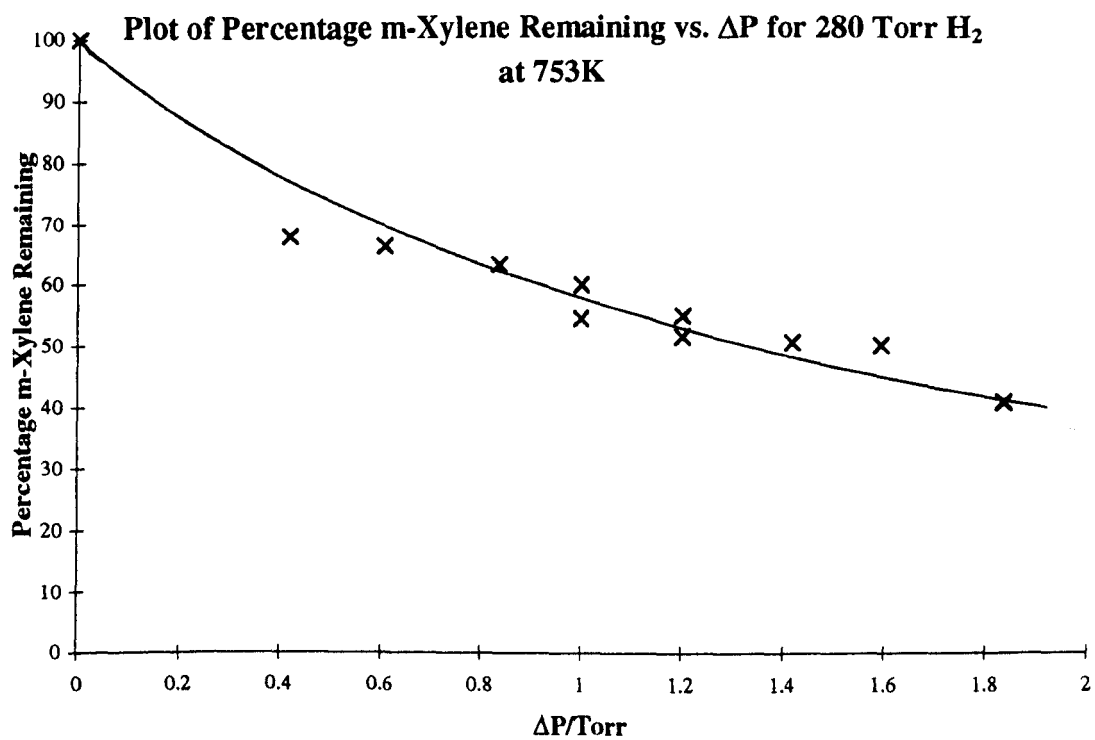


Figure 4. 20

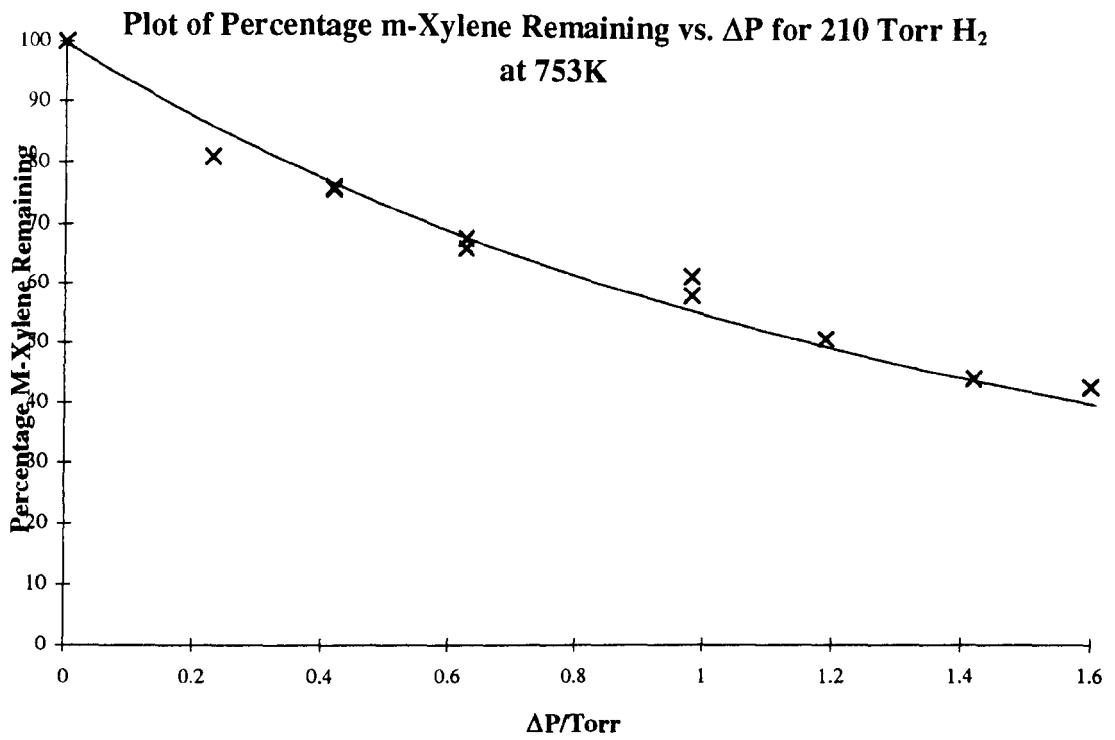


Figure 4. 21

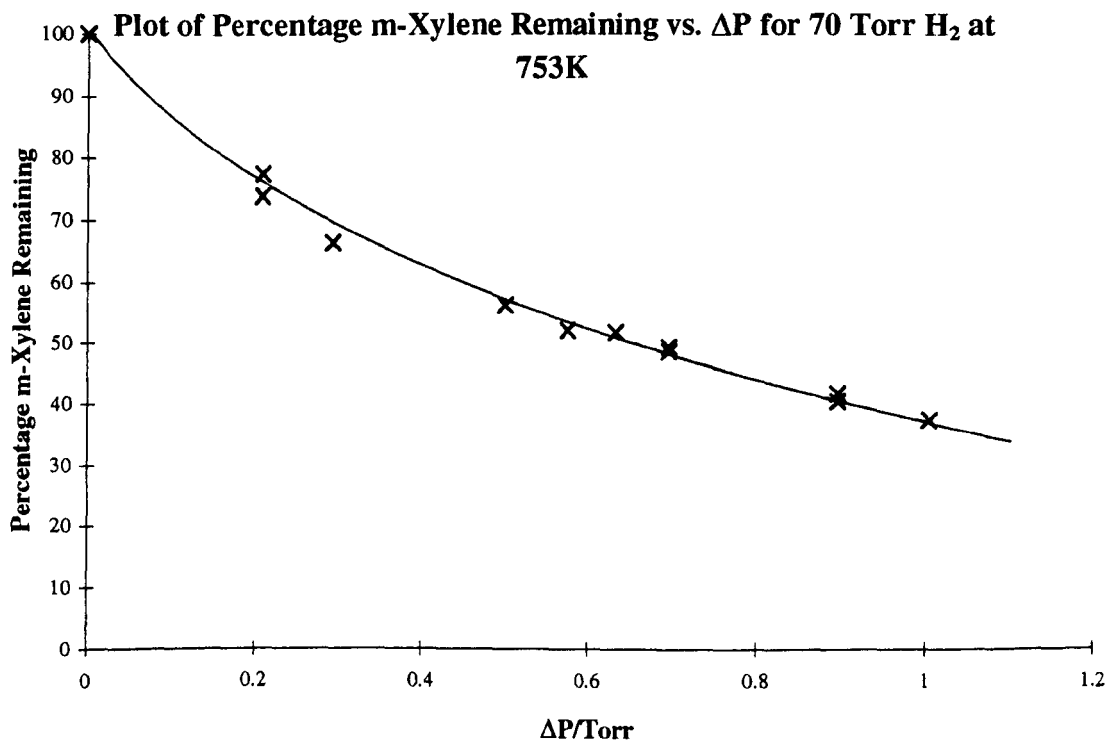
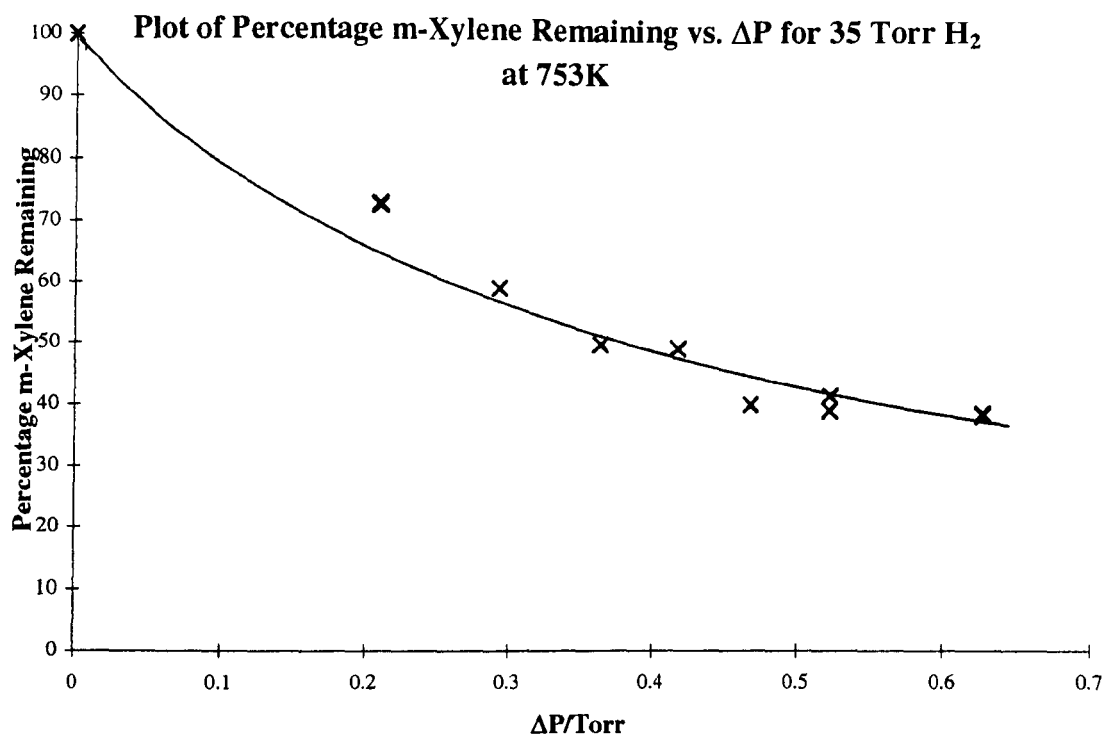


Figure 4. 22



Consumption Plots for *o*-Xylene Kinetics

Figures for 0.05 Torr *o*-Xylene + 140 Torr Hydrogen with variable Oxygen.

Figure 4. 23

Plot of Percentage *o*-Xylene Remaining vs. ΔP for 360 Torr O_2 at 753K

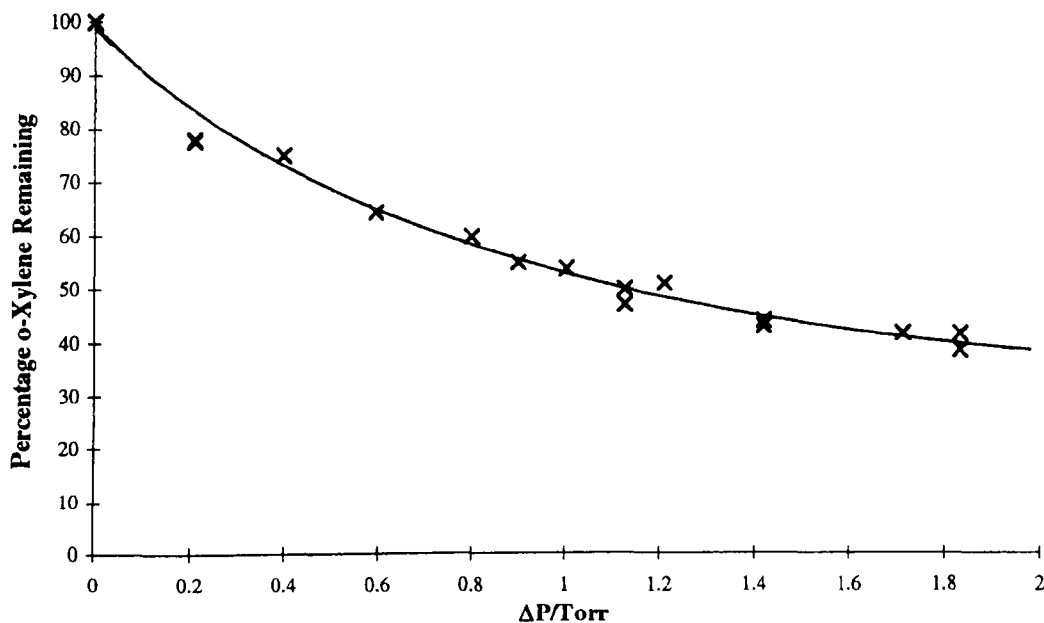


Figure 4. 24

Plot of Percentage *o*-Xylene Remaining vs. ΔP for 280 Torr O_2 at 753 K

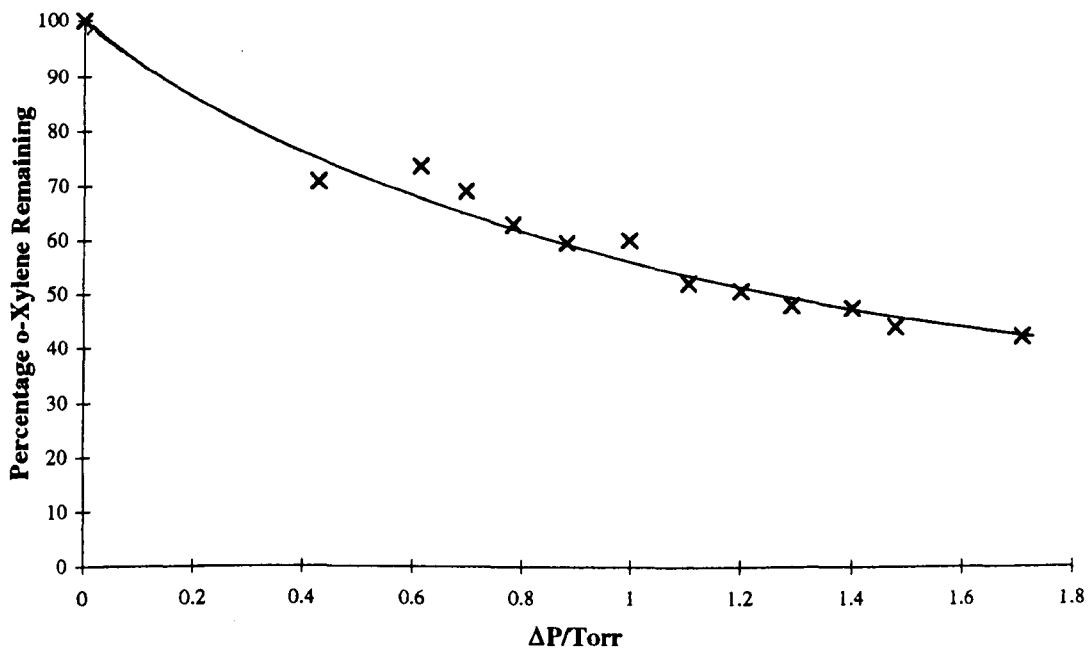


Figure 4. 25

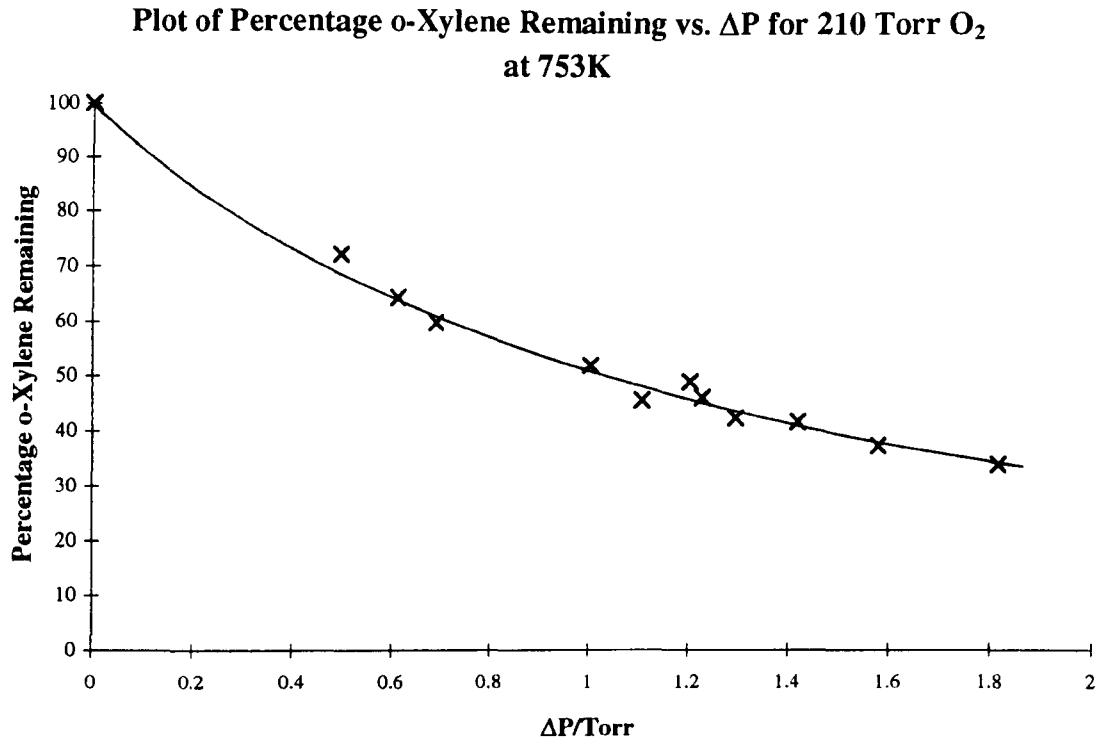


Figure 4. 26

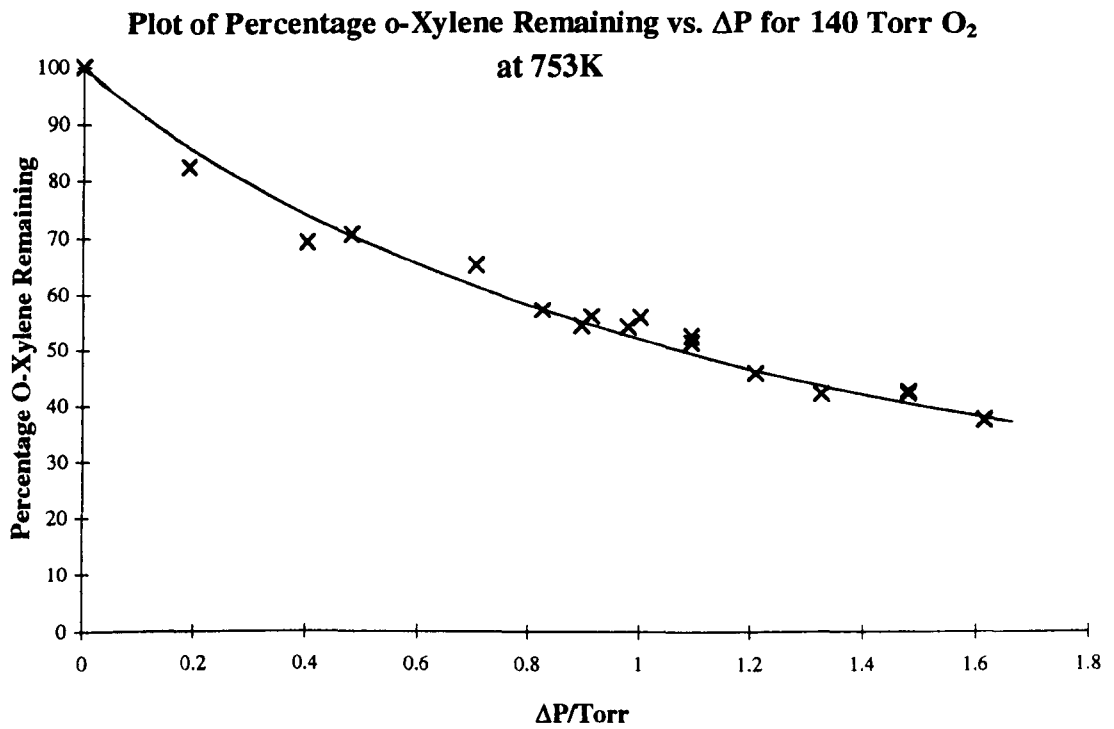


Figure 4. 27

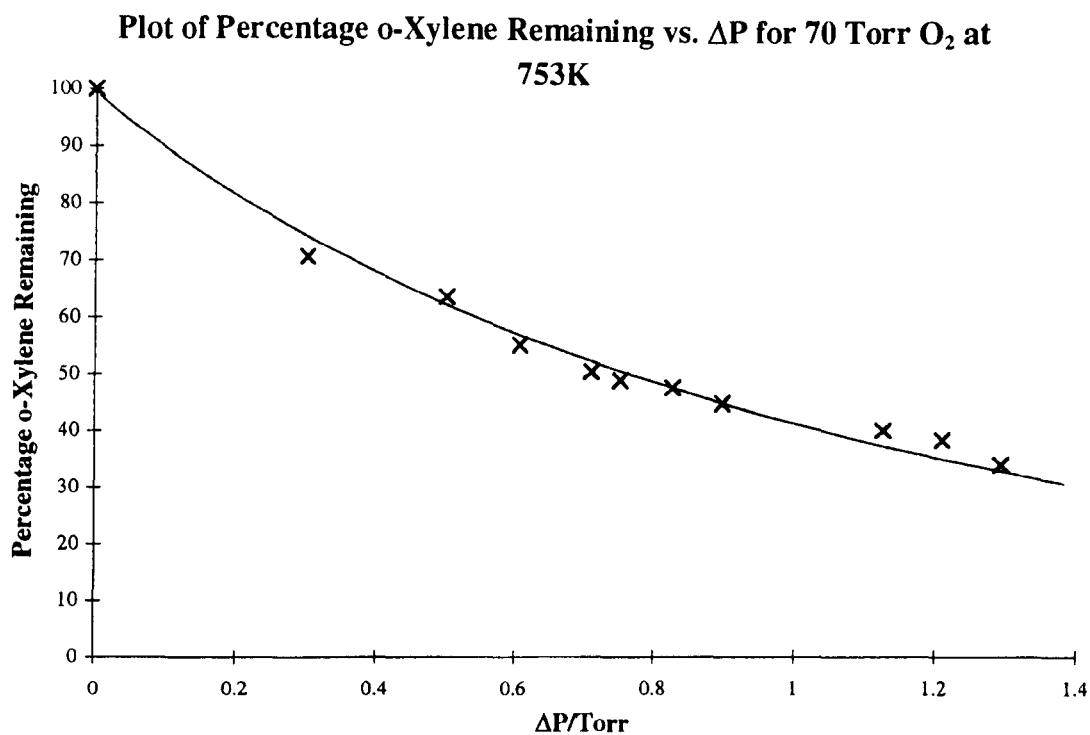
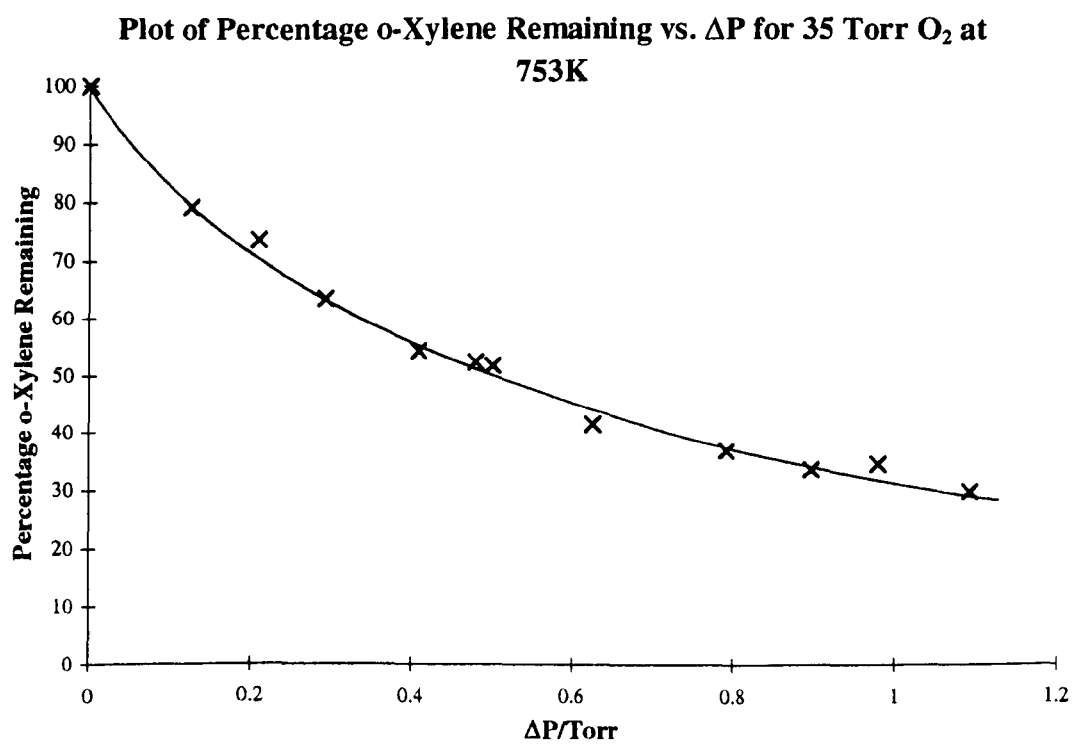


Figure 4. 28



Figures for 0.05 Torr o-Xylene + 70 Torr Oxygen with variable Hydrogen.

Figure 4. 29

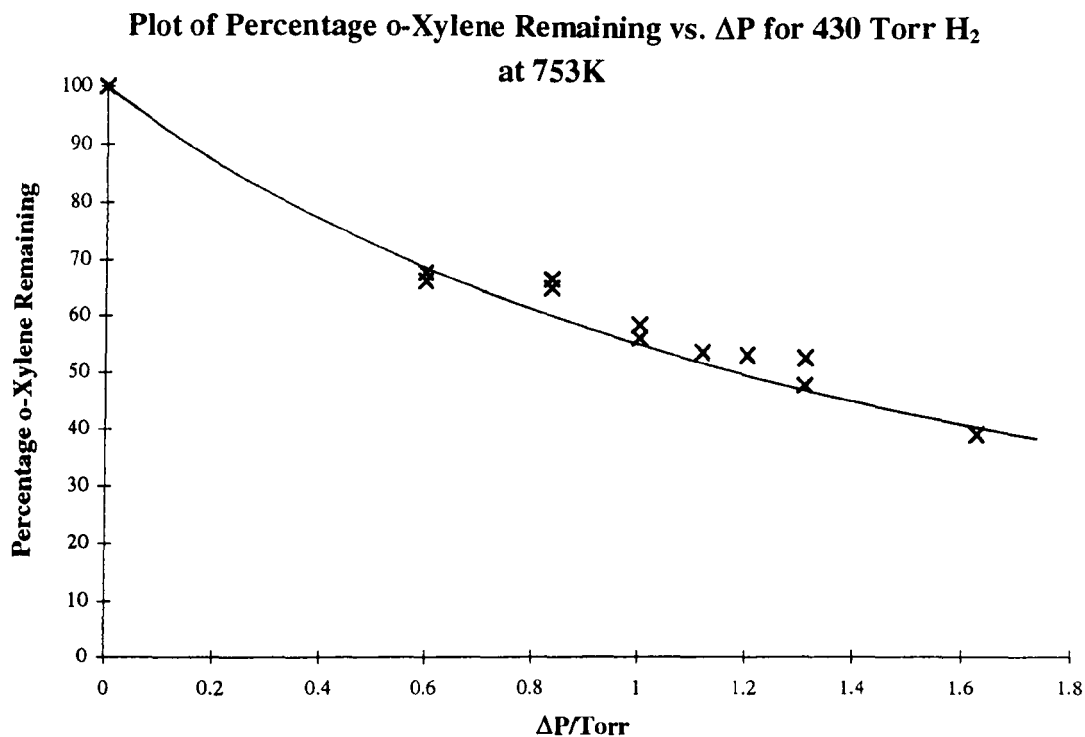


Figure 4. 30

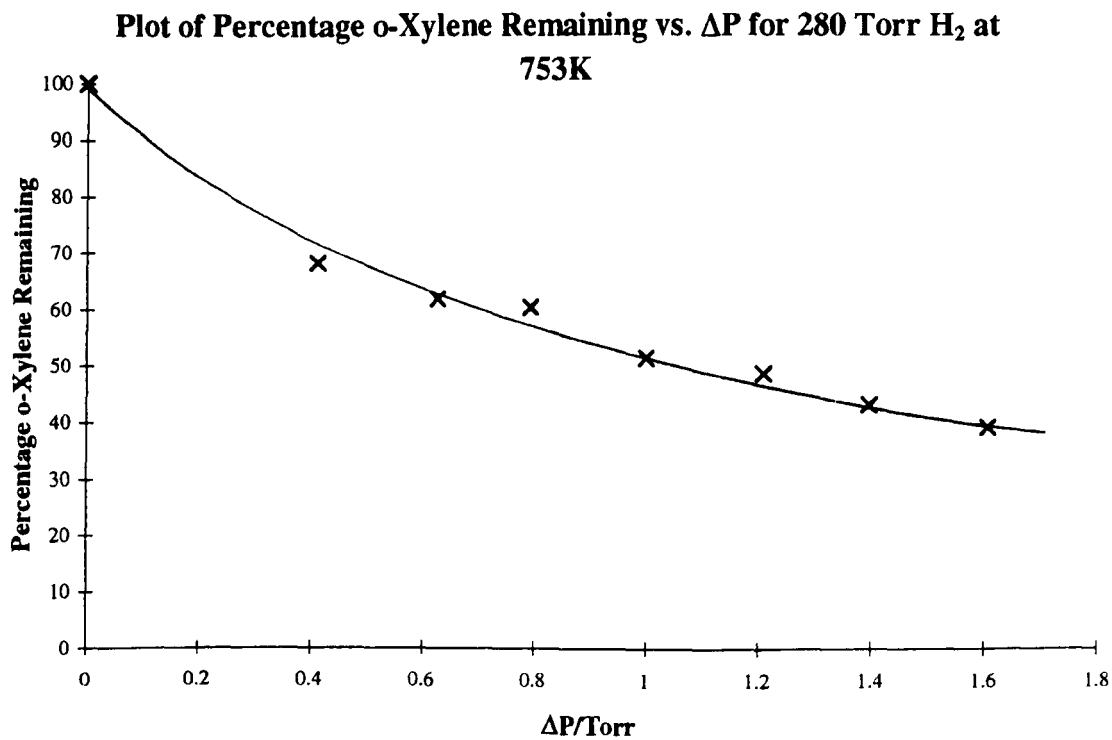


Figure 4. 31

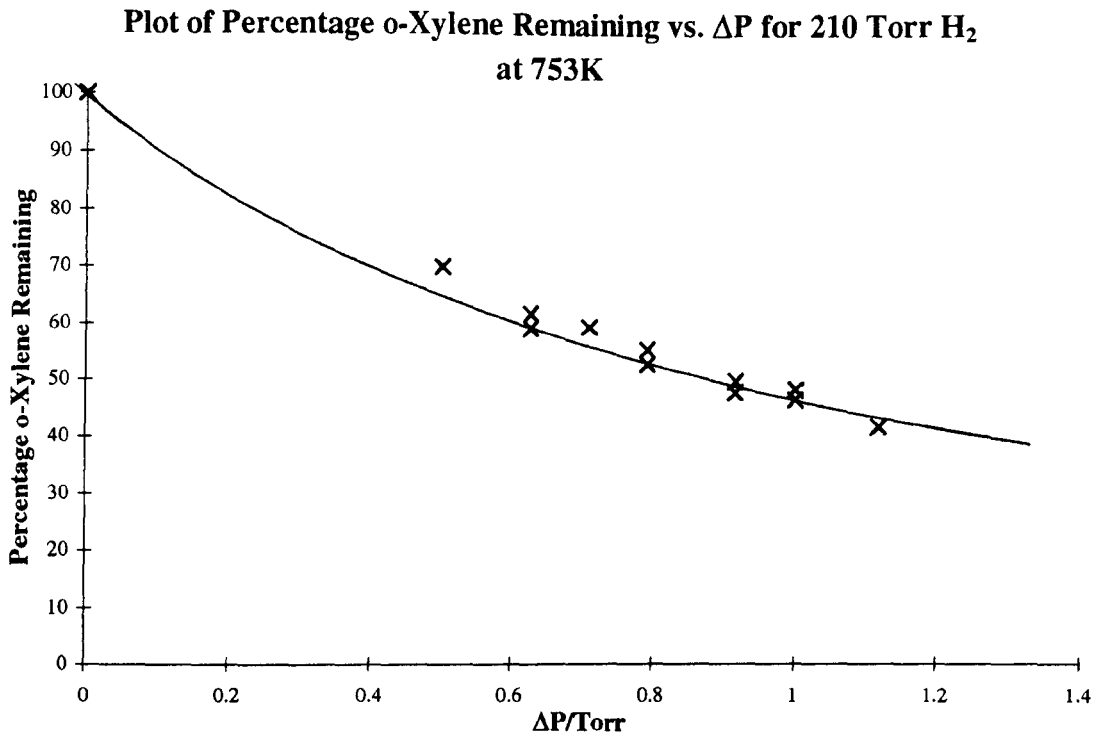


Figure 4. 32

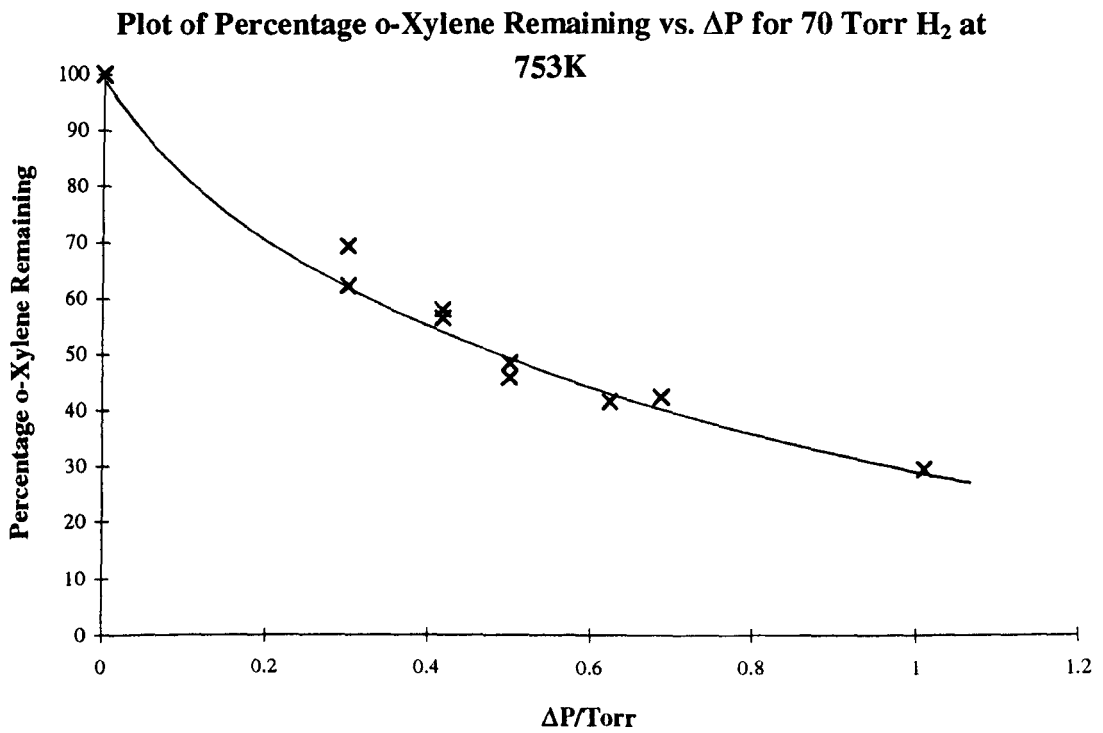
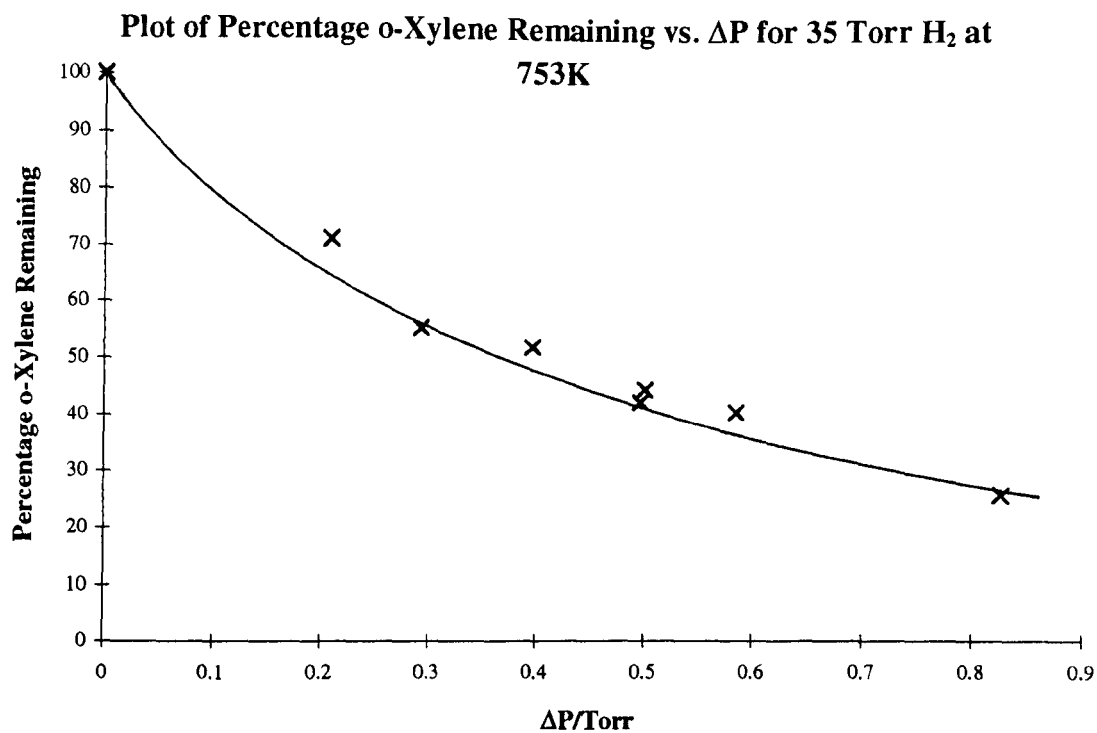


Figure 4. 33



ΔP_{50} for each mixture composition was obtained by drawing a smooth curve through the points on the graph of consumption of hydrocarbon v.s. ΔP . Curves were hand drawn using French curves rather than using a mathematical exponential fit. This is because the reactions generally follow a complex rather than a simple exponential relationship. Generally the reaction mixtures were carried out in order to obtain a large collection of points close to the position of ΔP_{50} and thus obtain as accurate a value as possible.

A summary of the ΔP_{50} values for each mixture and xylene is given in Table 4.3. These values are corrected for the 9.1% dead volume which encompasses the effect of the section of glass not enclosed in the reaction furnace.

The results display an increase in ΔP_{50} as either oxygen or hydrogen increases, as found with other additives (Figures 4.34 and 4.35). The overall relative reactivity of each xylene in the $H_2 + O_2$ mixtures can be illustrated from a simple inspection of the ΔP_{50} values. The results show p-xylene and m-xylene are similar in reactivity and o-xylene is slightly more reactive as seen by the lower ΔP_{50} values; this is in agreement with the conclusions of Wright^{3,4}. For each xylene, ΔP_{50} increases more noticeably with increasing H_2 than with increasing O_2 pressure. This is consistent with the OH radical being the major attacking species.

The results will be discussed, together with the computer program used to interpret the results and obtain the key relative rate constants, in Chapter 7.

Table 4. 3: Summary of ΔP_{50} values for the addition of each Xylene to the Hydrogen + Oxygen reaction. All values are corrected for the dead volume. Total Pressure is 500 Torr for all mixtures.

Pressure H ₂ / Torr	Pressure O ₂ / Torr	ΔP_{50} / Torr		
		p-Xylene	m-Xylene	o-Xylene
140	360	1.76	1.76	1.48
140	280	1.62	1.65	1.31
140	210	1.57	1.54	1.24
140	140	1.34	1.35	1.15
140	70	1.12	0.99	0.84
140	35	0.78	0.75	0.55
430	70	2.10	2.11	1.53
280	70	1.59	1.52	1.24
210	70	1.23	1.29	1.01
70	70	0.69	0.69	0.53
35	70	0.45	0.42	0.37

Figure 4. 34 : Variation of ΔP_{50} with Oxygen Pressure

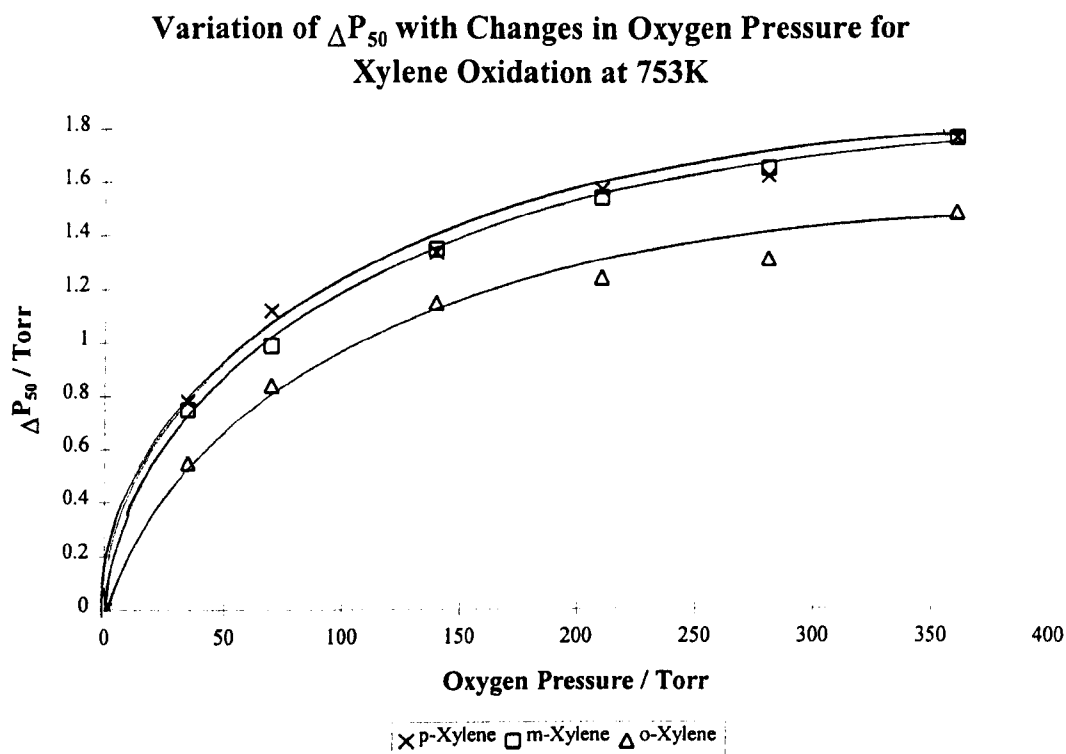
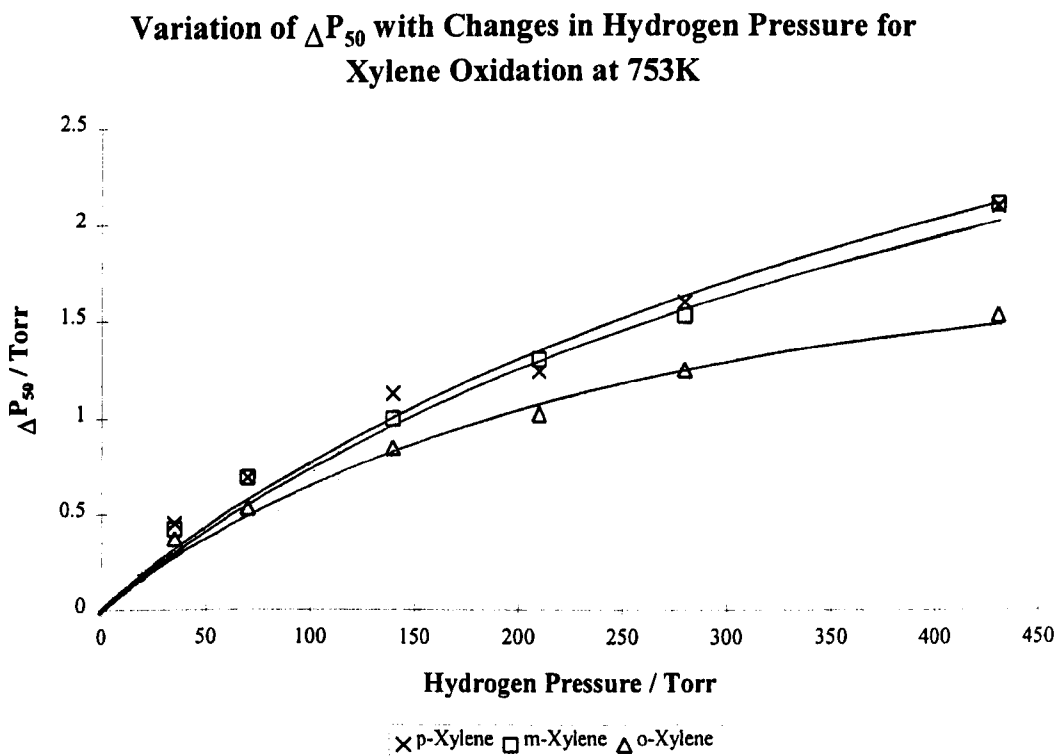


Figure 4. 35 : Variation of ΔP_{50} With Hydrogen Pressure.



4.2. References.

¹ Baker R.R., *Ph.D. Thesis, University of Hull*, 1969.

² Keen A., *Ph.D. Thesis, University of Hull*, 1989.

³ Wright F.J., *J. Phys. Chem.*, **64**, 1944, (1960).

⁴ Wright F.J., *J. Phys. Chem.*, **66**, 2023, (1962).

Chapter 5.

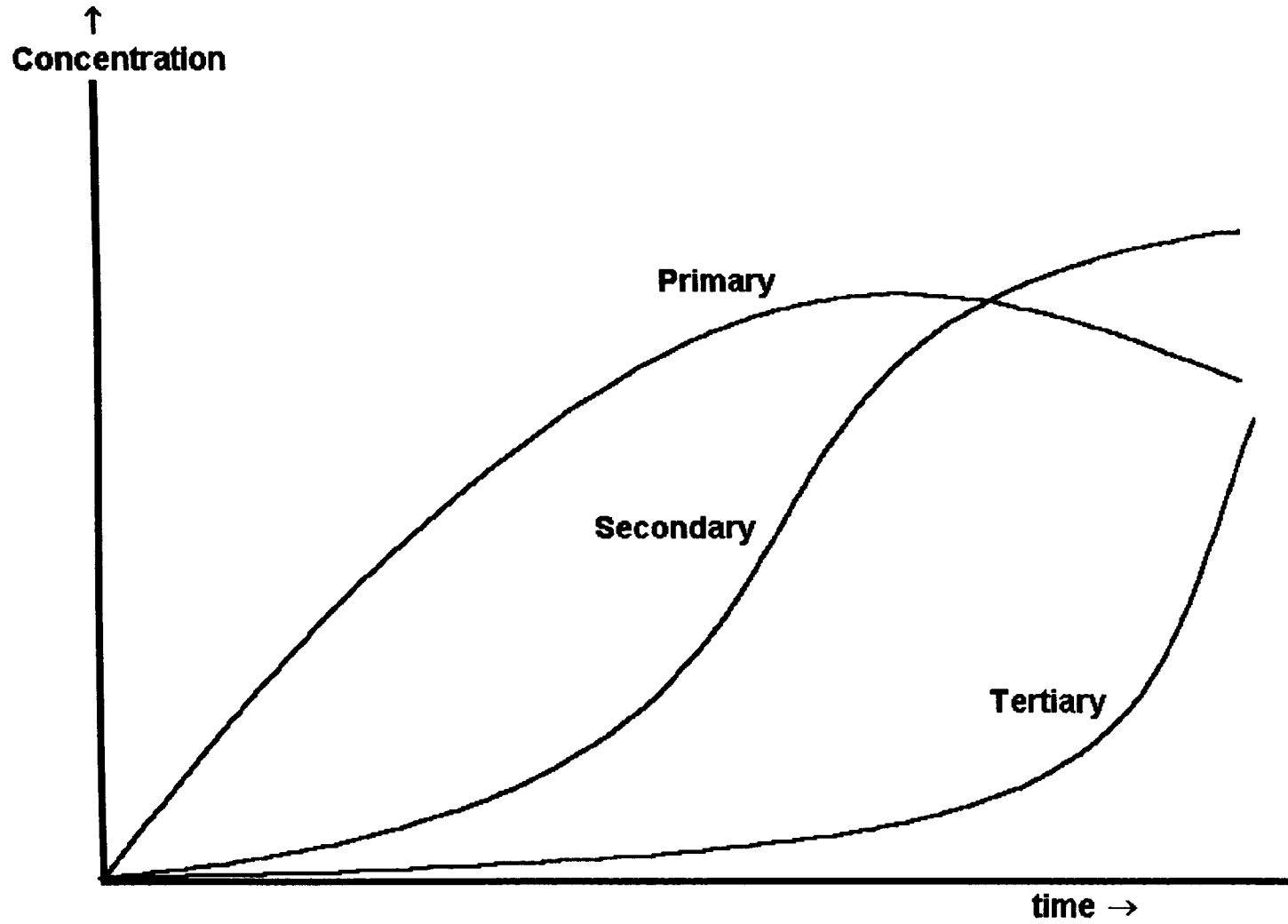
Results of the Analytical Experiments for the Oxidation of the Xylenes.

The separate addition of small amounts of each xylene to mixtures of hydrogen + oxygen at 480°C has also been used to elucidate the mechanism of their oxidation using the approach as described in Chapter 2.

The concentration of each xylene was increased from the 0.01% used in the kinetic study to 0.5% in order to enable more accurate detection of the products by gas chromatography particularly in the early stages of oxidation. This increase in the xylene concentration was found to have a minor, but not overly significant, effect on the maximum rate and induction period of the hydrogen + oxygen reaction (Table 4.2). The possibility of increasing the xylene concentration to 1.0% was discounted due to a tailing effect on the xylene peaks such that accurate measurement of the xylene concentration became very difficult.

The shape of the product profiles can give a good indication as to whether the product is formed in a primary, secondary or tertiary process (Figure 5.1). Primary products are ones which are produced effectively from the parent molecule whereas secondary or tertiary products are formed by the subsequent reactions of the primary or secondary molecular products, respectively.

Figure 5. 1: Primary, secondary and tertiary product profiles.



The auto-catalytic nature of the hydrogen + oxygen reaction means that plots of '*Pressure of Product*' vs. '*Reaction Time*' are of limited value here. In their place, plots of '*Pressure of Product*' vs. '*Pressure of Xylene Consumed*' are presented which give a clearer indication as to whether a product is primary, secondary or tertiary. The degree of consumption of the xylene is determined by difference using gas chromatography in the same manner as for the kinetic results discussed in Chapter 4.

All of the experiments were carried out at 480°C and 500 Torr total pressure in an aged boric-acid-coated Pyrex reaction vessel, as described in Chapter 3. Three reaction mixtures were chosen, as shown in Table 5.1 which give a wide variation in the radical pool and in the [H₂]:[O₂] ratio.

The variation in the oxygen pressure by a factor of 5 allows mechanisms to be tested, particularly where product yields are very sensitive to O₂ pressure. Similarly, the change in hydrogen pressure by a factor of 3 may be used in a similar way.

A detailed discussion of the product results will be given in a Chapter 8. A short summary is included here.

5.1. Xylene Product Summary.

The primary products generated agreed with those found by other workers¹⁻⁶, being benzaldehyde (**BA**), the isomeric tolualdehyde (**OTA**, **MTA**, **PTA**) and toluene (**T**), o-xylene also produces o-xylylene oxide (phthalan) (**OXO**) (Table 5.2).

Products such as dibenzyl and CH₃-Ph-CH₂-CH₂-Ph-CH₃ were not detected in the product analysis. The vapour pressure of dibenzyl in the literature⁷ is **0.0212Torr** at

Table 5. 1: Summary of Reaction Mixture Compositions Used For Product Study.

Pressure of Gas / Torr			
Hydrogen	Oxygen	Nitrogen	Xylene
140.0	357.5	0.0	2.5
140.0	70.0	287.5	2.5
427.5	70.0	0.0	2.5

Table 5. 2 : Summary of the Products from the oxidation of the Xylenes at 753K.

p-Xylene	o-Xylene	m-Xylene	1°, 2°, 3° Product
p-Tolualdehyde	o-Tolualdehyde	m-Tolualdehyde	Primary
	o-Xylylene oxide		Primary
Toluene			Primary
Benzaldehyde			Secondary
Benzene			Tertiary
Methane			Primary

25°C. It was concluded that should any of these dibenzyl-based compounds form they would condense on the surface of the lines outside the reaction vessel and on the surface of the sample bulbs and thus would not be detected using gas chromatography. Without doubt, quantitative analysis would be impossible.

The possibility of heating sections of the apparatus and sampling bulbs to prevent products from condensing was regarded as impractical with the probability of increasing error in the detection of the non-condensable products.

Figures 5.2, 5.8 and 5.14 show the degree of consumption of p-, m- and o-xylene respectively measured against time.

Figures 5.3 - 5.7 show the variation of p-xylene products with the variation of p-xylene consumption.

Figures 5.9 - 5.13 show the variation of m-xylene products with the variation of m-xylene consumption.

Figures 5.15 - 5.20 show the variation of o-xylene products with the variation of o-xylene consumption.

Tables 5.3 - 5.5 show the variation of p-xylene products with the variation of p-xylene consumption.

Tables 5.6 - 5.8 show the variation of m-xylene products with the variation of m-xylene consumption.

Tables 5.9 - 5.11 show the variation of o-xylene products with the variation of o-xylene consumption.

Tables 5.12 - 5.14 show the variation of xylene consumption with time.

Profiles for p-Xylene Addition to the $H_2 + O_2$ Reaction at 753K and 500 Torr Total Pressure.

Figure 5. 2

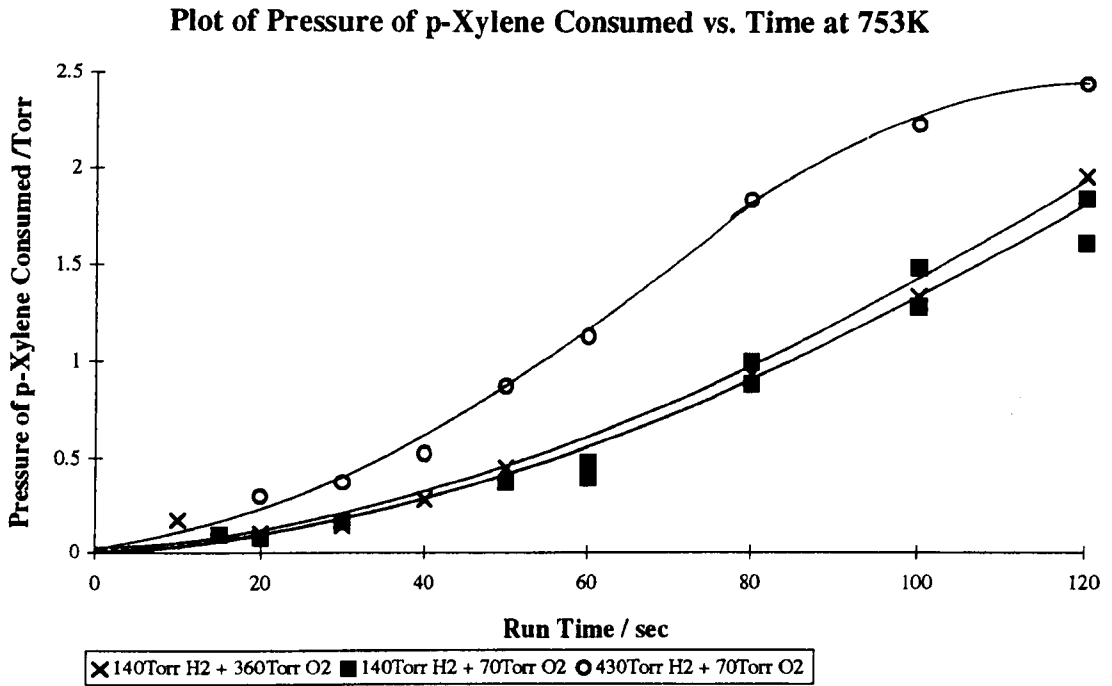


Figure 5. 3

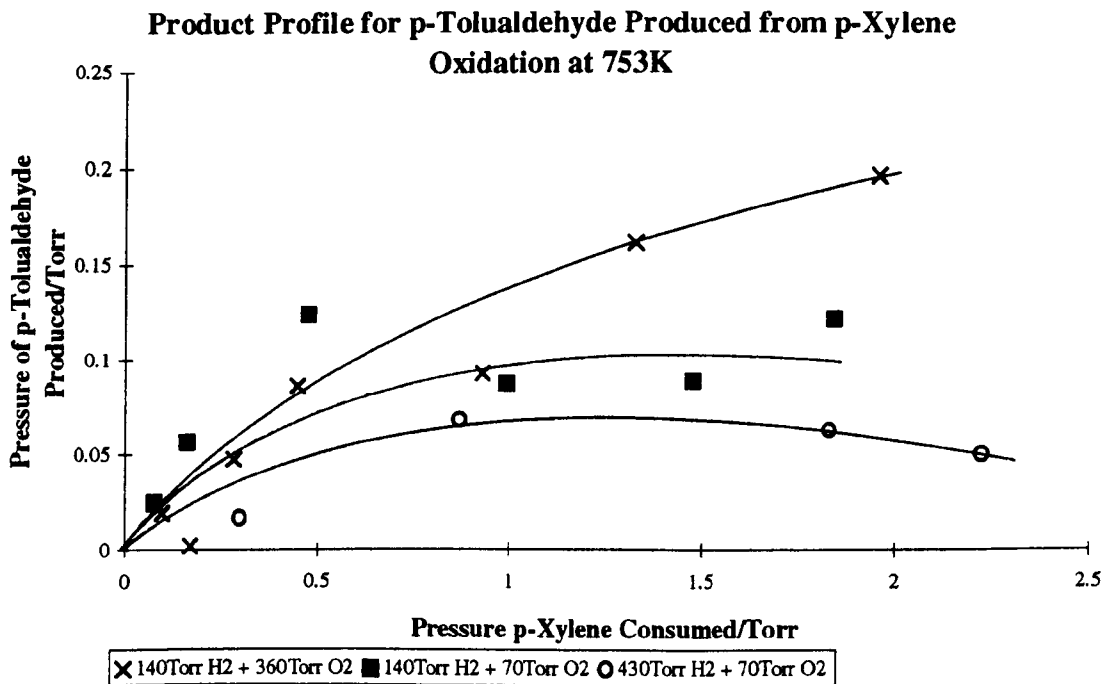


Figure 5. 4

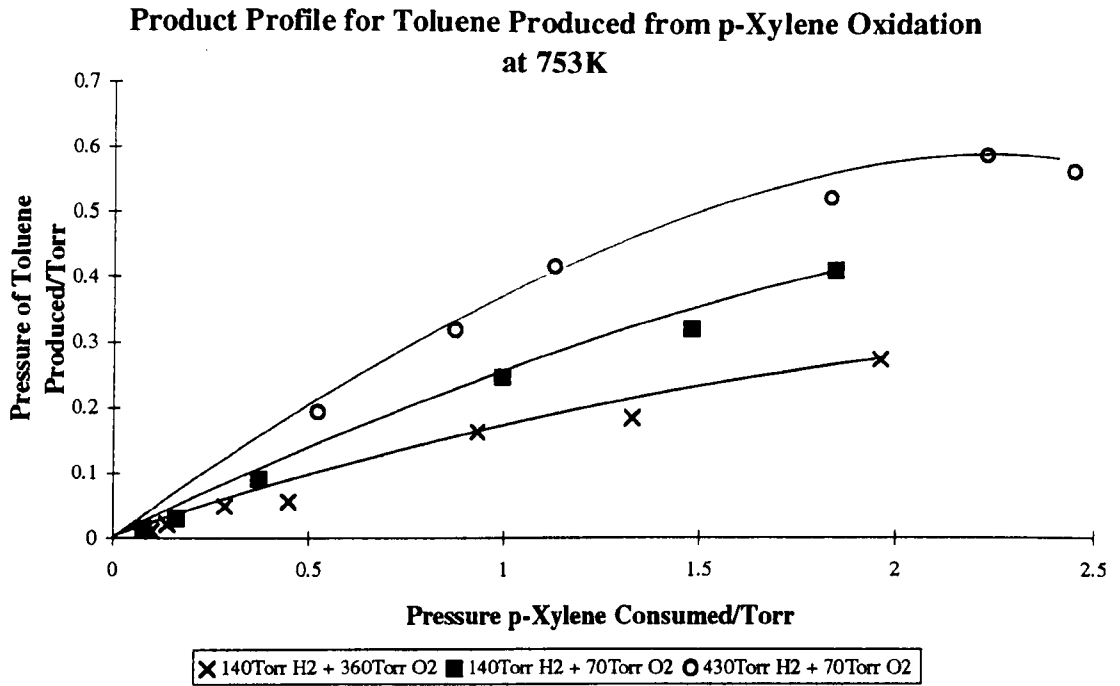


Figure 5. 5

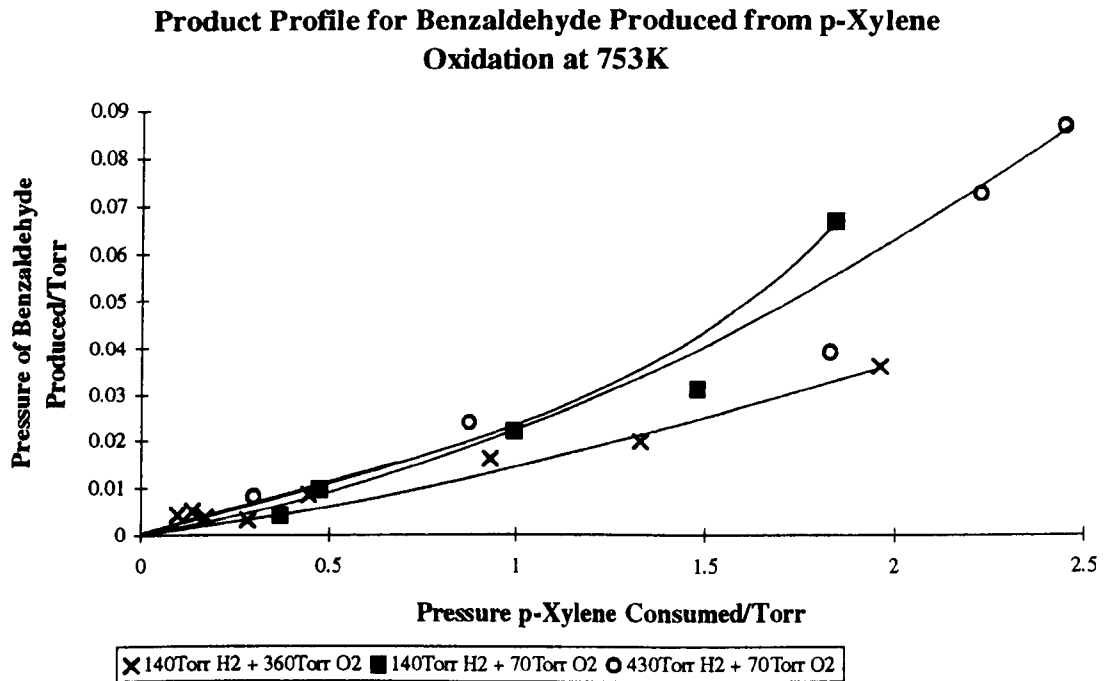


Figure 5.6

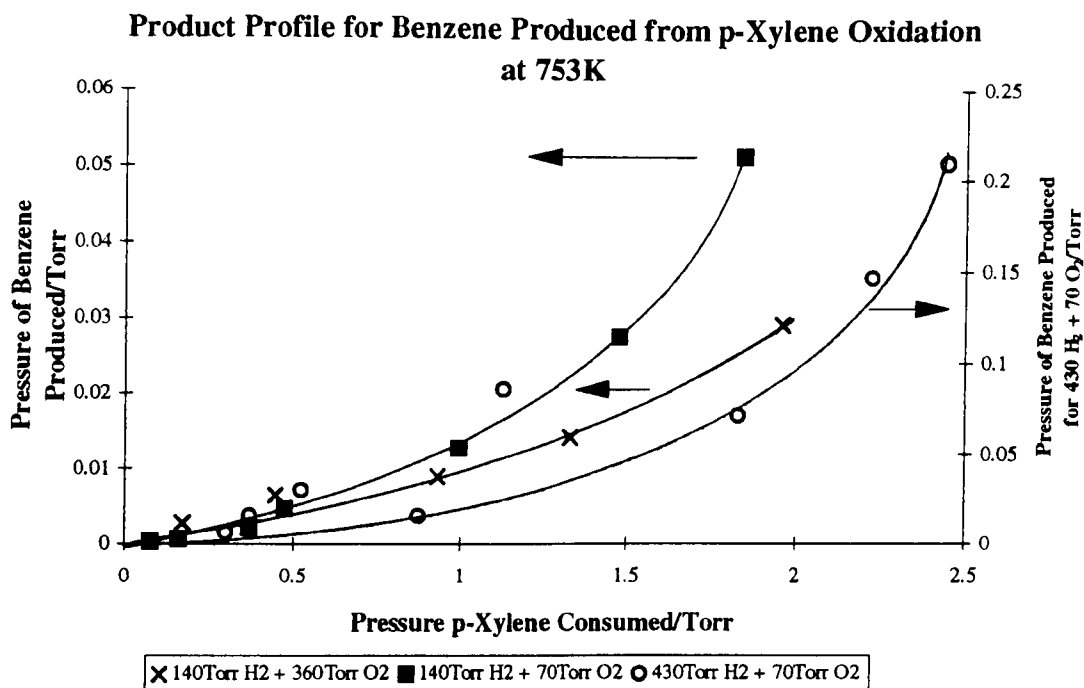
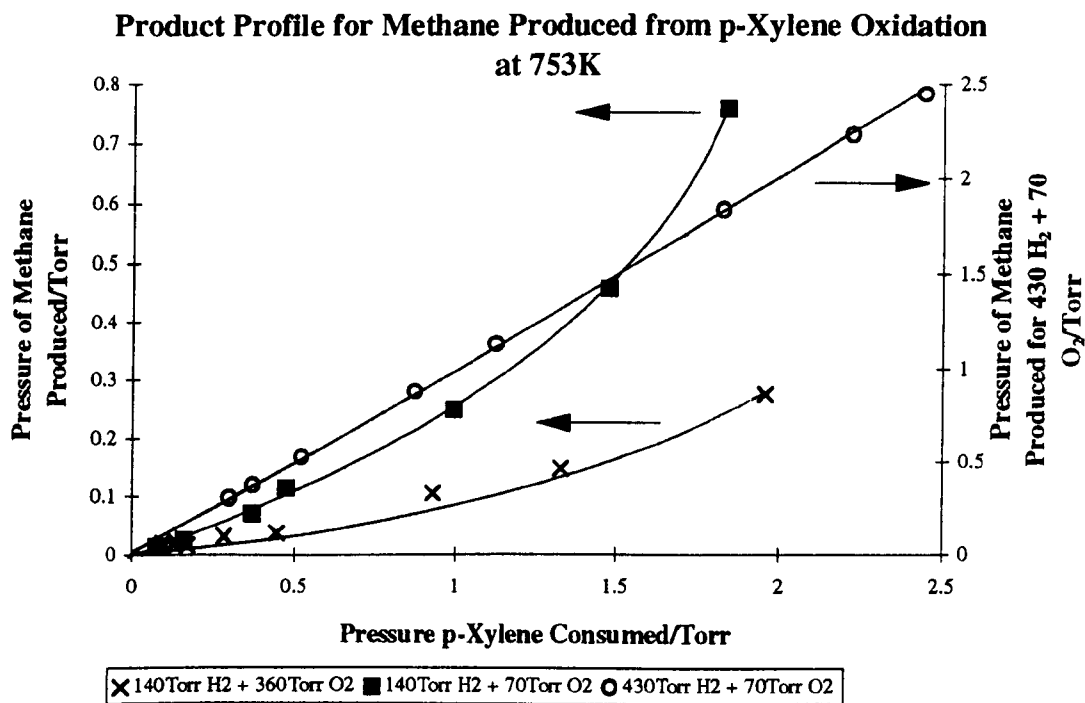


Figure 5.7



Profiles for *m*-Xylene Addition to the $H_2 + O_2$ Reaction at 753K and 500 Torr Total Pressure.

Figure 5. 8

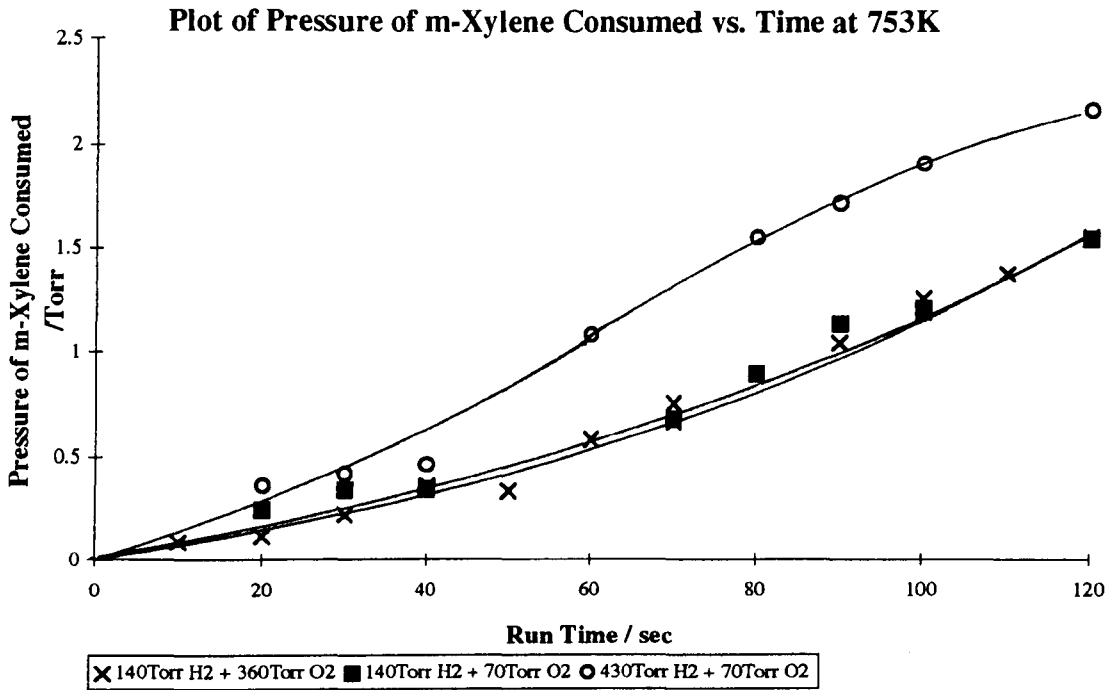


Figure 5. 9

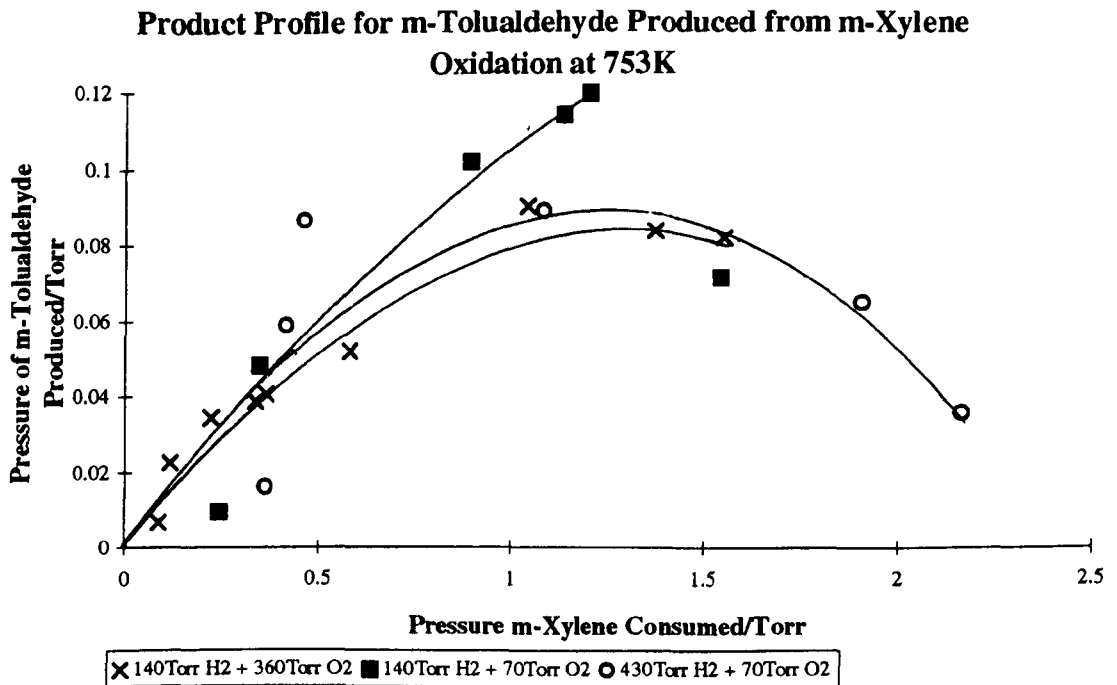


Figure 5.10

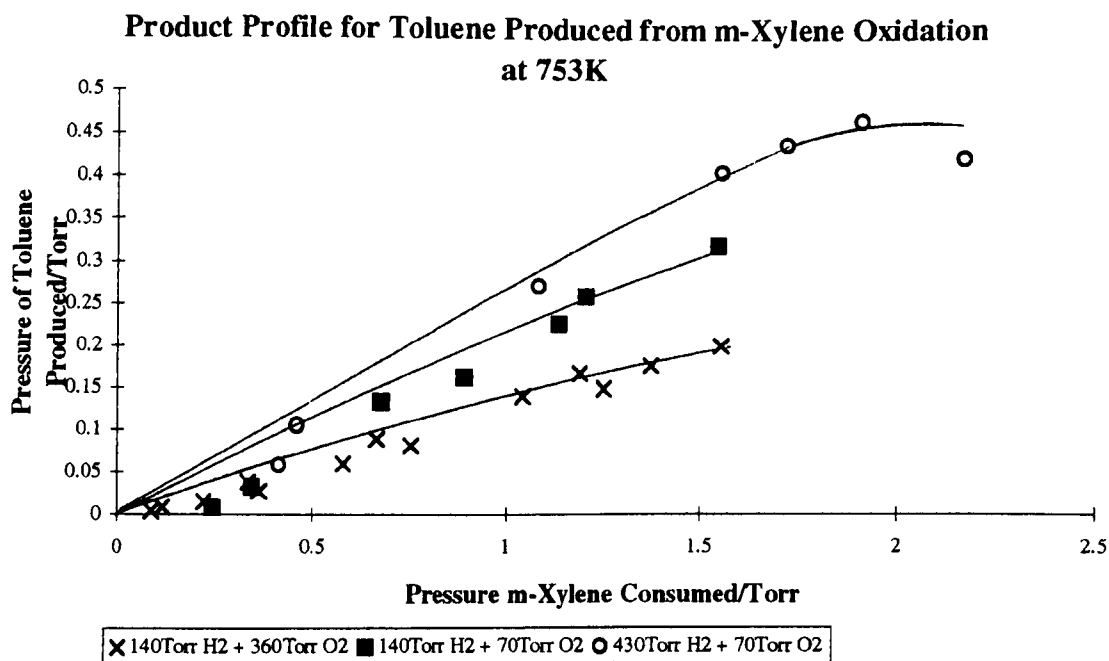


Figure 5.11

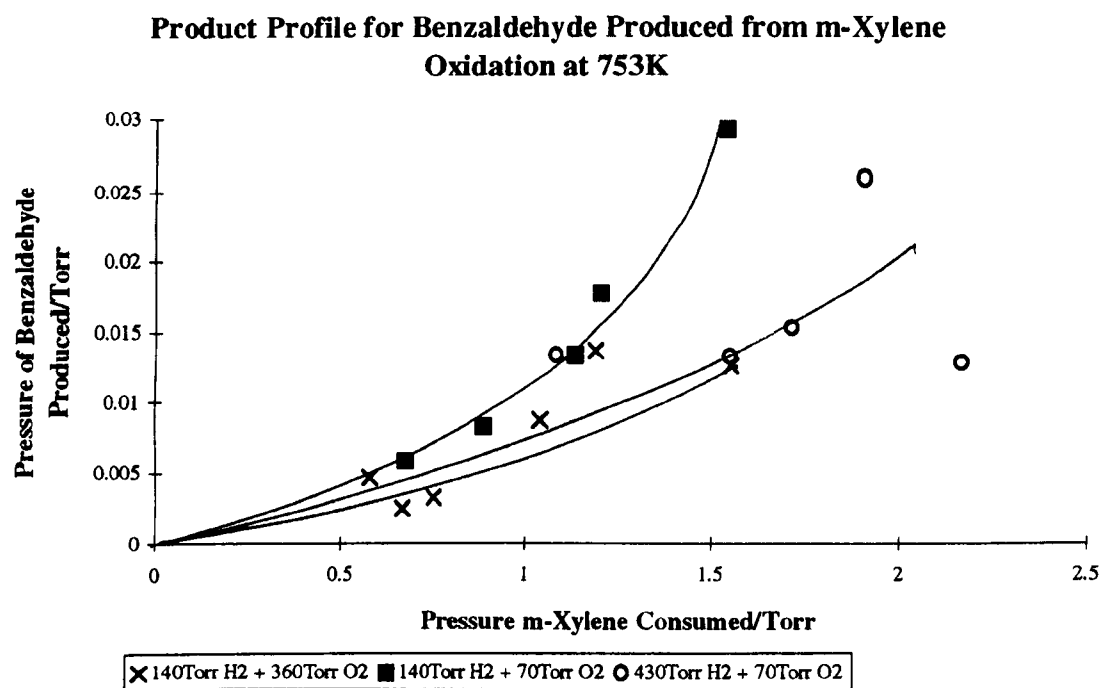


Figure 5. 12

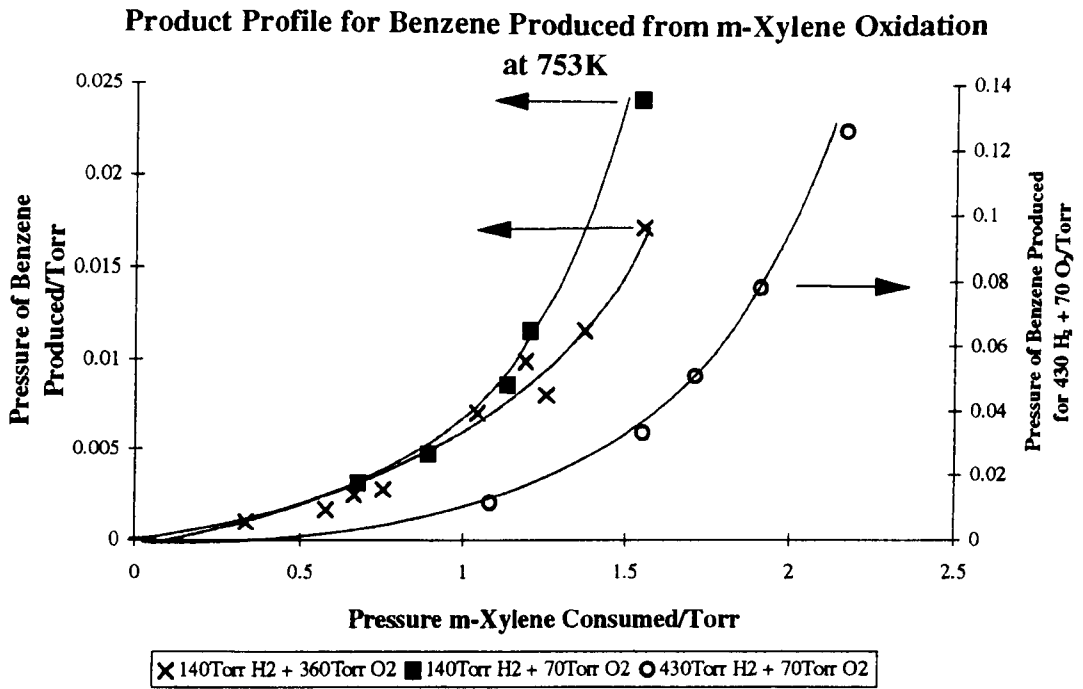
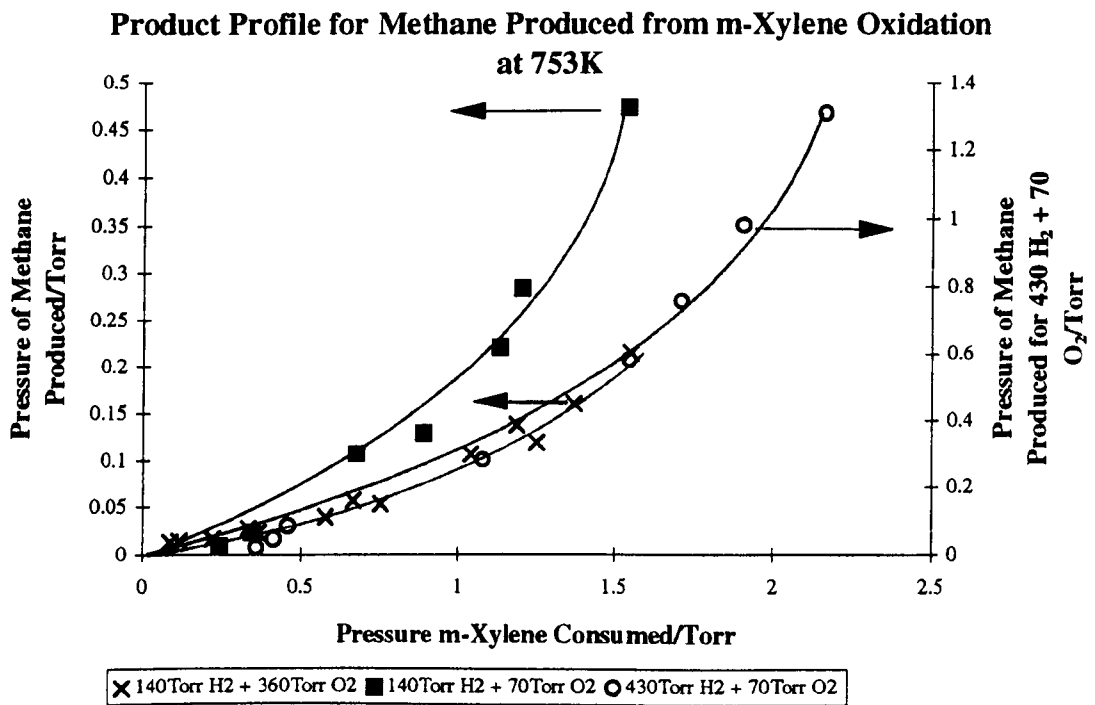


Figure 5. 13



Profiles for o-Xylene Addition to the H₂ + O₂ Reaction at 753K and 500 Torr Total Pressure.

Figure 5. 14

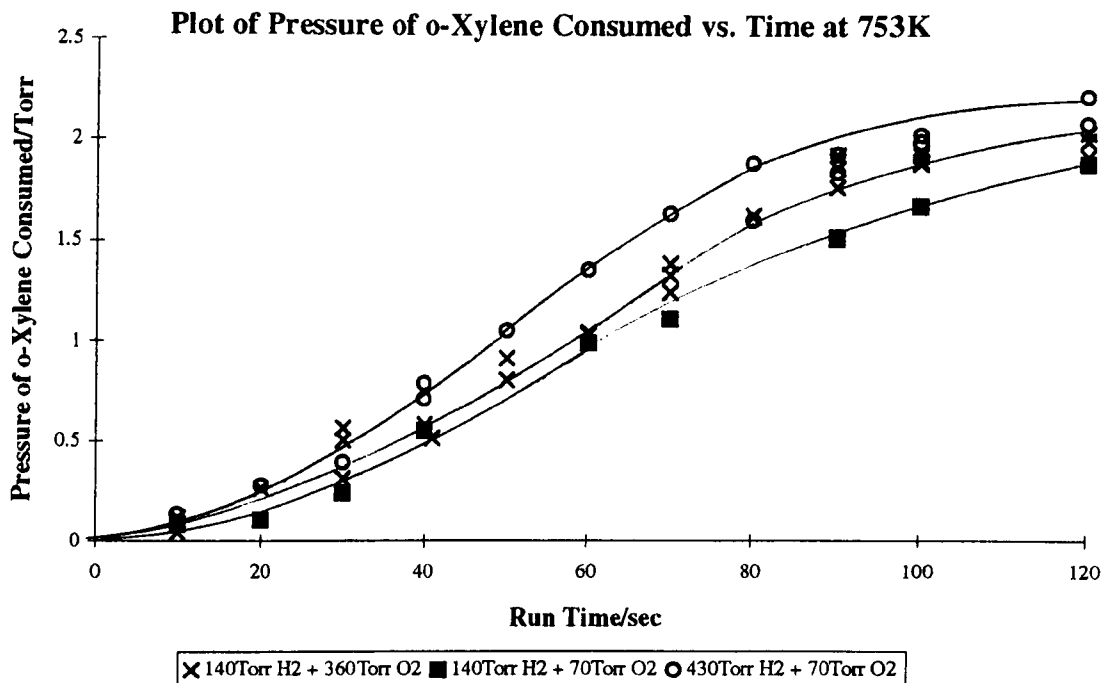


Figure 5. 15

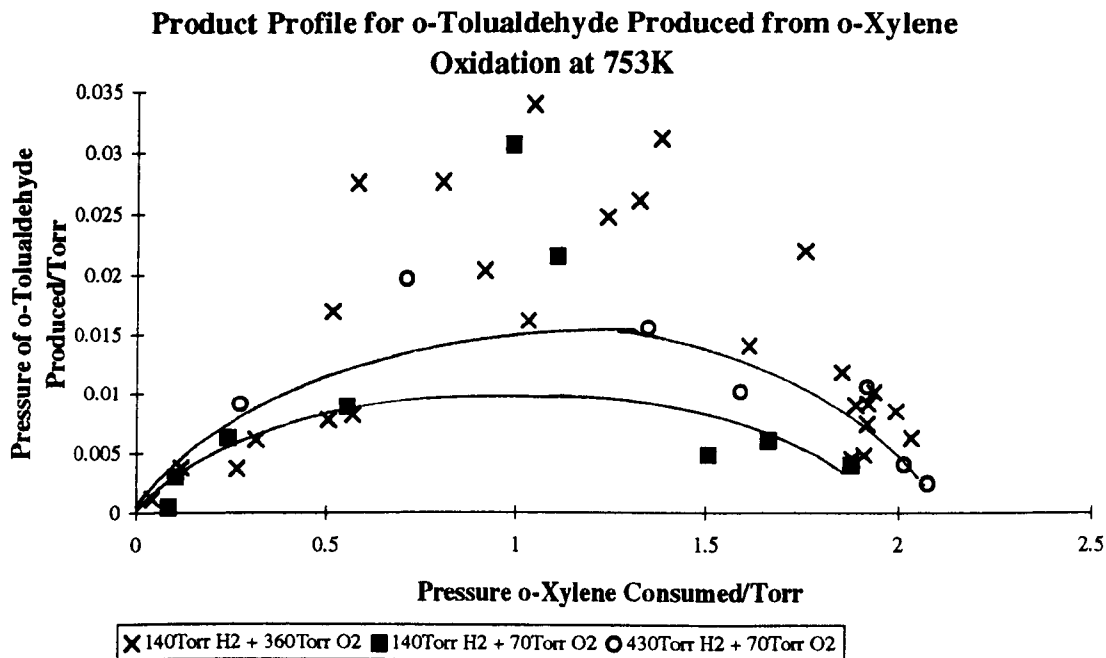


Figure 5. 16

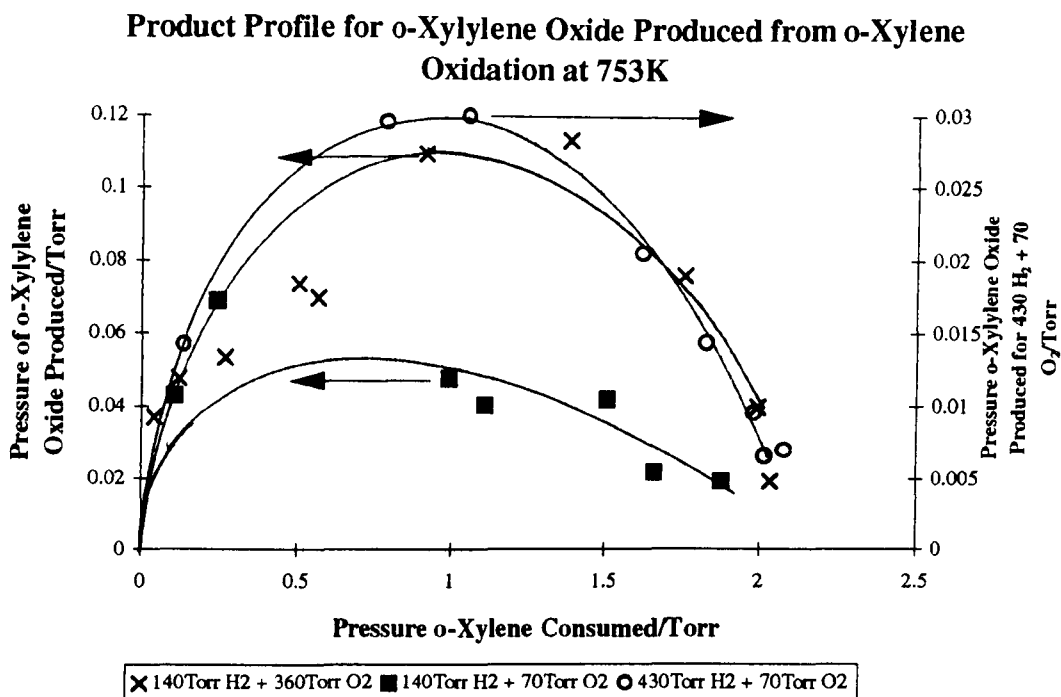


Figure 5. 17

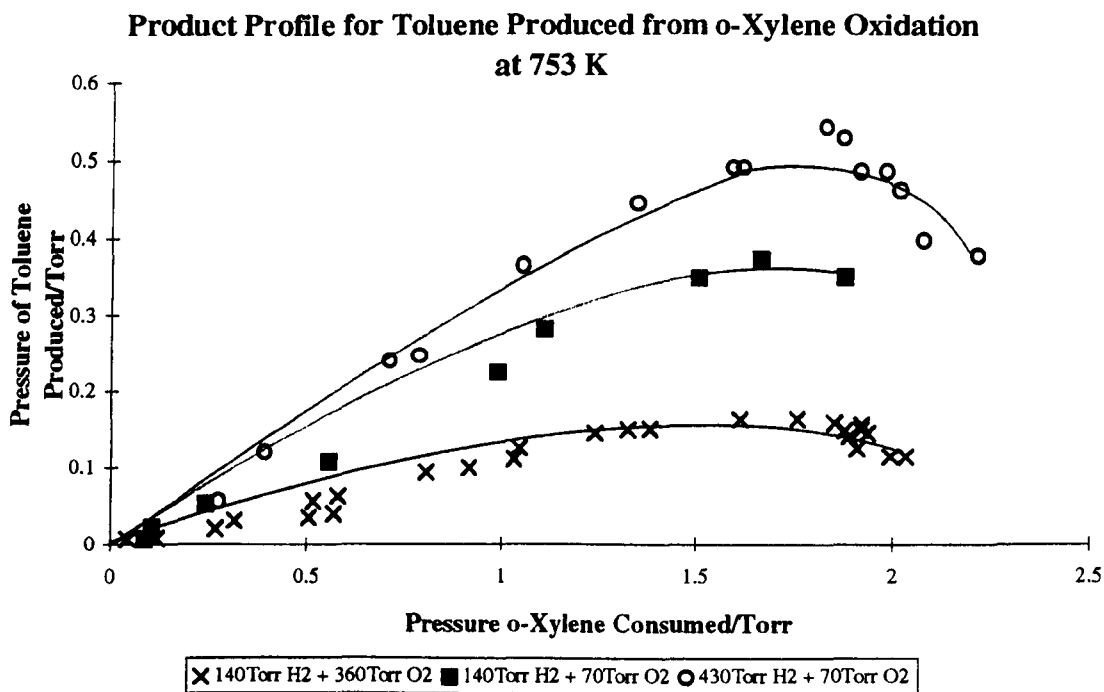


Figure 5.18

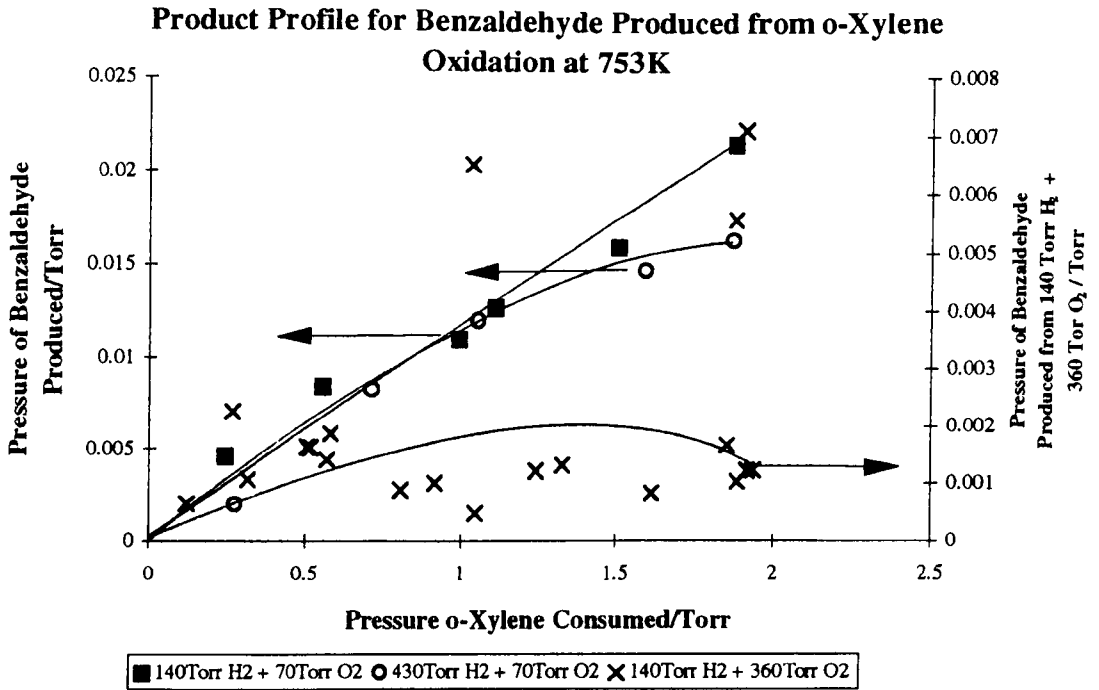


Figure 5.19

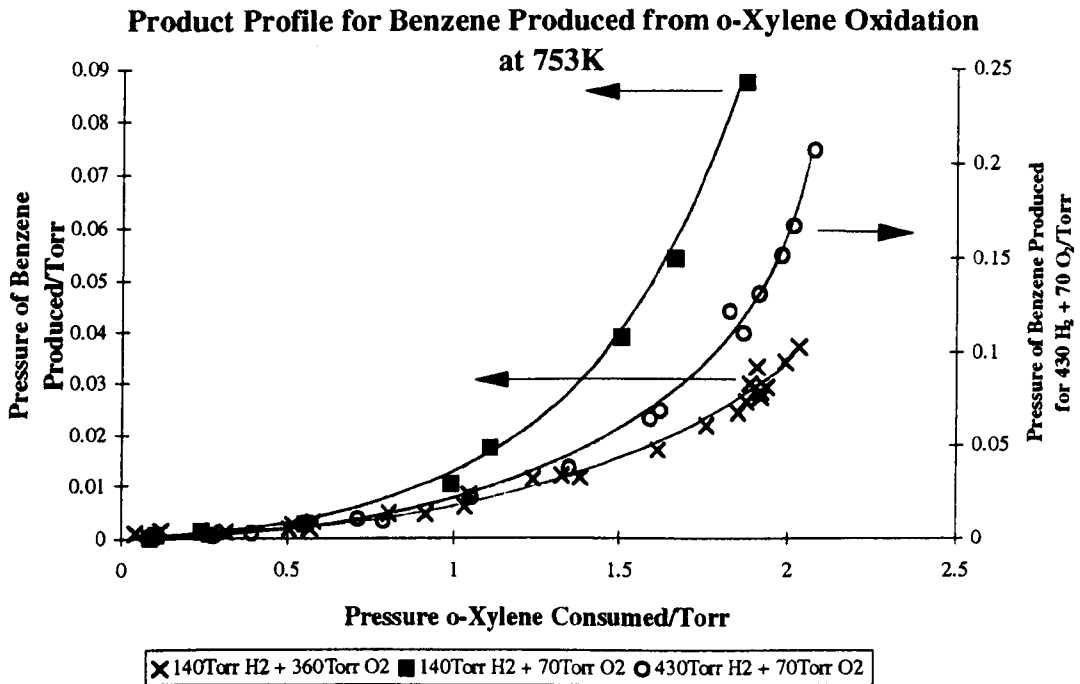


Figure 5. 20

Product Profile for Methane Produced from o-Xylene Oxidation
at 753K

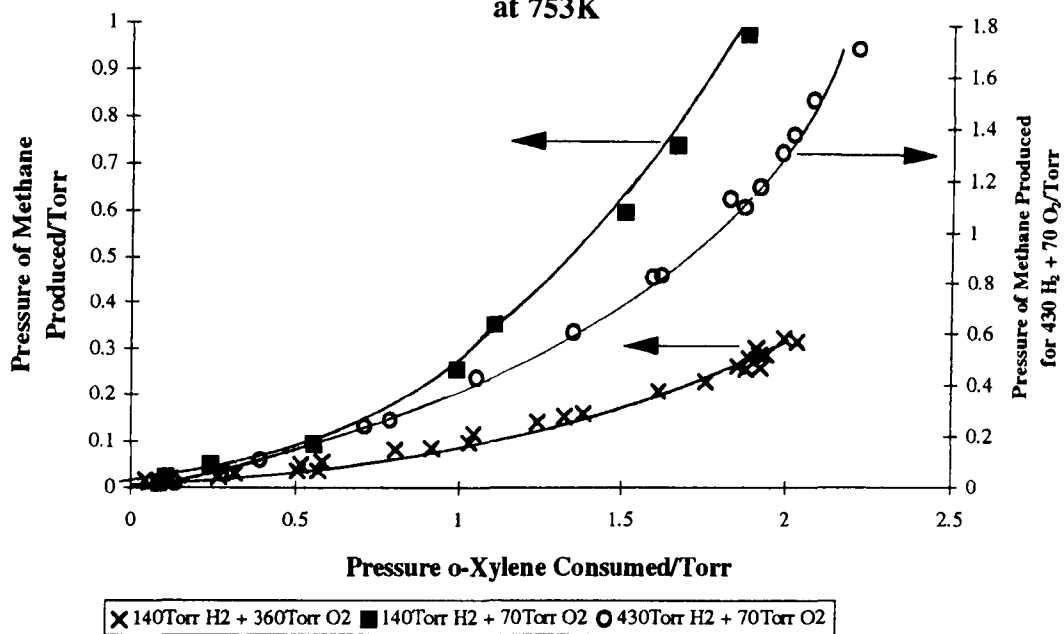


Table 5. 3: *p*-Xylene Oxidation Products for 140Torr H₂ + 360Torr O₂.

Pressure PX Consumed /Torr	Pressure of Product/Torr				
	PTA	Toluene	Methane	Benzaldehyde	Benzene
0.097	0.019	0.011	0.018	0.0042	0.003
0.138		0.021	0.021	0.0049	0.004
0.146		0.044	0.031	0.0072	0.005
0.171			0.015	0.0036	0.003
0.282	0.047	0.048	0.031	0.0031	
0.447	0.086	0.055	0.037	0.0085	0.006
0.930	0.092	0.164	0.105	0.0160	0.009
1.330	0.161	0.185	0.146	0.0197	0.014
1.959	0.196	0.274	0.275	0.0361	0.029

Table 5. 4: *p*-Xylene Oxidation Products for 140Torr H₂ + 70Torr O₂.

Pressure PX Consumed /Torr	Pressure of Product/Torr				
	PTA	Toluene	Methane	Benzaldehyde	Benzene
0.076	0.024	0.014	0.013		0.000
0.093		0.007	0.009		0.000
0.161	0.057	0.030	0.024		0.001
0.370	0.153	0.091	0.069	0.0041	0.002
0.389		0.181	0.140		0.006
0.475		0.145	0.114	0.0096	0.005
0.881	0.222	0.267	0.256	0.0264	0.013
0.994		0.247	0.248	0.0220	0.013
1.279		0.335	0.416	0.0464	0.026
1.479		0.321	0.454		0.027
1.610	0.189	0.398	0.664	0.0689	0.045
1.844	0.121	0.411	0.757	0.0667	0.051

Table 5. 5: *p*-Xylene Oxidation Products for 430Torr H₂ + 70Torr O₂.

Pressure PX Consumed /Torr	Pressure of Product/Torr				
	PTA	Toluene	Methane	Benzaldehyde	Benzene
0.299	0.016		0.034	0.008	0.006
0.310			0.014		0.002
0.371		0.163	0.086	0.020	0.015
0.523	0.105	0.192	0.166	0.039	0.029
0.873	0.068	0.318	0.309	0.024	0.015
1.127		0.417	0.485		0.086
1.831	0.062	0.522	0.959	0.039	0.071
2.225	0.050	0.589	1.615	0.073	0.147
2.444		0.563	2.013	0.087	0.209

Table 5. 6: *m*-Xylene Oxidation Products for 140Torr H₂ + 360Torr O₂.

Pressure MX Consumed /Torr	Pressure of Product/Torr				
	MTA	Toluene	Methane	Benzaldehyde	Benzene
0.116	0.023	0.008	0.014		
0.222	0.034	0.015	0.016		
0.335	0.039	0.038	0.027		0.0010
0.363	0.041	0.027	0.023		
0.579	0.052	0.059	0.039	0.00464	0.0016
0.666	0.041	0.089	0.057	0.00242	0.0025
0.753	0.097	0.081	0.053	0.00317	0.0028
1.042	0.090	0.139	0.106	0.00866	0.0071
1.191		0.166	0.137	0.01362	0.0099
1.253	0.072	0.148	0.118		0.0080
1.373	0.084	0.175	0.159		0.0116
1.553	0.082	0.199	0.214	0.01259	0.0171

Table 5. 7: *m*-Xylene Oxidation Products for 140Torr H₂ + 70Torr O₂.

Pressure MX Consumed /Torr	Pressure of Product/Torr				
	MTA	Toluene	Methane	Benzaldehyde	Benzene
0.244	0.010	0.008	0.008		
0.340			0.014		0.0003
0.345	0.048	0.032	0.023		
0.676		0.134	0.107	0.0058	0.0031
0.891	0.102	0.162	0.129	0.0082	0.0048
1.135	0.114	0.225	0.220	0.0133	0.0086
1.205	0.120	0.258	0.283	0.0176	0.0116
1.543	0.071	0.318	0.473	0.0292	0.0242

Table 5. 8: *m*-Xylene Oxidation Products for 430Torr H₂ + 70Torr O₂.

Pressure MX Consumed /Torr	Pressure of Product/Torr				
	MTA	Toluene	Methane	Benzaldehyde	Benzene
0.346		0.020	0.010		
0.361	0.016	0.020	0.018		
0.414	0.059	0.059	0.044		
0.461	0.087	0.105	0.083		
1.082	0.089	0.271	0.280	0.0133	0.011
1.551		0.403	0.579	0.0132	0.033
1.715		0.435	0.751	0.0152	0.051
1.908	0.065	0.462	0.976	0.0257	0.078
2.165	0.035	0.420	1.305	0.0129	0.126

Table 5. 9: *o*-Xylene Oxidation Products for 140Torr H₂ + 360Torr O₂.

Pressure OX Consumed /Torr	Pressure of Product/Torr					
	OTA	OXO	Toluene	Methane	Benzaldehyde	Benzene
0.043	0.001	0.037	0.007	0.015		0.0009
0.119	0.004	0.048	0.008	0.018	0.0007	0.0014
0.265	0.004	0.053	0.020	0.023	0.0022	0.0008
0.314	0.006		0.031	0.030	0.0011	0.0011
0.505	0.008	0.074	0.035	0.036	0.0016	0.0017
0.515	0.017		0.057	0.048	0.0016	0.0027
0.568	0.008	0.070	0.040	0.036	0.0014	0.0018
0.579	0.028		0.063	0.056	0.0019	0.0032
0.806	0.028		0.093	0.083	0.0009	0.0047
0.916	0.020	0.109	0.098	0.086	0.0010	0.0046
1.033	0.016		0.110	0.097	0.0065	0.0060
1.046	0.034		0.124	0.117	0.0005	0.0083
1.241	0.025		0.143	0.142	0.0012	0.0113
1.325	0.026		0.148	0.154	0.0013	0.0119
1.382	0.031	0.113	0.149	0.162		0.0116
1.613	0.014		0.162	0.209	0.0008	0.0169
1.757	0.022	0.076	0.163	0.229		0.0217
1.854	0.012		0.158	0.263	0.0017	0.0241
1.879	0.004		0.148	0.256	0.0056	0.0263
1.889	0.009		0.140	0.280	0.0010	0.0297
1.910	0.005		0.125	0.302	0.0071	0.0330
1.920	0.007		0.150	0.288	0.0012	0.0281
1.921	0.009		0.156	0.259		0.0271
1.937	0.010		0.145	0.288	0.0012	0.0290
1.994	0.008	0.040	0.114	0.323		0.0340
2.033	0.006	0.019	0.114	0.316		0.0369

Table 5. 10: *o*-Xylene Oxidation Products for 140Torr H₂ + 70Torr O₂.

Pressure OX Consumed /Torr	Pressure of Product/Torr					
	OTA	OXO	Toluene	Methane	Benzaldehyde	Benzene
0.083	0.000		0.007	0.010		
0.106	0.003	0.043	0.022	0.022		0.001
0.242	0.006	0.069	0.053	0.049	0.0046	0.001
0.554	0.009		0.107	0.094	0.0084	0.003
0.991	0.031	0.048	0.224	0.256	0.0110	0.010
1.110	0.021	0.041	0.280	0.355	0.0127	0.017
1.507	0.005	0.042	0.348	0.599	0.0159	0.039
1.664	0.006	0.022	0.371	0.743		0.054
1.878	0.004	0.019	0.350	0.981	0.0214	0.087

Table 5. 11: *o*-Xylene Oxidation Products for 430Torr H₂ + 70Torr O₂.

Pressure OX Consumed /Torr	Pressure of Product/Torr					
	OTA	OXO	Toluene	Methane	Benzaldehyde	Benzene
0.135		0.0143		0.015		
0.274	0.0090		0.056	0.052	0.0020	0.0009
0.392			0.119	0.105		0.0026
0.711	0.0197		0.240	0.239	0.0083	0.0099
0.789		0.0295	0.247	0.262		0.0085
1.054		0.0300	0.364	0.428	0.0120	0.0212
1.350	0.0155		0.442	0.605		0.0366
1.593	0.0101		0.489	0.823	0.0147	0.0634
1.621		0.0205	0.488	0.829		0.0674
1.828		0.0144	0.542	1.131		0.1216
1.873			0.528	1.097	0.0163	0.1097
1.919	0.0105		0.485	1.177		0.1306
1.983		0.0095	0.484	1.309		0.1510
2.017	0.0040	0.0065	0.461	1.376		0.1667
2.078	0.0024	0.0070	0.396	1.511		0.2062
2.215			0.377	1.707		

Table 5. 12: Pressure of *p*-Xylene Lost for Varying Mixture Composition.

Run Time /sec	Pressure of <i>p</i> -Xylene Consumed / Torr		
	140Torr H ₂ + 360Torr O ₂	140Torr H ₂ + 70Torr O ₂	430Torr H ₂ + 70Torr O ₂
20	0.097	0.076	0.299
30	0.138	0.161	0.371
40	0.146		0.523
40	0.282		
50	0.447	0.370	0.873
60		0.475	1.127
60		0.389	
80	0.930	0.994	1.831
80		0.881	
100	1.330	1.479	2.225
100		1.279	
120	1.959	1.844	2.444
120		1.610	

Table 5. 13: Pressure of m-Xylene Lost for Varying Mixture Composition.

Run Time /sec	Pressure of m-Xylene Consumed /Torr		
	140Torr H₂ + 360Torr O₂	140Torr H₂ + 70Torr O₂	430Torr H₂ + 70Torr O₂
20	0.116	0.244	0.361
30	0.222	0.340	0.414
40	0.363	0.345	0.461
50	0.335		
60	0.579		1.082
70	0.753	0.676	
70	0.666		
80		0.891	1.551
90	1.042	1.135	1.715
100	1.191	1.205	1.908
100	1.253		
110	1.373		
120	1.553	1.543	2.165

Table 5. 14: Pressure of o-Xylene Lost for Varying Mixture Composition.

Run Time /sec	Pressure of o-Xylene Consumed / Torr		
	140Torr H ₂ + 360Torr O ₂	140Torr H ₂ + 70Torr O ₂	430Torr H ₂ + 70Torr O ₂
20	0.265	0.106	0.274
30	0.314	0.242	0.392
30	0.568		
30	0.505		
40	0.579	0.554	0.789
40			0.711
50	0.806		1.054
50	0.916		
60	1.033	0.991	1.350
60	1.046		
70	1.241	1.110	1.621
70	1.325		
70	1.382		
80	1.613		1.873
80			1.493
90	1.757	1.507	1.828
90	1.921		1.919
90	1.854		
100	1.879	1.664	1.983
100	1.889		2.017
100	1.937		
100	1.920		
120	1.910	1.878	2.078
120	2.033		2.215
120	1.994		

Table 5.2 summarises the products under the headings primary, secondary and tertiary, for the respective xylenes.

A fuller discussion of these results will be given in Chapter 8 but it is clear that the total product yield observed is well below that expected. The major products agree well with those of previous workers such as Emdee et al.⁶ who studied the oxidation of o-xylene in a flow system at 1150K. However, under the analytical conditions used it was not possible to detect such compounds as phenol, cresols, indene and naphthalene together with any di-methylbenzyl ($\text{CH}_3\text{-C}_6\text{H}_4\text{-CH}_2\text{-CH}_2\text{-C}_6\text{H}_4\text{-CH}_2$) or dibenzyl. Henceforth the discussion of the products will be looking only at part of the mechanism rather than attempting to obtain a full appraisal of the oxidation mechanism for the xylenes. The main concern will be to look at the effect of the reactions between the methylbenzyl radicals and HO_2 in order to assess the importance of this reaction and in comparison with the benzyl + HO_2 reaction (from Chapter 6).

5.2. References.

¹Wright F.J., *J. Phys. Chem.*, **64**, 1944, (1960).

²Wright F.J., *J. Phys. Chem.*, **66**, 2023, (1962).

³Barnard J.A., and Sankey B.M., *Comb. Flame.*, **12**, 345, (1968).

⁴Nicovich J.M., Thompson R.L. and Ravishankara A.R., *J. Phys. Chem.*, **85**, 2913, (1981).

⁵Emdee J.L., Brezinsky K., and Glassman I., *J. Phys. Chem.*, **95**, 1626, (1991).

⁶Emdee J.L., Bresinsky K. and Glassman I., *23rd Symposium (International) on Combustion*, **77**, (1990).

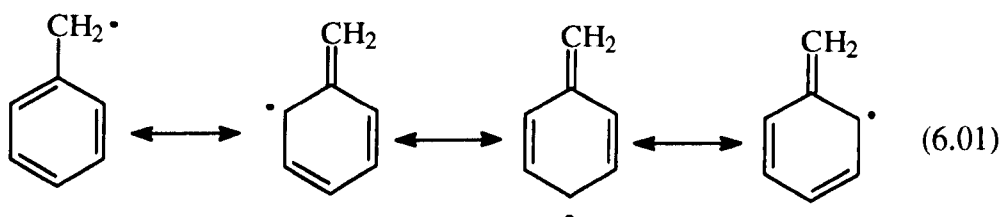
⁷CRC Handbook of Chemistry and Physics, 51st Edition (1970-1971), The Chemical Rubber Company, pp163.

Chapter 6.

The Decomposition of Neopentylbenzene in the Presence of Oxygen.

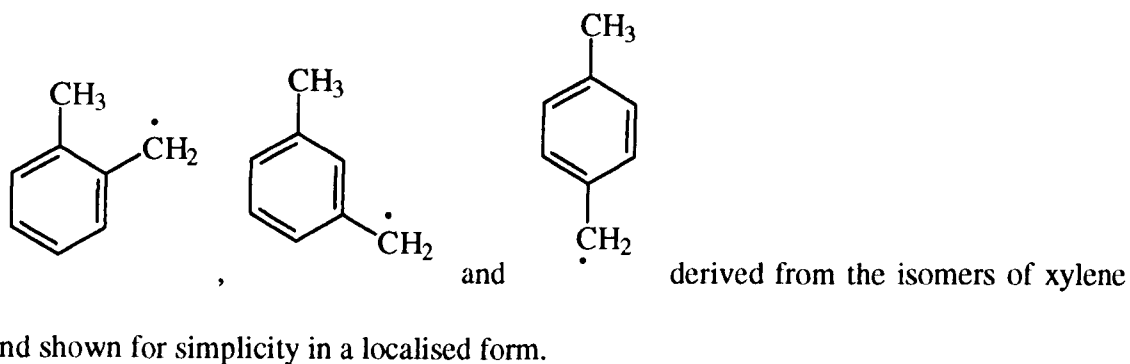
6.1. Introduction

Benzyl radicals are particularly important in the combustion chemistry of toluene¹ and also because they share characteristics of many radicals formed from aromatic hydrocarbons. As benzyl radicals are stabilised by electron delocalisation (6.01), they are less prone to oxidation via molecular oxygen because the equilibrium $C_6H_5-CH_2 + O_2 \rightleftharpoons C_6H_5-CH_2O_2$ is well to the left at temperatures above $500K^2$.

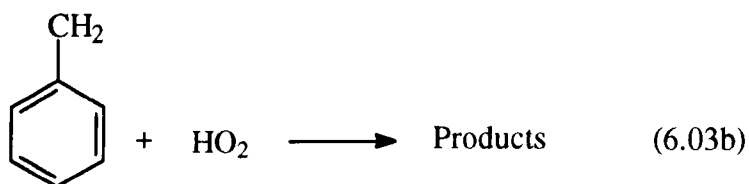
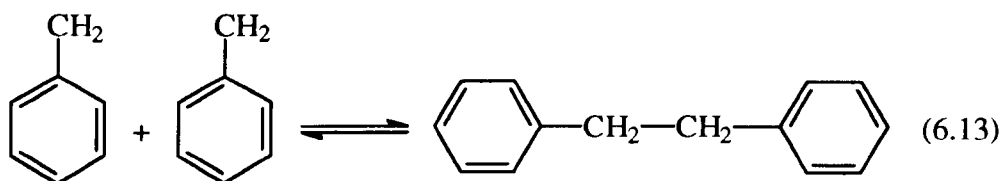


As a consequence, radical-radical reactions are of considerable importance in the oxidation chemistry of $C_6H_5-CH_2$ under conditions where normally such processes would have minor impact.

Similar arguments apply to the related delocalised radicals such as

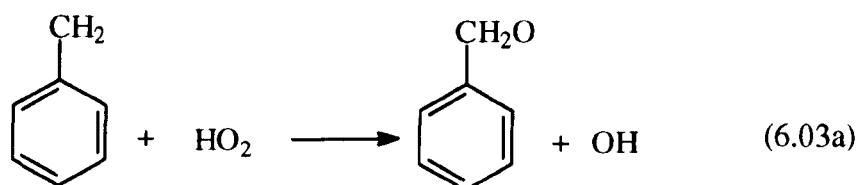
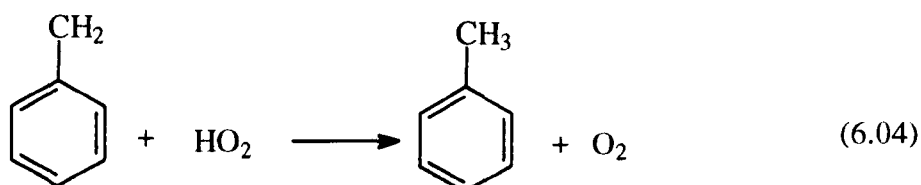


Below ca. 800K, where rates of oxidation are usually relatively low, so that the concentrations of non-stabilised organic radicals and of reactive radicals such as OH are low, radical-radical reactions will tend to occur most importantly between relatively stable species. Under these conditions, in systems where HO₂ and benzyl radicals are formed, then three radical-radical reactions will inevitably be of importance.



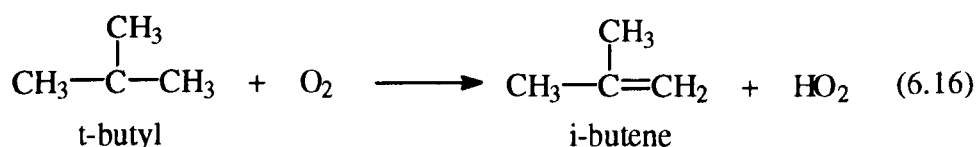
Rate data are available for the reaction of benzyl radicals with O₂². However, there are no kinetic data below 1000K currently available for the reactions of benzyl radicals with HO₂. As importantly, there is little information on the reaction path or products.

For those concerned with modelling toluene oxidation, particularly at moderate temperatures, it is essential to have information on the relative importance of the reaction paths. For example, reaction (6.04) involves termination whereas (6.03a) is at least a propagation process and could under certain circumstances be regarded as a branching process.

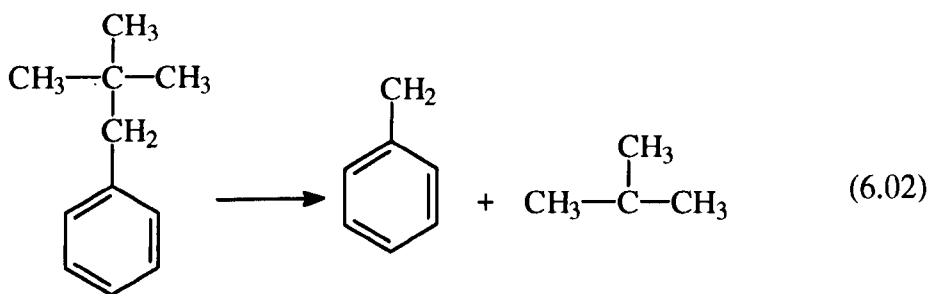
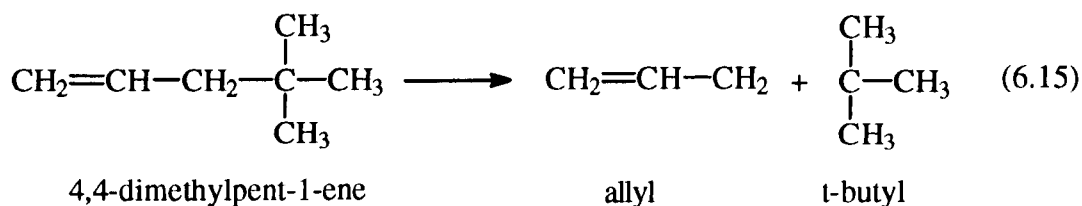


6.2. Approach used to study the reaction $\text{HO}_2 + \text{Benzyl}$.

As discussed in section 2.3 of Chapter 2, the decomposition of tetramethylbutane (TMB) in the presence of O_2 has been shown to be an excellent and clean source of HO_2 and t-butyl radicals in the temperature range 700-800K³. The t-butyl radicals produced from the decomposition of TMB react with 99% efficiency to produce i-butene and HO_2 , reaction (6.16).



In order to produce benzyl in the presence of HO₂ it might have been possible to add dibenzyl to a mixture of O₂ and TMB at ~750K, but as dibenzyl has a very low volatility at room temperature, quantitative experiments in the gas phase are difficult. Almost certainly absorption/adsorption effects would make reproducibility difficult to achieve. Neopentylbenzene decomposition in the presence of O₂ was considered because, from consideration of its structure, simple homolysis of the strained C-C bond gives the two important radicals, benzyl and t-butyl (reaction 6.02). This is analogous to the use of 4,4-dimethylpent-1-ene by Lohdi and Walker⁴ when examining the oxidation chemistry of allyl radicals (discussed in Chapter 2).



In the two cases, both strain in the central C-C bond and the release of electron delocalisation energy (in the allyl and benzyl radicals respectively) contribute to the considerable lowering of the activation energy for the homolysis.

Table 6.1 compares the activation energies for the two strained hydrocarbons with those for the homolysis of TMB³ (to give 2 *t*-butyl radicals) and of butane⁵ (to give 2 C₂H₅ radicals). Also shown are the A factors and the rate constants at 753K. As can be seen $k_{6.15}$ ($1.4 \cdot 10^{-4} \text{ s}^{-1}$) and $k_{6.02}$ ($6.9 \cdot 10^{-4} \text{ s}^{-1}$) are a factor of 10^4 higher than the rate constant for the homolysis of butane ($1.7 \cdot 10^{-8} \text{ s}^{-1}$) and similar to that for the homolysis of TMB.

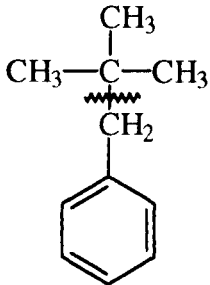
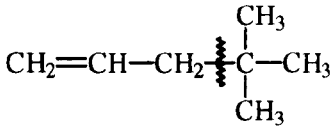
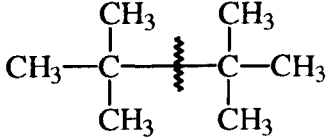
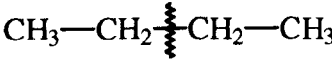
Robaugh et al.⁶ studied the thermal decomposition of propyl, isopropyl and neopentylbenzene between 918-1064K. From their results the rate constant for the reaction NPB \rightarrow benzyl + *t*-butyl at 750K is $6.9 \cdot 10^{-4} \text{ s}^{-1}$. This value was considered suitable for a study of the reaction between benzyl and HO₂ radicals, which as indicated above are formed in 99% yield³ in the reaction *t*-butyl + O₂ \rightarrow *i*-butene + HO₂ (6.16).


6.3. Experimental Results.

The experiments were carried out as described in section 3.5.5 of Chapter 3. The main set of data has been obtained at 753K.

1. From a detailed examination of the ratio of the yield of benzaldehyde to that of toluene it has proved possible to obtain relative rate data for the two important reactions (6.03) and (6.04) of benzyl radicals with HO₂ radicals.
2. From a partial analytical investigation, a preliminary study has been carried out of the chemistry of the decomposition of neopentylbenzene (NPB) in the presence of O₂.

Table 6. 1 : Kinetic Data for the homolysis of strained hydrocarbons.

Reference	Hydrocarbon [•]	E _A / kJ mol ⁻¹	A / s ⁻¹	k ₇₅₃ / s ⁻¹
6	 <p style="text-align: center;">NPB</p>	269	3.16*10 ¹⁵	6.9*10 ⁻⁴
4	 <p style="text-align: center;">4,4-dimethylpent-1-ene</p>	256	1.55*10 ¹⁴	1.4*10 ⁻⁴
3	 <p style="text-align: center;">TMB</p>	295	1.04*10 ¹⁷	3.8*10 ⁻⁴
5	 <p style="text-align: center;">Butane</p>	364	1.58*10 ¹⁷	1.7*10 ⁻⁸

•  indicates the bond being broken.

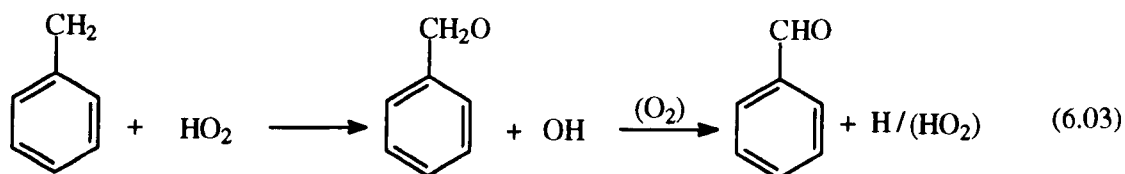
6.3.1. Introduction.

The homolyses were carried out at 753K in an aged boric-acid-coated Pyrex reaction vessel. The mixture composition was 0.48 Torr (0.8%) NPB + 5, 10[⊗], 15, 30 or 59.5 Torr of oxygen, (with nitrogen to make up the total pressure to 60 Torr where required). The reactions were carried out at a maximum pressure of 60 Torr to reduce the decomposition of hydrogen peroxide³ which leads to rapid auto-catalysis at this temperature through the reaction $\text{H}_2\text{O}_2 + \text{M} \rightarrow 2\text{OH} + \text{M}$.

Analysis of the product profiles indicated that the primary products include CH_4 , C_2H_6 , benzaldehyde (BA), toluene (T), i-butene and 2-methyl-1-phenylprop-1-ene (MPP). (Figures 6.02-6.10). No analysis was made for HCHO, which will be formed as a primary oxidation product of CH_3 radicals (see later), or for CO and CO_2 , both of which are unlikely to be formed in primary processes.

As is common with this type of study, which is essentially a *relative rate* investigation, it is ratios of product concentrations which are critically important, often independently of the consideration of other product yields.

The approach emerges during the course of the current work. A very simple case emerges if toluene (T) and benzaldehyde (BA) are formed uniquely (as initial products) from NPB in reactions (6.03) and (6.04).



[⊗] The reaction mixture containing 10 Torr O_2 was only used in the presence of propene.

Profiles from NPB + O₂ only at 753K and 60 Torr Maximum Pressure.

Figure 6. 1

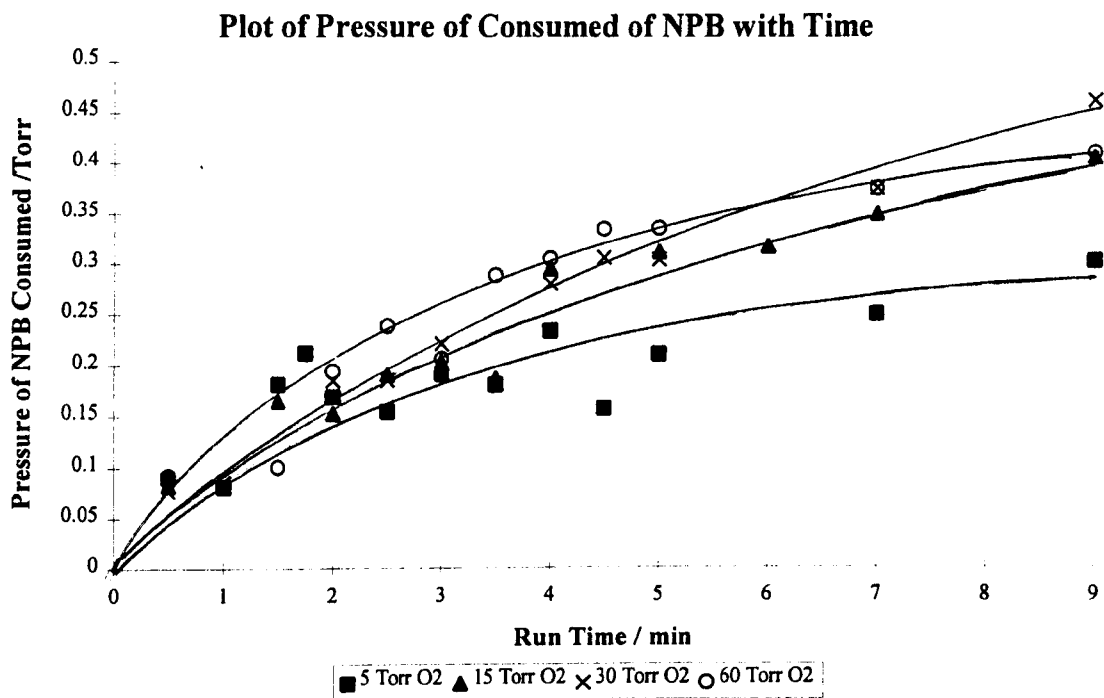


Figure 6. 2

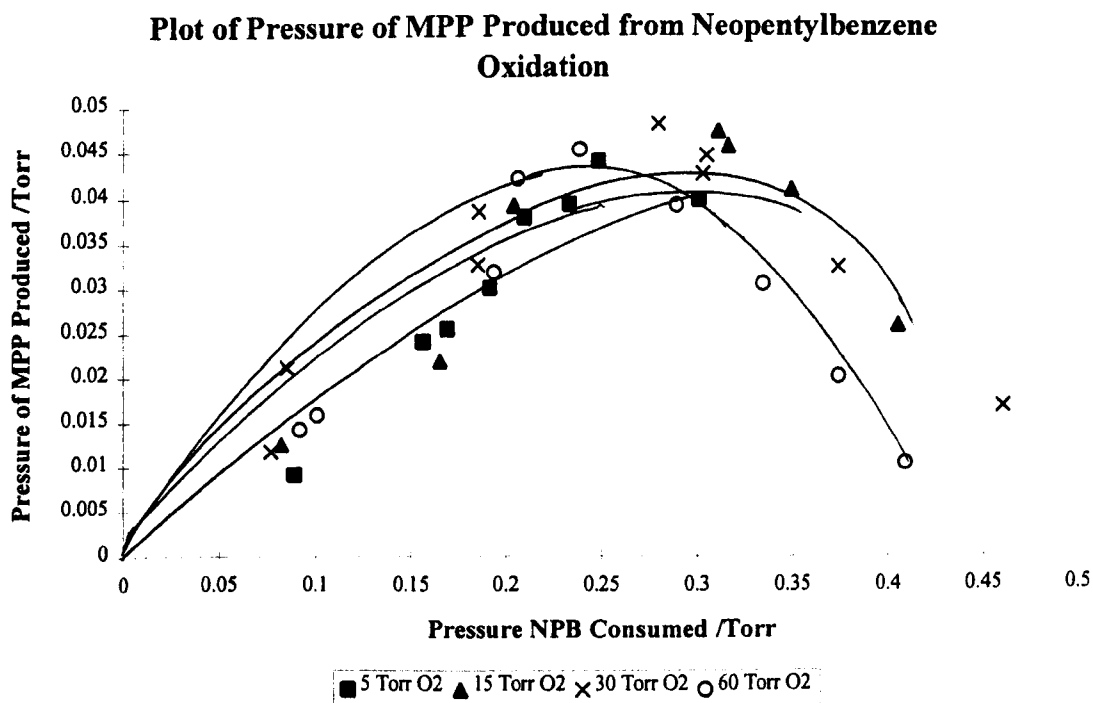


Figure 6. 3

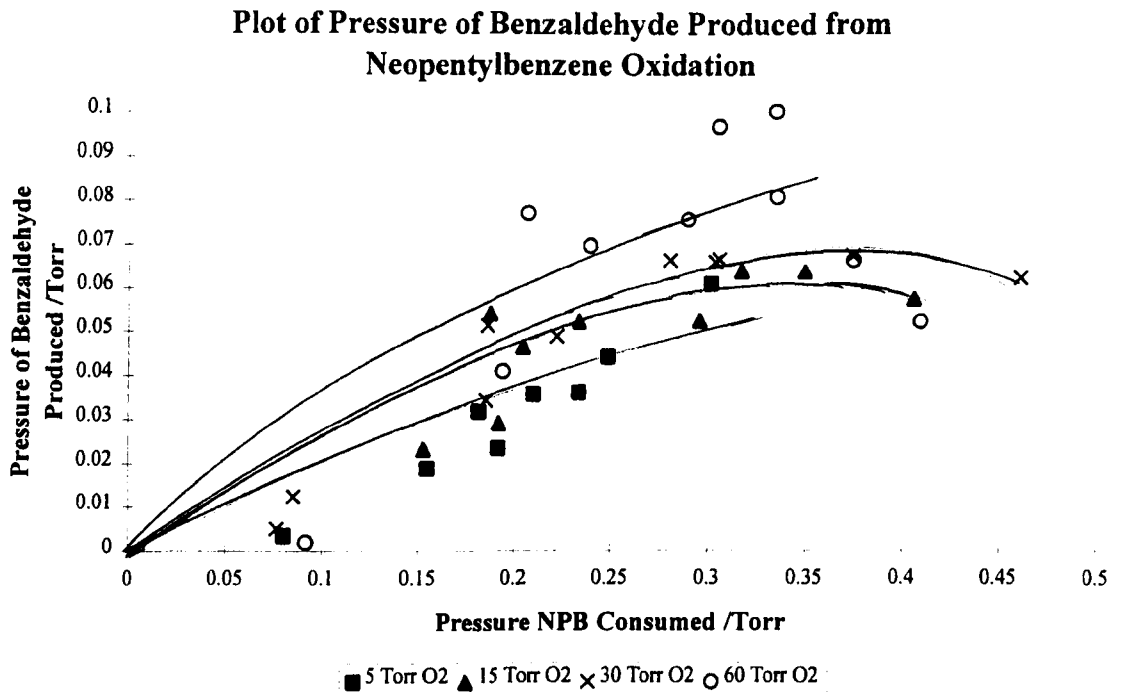


Figure 6. 4

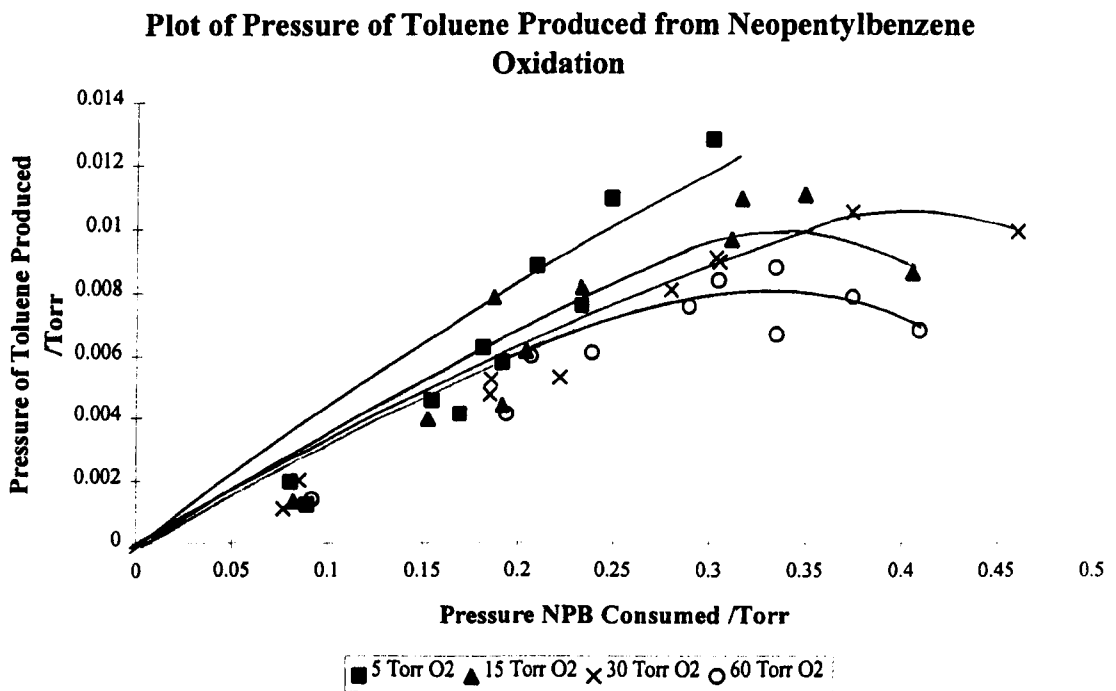


Figure 6. 5

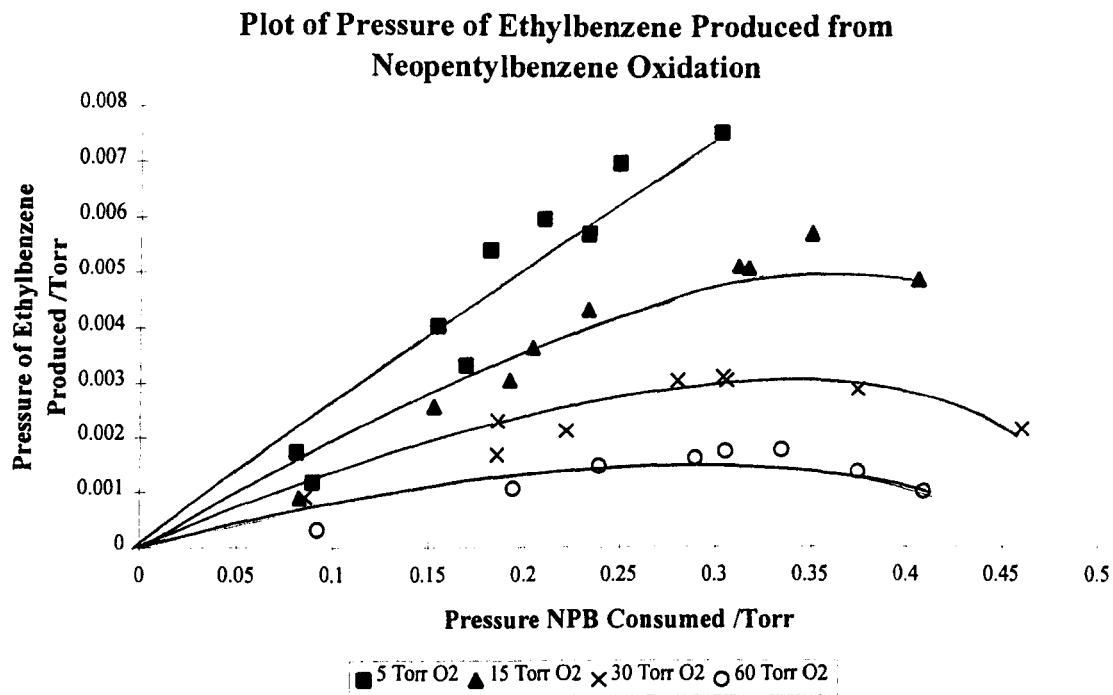


Figure 6. 6

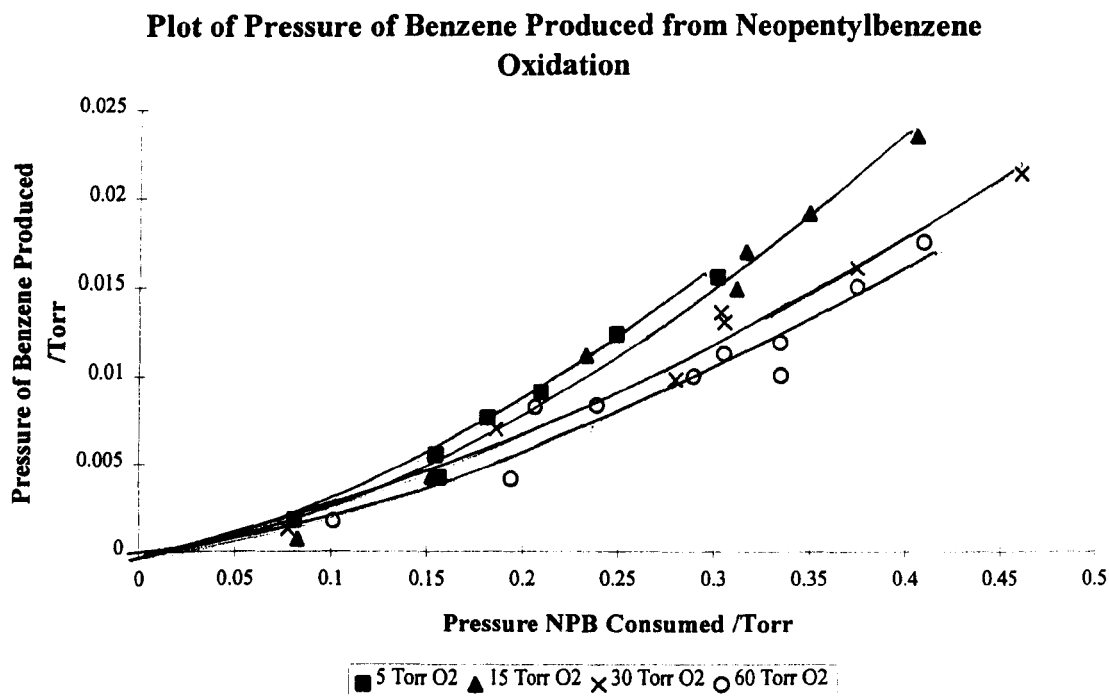


Figure 6. 7

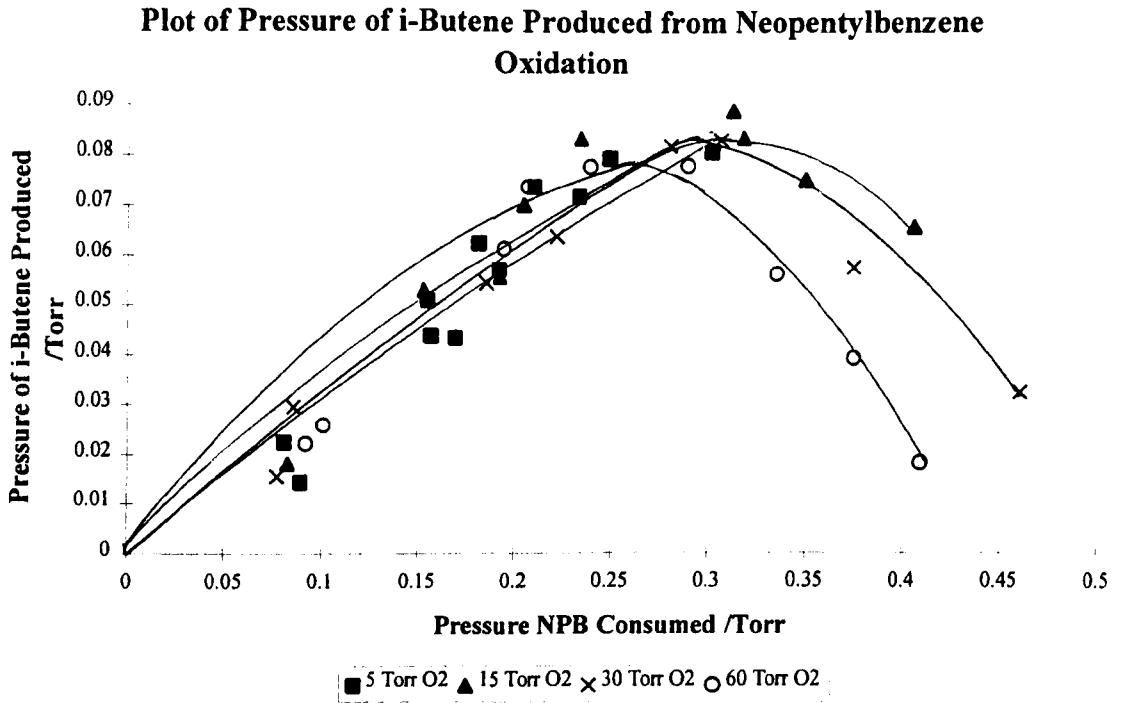


Figure 6. 8

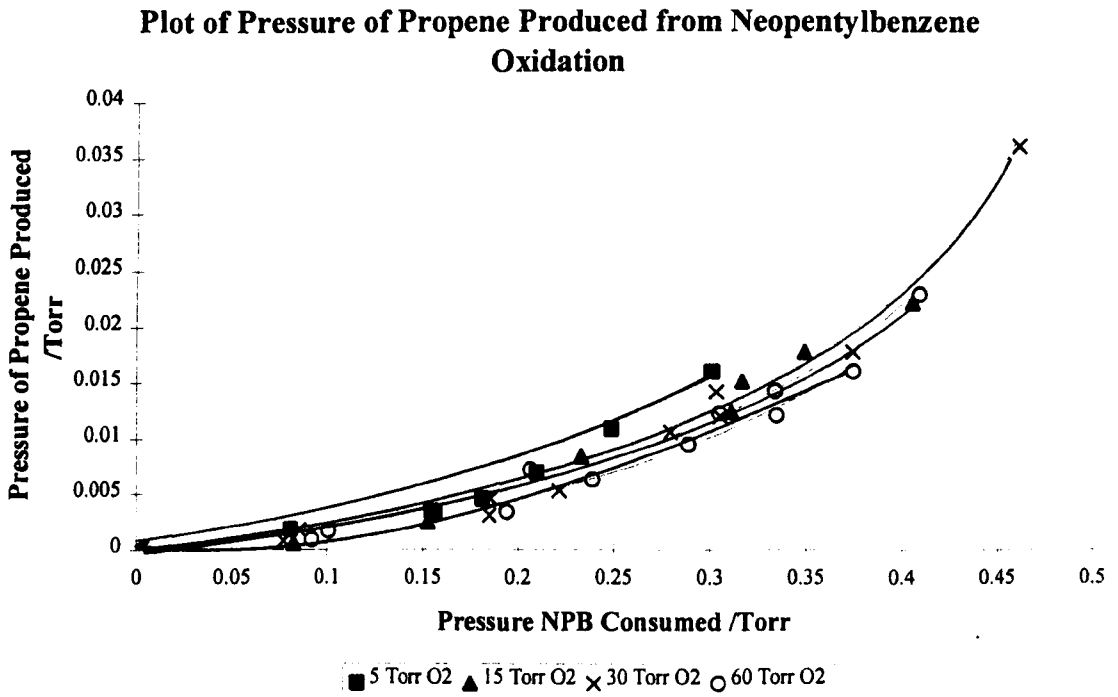


Figure 6. 9

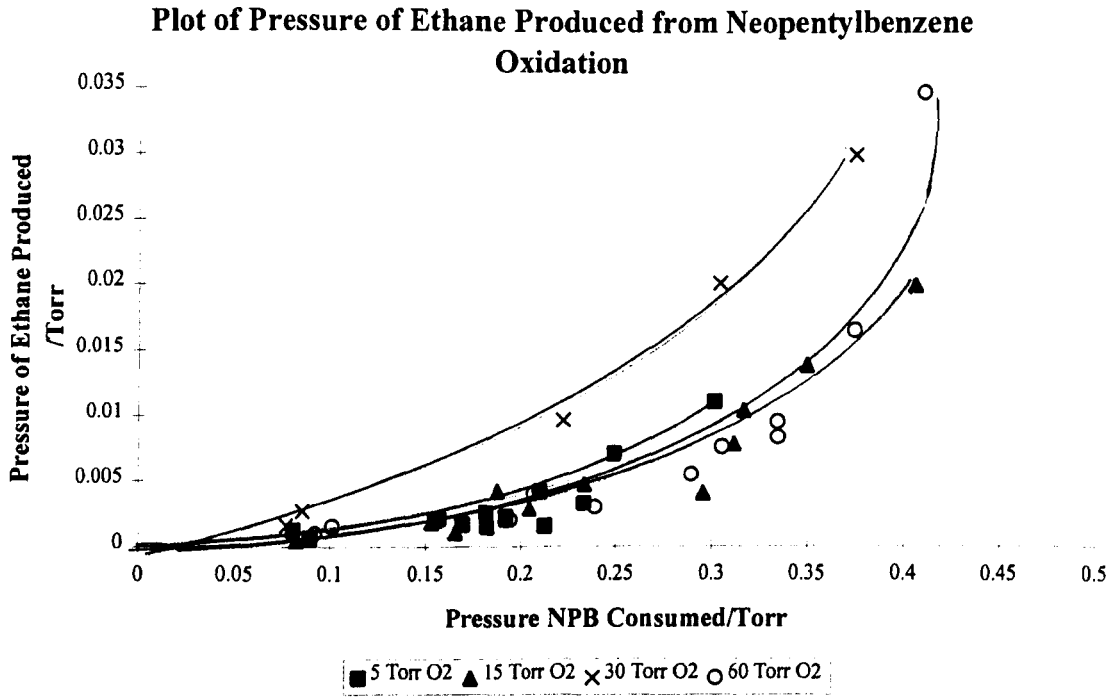
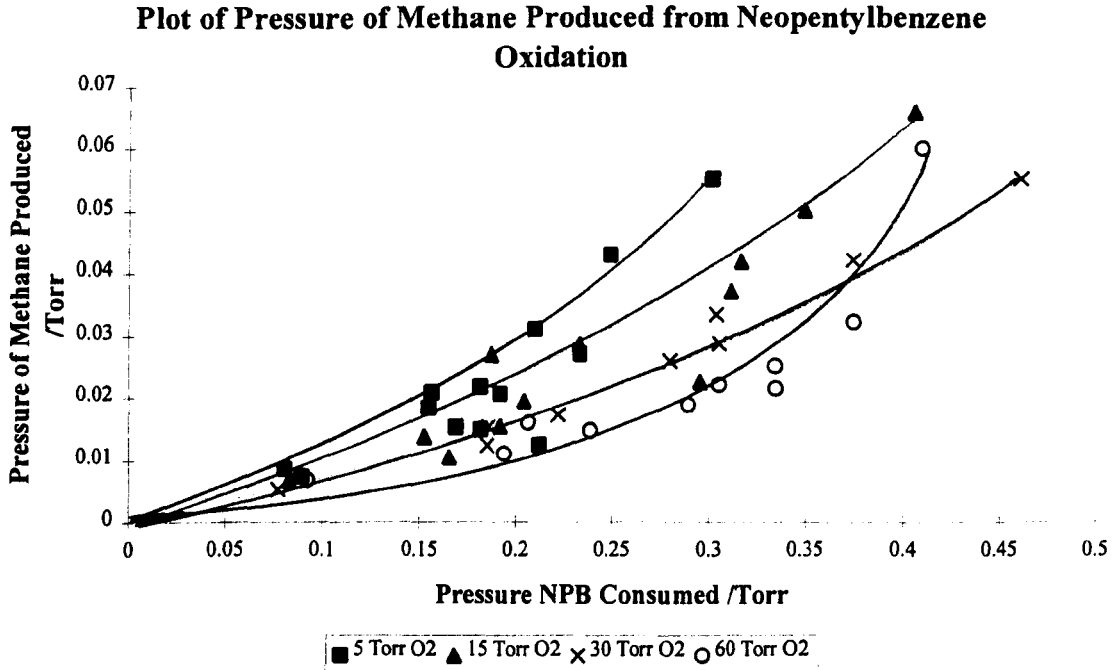
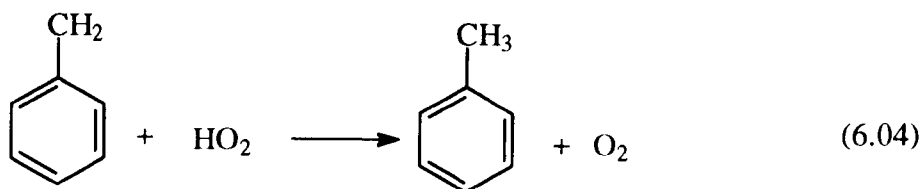


Figure 6. 10





The initial relative rate of formation of benzaldehyde and toluene is given by equation (i)

$$\frac{d[BA]}{d[T]} = \frac{[BA]}{[T]} = \frac{k_{6.03}}{k_{6.04}} \quad (i)$$

Consequently the initial values of $[BA]/[T]$ should be completely independent of mixture composition and dependent only on any difference in the temperature coefficients for the two reactions (assuming no pressure effects). Clearly this can be tested experimentally without a full knowledge of all the other reaction products.

6.3.2. Results : Decomposition of NPB in the presence of O₂ at 753K.

Figure 6.1 shows a plot of the consumption of NPB against time for different oxygen pressures. The consumption was measured by difference. Although the data points are not entirely consistent, the results show that the rate of consumption increases with O₂ pressure. Between O₂ = 5 Torr and 60 Torr, the rate of consumption increases by about 50%, presumably due to an enhanced radical attack on NPB.

Figures 6.2 - 6.10 show the product yields for the various mixtures of differing O₂ pressures. 2-methyl-1-phenylprop-1-ene (MPP), toluene (T), benzaldehyde (BA), i-butene, ethylbenzene and methane are clearly formed in primary processes. Benzene and propene are secondary products. It is likely that C₂H₆ is formed (in minor amounts) as a

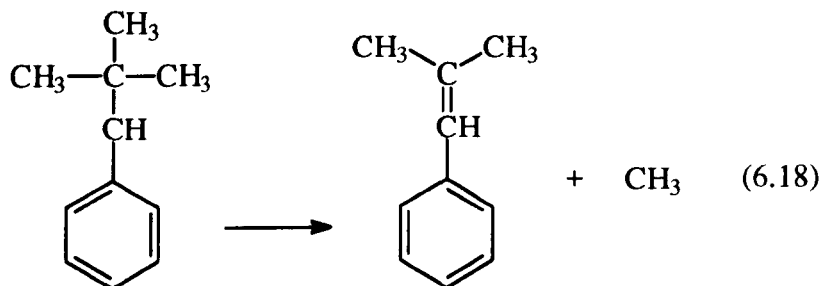
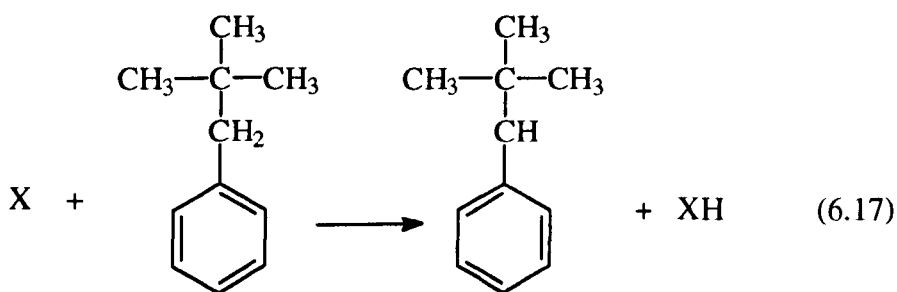
primary product and that the auto-catalytic rise shown in Figure 6.9 is at least partly due to the formation of C_2H_4 as a secondary or tertiary product because on the column used, C_2H_6 and C_2H_4 were not easily resolved. The product yields are also presented in Tables 6.2 to 6.5.

6.3.3. Formation of Products in the NPB + O_2 Experiments.

The mechanism for the formation of toluene and benzaldehyde will be considered shortly. As indicated, earlier i-butene is formed in 99% yield from t-butyl radicals in the reaction



MPP, CH_4 and C_2H_6 are probably formed as a consequence of radical (**X**) attack on the benzylic (CH_2) group in NPB.



2-methyl-1-phenylprop-1-ene (MPP)

Table 6. 2: NPB + 60 Torr O₂ Oxidation Products.

Pressure NPB Consumed/Torr	Pressure of Product/Torr								
	Benzaldehyde	Toluene	MPP	Ethylbenzene	i-Butene	Benzene	Methane	Ethane	Propene
0.092	0.002	0.0014	0.014	0.0003	0.022		0.006	0.0009	0.0009
0.101			0.015		0.026	0.002		0.0015	0.0017
0.156	0.016	0.0021			0.034	0.003	0.008	0.0011	0.0012
0.194	0.040	0.0041	0.031	0.0011	0.061	0.004	0.011	0.0020	0.0034
0.206	0.076	0.0060	0.042		0.073	0.008	0.015	0.0040	0.0072
0.239	0.069	0.0061	0.045	0.0015	0.077	0.008	0.014	0.0030	0.0063
0.289	0.075	0.0075	0.039	0.0016	0.077	0.009	0.018	0.0055	0.0095
0.305	0.096	0.0084		0.0017		0.011	0.022	0.0076	0.0122
0.334	0.099	0.0088		0.0018		0.011	0.025	0.0096	0.0143
0.334	0.080	0.0067	0.030		0.056	0.010	0.021	0.0083	0.0120
0.374	0.066	0.0079	0.020	0.0014	0.039	0.015	0.032	0.0165	0.0162
0.408	0.051	0.0068	0.010	0.0010	0.018	0.017	0.059	0.0347	0.0230

Table 6. 3: NPB + 30 Torr O₂ Oxidation Products.

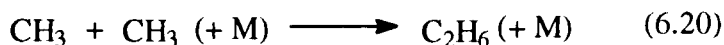
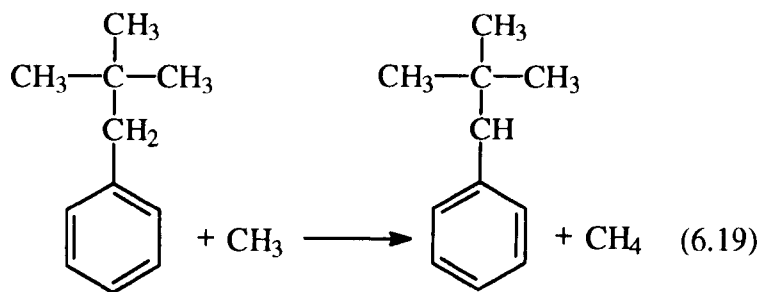
Pressure NPB Consumed/Torr	Pressure of Product/Torr								
	Benzaldehyde	Toluene	MPP	Ethylbenzene	i-Butene	Benzene	Methane	Ethane	Propene
0.077	0.005	0.0011	0.012		0.015	0.001	0.005	0.0015	0.0008
0.085	0.012	0.0020	0.021	0.0009	0.029		0.007	0.0027	0.0018
0.103							0.003		
0.126			0.024		0.039	0.003		0.0064	0.0027
0.185	0.034	0.0047	0.032	0.0017	0.054		0.012		0.0030
0.185	0.513	0.0052	0.038	0.0023		0.007	0.015		0.0045
0.221	0.048	0.0053		0.0021	0.063		0.017	0.0097	0.0052
0.251								0.0102	0.0105
0.279	0.066	0.0080	0.048	0.0030	0.081	0.009	0.025		0.0106
0.303	0.065	0.0090	0.042	0.0031		0.013	0.033	0.0200	0.0142
0.305	0.066	0.0089	0.044	0.0031	0.082	0.013	0.028		0.0120
0.374	0.067	0.0105	0.032	0.0029	0.057	0.016	0.042	0.0299	0.0179
0.460	0.062	0.0099	0.016	0.0021	0.032	0.021	0.055		0.0360

Table 6. 4: NPB + 15 Torr O₂ Oxidation Products.

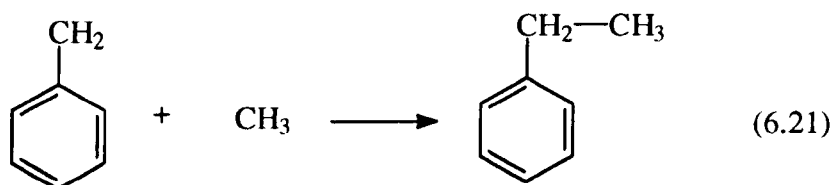
Pressure NPB Consumed/Torr	Pressure of Product/Torr								
	Benzaldehyde	Toluene	MPP	Ethylbenzene	i-Butene	Benzene	Methane	Ethane	Propene
0.082		0.0013	0.012	0.0008	0.018	0.001	0.006	0.0005	0.0006
0.153	0.023	0.0040		0.0026	0.053	0.004	0.013	0.0018	0.0025
0.165			0.021				0.010	0.0011	
0.187	0.054	0.0079					0.027	0.0043	
0.191							0.009	0.0013	
0.192			0.032	0.0031	0.074	0.008	0.037	0.0037	0.0057
0.192	0.029	0.0044	0.030		0.055		0.015	0.0021	
0.204	0.046	0.0061	0.039	0.0036	0.070		0.019	0.0029	
0.233	0.052	0.0081		0.0043	0.083	0.011	0.028	0.0048	0.0084
0.295	0.052						0.022	0.0040	
0.311		0.0096	0.047	0.0051	0.088	0.014	0.037	0.0078	0.0124
0.317	0.063	0.0109	0.045	0.0051	0.083	0.016	0.041	0.0104	0.0152
0.349	0.063	0.0110	0.040	0.0057	0.075	0.019	0.050	0.0138	0.0179
0.405	0.057	0.0086	0.025	0.0049	0.065	0.023	0.065	0.0199	0.0223
0.476									
0.499			0.019		0.046				
0.511	0.030	0.0053							
0.511					0.037				
0.511			0.015						

Table 6. 5: NPB + 5 Torr O₂ Oxidation Products.

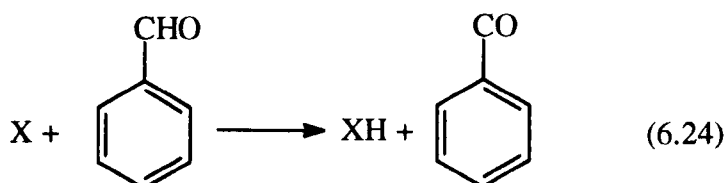
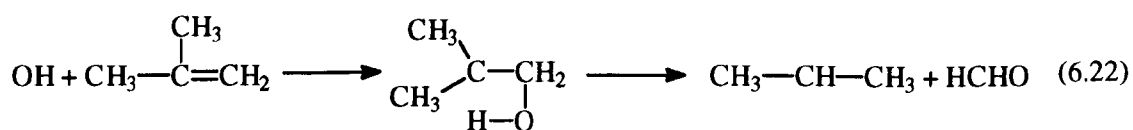
Pressure NPB Consumed/Torr	Pressure of Product/Torr								
	Benzaldehyde	Toluene	MPP	Ethylbenzene	i-Butene	Benzene	Methane	Ethane	Propene
0.081	0.003	0.002		0.0017	0.022	0.002	0.008	0.0012	0.0018
0.089		0.001	0.009	0.0012	0.014		0.007	0.0006	
0.104							0.004	0.0005	
0.155	0.019	0.005		0.0040	0.051	0.005	0.018	0.0020	0.0034
0.157			0.024		0.044	0.004	0.021	0.0021	0.0032
0.169		0.004	0.025	0.0033	0.043		0.015	0.0017	
0.181	0.032	0.006		0.0054	0.062	0.007	0.021	0.0025	0.0045
0.182							0.014	0.0014	
0.192	0.023	0.006	0.030		0.057		0.020	0.0022	
0.210	0.036	0.009	0.038	0.0060	0.074	0.009	0.031	0.0042	0.0069
0.212							0.012	0.0015	
0.233	0.036	0.008	0.039	0.0057	0.072		0.027	0.0033	
0.249	0.044	0.011	0.044	0.007	0.079	0.012	0.042	0.0071	0.0108
0.301	0.061	0.013	0.040	0.0075	0.080	0.015	0.055	0.0111	0.0160

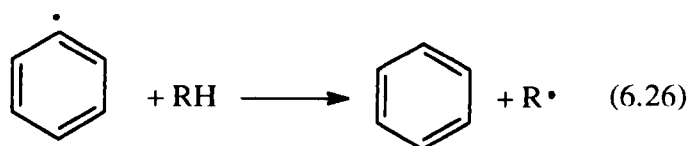
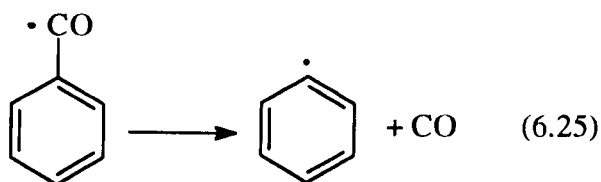


The formation of ethylbenzene may well occur through a radical-radical reaction between benzyl radicals and CH_3 radicals, reaction (6.21).



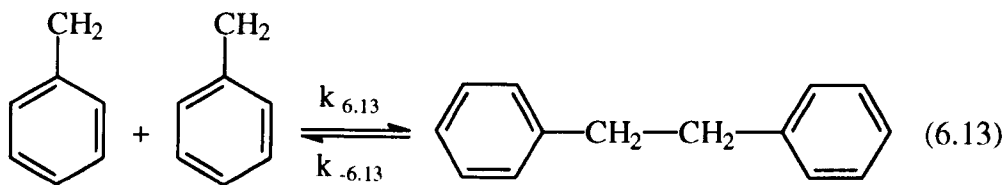
As indicated above, C_3H_6 and benzene are formed from secondary processes. The most likely mechanism involves OH addition to i-butene and radical attack on benzaldehyde, respectively.





One major problem in the results illustrated in this chapter is the difference in the total pressure of aromatic compounds produced initially relative to the amount of NPB consumed given that the aromatic ring is not lost in the initial products. Several checks have been used on the equipment in order to establish why this has occurred. Tests have shown that a maximum of about 10% consumption may be caused by condensation of NPB on the cold parts of the apparatus and additionally by tailing effects occurring on the GC peaks for NPB.

Accounting for this 10% still leaves a major quantity of aromatic products not accounted for. The only other explanation that can be postulated is that dibenzyl and other heavy aromatics are being produced. Rate data are available for the formation of dibenzyl from benzyl radicals and the decomposition of dibenzyl to give benzyl radicals between two different temperature ranges. Müller-Markgraf and Troe⁷ determined values for both $k_{6.13} = 2.45 \cdot 10^9 \cdot (T/298)^{0.4} \text{ l mol}^{-1} \text{ s}^{-1}$ between 300 and 1500K such that $k_{6.13} = 3.55 \cdot 10^9 \text{ l mol}^{-1} \text{ s}^{-1}$ at 753K and $k_{6.13} = 7.94 \cdot 10^{14} \exp(-30069\text{K}/T) \text{ s}^{-1}$ between 900 and 1500K. Korobkov and Kalechits⁸ determined $k_{6.13} = 9.48 \cdot 10^{14} \exp(-30911\text{K}/T) \text{ s}^{-1}$ between 683 and 713K; which leads to a decomposition rate constant for $k_{6.13} = 2.97 \cdot 10^{-3} \text{ s}^{-1}$ at 753K.



Consequently when [Benzyl] is high it is very likely that dibenzyl will be the significant product. Dibenzyl and any other heavy aromatics would condense on the sections of glassware connecting the reaction vessel with the sampling bulb. Since dibenzyl has a vapour pressure of 0.0212 Torr at 298K⁹, it was not possible to get a sample of dibenzyl in a form whereby a quantitative estimation could be performed using the available analytical techniques; also the initial concentration of NPB used was 0.48 Torr (0.8%) and consequently any quantity of dibenzyl produced would probably condense on any surface at room temperature preventing it from being detected. Other possible products such as cresol could not be detected quantitatively with the analytical techniques available.

6.3.4. [BA]/[T] Ratios.

Figures 6.11 - 6.14 show the values of [BA]/[T] plotted as a function of time for four mixtures of varying O₂ pressure. In all cases, the value of the ratio falls off with reaction time. Accurate measurement of the ratio at lower times was not possible because of the difficulty of measuring the area of the benzaldehyde peak on the gas chromatogram. The fall in the product ratio tends to increase slightly as the O₂ pressure increases. However, in all cases, the values may be extrapolated to zero time to obtain a reasonably reliable initial value of ([BA]/[T])₀. Table 6.6 summarises the values of these ratios.

[BA]/[T] Plots from NPB + O₂ at 753K and 60 Torr maximum pressure.

Figure 6. 11

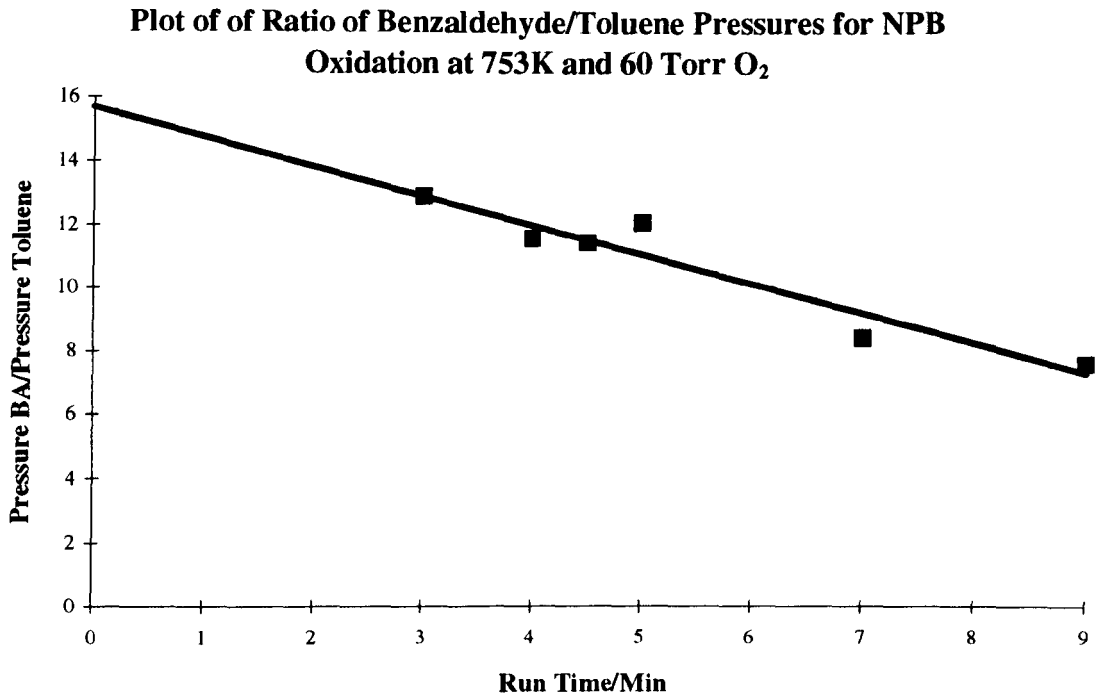


Figure 6. 12

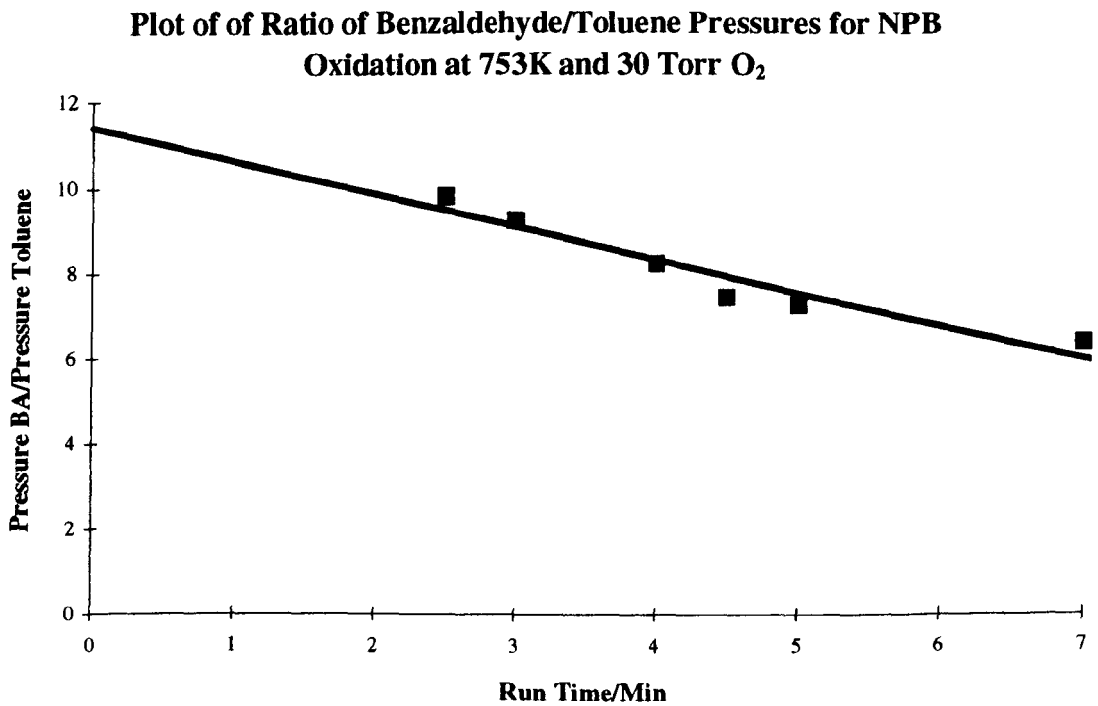


Figure 6. 13

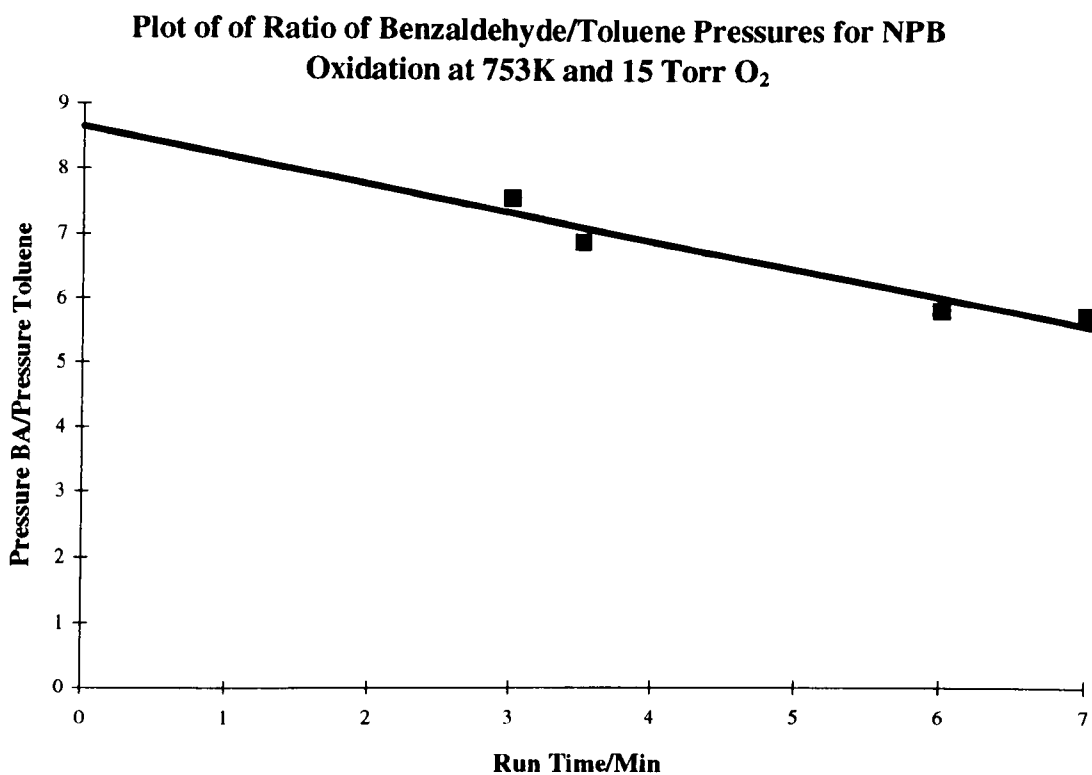


Figure 6. 14

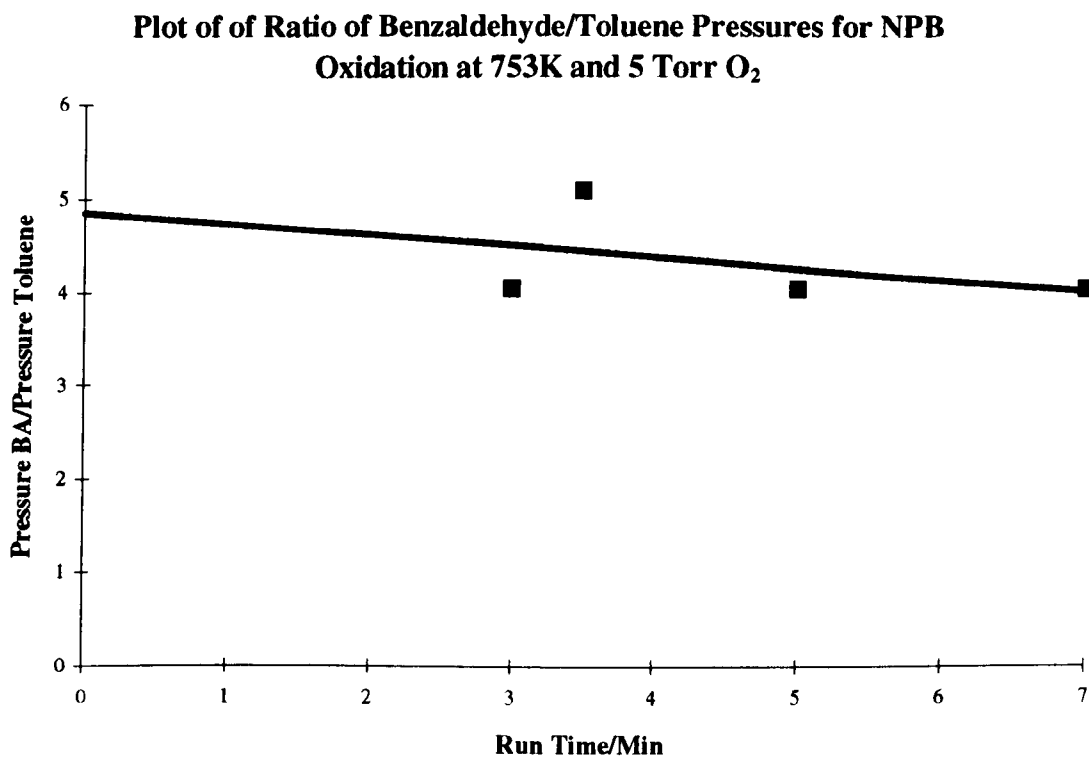
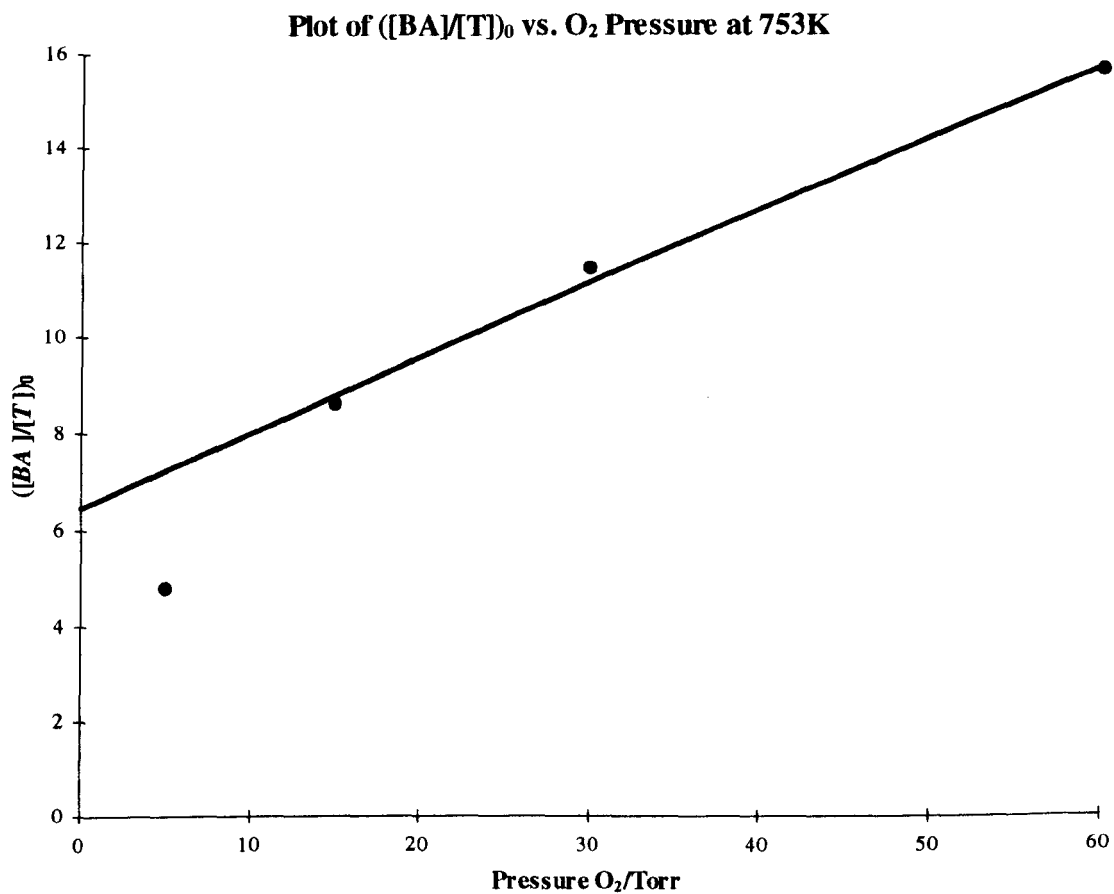


Table 6. 6 : Extrapolated Ratio of Benzadehyde : Toluene $([BA]/[T])_0$ for NPB Oxidation at 753K.

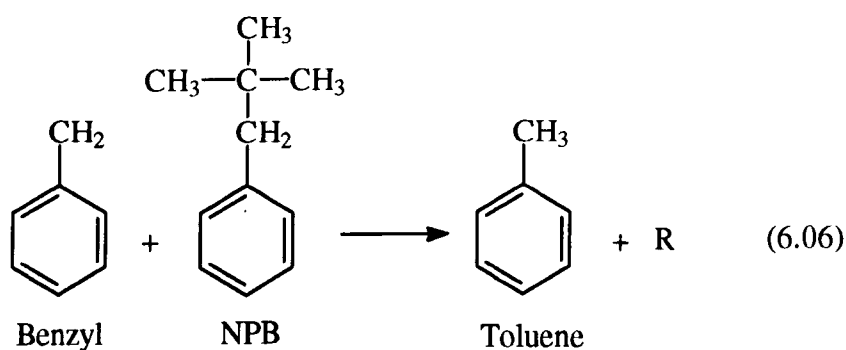
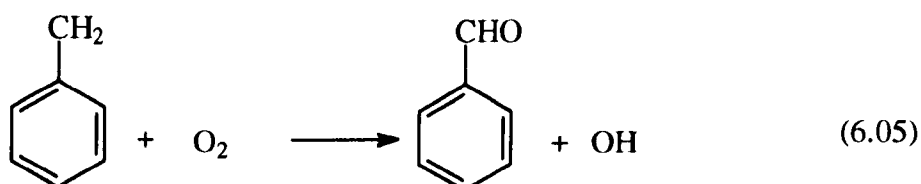
Pressure O ₂ / Torr	$([BA]/[T])_0$
60	15.7
30	11.4
15	8.6
5	4.8

Figure 6. 15

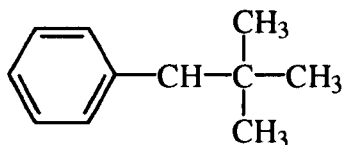


If, as indicated earlier by equation (i), benzaldehyde and toluene are formed only from reactions (6.04) and (6.03), then the values of $([BA]/[T])_0$ should be independent of mixture composition and as such should be independent of O_2 pressure. Table 6.6 and Figure 6.15 show that there is a near linear increase with O_2 pressure and an intercept of 6.5 ± 1 . Clearly other reactions are involved in the formation of benzaldehyde and toluene.

Two other reactions may be considered for the formation of benzaldehyde and toluene in the initial stages of reaction, where (6.05) represents the overall process,



where **R** represents a radical formed by H abstraction from NPB and is most likely to be the delocalised radical.



If benzaldehyde and toluene are formed solely from reactions (6.05) and (6.06), then the initial product ratio is given by equation (ii)

$$\left(\frac{[BA]}{[T]}\right)_0 = \frac{k_{6.05}}{k_{6.06}} \times \frac{[O_2]}{[NPB]} \quad (\text{ii})$$

However, as shown in Table 6.6 and Figure (6.15), although $([BA]/[T])_0$ does increase with the pressure of O_2 , the increase is significantly less than first power and further equation (ii) does not predict the intercept found in Figure (6.15). Further, as shown later, the addition of 1.5 Torr of propene to the $NPB + O_2$ mixtures does not reduce the values of $([BA]/[T])_0$, even though H abstraction from C_3H_6 by benzyl to give toluene would be very significant if reaction (6.06) is important.

Analytically, there are combinations of reactions (6.03) - (6.06) which might lead to the form of relationship between $([BA]/[T])_0$ and $[O_2]$ shown in Figure (6.15).

A) BA is formed in reaction (6.03) and (6.05), T is formed in (6.04).

In this case $([BA]/[T])_0$ is given by equation (iii)

$$\left(\frac{[BA]}{[T]}\right)_0 = \frac{k_{6.03}[HO_2] + k_{6.05}[O_2]}{k_{6.04}[HO_2]} \quad (\text{iii})$$

which upon rearrangement gives equation (iv)

$$\left(\frac{[BA]}{[T]}\right)_0 = \frac{k_{6.03}}{k_{6.04}} + \frac{k_{6.05}[O_2]}{k_{6.04}[HO_2]} \quad (\text{iv})$$

As shown later, $[HO_2] \propto [O_2]^n$, where $n < 1$ and positive, so that equation (iv) predicts an intercept and an increase in the $([BA]/[T])_0$ ratio when it is plotted against $[O_2]$.

B) BA is formed in reaction (6.03), T is formed in (6.04) and (6.06).

$([BA]/[T])_0$ is given by equation (v)

$$\left(\frac{[BA]}{[T]}\right)_0 = \frac{k_{6.03}[HO_2]}{k_{6.04}[HO_2] + k_{6.06}[NPB]} \quad (v)$$

If $k_{6.06}[NPB] \ll k_{6.04}[HO_2]$, then equation (v) reduces to equation (i) and hence a plot of $([BA]/[T])_0$ against $[O_2]$ would give a horizontal line with an intercept equal to $k_{6.03}/k_{6.04}$.

If $k_{6.06}[NPB] \gg k_{6.04}[HO_2]$ and $[HO_2] \propto [O_2]^n$, then the $([BA]/[T])_0$ would rise with $[O_2]$, again given that $n < 1$ and positive.

C) BA is formed in reactions (6.03) and (6.05) and T in (6.04) and (6.06).

In this case, the initial value of the product ratio is given by equation (vi),

$$\left(\frac{[BA]}{[T]}\right)_0 = \frac{k_{6.03}[HO_2] + k_{6.05}[O_2]}{k_{6.04}[HO_2] + k_{6.06}[NPB]} \quad (vi)$$

which predicts that $([BA]/[T])_0$ will increase with $[O_2]$.

Two cases can be considered

I. If $k_{6.04}[HO_2] \gg k_{6.06}[NPB]$ then equation (vi) simplifies to equation (iii) discussed earlier (heading A).

II. If $k_{6.04}[HO_2] \ll k_{6.06}[NPB]$ then equation (vi) simplifies to (vii) which predicts an increase in $([BA]/[T])_0$ as O_2 pressure increases and a zero intercept unless $[HO_2] \propto [NPB]$.

$$\left(\frac{[BA]}{[T]}\right)_0 = \frac{k_{6.03}[HO_2] + k_{6.05}[O_2]}{k_{6.06}[NPB]} \quad (vii)$$

It is clear that each combination of reactions **A**, **B** and **C** may predict an increase in $([BA]/[T])_0$ with $[O_2]$ similar to that observed experimentally. In order to discriminate further, it is necessary to measure the concentration of HO_2 radicals. As in previous studies¹⁰, this has been accomplished by the addition of C_3H_6 to the $NPB + O_2$ mixtures. By measurement of the rate of formation of propene oxide (**PO**) produced in reaction (6.07), together with a knowledge of $k_{6.07}$ ⁽¹¹⁾, $[HO_2]$ may be calculated from equation (viii), where R_{po} is the initial rate of formation of propene oxide (**PO**).

$$R_{po} = k_{6.07} [HO_2] [C_3H_6] \quad \text{(viii)}$$

It has been shown¹¹ that under the conditions used in the present work, **PO** is formed uniquely in reaction (6.07).



6.3.5. Formation of products from $NPB + O_2 + C_3H_6$ mixtures.

Figure 6.16 and 6.17 show plots of NPB and C_3H_6 consumption for varying O_2 pressures with $NPB = 0.48$ Torr and $C_3H_6 = 1.5$ Torr. In general, the addition of C_3H_6 leads to a small (c.a. 20 - 30%) increase in the rate of consumption of NPB . The rate of consumption of C_3H_6 is more markedly dependent on O_2 pressure, as might be expected because of the absence of any significant pyrolysis reaction.

The products are shown in Figures 6.18 - 6.26 and follow the same trend as observed in the absence of C_3H_6 , discussed earlier, with the product yields presented in Tables 6.7 - 6.10. C_3H_6O (propylene oxide) was the only C_3H_6 product monitored (Figure 6.23) although it is known that CH_3CHO , C_2H_4 , 1,5-hexadiene, $HCHO$, CO and allene are important initial products under the present conditions¹². Benzene (from NPB) was detected but the yield was not quantified since benzene is only a secondary product; also

Profiles from NPB + O₂ + 1.5 Torr Propene at 753K and 60 Torr maximum pressure.

Figure 6. 16

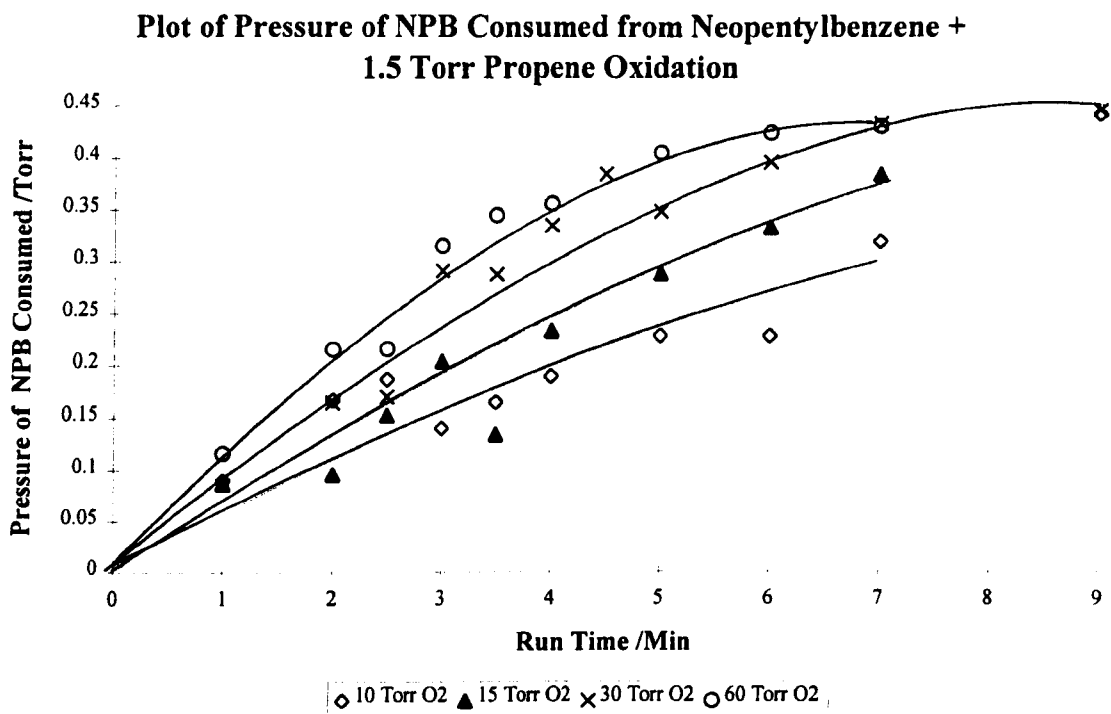


Figure 6. 17

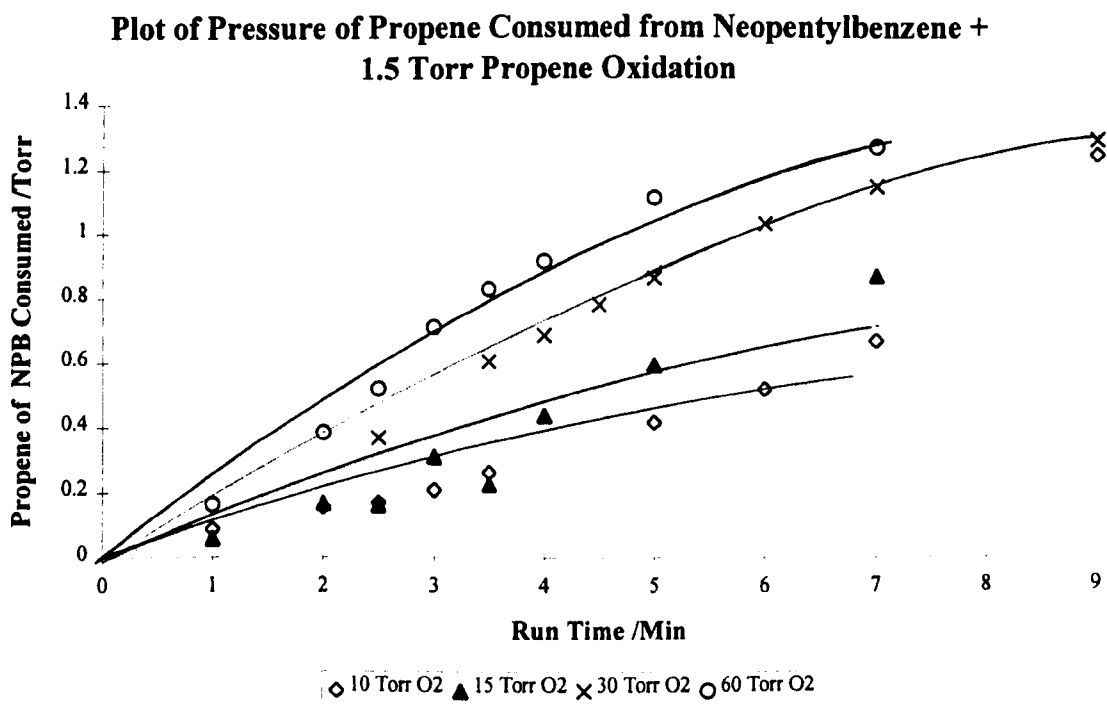


Figure 6. 18

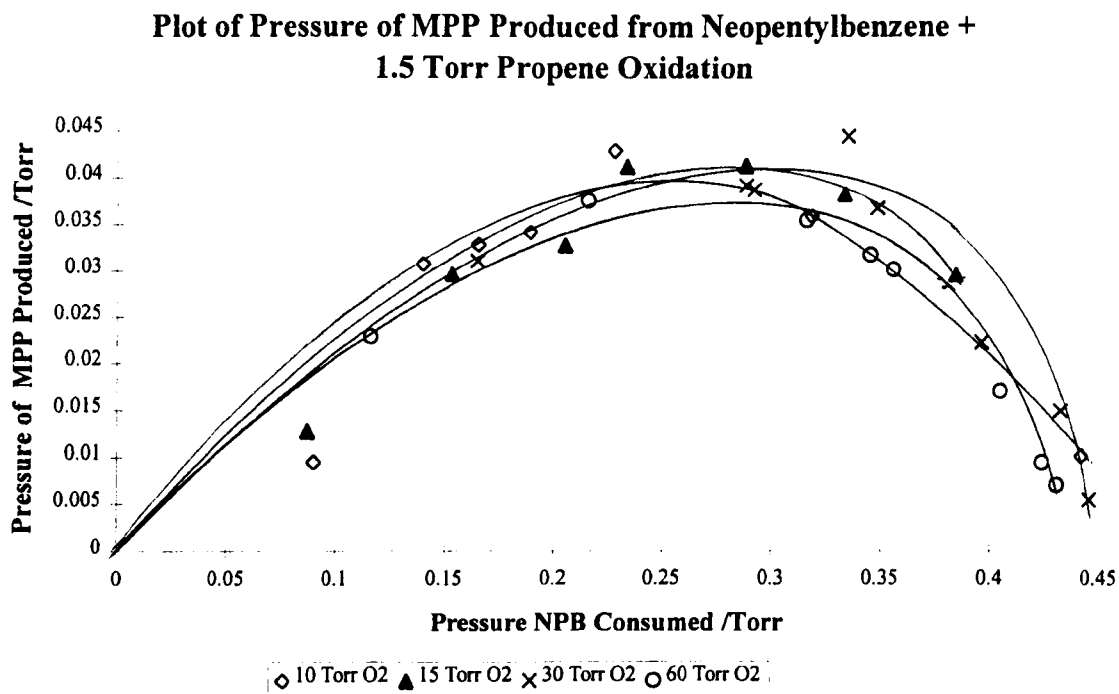


Figure 6. 19

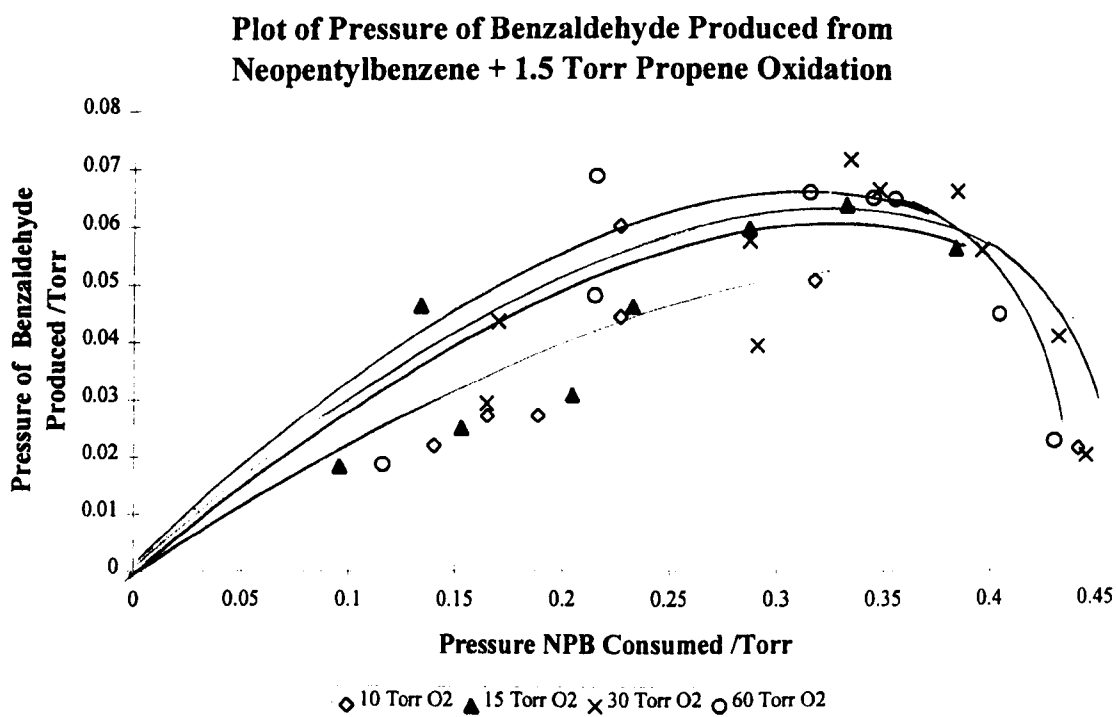


Figure 6. 20

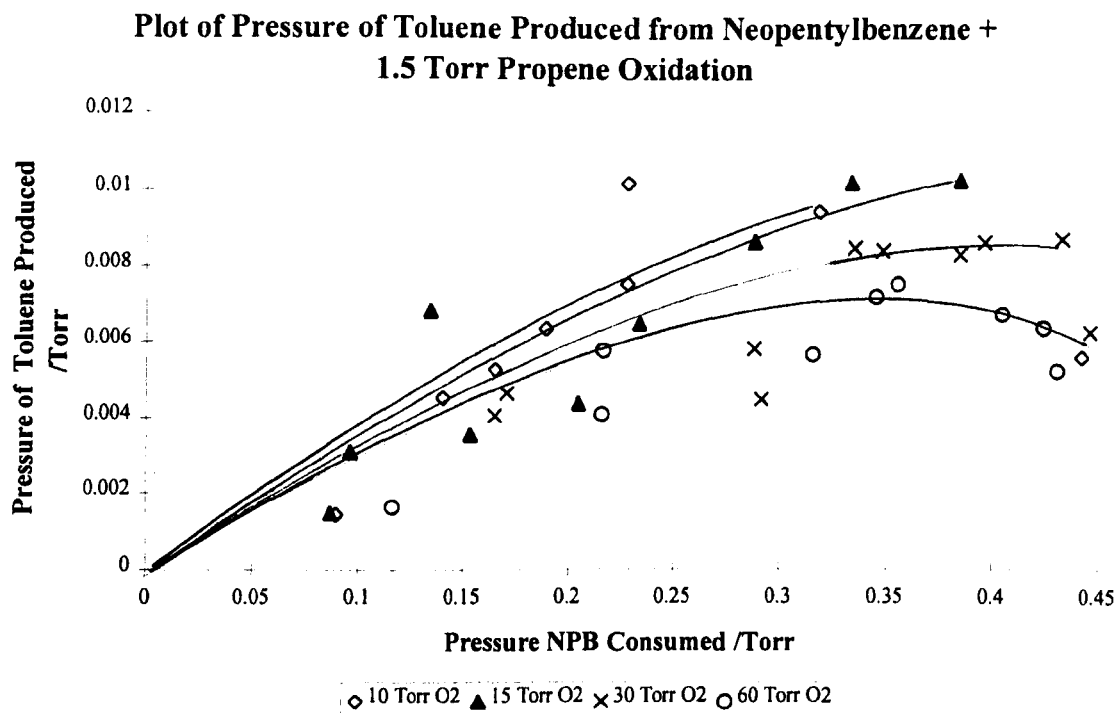


Figure 6. 21

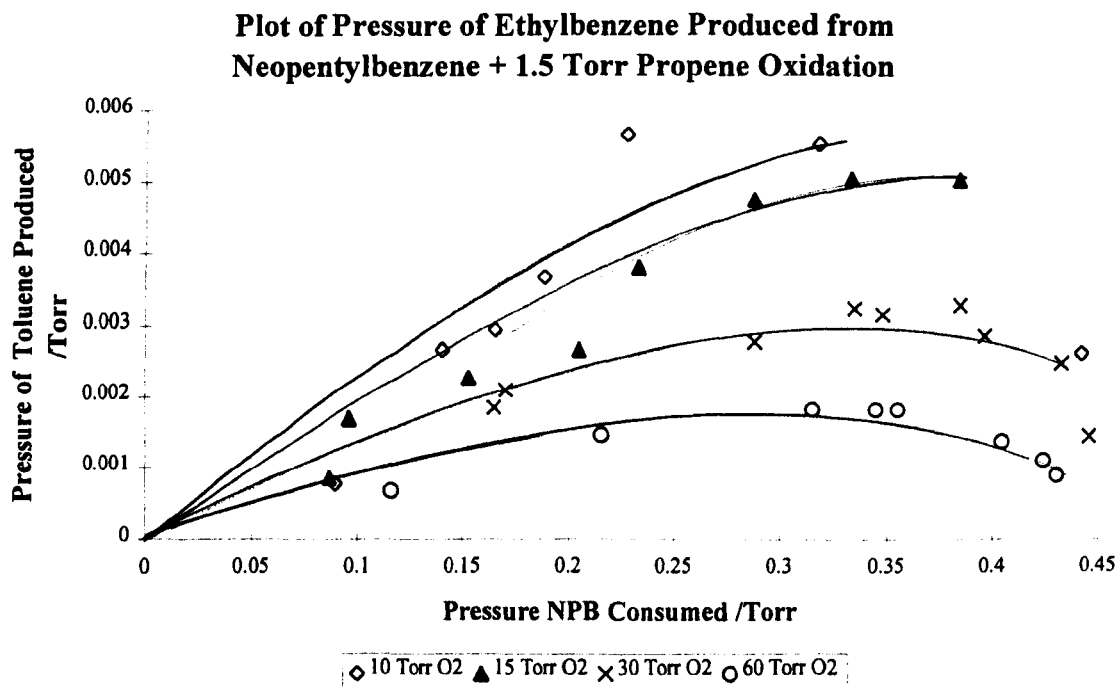


Figure 6. 22

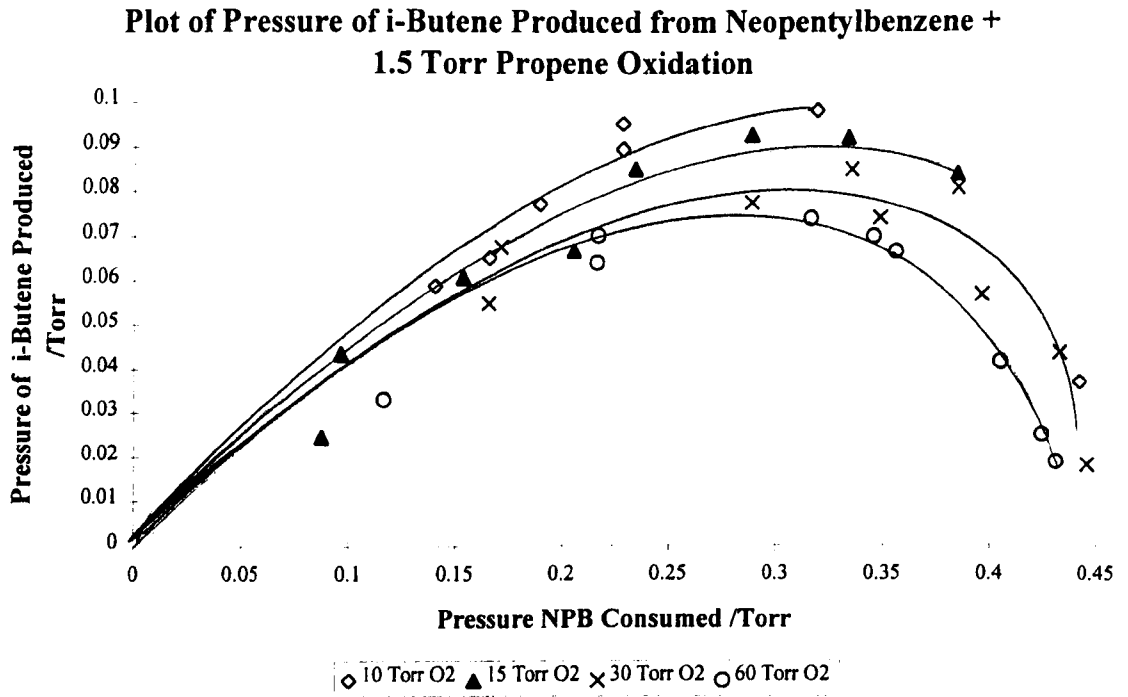


Figure 6. 23

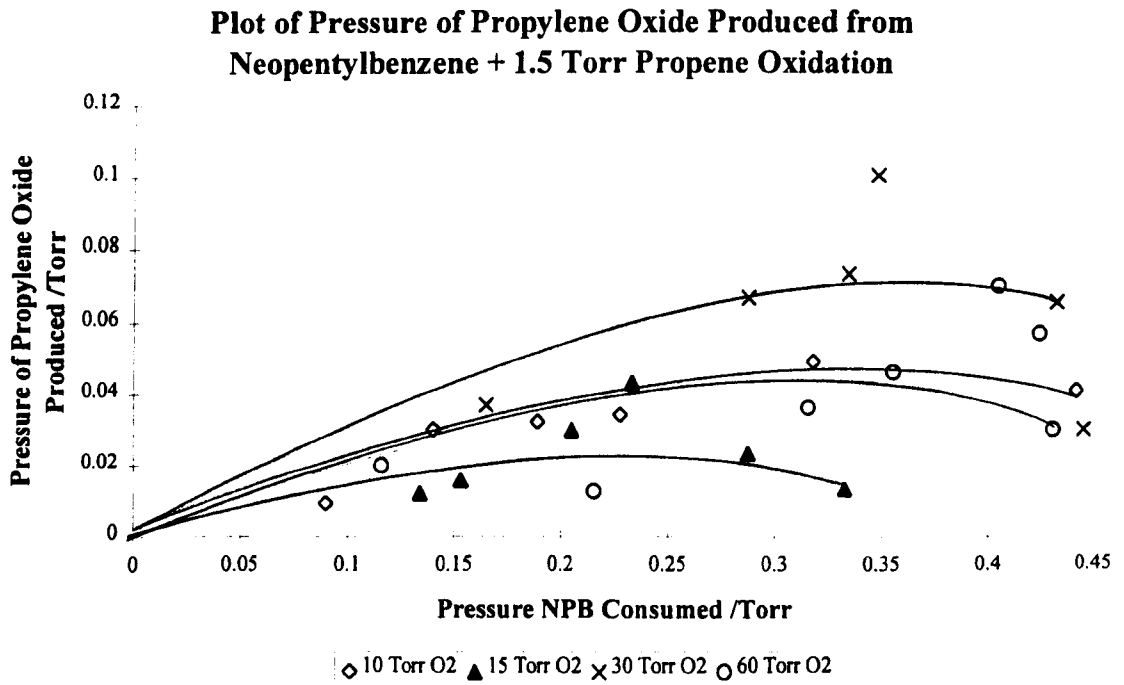


Figure 6. 24

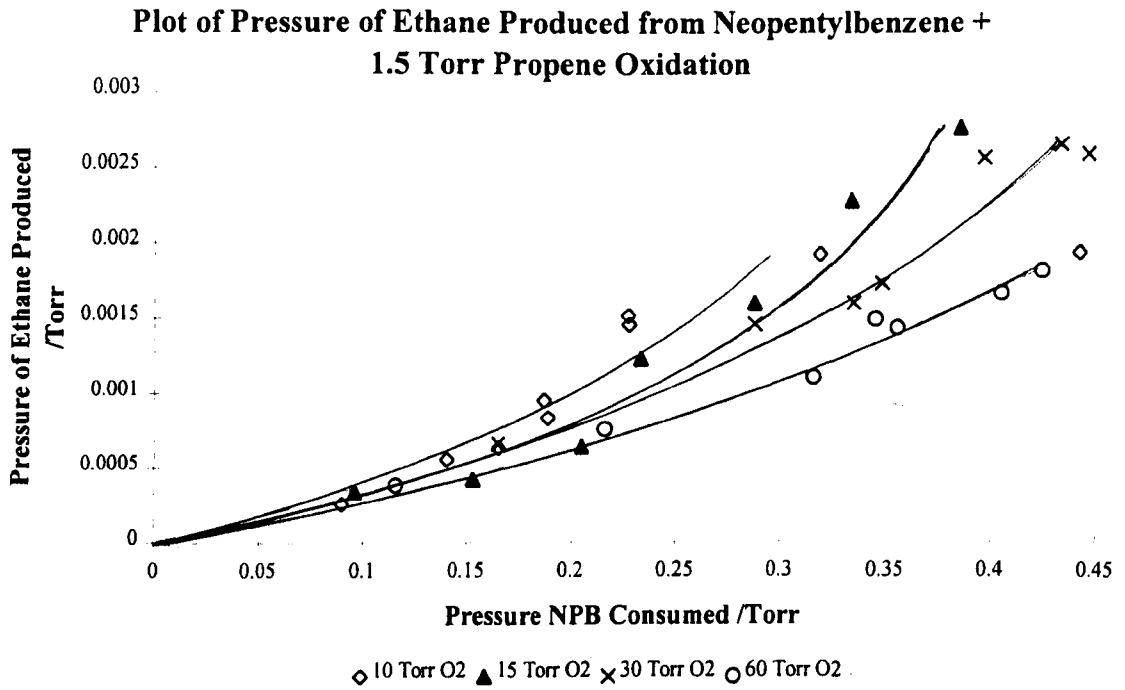


Figure 6. 25

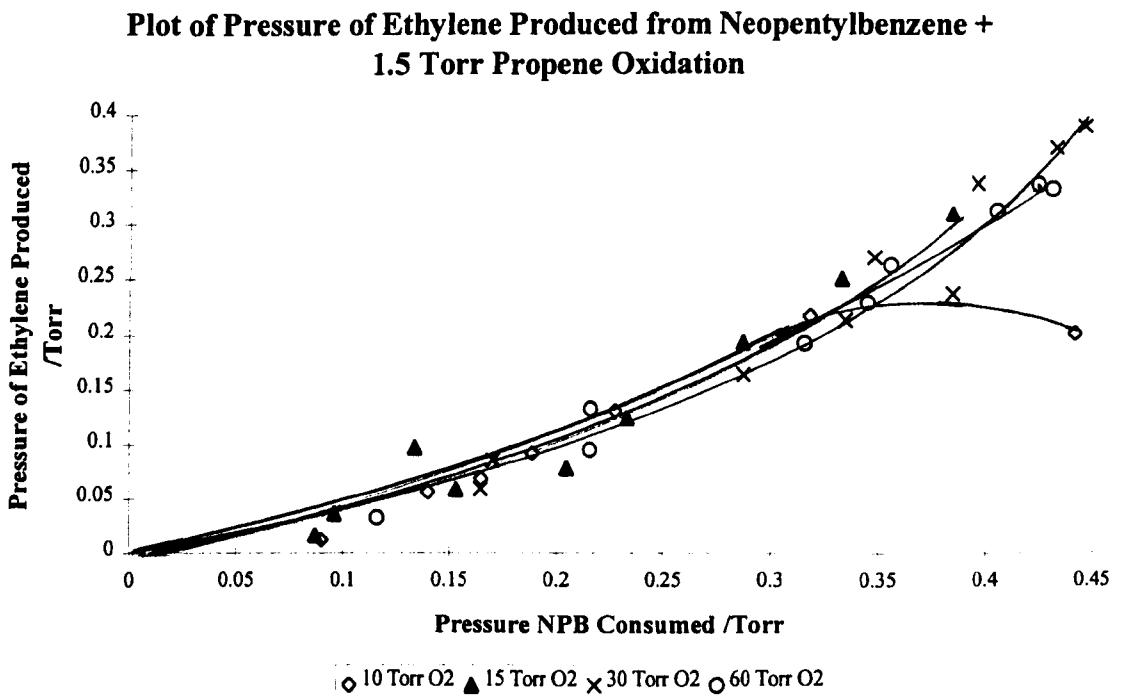


Figure 6. 26

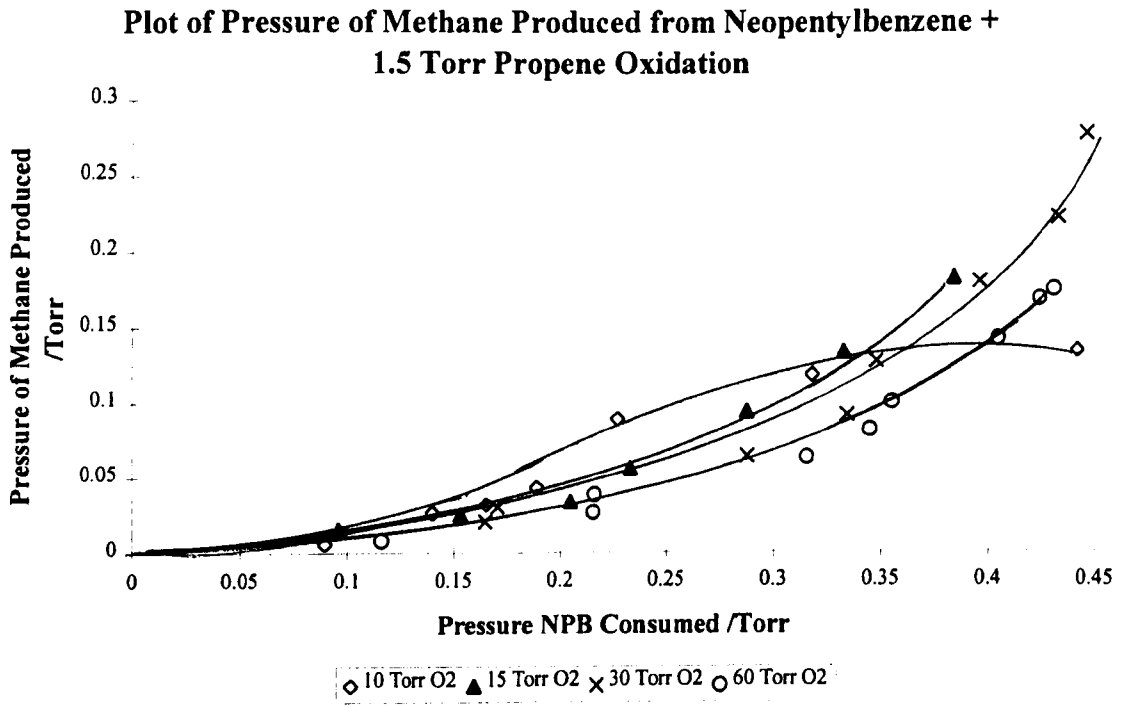


Table 6. 7: NPB +1.5 Torr Propene + 60 Torr O₂ Oxidation Products.

Pressure NPB Consumed/Torr	Pressure of Product/Torr								
	Benzaldehyde	Toluene	MPP	Ethylbenzene	i-Butene	Propylene Oxide	Methane	Ethylene	Ethane
0.116	0.018	0.0016	0.023	0.0007	0.033	0.019	0.008	0.032	0.0004
0.215	0.047	0.0041	0.037	0.0015	0.064	0.012	0.026	0.094	
0.216	0.068	0.0058	0.047		0.070		0.038	0.132	0.0008
0.315	0.065	0.0057	0.035	0.0018	0.073	0.036	0.062	0.191	0.0011
0.344	0.064	0.0072	0.031	0.0018	0.069		0.080	0.229	0.0015
0.355	0.064	0.0075	0.030	0.0018	0.066	0.046	0.099	0.262	0.0014
0.404	0.045	0.0067	0.017	0.0014	0.041	0.070	0.141	0.312	0.0017
0.423		0.0064	0.009	0.0011	0.025	0.057	0.167	0.335	0.0018
0.430	0.022	0.0052	0.007	0.0009	0.018	0.030	0.173	0.332	

Table 6. 8: NPB +1.5 Torr Propene + 30 Torr O₂ Oxidation Products.

Pressure NPB Consumed/Torr	Pressure of Product/Torr								
	Benzaldehyde	Toluene	MPP	Ethylbenzene	i-Butene	Propylene Oxide	Methane	Ethylene	Ethane
0.164	0.029	0.0041	0.031	0.0018	0.054	0.036	0.020	0.058	0.0007
0.170	0.043	0.0047		0.0021	0.067		0.030	0.085	
0.287	0.057	0.0058	0.039	0.0028	0.077	0.066	0.063	0.163	0.0015
0.291	0.039	0.0048							
0.334	0.071	0.0085	0.044	0.0032	0.084	0.073	0.091	0.213	0.0016
0.347	0.066	0.0084	0.036	0.0032	0.073	0.100	0.126	0.269	0.0017
0.384	0.066	0.0083		0.0033	0.080			0.237	
0.395	0.056	0.0086	0.022	0.0029	0.056		0.179	0.337	0.0026
0.432	0.041	0.0087	0.014	0.0025	0.043	0.065	0.221	0.369	0.0026
0.445	0.020	0.0062	0.005	0.0015	0.018	0.030	0.276	0.389	0.0026

Table 6. 9: NPB +1.5 Torr Propene + 15 Torr O₂ Oxidation Products.

Pressure NPB Consumed/Torr	Pressure of Product/Torr								
	Benzaldehyde	Toluene	MPP	Ethylbenzene	i-Butene	Propylene Oxide	Methane	Ethylene	Ethane
0.087		0.001	0.012	0.0009	0.024			0.016	
0.096	0.018	0.003	0.026	0.0017	0.043		0.015	0.036	0.0003
0.134	0.046	0.006				0.012		0.096	
0.153	0.024	0.003	0.029	0.0023	0.060	0.015	0.025	0.058	0.0004
0.204	0.030	0.004	0.032	0.0027	0.066	0.029	0.033	0.078	0.0006
0.233	0.046	0.006	0.041	0.0038	0.084	0.043	0.055	0.124	0.0012
0.287	0.059	0.008	0.041	0.0047	0.092	0.023	0.093	0.192	0.0016
0.332	0.063	0.010	0.038	0.0050	0.091	0.013	0.133	0.251	0.0023
0.383	0.056	0.010	0.029	0.0050	0.083		0.182	0.310	0.0028

Table 6. 10: NPB +1.5 Torr Propene + 10 Torr O₂ Oxidation Products.

Pressure NPB Consumed/Torr	Pressure of Product/Torr								
	Benzaldehyde	Toluene	MPP	Ethylbenzene	i-Butene	Propylene Oxide	Methane	Ethylene	Ethane
0.089		0.001	0.009	0.0008		0.009y	0.005	0.012	0.0003
0.140	0.021	0.004	0.030	0.0027	0.058	0.029	0.026	0.056	0.0006
0.165	0.027	0.005	0.032	0.0039	0.065		0.031	0.068	0.0006
0.189	0.027	0.006	0.034	0.0037	0.076	0.032	0.042	0.091	0.0008
0.227	0.059	0.010		0.0056	0.095		0.088		0.0015
0.227	0.044	0.007	0.042		0.089	0.034		0.130	0.0015
0.317	0.050	0.009	0.035	0.0055	0.097	0.049	0.117	0.216	0.0019
0.441	0.021	0.005	0.010	0.0026	0.037	0.041	0.133	0.201	0.0019

the addition of propene complicated the analysis such that it was not possible to quantitatively determine the benzene yields.

The yield of CH₄ increased noticeably on addition of C₃H₆, presumably due to the occurrence of the abstraction process (6.07a)



As for the decomposition of NPB in the absence of propene, the detected total product yield was noticeably less than 100% indicating that there are a number of products, such as dibenzyl and cresol, which were not detectable by use of the analytical techniques available.

6.3.6. $([BA]/[T])_0$ values in the presence of C₃H₆

Figures (6.27) - (6.30) show the plots of $([BA]/[T])$ against time for varying O₂ pressures when 1.5 Torr of C₃H₆ is added to the mixtures containing 0.48 Torr NPB. As in the absence of C₃H₆, the $[BA]/[T]$ values fall with time, and the initial values of $([BA]/[T])_0$, are obtained by extrapolation to zero time. Table 6.11 compares the values for $([BA]/[T])_0$ in the presence and absence of C₃H₆ for the range of O₂ pressure used. Significantly, within experimental error, the values are unchanged. This observation is important because if toluene is formed predominantly from reaction (6.06), then $([BA]/[T])_0$ would be expected to fall noticeably upon addition of C₃H₆ due to toluene formation in reaction (6.08) because of the similar thermochemistry involved in the two reactions.

[BA]/[T] Plots from NPB + O₂ + 1.5 Torr propene at 753K and 60 Torr maximum pressure.

Figure 6. 27

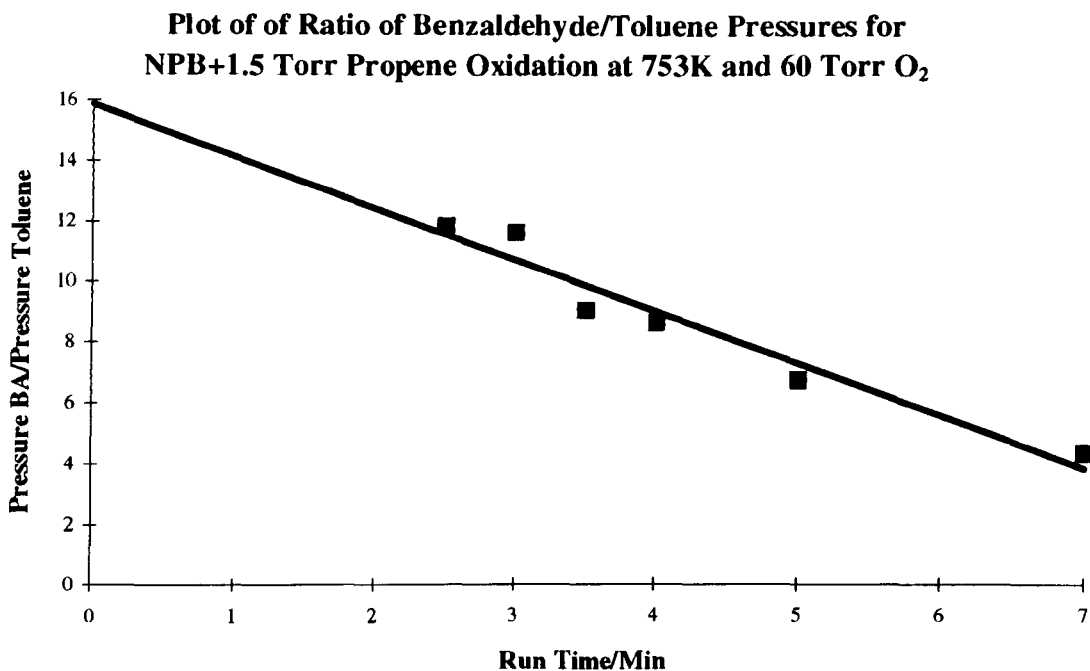


Figure 6. 28

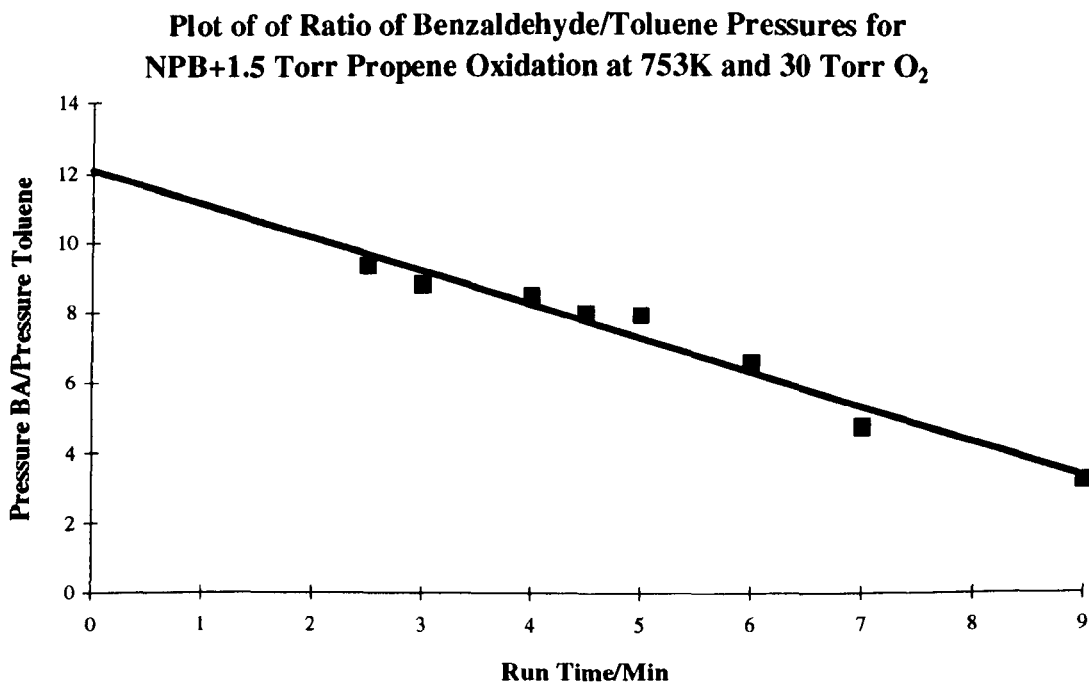


Figure 6. 29

**Plot of of Ratio of Benzaldehyde/Toluene Pressures for
NPB+1.5 Torr Propene Oxidation at 753K and 15 Torr O₂**

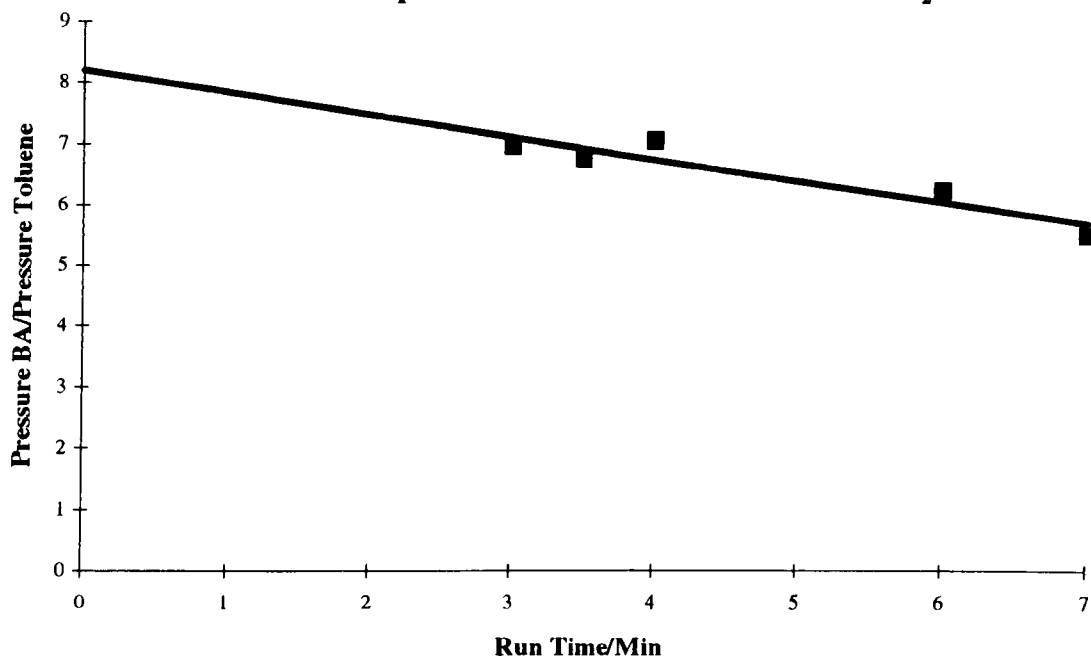


Figure 6. 30

**Plot of of Ratio of Benzaldehyde/Toluene Pressures for
NPB+1.5 Torr Propene Oxidation at 753K and 10 Torr O₂**

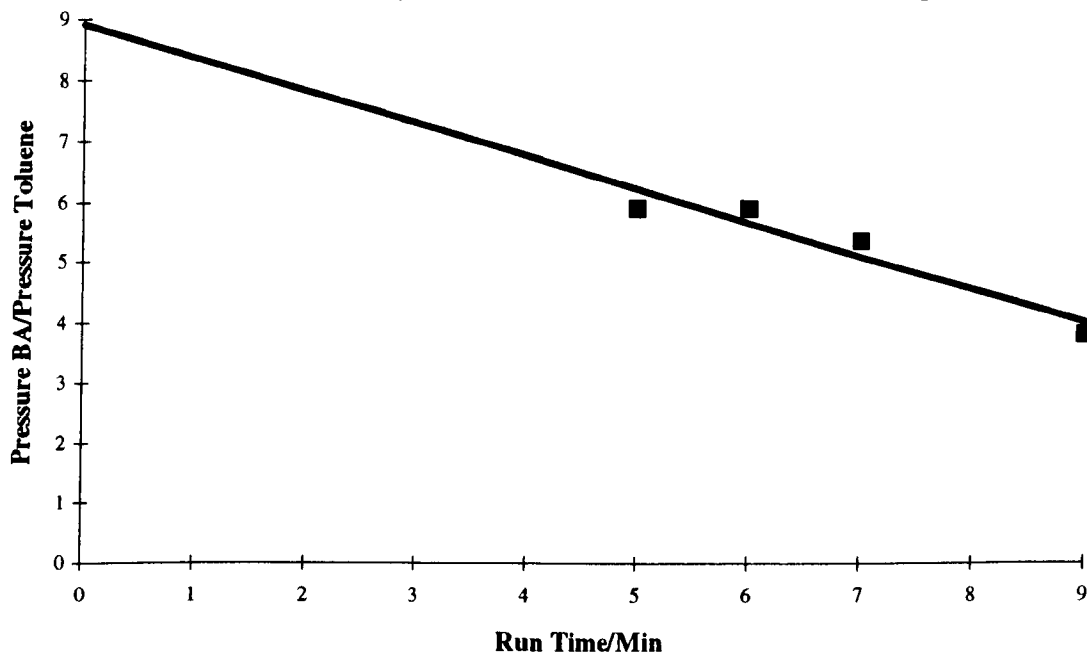
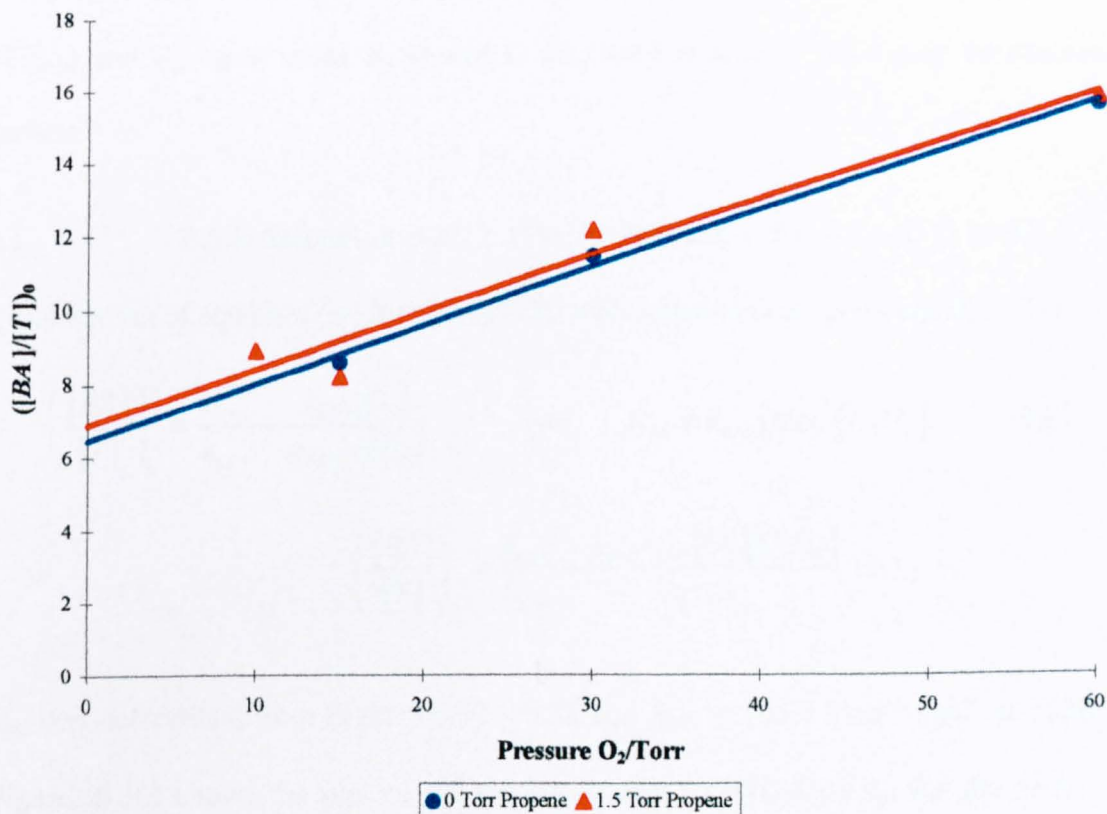


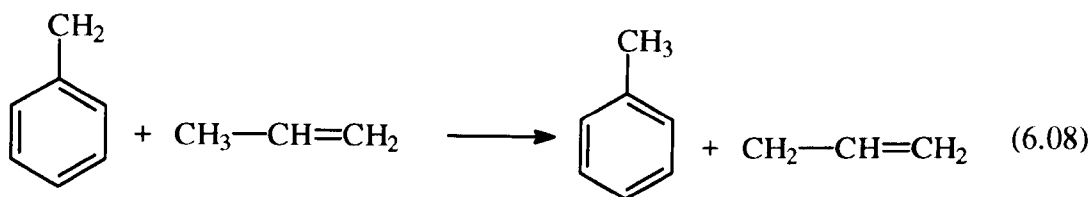
Table 6. 11 : $([BA]/[T])_0$ for NPB Oxidation and variable Propene at 753K.

Pressure O₂ / Torr	0 Torr (0 %) Propene	1.5 Torr (2.5%) Propene
60	15.7	15.9
30	11.4	12.1
15	8.6	8.2
10	-	8.9

Figure 6. 31

Plot of $([BA]/[T])_0$ for variable Propene against O₂ Pressure at 753K





This point will be discussed in more detail later.

Figure (6.31) shows the $([BA]/[T])_0$ values plotted against the pressure of O_2 when 1.5 Torr C_3H_6 is added to the $\text{NPB} + \text{O}_2$ mixtures and also in the absence of C_3H_6 . The intercepts are effectively indistinguishable and a maximum value for $k_{6.03}/k_{6.04}$ of 6.9 is obtained from application of equation (vi). The value is an upper limit because $[\text{HO}_2]$ increases slightly with O_2 pressure.

As $[\text{HO}_2]$ may be calculated for each mixture by use of equation (viii) and a knowledge of $k_{6.07}$ and R_{po} , then cases **A**, **B** and **C** discussed in section 6.3.4 may be examined further.

A) BA is formed in reaction (6.03) and (6.05), T is formed in (6.04).

Combination of equation (iv) for $([BA]/[T])_0$ with equation (viii) gives equation (ix)

$$\left(\frac{[BA]}{[T]} \right)_0 = \frac{k_{6.03}}{k_{6.04}} + \frac{k_{6.05}[\text{O}_2]}{k_{6.04}[\text{HO}_2]} \quad (\text{iv}), \quad R_{po} = k_{6.07}[\text{HO}_2][\text{C}_3\text{H}_6] \quad (\text{viii})$$

$$\left(\frac{[BA]}{[T]} \right)_0 = \frac{k_{6.03}}{k_{6.04}} + \frac{k_{6.05}k_{6.07}[\text{O}_2][\text{C}_3\text{H}_6]}{k_{6.04}R_{po}} \quad (\text{ix})$$

R_{po} was determined from Figures 6.32 - 6.35 and $k_{6.07} = 105.5 \text{ Torr}^{-1} \text{ min}^{-1}$ at 753K^{11} .

Figure (6.36) shows the plot of $([BA]/[T])_0$ against $([\text{O}_2][\text{C}_3\text{H}_6])/R_{po}$ for the series of experiments with $\text{C}_3\text{H}_6 = 1.5 \text{ Torr}$. The data for the plot are summarised in Table 6.12.

As can be seen, a good straight line can be drawn through the points (equally weighted),

Rate of Production of Propylene Oxide graphs for NPB + O₂ + 1.5 Torr Propene at 60 Torr Maximum Pressure.

Figure 6. 32

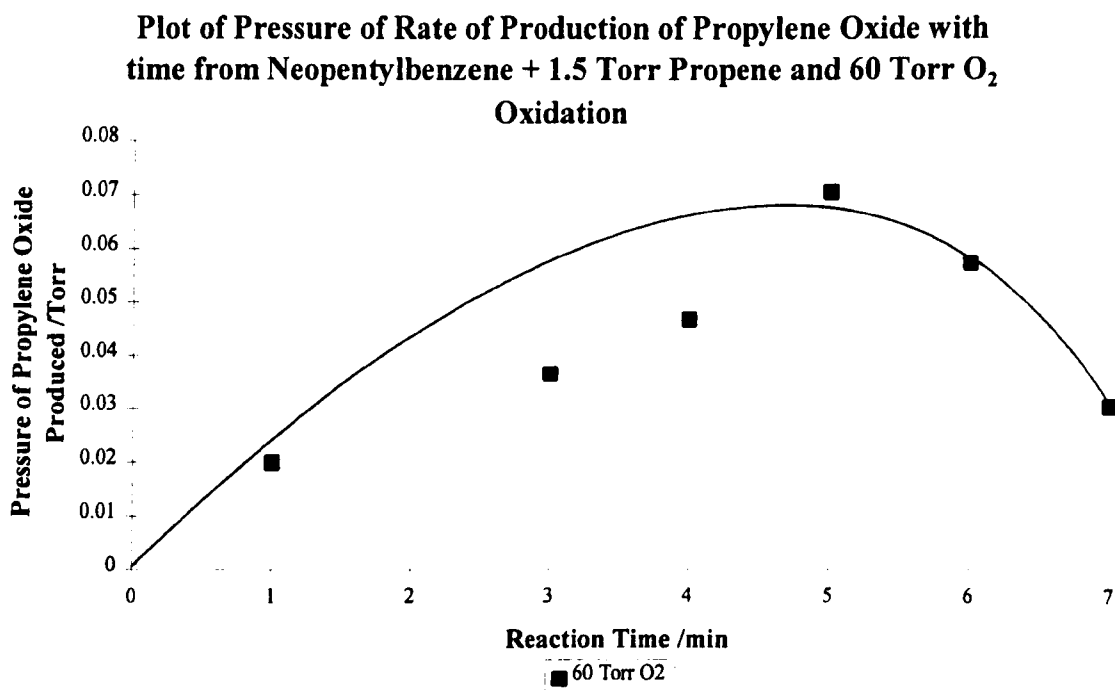


Figure 6. 33

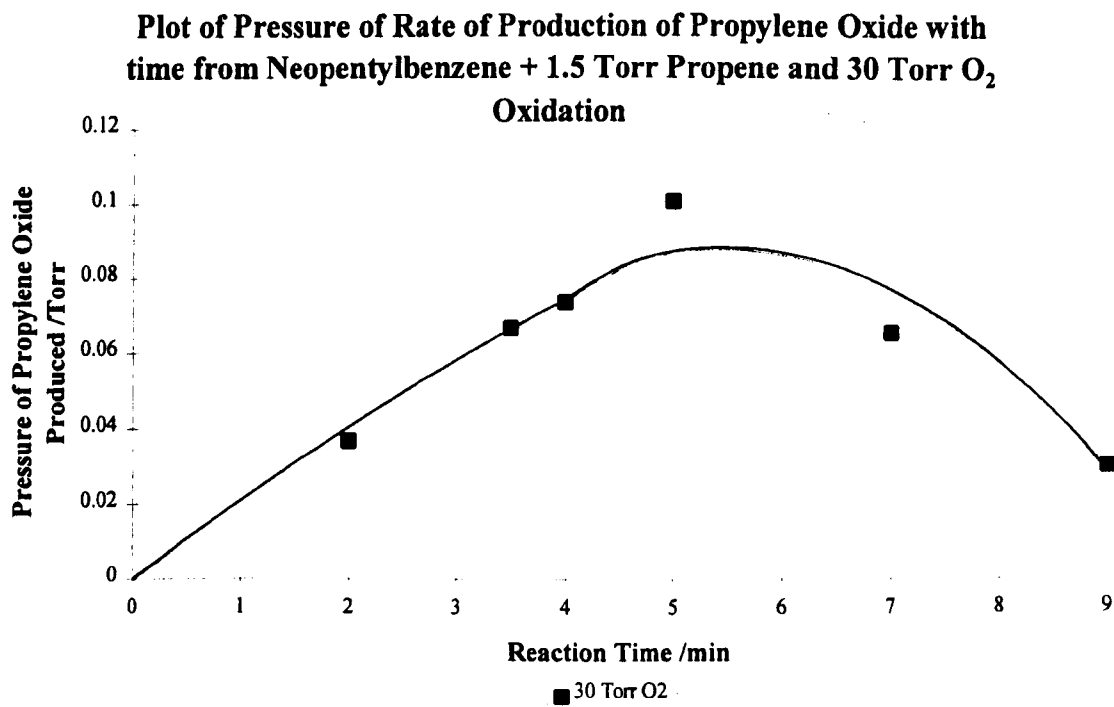


Figure 6. 34

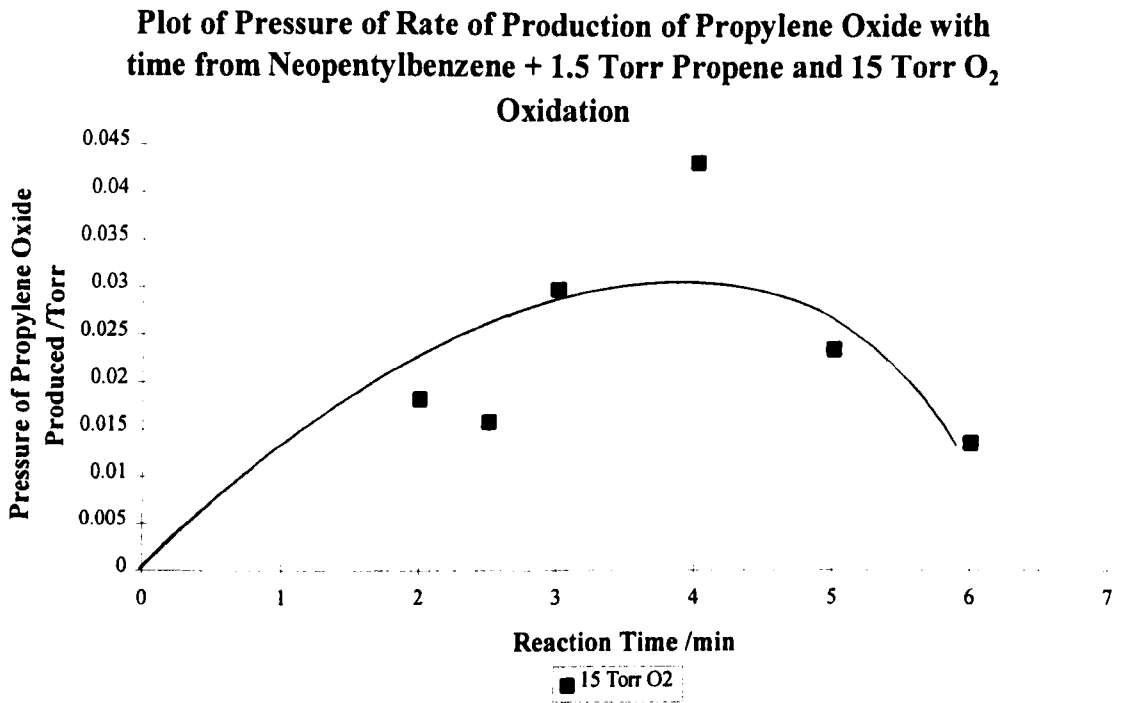


Figure 6. 35

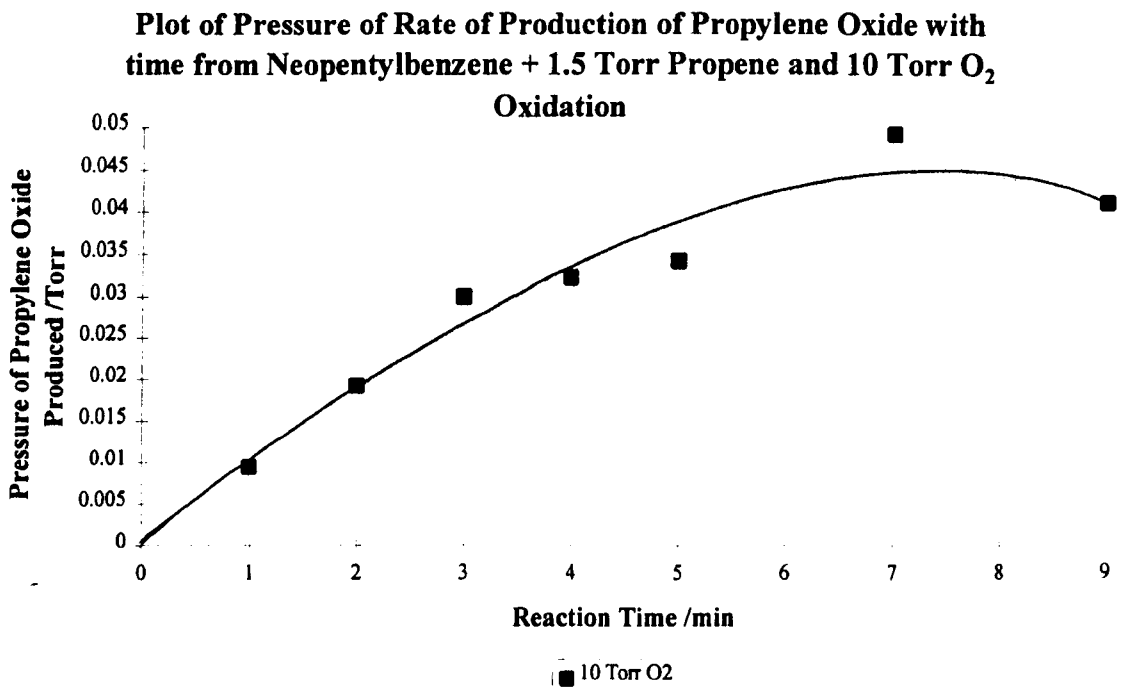
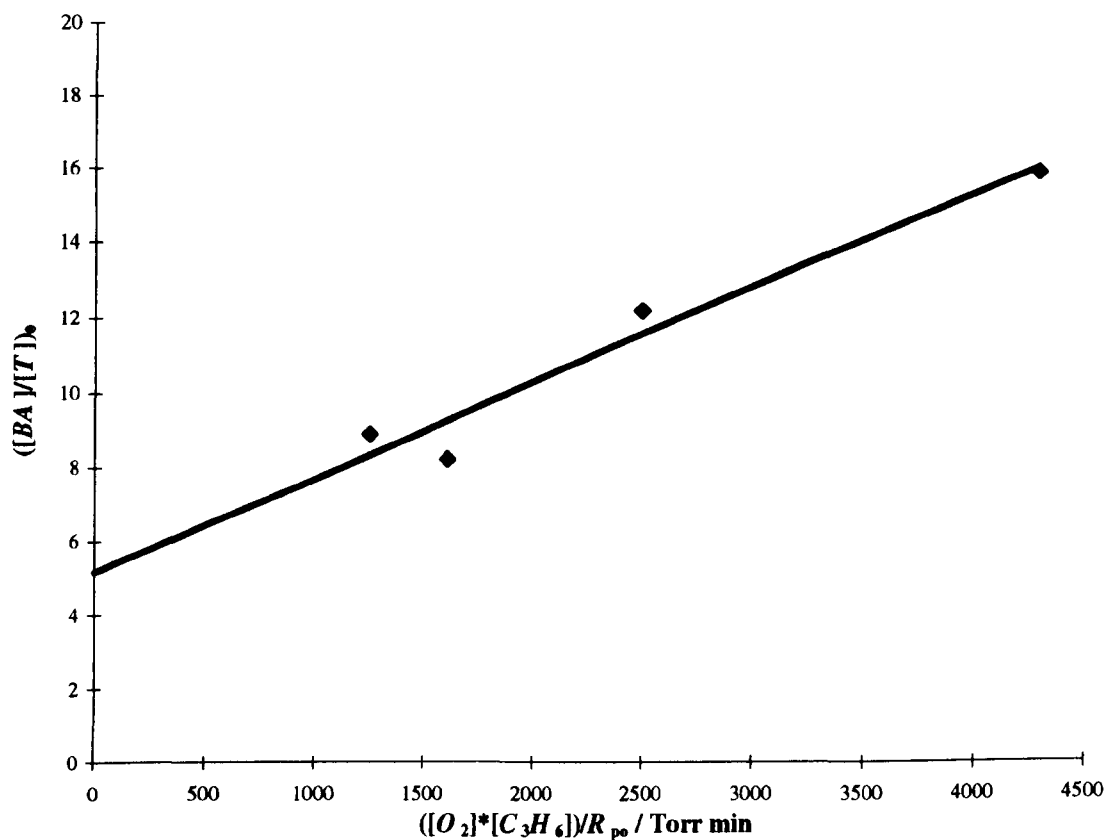


Table 6. 12 : Data for plot of $([BA]/[T])_0$ vs. $([O_2]*[C_3H_6])/R_{po}$ for 0.48 Torr NPB + 1.5 Torr Propene + Oxygen at 753K.

Pressure of O_2 / Torr	R_{po} / Torr min^{-1}	$\frac{[O_2]*[C_3H_6]}{R_{po}}$ /Torr min	$([BA]/[T])_0$ (Pressures)
58.0	0.021	4285	15.9
30.0	0.018	2500	12.1
15.0	0.014	1607	8.2
10.0	0.012	1250	8.9

Figure 6. 36

Plot of $([BA]/[T])_0$ vs. $([O_2]*[C_3H_6])/R_{po}$ for 0.48 Torr NPB + O_2 + 1.5 Torr Propene at 753K



and values of $k_{6.03}/k_{6.04} = 5.2 \pm 0.5$ and $(k_{6.05}k_{6.07})/k_{6.04} = 2.5 \cdot 10^{-3} \text{ Torr}^{-1} \text{ min}^{-1}$ are obtained from the intercept and gradient, respectively.

The values of the rate constant ratios will be discussed further later, although it is worth noting that the value of $k_{6.03}/k_{6.04} = 6.5$ obtained from Figure 6.15 and $k_{6.03}/k_{6.04} = 6.9$ obtained from Figure 6.31 are only slightly higher than the more reliable value of 5.2 ± 1.0 above.

B) BA is formed in reaction (6.03), T is formed in (6.04) and (6.06).

This case is best treated analytically by inverting equation (v) so that the initial product ratio $([T]/[BA])_0$ is given by equation (x)

$$\left(\frac{[BA]}{[T]}\right)_0 = \frac{k_{6.03}[HO_2]}{k_{6.04}[HO_2] + k_{6.06}[NPB]} \quad (\text{v}) \rightarrow \left(\frac{[T]}{[BA]}\right)_0 = \frac{k_{6.04}}{k_{6.03}} + \frac{k_{6.06}[NPB]}{k_{6.03}[HO_2]} \quad (\text{x})$$

Combination with equation (viii) then gives equation (xi)

$$\left(\frac{[T]}{[BA]}\right)_0 = \frac{k_{6.04}}{k_{6.03}} + \frac{k_{6.06}k_{6.07}[C_3H_6][NPB]}{k_{6.03}R_{po}} \quad (\text{xi})$$

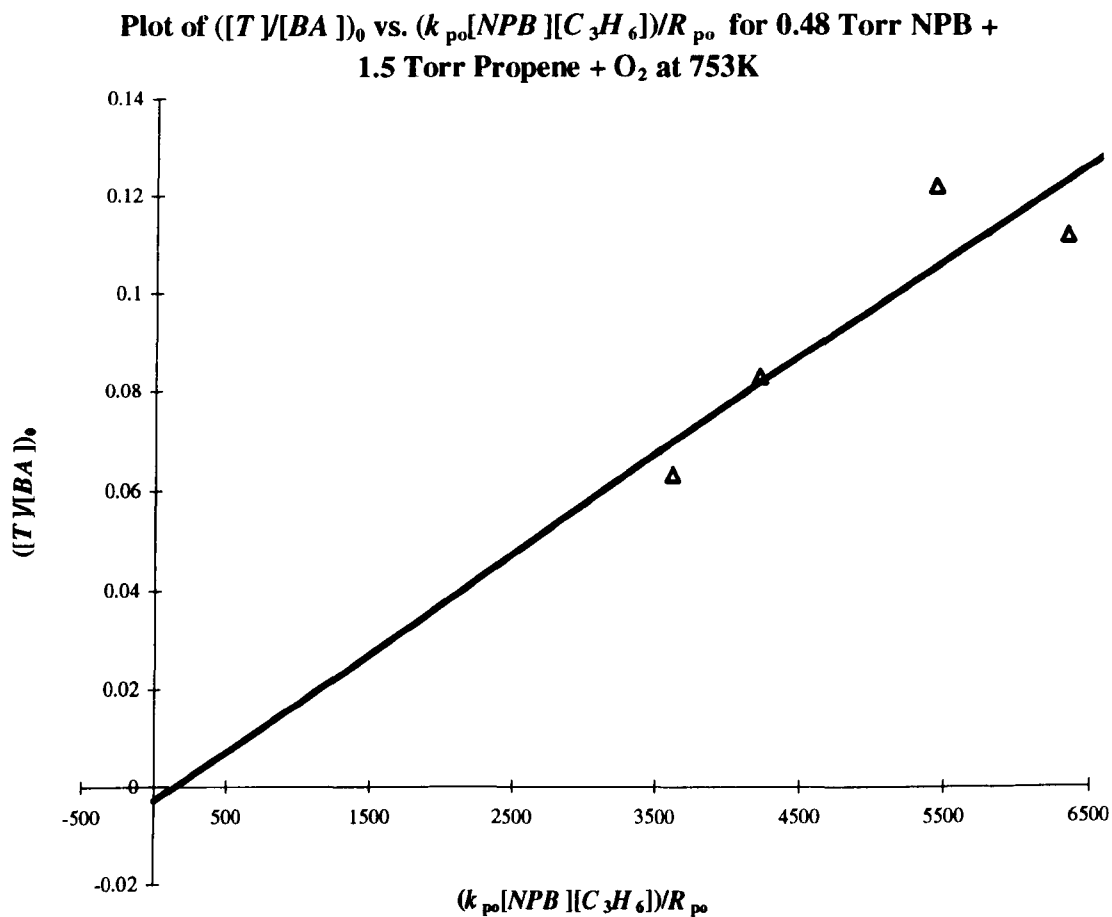
Figure (6.37) shows that a plot of $([T]/[BA])_0$ against $([C_3H_6][NPB])/R_{po}$ (Table 6.13) gives a reasonably good straight line through the origin. If this mechanism is correct, a major conclusion from the fact that the intercept has an effective value of zero is that toluene is formed almost uniquely in reaction (6.06) even at very high $[O_2]$ (and high $[HO_2]$) and further that $k_{6.04}/k_{6.03} \leq 0.03$.

There are two key reasons for the view that **B** is not the correct combination of reactions for benzaldehyde and toluene formation.

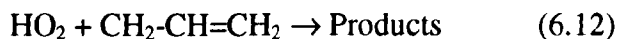
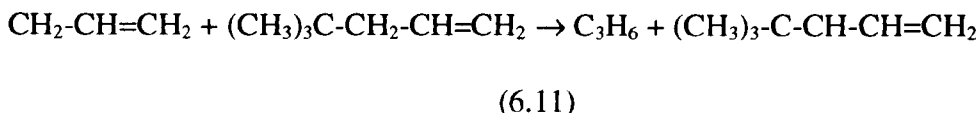
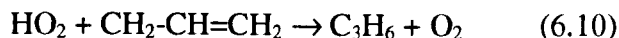
Table 6. 13 : Data for plot of Benzaldehyde:Toluene vs. $(k_{po}[NPB]*[Propene])/R_{po}$ for 0.48 Torr NPB + 1.5Torr Propene + Oxygen oxidation at 75K.

Pressure of O ₂ / Torr	$R_{po} / \text{Torr min}^{-1}$	$\frac{k_{po} * [NPB] * [C_3H_6]}{R_{po}}$	$([T]/[BA])_0$
60	0.021	3617	0.063
30	0.018	4220	0.083
15	0.014	5426	0.122
10	0.012	6330	0.112

Figure 6. 37

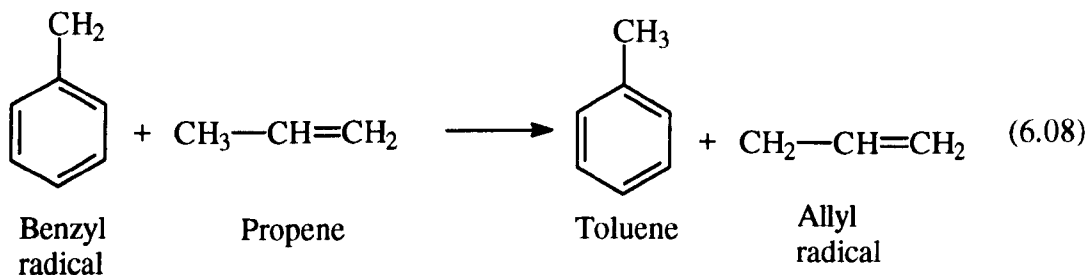


- i. When 4,4-dimethylpent-1-ene was decomposed under virtually the same conditions⁴, it was shown that C₃H₆ was formed in reaction (6.10) rather than (6.11) and that the ratio $k_{6.12}/k_{6.10} = 2.2$ at 753K⁴.



The thermochemistry involved in the two systems is very similar, so that even allowing for the uncertainty of the reaction path in (6.12), it would be expected that $k_{6.03}/k_{6.04} \approx k_{6.12}/k_{6.10}$ at about 750K.

- ii. If toluene is formed in reaction (6.06) in the absence of C₃H₆, then when C₃H₆ is present, the rate of formation of toluene = $k_{6.06}[\text{benzyl}][\text{NPB}] + k_{6.08}[\text{benzyl}][\text{C}_3\text{H}_6]$



Given that a secondary allylic H atom is abstracted in (6.06) and a primary allylic in (6.08), it is probable that with both reactions being nearly thermoneutral, $E_{A6.08} = E_{A6.06} + 8(\pm 1) \text{ kJ mol}^{-1}$. With the path degeneracy included then the activation energy difference gives $k_{6.08}/k_{6.06} = 2.5$ at 753K. In consequence, addition of 1.5 Torr of C₃H₆ to mixtures containing 0.48 Torr NPB would be expected to reduce the

$[BA]/[T]$ ratios by at least a factor of 2. In contrast, as shown in Figure 6.31, no significant change is observed experimentally.

C) **BA is formed in reactions (6.03) and (6.05) and T in (6.04) and (6.06).**

$$\left(\frac{[BA]}{[T]}\right)_0 = \frac{k_{6.03}[HO_2] + k_{6.05}[O_2]}{k_{6.04}[HO_2] + k_{6.06}[NPB]} \quad (\text{vi})$$

If, as discussed above under heading **B**, it is accepted that reaction (6.06) is of only minor importance such that $k_{6.04}[HO_2] \gg k_{6.06}[NPB]$ then equation (vi) reduces to equation (iv), discussed under heading **A**.

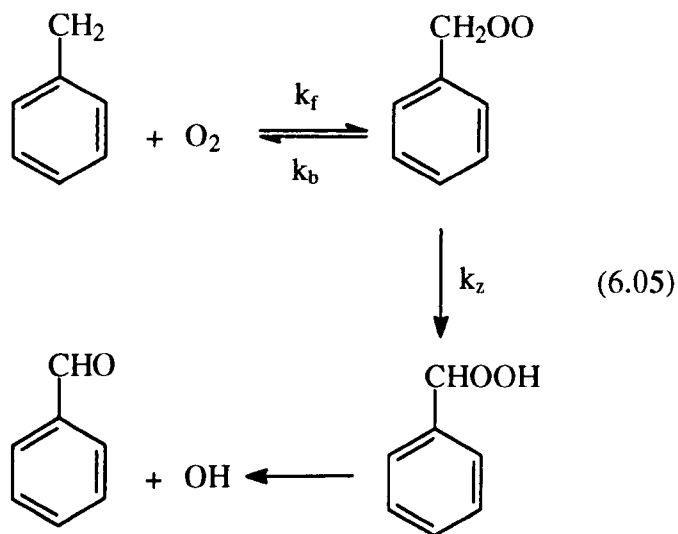
$$\left(\frac{[BA]}{[T]}\right)_0 = \frac{k_{6.03}}{k_{6.04}} + \frac{k_{6.05}[O_2]}{k_{6.04}[HO_2]} \quad (\text{iv})$$

6.4. Interpretation of the Kinetic Data.

It has been argued in the previous sections that the variation of the $([BA]/[T])_0$ ratios with O_2 pressure are best explained if BA is formed in reactions (6.03) and (6.05) and T in reaction (6.04). It is now possible to estimate reasonably accurate rate constants for the reactions of benzyl with HO_2 radicals to give both benzaldehyde and toluene.

From a plot of $([BA]/[T])_0$ against $([O_2][C_3H_6])/R_{p0}$ shown in Figure 6.36 for a series of experiments with $[C_3H_6] = 1.5$ Torr, the gradient = $(k_{6.05}k_{6.07})/k_{6.04} = 0.0025 \text{ Torr}^{-1} \text{ min}^{-1}$ and intercept = $k_{6.03}/k_{6.04} = 5.2 \pm 0.5$. It is considered that the mechanism for benzyl + O_2 is likely to involve the sequence shown below. Although the $\text{PhCH}_2 + O_2 \rightleftharpoons \text{PhCHOO}$ equilibrium is well to the left, formation of the QOOH radical by H

transfer will be rapid. With this mechanism then $k_{6.05} = K_c k_z$, where $K_c = k_f/k_b$, it being assumed that the formation of the hydroperoxide radical is effectively irreversible



The value for $k_{6.05}$ can be estimated using data from two sources. Two different research groups have determined the equilibrium constant, $K_c = k_f/k_b$, for the reaction between benzyl radicals and oxygen producing the R-O₂ radical. A brief examination of their data is given below.

6.4.1. Determination of K_c by Fenter *et al.*²

Fenter *et al.*² determined K_c between 398 and 525K using flash photolysis experiments. Their results are summarised in Table 6.14 together with a van't Hoff plot of the data in Figure 6.38. The least squares Second law best fit to the data gives the following expression for K_c between 398 and 525K.

$$K_c = 9.73 * 10^{-6} e^{\frac{10366}{T}} \text{ l mol}^{-1}$$

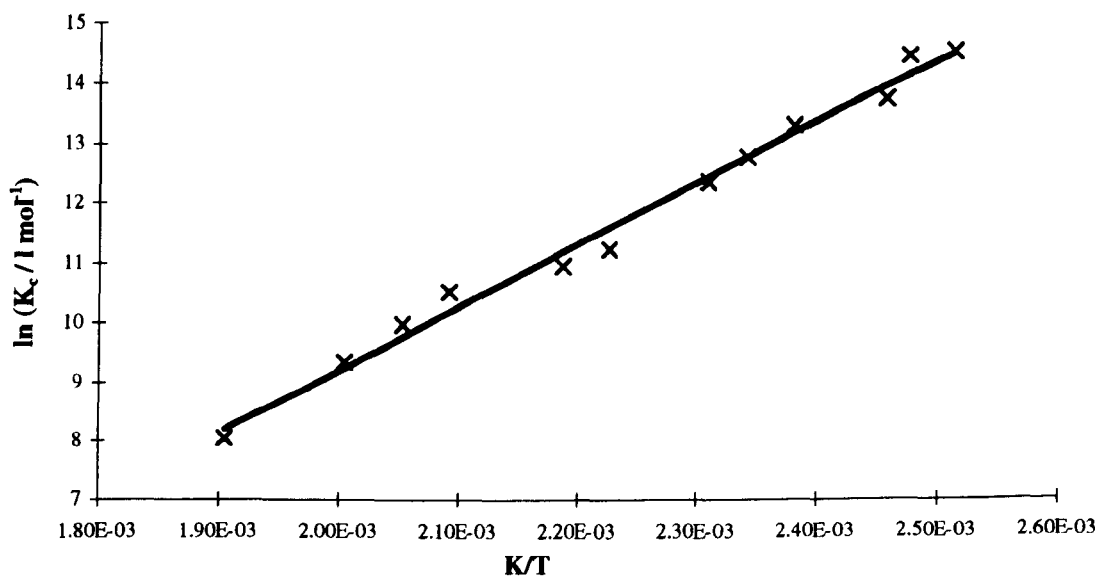
This expression gives $K_c = 9.26 \text{ l mol}^{-1}$ at 753K.

Table 6. 14 : Values of K_c obtained by Fenter et al.²

T/K	$K_c / \text{l mol}^{-1}$	K/T	$\ln (K_c / \text{l mol}^{-1})$
525	$3.13 \cdot 10^3$	$1.90 \cdot 10^{-3}$	8.05
499	$1.14 \cdot 10^4$	$2.00 \cdot 10^{-3}$	9.34
487	$2.11 \cdot 10^4$	$2.05 \cdot 10^{-3}$	9.96
478	$3.55 \cdot 10^4$	$2.09 \cdot 10^{-3}$	10.48
457	$5.42 \cdot 10^4$	$2.19 \cdot 10^{-3}$	10.90
449	$7.23 \cdot 10^4$	$2.23 \cdot 10^{-3}$	11.19
433	$2.23 \cdot 10^5$	$2.31 \cdot 10^{-3}$	12.31
427	$3.37 \cdot 10^5$	$2.34 \cdot 10^{-3}$	12.73
420	$5.72 \cdot 10^5$	$2.38 \cdot 10^{-3}$	13.26
407	$9.03 \cdot 10^5$	$2.46 \cdot 10^{-3}$	13.71
404	$1.87 \cdot 10^6$	$2.48 \cdot 10^{-3}$	14.44
398	$2.05 \cdot 10^6$	$2.51 \cdot 10^{-3}$	14.53

Figure 6. 38

Plot of $\ln K_c$ vs. K/T from the work of Fenter et al.



6.4.2. Determination of K_c by Elmaimouni et al.¹³

Elmaimouni et al.¹³ determined values for K_c between 393 and 433K; the data are summarised in Table 6.15 and are plotted in logarithmic form in Figure 6.39. The least squares Second law best fit to the data gives the following expression for K_c between 393 and 433K.

$$K_c = 1.67 * 10^{-4} e^{\frac{9221.3}{T}} \text{ l mol}^{-1}$$

This expression gives $K_c = 34.9 \text{ l mol}^{-1}$ at 753K.

6.4.3. Comments.

The overall accuracy of extrapolating each of the above sets of results from 525K or 433K respectively to 753K will lead to an uncertainty in the final answer greater than if true experimental data had been available at 753K. Figure 6.40 shows the data for both Elmaimouni et al.¹³ and Fenter et al.² on a single plot. Over the same temperature range there is excellent agreement between the two sets of data. However, since the spread of data between 393 and 525K obtained from the work of Fenter et al. is of a suitable accuracy and determined over a larger temperature range than that obtained by Elmaimouni et al., a reasonable conclusion is that a more reliable value for K_c can be obtained at 753K via extrapolation of data obtained by Fenter et al.

6.4.4. Estimation of k_z .

A value of k_z can be estimated from the data available for a 1,3t transition for $\text{RO}_2 \rightarrow \text{QOOH}$. The A factor and activation energy for a normal 1,3t transition has been given by Walker et al.^{3,20} as $1.15 * 10^{13} \text{ s}^{-1}$ and 160 kJ mol^{-1} , respectively. The A factor may be reduced by a factor of 4.35 from $1.15 * 10^{13} \text{ s}^{-1}$ to $2.64 * 10^{12} \text{ s}^{-1}$, arising from a reduction by a factor of 8.7 due to delocalisation effects and an increase by a factor of 2

Table 6. 15 : Values of K_c obtained by Elmaimouni et al.¹³

T/K	$K_c / \text{l mol}^{-1}$	K/T	$\ln (K_c / \text{l mol}^{-1})$
393	$2.76 \cdot 10^6$	$2.54 \cdot 10^{-3}$	14.83
393	$3.08 \cdot 10^6$	$2.54 \cdot 10^{-3}$	14.94
403	$1.50 \cdot 10^6$	$2.48 \cdot 10^{-3}$	14.22
403	$1.13 \cdot 10^6$	$2.48 \cdot 10^{-3}$	13.94
407	$9.52 \cdot 10^5$	$2.46 \cdot 10^{-3}$	13.77
413	$8.21 \cdot 10^5$	$2.42 \cdot 10^{-3}$	13.62
423	$5.87 \cdot 10^5$	$2.36 \cdot 10^{-3}$	13.28
423	$4.76 \cdot 10^5$	$2.36 \cdot 10^{-3}$	13.07
433	$3.20 \cdot 10^5$	$2.31 \cdot 10^{-3}$	12.68
433	$2.77 \cdot 10^5$	$2.31 \cdot 10^{-3}$	12.53

Figure 6. 39

Plot of $\ln K_c$ vs. K/T from the work of Elmaimouni et al.

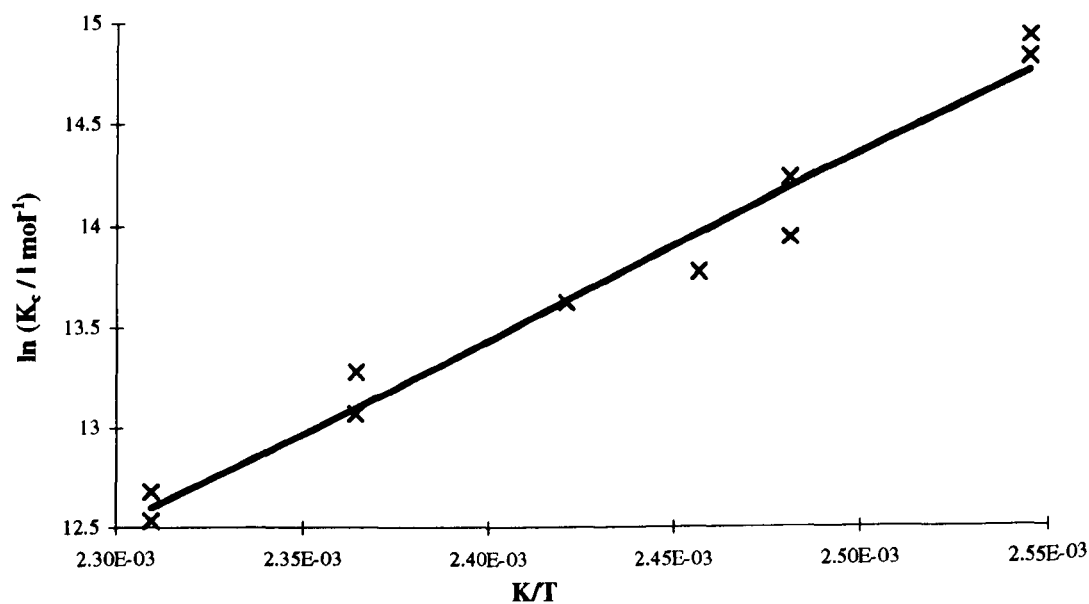
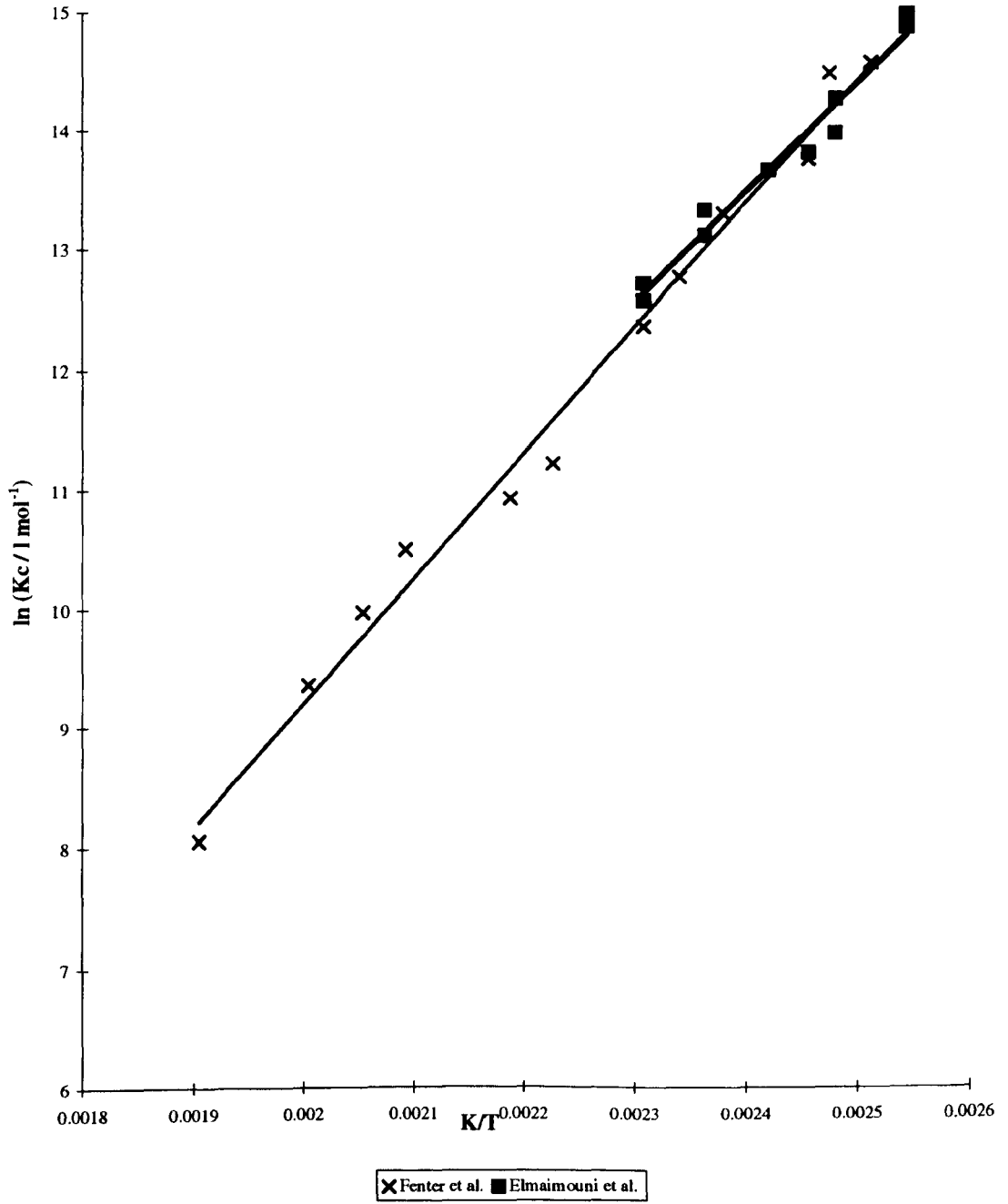


Figure 6. 40

Plot of $\ln K_c$ vs. K/T combining the data from Fenter et al. and Elmaimouni et al.



to account for path degeneracy. Walker et al.^{3,20} have shown that the difference in activation energy for H atom transfer for $\text{RO}_2 \rightarrow \text{QOOH}$ processes for ring transition states containing the same number of atoms equals the differences in the endothermicity involved. Although this has only been established for primary, secondary and tertiary C-H atoms in alkylperoxy radicals, it has been extended here to allylic systems. In consequence the activation energy was reduced from 160 for the 1,3t to 131 kJ mol^{-1} taking the bond energy for a *t*-C-H bond as 393 kJ mol^{-1} and the bond energy for the C-H bond in $\text{Ph-CH}_2\text{OO} = 364 \text{ kJ mol}^{-1}$.

Consequently $k_z = 2.64 \cdot 10^{12} \exp(-15756/T) \text{ s}^{-1}$ and therefore $k_z = 2.16 \cdot 10^3 \text{ s}^{-1}$ at 753K.

6.4.5. Evaluation of $k_{6.03}$ and $k_{6.04}$

Combination with the results of Fenter et al. discussed previously leads to a value of $k_{6.05} = K_c \cdot k_z = 9.27 \cdot 2.16 \cdot 10^3 = 2.0 \cdot 10^4 \text{ l mol}^{-1} \text{ s}^{-1}$ at 753K.

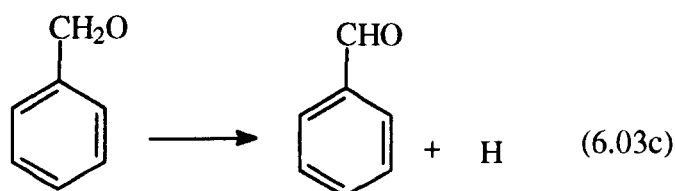
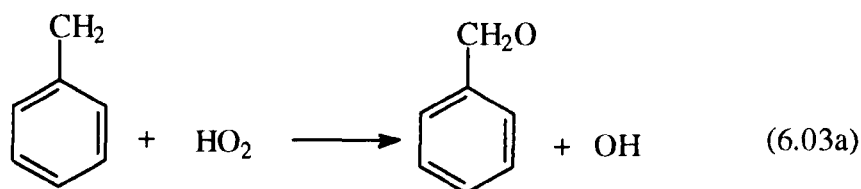
Given $k_{6.07} = 8.3 \cdot 10^4 \text{ l mol}^{-1} \text{ s}^{-1}$ or $105.5 \text{ Torr}^{-1} \text{ min}^{-1}$ at 753K¹¹, it is possible to determine $k_{6.04}$ from $(k_{6.05}k_{6.07})/k_{6.04} = 0.0025 \text{ Torr}^{-1} \text{ min}^{-1}$ such that $k_{6.04} = 8.4 \cdot 10^8 \text{ l mol}^{-1} \text{ s}^{-1}$ at 753K. Consequently if $k_{6.03}/k_{6.04} = 5.2$ then $k_{6.03} = 4.4 \cdot 10^9 \text{ l mol}^{-1} \text{ s}^{-1}$ at 753K.

6.4.6. Comparison with other data.

There is only a very limited kinetic information on the reactions of benzyl radicals at temperatures below 1000K. Previous studies on the reactions between HO_2 and benzyl radicals have been carried out by two research groups^{1,14}. This work was carried out at temperatures in excess of 900K and no values for activation energies or A factors have been given.

6.4.6.1. Benzyl + HO₂ → Benzaldehyde, reaction (6.03).

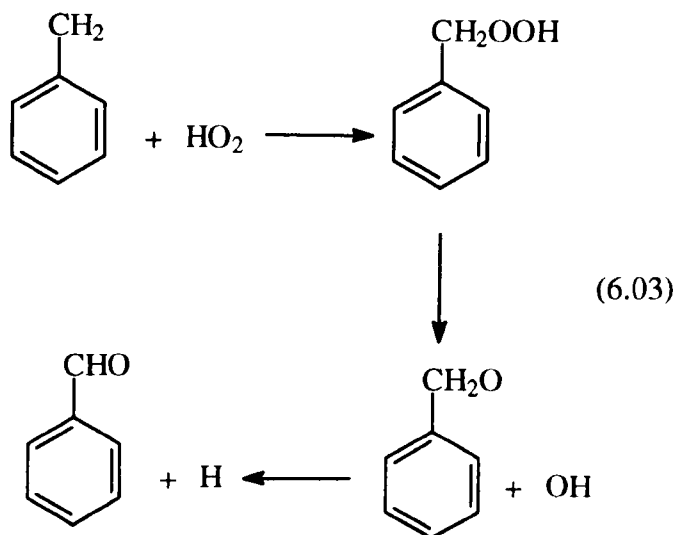
From an interpretation of a complex reaction involving the oxidation of toluene, Brezinsky et al.¹ estimated $k_{6.03a} = 3.2 \pm 1.5 \cdot 10^9 \text{ l mol}^{-1} \text{ s}^{-1}$ between 990-1100K and $k_{6.03c} = 6.5 \cdot 10^{13} \text{ s}^{-1}$ ($k_{6.03c} = 1.27 \cdot 10^{14} \exp(-555/T) \text{ s}^{-1}$) between 300 and 1180K).



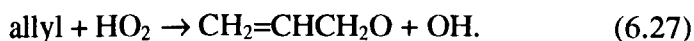
If it is assumed that reaction 6.03a is the rate determining step in the overall sequence of reactions in the production of benzaldehyde by reaction (6.03) then it can be assumed that $k_{6.03a} = k_{6.03}$. Since from this work $k_{6.03} = 4.4 \pm 2 \cdot 10^9 \text{ l mol}^{-1} \text{ s}^{-1}$ at 753K then the agreement with value obtained by Brezinsky et al.¹ is very good and it may be concluded that within experimental error the activation energy for reaction (6.03) is effectively zero. The data are summarised in Table 6.16.

Table 6. 16 : Summary of Rate Constants for R+ HO₂ → X

R	X	T/K	k / l mol ⁻¹ s ⁻¹	Reference
Benzyl	PhCHO	753	4.4 ± 2 · 10 ⁹	This work
Benzyl	PhCH ₂ O	990 - 1100	3.2 ± 1.5 · 10 ⁹	1
Allyl	CH ₂ =CHCH ₂ O	300 - 2500	9.6 · 10 ⁹	12



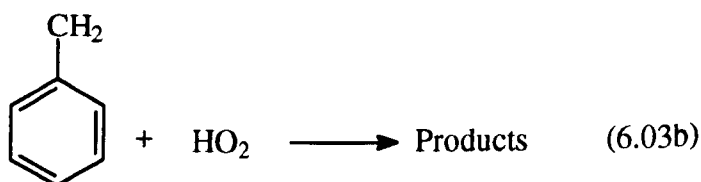
No experimental rate data are available for the analogous reaction between allyl radicals and HO_2 . Tsang¹² recommended a value $k_{(\text{allyl}+\text{HO}_2 \rightarrow \text{CH}_2=\text{CHCH}_2\text{O})} = 9.6 \cdot 10^9 \text{ l mol}^{-1} \text{ s}^{-1}$ between 300 and 2500K for reaction (6.27).



As for the benzyl radical system described above, no activation energy is given and the rate constant for the allyl radical is of the same order of magnitude as that for benzyl radicals.

6.4.6.2. Benzyl + $\text{HO}_2 \rightarrow$ Products, reaction (6.03b).

Hippler et al.¹⁴ obtained the rate constant $k_{6.03b} = 5.0 \cdot 10^9 \text{ l mol}^{-1} \text{ s}^{-1}$ between 1180-1450K.



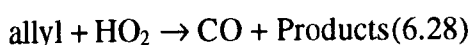
If it is assumed that the only major products for the reaction between HO₂ and benzyl radicals in the present study are benzaldehyde and toluene, then an estimated rate constant for $k_{6.03b}$ may be obtained from the summation $k_{6.03b} = k_{6.03} + k_{6.04} = 5.20 \pm 2 * 10^9$ l mol⁻¹ s⁻¹ at 753K. This value is in excellent agreement with the value obtained by Hippler et al. on the assumption that the activation energy for this reaction is effectively zero, which is not unreasonable. The data are summarised in Table 6.17.

Table 6. 17 : Summary of Rate Constants for R + HO₂ → Products

Reaction	T/K	k / l mol ⁻¹ s ⁻¹	Reference
Benzyl + HO₂ → Products	753	$5.2 \pm 2 * 10^9$	This Work
Benzyl + HO₂ → Products	1180 - 1450	$5 \pm 1.5 * 10^9$	14
allyl + HO₂ → CO + Products	753	$5.8 * 10^9$	22

$k_{allyl} = 9.38 * 10^9 \exp(-352/T)$ l mol⁻¹ s⁻¹ between 698-753K.

Lodhi and Walker²² have obtained experimental rate data for the reaction of allyl radicals with HO₂ radicals (6.28) and give $k_{6.28} = 9.38 * 10^9 \exp(-2.9 * 10^3/RT)$ l mol⁻¹ s⁻¹ between 689 and 753K such that $k_{6.28} = 5.8 * 10^9$ l mol⁻¹ s⁻¹ at 753K



Given the similarity in the nature of the two systems, the closeness of the rate constants suggests that the data are generally reliable.

6.4.6.3. Estimation of the A factor for reaction (6.04).

An estimation of the A factor for reaction (6.04) can be made by use of the entropy and heat capacity data given in Table 6.18.

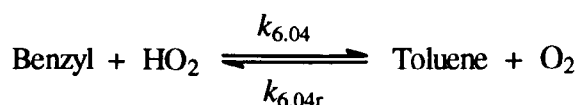


Table 6. 18 : Thermodynamic Properties for the Species in reaction (6.04) - Summary for Calculation of ΔS°_{300} and $\Delta C_p^\circ_{500}$.

Reaction (6.04)	Benzyl	+	HO ₂	→	Toluene	+	O ₂
$S^\circ_{300} / \text{J mol}^{-1} \text{K}^{-1}$	321.3		227.6		320.5		205.0
$C_p^\circ_{500} / \text{J mol}^{-1} \text{K}^{-1}$	170.7		39.7		202.25		31.0
Reference	15		16		17		16

$$\Delta S^\circ_{300} = -23.4 \text{ J mol}^{-1} \text{K}^{-1}$$

$$\Delta C_p^\circ_{500} = +22.9 \text{ J mol}^{-1} \text{K}^{-1}$$

At 300K, $\Delta S^\circ_{300} = -23.4 \text{ J mol}^{-1} \text{K}^{-1}$ for reaction (6.04). However, the entropy change is required at 753K, which can be estimated using equation (xii) below, where $\Delta C_p^\circ_{TM}$ is the value at the medium temperature 527K.

$$\Delta S^\circ_T = \Delta S^\circ_{300} + \Delta C_p^\circ_{TM} * \ln(T/300) \quad (\text{xii})$$

Although values for C_p° for individual species may be large and may change grossly over temperature intervals of 500K, ΔC_p° for reactions tend to change very little over such intervals. Consequently it is possible, with little error, to take an average value of $\Delta C_p^\circ_{TM}$ over the interval 753-300K. Data for C_p° at 500K are available and have been used to calculate $\Delta C_p^\circ_{TM}$ and hence ΔS°_{753} since it is unlikely that there will be any significant change in the value of ΔC_p° for an increase of 27K; as a result $\Delta C_p^\circ_{TM} = +22.9 \pm 0.5 \text{ J mol}^{-1} \text{K}^{-1}$. Application of equation (xii) gives $\Delta S^\circ_T = -2.4 \pm 1.0 \text{ J mol}^{-1} \text{K}^{-1}$ at

753K. From transition state theory $\frac{A_{6.04}}{A_{6.04r}} = \exp\left(\frac{\Delta S^\circ_T}{R}\right)$ so that $A_{6.04}/A_{6.04r} = 0.75 \pm 0.10$.

Emdee et al.¹⁸ quote a value for $A_{6.04r} = 3 \times 10^{11} \text{ l mol}^{-1} \text{ s}^{-1}$ between 1100 and 1200K for reaction (6.04r) from a complex analysis of toluene oxidation. From a shock-tube study of toluene oxidation Eng et al.¹⁹ also gave $A_{6.04r} = 3 \times 10^{11} \text{ l mol}^{-1} \text{ s}^{-1}$ over a similar temperature range 1050 - 1400K. Walker²⁰ has considered this value to be

approximately two orders of magnitude too high arising from the neglect of important branching reactions in the mechanism used. Since the chemistry involved in the removal of one of the primary hydrogens in the CH₃ in toluene is similar in that for propene reacting with oxygen to produce allyl radicals²¹, (i.e. similar chemical environment, similar C-H bond energy and the production of a resonance stabilised radical as a result of the reaction,) an estimate for an A factor should be near to $1.95 \times 10^9 \text{ l mol}^{-1} \text{ s}^{-1}$ between 673 and 793K which is the experimental value for $\text{C}_3\text{H}_6 + \text{O}_2 \rightarrow \text{allyl} + \text{HO}_2$ ²¹; consequently a value of $A_{6.04r} = 2 \times 10^9 \text{ l mol}^{-1} \text{ s}^{-1}$ between 750 and 1200K is given as a reasonable estimate.

With $A_{6.04}/A_{6.04r} = 0.75$ and $k_{6.04r} = 2.0 \times 10^9 \text{ l mol}^{-1} \text{ s}^{-1}$ then $A_{6.04} = 1.5 \pm 0.2 \times 10^9 \text{ l mol}^{-1} \text{ s}^{-1}$ at 753K. This value is very close to the value of $k_{6.04} = 8.4 \times 10^8 \text{ l mol}^{-1} \text{ s}^{-1}$ at 753K obtained above. On this basis the value of $k_{6.04r} = 3 \times 10^{11} \text{ l mol}^{-1} \text{ s}^{-1}$ recommended by Emdee et al.¹⁸ and Eng et al.¹⁹ appears to be a factor of about 100 too high. As Emdee et al.'s¹⁸ value was obtained by use of a complex mechanism which undoubtedly ignored alternative primary and secondary initiation reactions, it is not surprising that they obtained a value much higher than expected. Further, Eng et al.'s¹⁹ system may be more complex than at first thought. For example at 1400K, under the conditions used, primary initiation through



may be faster than reaction (6.04r). At lower temperatures, reaction (6.04r) may be too slow to obtain a precise value of $k_{6.04r}$.

The corresponding reaction,

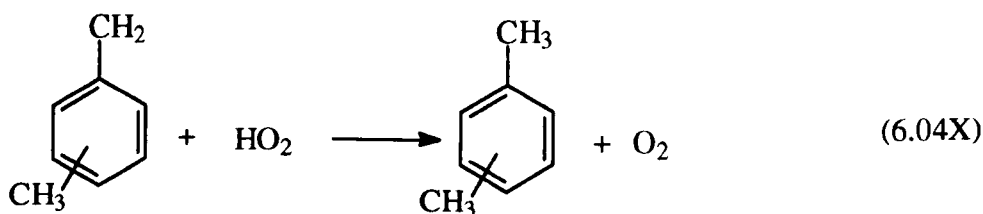


has an A factor of $7.35 \times 10^9 \text{ l mol}^{-1} \text{ s}^{-1}$ and activation energy of 5.5 kJ mol^{-1} between 689 and 753K²² such that a rate constant of $k_{6.30} = 3.1 \times 10^9 \text{ l mol}^{-1} \text{ s}^{-1}$ at 753K can be obtained. The value obtained in this work for $k_{6.04} = 8.44 \times 10^8 \text{ l mol}^{-1} \text{ s}^{-1}$ at 753K thus appears reasonable considering the increased delocalisation present in the benzyl radical reducing the reactivity compared with that of allyl radicals.

6.5. Application of the Rate Constants.

One clear conclusion that can be drawn from the above study is that the chemistry of benzyl radicals is very similar to that for allyl radicals. Consequently it is possible to use the rate constant values for allyl radicals as a rough estimate for radicals such as benzyl and the methylbenzyls. Further, it should be possible to estimate with reasonable accuracy rate constants for the di- and tri- substituted methylbenzyls reacting with HO_2 and O_2 from the results contained in this chapter.

The rate constant ratios calculated from this study, $k_{6.03}/k_{6.04} = 5.2$ and $k_{6.05}/k_{6.04} = 2.37 \times 10^{-5}$ at 753K, will be used to correct the estimates of $k_{(\text{H} + \text{Xylene})}$ and $k_{(\text{HO}_2 + \text{Xylene})}$ obtained in Chapter 7. Since no data are available at 753K for the reverse reaction of the methyl benzyl radical back to xylene (reaction 6.04X), the data obtained here for benzyl radicals will be applied in order to assess the importance of methylbenzyl reactions occurring in the xylene oxidation system. This will be discussed in more detail in Chapter 7.



6.6. References.

- ¹ Brezinsky K., Litzinger T. A. and Glassman I., *Int. J. Chem. Kinet.*, **16**, 1053, (1984).
- ² Fenter F. F., Noziere B., Caralp F and Lesclaux R., *Int. J. Chem. Kinet.*, **26**, 171, (1994).
- ³ Baldwin R. R., Hisham M. W. M., Keen A. and Walker R. W., *J. Chem. Soc. Faraday Trans. 1*, **78**, 1165, (1982).
- ⁴ Lodhi Z.H. and Walker R.W., *J. Chem. Soc Faraday Trans. 1*, **87**, 681, (1991).
- ⁵ Tsang W., *Int. J. Chem. Kinet.*, **10**, 821, (1978).
- ⁶ Robaugh D. A., Barton B. D. and Stein S. E., *J. Phys. Chem.*, **85**, 2378, (1981).
- ⁷ Müller-Markgraf W. and Troe J., *J. Phys. Chem.*, **92**, 4899, (1988).
- ⁸ Korobkov V.Y. and Kalechits I.V., *Russ. J. Phys. Chem.*, **65**, 346, (1991).
- ⁹ CRC Handbook of Chemistry and Physics, 51st Edition (1970-1971), The Chemical Rubber Company, pp163.
- ¹⁰ Stothard N.D. and Walker R.W., *J. Chem. Soc. Faraday Trans.*, **86**, 2115, (1990).
- ¹¹ Baldwin R. R., Hisham M. W. M. and Walker R. W., *Symp. Int. Combust. Proc.*, **20**, 743, (1985).
- ¹² Tsang W., *J. Phys. Chem. Ref. Data*, **20**, 221, (1991).
- ¹³ Elmaimouni L., Minetti R., Sawerysyn J. P. and Devalder P., *Int. J. Chem. Kinet.*, **25**, 399, (1993).
- ¹⁴ Hippler H., Reihls C. and Troe J., *Symp. Int. Combust. Proc.*, **23**, 31, (1991).
- ¹⁵ Hippler H. and Troe J., *J. Phys. Chem.*, **94**, 3803, (1990).
- ¹⁶ Benson S.W., "*Thermochemical Kinetics*", Wiley, New York, (1976).

- ¹⁷ Burcat A., *Combustion Chemistry*, Gardiner Jr. W.C., Ed., Springer-Verlag: New York, (1984), Appendix C.
- ¹⁸ Emdee J.L., Brezinsky K. and Glassman I., *J. Phys. Chem.*, **96**, 2151, (1992).
- ¹⁹ Eng R.A., Fittschen C., Gebert A., Hibomvschi P., Hippler H. and Unterreiner A.-N., Paper presented at *27th International Symposium on Combustion, Boulder, Colorado*, Book of abstracts pp31, (1998).
- ²⁰ Walker R.W., "Some Burning Problems in Combustion Chemistry," *Research In Chemical Kinetics, Volume 3*, pp1, Compton R.G. and Hancock G. (editors), © 1995 Elsevier Science B.V., Amsterdam.
- ²¹ Stothard N.D. and Walker R.W., *J. Chem. Soc. Faraday Trans.*, **87**, 241, (1991).
- ²² Lodhi Z.H. and Walker R.W., *J. Chem. Soc. Faraday Trans.*, **87**, 2361, (1991).

Chapter 7.

Discussion of the Kinetic Experiments for the Oxidation of the Xylenes.

7.1. Introduction.

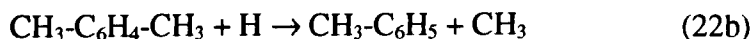
The experimental data obtained in **Chapter 4** can be used to determine rate constants for the attack of OH, H, or HO₂ on the three xylenes. The basic algebraic stationary state approach, outlined in **Chapter 2**, is a good method of estimating approximate rate constants for the attack of the radicals on the hydrocarbon but this approach does not permit the use of a comprehensive mechanism. Further, effects such as self-heating and pressure changes due to the oxidation of the additive are not taken into account. All of these effects can be taken into consideration by using an comprehensive computer program.

7.2. Description of the Computer Program and Mechanism Used.

A brief outline of some of the important features of the computer program used to interpret the experimental data and obtain the rate constants for $k(\text{HO}_2 + \text{Xylene})$ and $k(\text{H} + \text{Xylene})$ is given below.

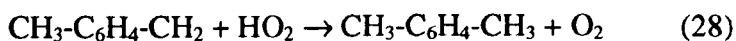
The computer program used to calculate the relative rate constants was written using the C programming language running under *UNIX-SunOS(4.1)*. The program is comprised of a number of sections.

Section 1 incorporates a series of differential equations for formation and consumption of the products and stable intermediates such as H₂O₂. The concentrations of the radicals are obtained by solving a steady state mechanism derived from the hydrogen + oxygen reaction (Table 7.1 reactions 0-4, 7, 8, 10, 11 13, 14, 14a and 15) together with the important reactions for the removal of the hydrocarbon by radical attack, the decomposition of the additive, the reaction of the additive with oxygen, a few subsequent reactions for the radicals generated from the parent hydrocarbon and the necessary termination reactions (Table 7.1 reactions 21-24, 27-31 and 37). For the purposes of the kinetic analysis it is assumed that apart from the occurrence of reaction (22b), radical attack occurs solely through H abstraction from one of the CH₃ groups.



Reactions (27) and (28) are written to account for the removal of methylbenzyl radicals.

The consequences of this undoubted *oversimplification* are addressed below.



(i) **Production of OH, H, O and HO₂ radicals from methylbenzyl reactions.**

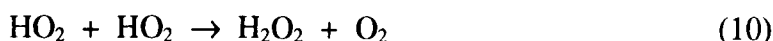
Production of H, O or OH from methylbenzyl radicals will not affect the relative rate of attack on the additive and H₂ (directly related to ΔP₅₀) since each pair of reactions involved is linear in radical concentration. However, production of HO₂

Table 7. 1: Important reactions used in computer program

Reaction Number	Reaction	Rate Constant Parameter	Rate Equation
0	$H_2 + O_2 \rightarrow H_2O_2$	R_1	k_0
1	$OH + H_2 \rightarrow H_2O + H$	K	$K = k_1 [OH][H_2]$
2	$H + O_2 \rightarrow OH + O$	Q	$Q = k_2 [H][O_2]$
3	$O + H_2 \rightarrow OH + H$	J	$J = k_3 [O][H_2]$
4	$H + O_2 + M \rightarrow HO_2 + M$	A_1Q	$A_1 = k_4 [M_4] / k_2$
7	$H_2O_2 + M' \rightarrow 2OH + M'$	$0.5A_7I$	$A_7 = 2k_7M'_7$
8	$H + HO_2 \rightarrow 2OH$	A_3QG	$A_3 = k_8 / k_2k_{10}^{1/2}[O_2]$
10	$HO_2 + HO_2 \rightarrow H_2O_2 + O_2$	G^2	$G = k_{10}^{1/2}[HO_2]$
11	$H_2 + HO_2 \rightarrow H_2O_2 + H$	A_6G	$A_6 = k_{11}[H] / k_{10}^{1/2}$
13	$O + H_2O_2 \rightarrow H_2O + O_2$	A_4IJ	$A_4 = k_{13} / k_3[H_2]$
14	$H + H_2O_2 \rightarrow H_2O + OH$	A_2IQ	$A_2 = k_{14} / k_2[O_2]$
14a	$H + H_2O_2 \rightarrow H_2 + HO_2$	$A_{14}IQ$	$A_{14} = k_{14a} / k_2[O_2]$
15	$OH + H_2O_2 \rightarrow H_2O + HO_2$	A_5IK	$A_5 = k_{15} / k_1[H_2]$
21	$CH_3-C_6H_4-CH_3 + OH \rightarrow CH_3-C_6H_4-CH_2 + H_2O$	B_2K	$B_2 = R_9[XY] / [H_2]$
22	$CH_3-C_6H_4-CH_3 + H \rightarrow CH_3-C_6H_4-CH_2 + H_2$	B_4Q	$B_4 = R_{11}[XY] / [O_2]$
23	$CH_3-C_6H_4-CH_3 + O \rightarrow CH_3-C_6H_4-CH_2 + OH$	B_3J	$B_3 = R_{10}[XY] / [H_2]$
24	$CH_3-C_6H_4-CH_3 + HO_2 \rightarrow CH_3-C_6H_4-CH_2 + H_2O_2$	B_5G	$B_5 = R_{12}[XY]$
27	$CH_3-C_6H_4-CH_2 + HO_2 \rightarrow CH_3-C_6H_4-CH_2O + OH$	F_2	$F_2 = G / (G + R_{23}G + R_{16}[O_2])$
28	$CH_3-C_6H_4-CH_2 + HO_2 \rightarrow CH_3-C_6H_4-CH_3 + O_2$	$F_3 = 1 - F_2$	$F_3 = R_{23}G / (G + R_{23}G + R_{16}[O_2])$
37	$CH_3-C_6H_4-CH_2 + O_2 \rightarrow CH_3-C_6H_4-CHO + OH$	F_9	$F_9 = R_{16}[O_2] / (G + R_{23}G + R_{16}[O_2])$
29	$CH_3-C_6H_4-CH_2O \rightarrow CH_3-C_6H_4-CHO + H$	$F_2 * F_4$	$F_4 = 1 / (1 + R_{24}[O_2])$
30	$CH_3-C_6H_4-CH_2O + O_2 \rightarrow CH_3-C_6H_4-CHO + HO_2$	$F_2 * F_5 = F_2(1 - F_4)$	
31	$CH_3 + H_2 \rightarrow CH_4 + H$	F_6	$F_6 = [H_2] / ([H_2] + R_{25}[O_2])$
32	$CH_3 + O_2 \rightarrow HCHO + OH$	$F_7 = 1 - F_6$	
33	$CH_3-C_6H_4-CH_3 + O_2 \rightarrow CH_3-C_6H_4-CH_2 + HO_2$	IN	$IN = R_{15}[XY][O_2]$
41	$HCHO + OH \xrightarrow{(O_2)} CO + H_2O + HO_2$	E_2K	$E_2 = R_{27}[HCHO] / [H_2]$
42	$HCHO + H \xrightarrow{(O_2)} CO + H_2 + HO_2$	E_4Q	$E_4 = R_{28}[HCHO] / [O_2]$
43	$HCHO + HO_2 \xrightarrow{(O_2)} CO + H_2O_2 + HO_2$	E_5G	$E_5 = R_{29}[HCHO]$
44	$HCHO + O_2 \xrightarrow{(O_2)} CO + HO_2 + HO_2$	FI	$FI = k_{44}[HCHO][O_2]$

[XY] = concentration of Xylene.

will affect ΔP_{50} . Reaction (24) competes with reaction (10), the rate of which is proportional to $[\text{HO}_2]^2$.

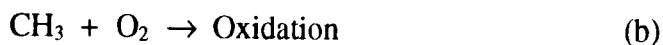


Consequently an increase in $[\text{HO}_2]$ will effectively reduce the relative rate of attack on xylene by HO_2 .

(ii) Oxidation of xylene results in a positive pressure change which will reduce the observed negative pressure change due to the $\text{H}_2 + \text{O}_2$ reaction. Consequently the observed value of ΔP_{50} will be lower than the real value. The magnitude of the pressure change due to the oxidation of xylene is determined by the chemical reactions, which follow the formation of the methylbenzyl radicals. Given that ΔP_{50} is the pressure change at 50% consumption of the xylene, it is clear that a considerable amount of complex oxidation chemistry will have occurred. The problem is potentially compounded by the fact that it has not been possible to determine good carbon balances in the analytical studies (Chapter 8).

(iii) With most hydrocarbon additives, particularly alkanes, the radical homolysis reactions and reactions with O_2 are so fast that reactions which reform the additive are negligible. In this situation the precise chemistry removing the radicals formed from the additive is of no interest in determining the full rate of radical attack on the additive.

An example of a system where regeneration is important is found when CH_4 is added to $\text{H}_2 + \text{O}_2$ mixtures at 773K^1 . For equal amounts of $\text{H}_2 + \text{O}_2$ at 500 Torr total pressure reaction (a) is significantly faster than (b),



Consequently the fraction of CH_3 removed is $k_b[\text{O}_2]/(k_b[\text{O}_2] + k_a[\text{H}_2])$, and is considerably less than unity. Clearly this must be taken into account when measuring the loss of CH_4 .

In carrying out this work, points (i) and (ii) have been dealt with by using an extremely low amount of additive, namely 0.05 Torr. In consequence, whatever the reactions of the methylbenzyl radicals the H, O, OH and (of particular importance) HO_2 , concentrations will only be negligibly perturbed from the values observed in the absence of the xylene. Further, from direct detailed experimental observations and computer analysis, the pressure change due to the oxidation of the xylene is unlikely to affect ΔP_{50} by more than 5%.

Tables 7.2 to 7.4 show the computer analysis of the ΔP_{50} values for different quantities of each additive. It is clear that there is negligible effect up to 0.1% (0.5 Torr) which confirms the view that the reaction concentrations have not been perturbed and that effects due to the oxidation of the xylene are minimal. The conclusion is very different with 1% of the additive.

In respect to point (iii), analysis of the benzyl radical oxidation chemistry (Chapter 6) indicates that there is some evidence for the regeneration of xylene from methylbenzyl reactions. This point will be discussed later.

Section 2 uses a Kutta-Runga integration method to solve numerically the differential equations obtained from the steady-state treatment as outlined in *section 1*. *Section 2* also contains a set of equations which account for the heats of reaction (Table 7.5) and

Table 7. 2 : A comparison between the observed the ΔP_{50} and computer calculated ΔP_{50} for different quantities of p-xylene.

H₂ / Torr	O₂ / Torr	N₂ / Torr	p-Xylene ΔP_{50} / Torr						
			Observed	0.005	0.05	0.1	0.2	0.5	5.0
140	35	325	0.78	0.704	0.702	0.700	0.697	0.690	0.412
140	70	290	1.11	1.047	1.049	1.055	1.053	1.054	0.983
140	140	220	1.34	1.390	1.388	1.391	1.388	1.389	1.595
140	210	150	1.57	1.556	1.550	1.549	1.540	1.538	1.875
140	280	80	1.62	1.643	1.642	1.637	1.632	1.617	2.031
140	360	0	1.76	1.711	1.707	1.702	1.694	1.671	2.140
35	70	395	0.45	0.434	0.436	0.438	0.439	0.435	0.249
70	70	360	0.69	0.685	0.686	0.688	0.685	0.685	0.513
140	70	290	1.11	1.047	1.049	1.055	1.053	1.054	0.983
210	70	220	1.23	1.353	1.349	1.349	1.354	1.367	1.409
280	70	150	1.59	1.633	1.634	1.640	1.634	1.659	1.806
430	70	0	2.10	2.215	2.215	2.223	2.218	2.253	2.595

Table 7. 3: A comparison between the observed the ΔP_{50} and computer calculated ΔP_{50} for different quantities of m-xylene.

			m-Xylene ΔP_{50} / Torr						
H ₂ / Torr	O ₂ / Torr	N ₂ / Torr	Observed	0.005	0.05	0.1	0.2	0.5	5.0
140	35	325	0.75	0.677	0.675	0.670	0.670	0.661	0.403
140	70	290	0.99	1.019	1.021	1.019	1.022	1.023	0.966
140	140	220	1.35	1.364	1.366	1.366	1.367	1.358	1.558
140	210	150	1.54	1.538	1.532	1.534	1.528	1.516	1.826
140	280	80	1.65	1.630	1.630	1.626	1.621	1.601	1.991
140	360	0	1.76	1.700	1.695	1.697	1.688	1.658	2.104
35	70	395	0.42	0.433	0.436	0.438	0.439	0.433	0.223
70	70	360	0.69	0.674	0.675	0.676	0.676	0.674	0.490
140	70	290	0.99	1.019	1.021	1.019	1.022	1.023	0.966
210	70	220	1.29	1.305	1.302	1.303	1.311	1.315	1.387
280	70	150	1.52	1.575	1.576	1.573	1.569	1.587	1.787
430	70	0	2.11	2.124	2.126	2.120	2.121	2.163	2.548

Table 7.4 : A comparison between the observed the ΔP_{50} and computer calculated ΔP_{50} for different quantities of *o*-xylene.

H₂ / Torr	O₂ / Torr	N₂ / Torr	<i>o</i>-Xylene ΔP_{50} / Torr						
			Observed	0.005	0.05	0.1	0.2	0.5	5.0
140	35	325	0.55	0.524	0.502	0.518	0.513	0.505	0.304
140	70	290	0.83	0.806	0.809	0.806	0.808	0.814	0.684
140	140	220	1.14	1.108	1.110	1.111	1.112	1.112	1.272
140	210	150	1.24	1.266	1.262	1.267	1.236	1.262	1.576
140	280	80	1.31	1.354	1.355	1.354	1.349	1.346	1.757
140	360	0	1.48	1.425	1.417	1.424	1.417	1.403	1.892
35	70	395	0.37	0.361	0.363	0.364	0.364	0.355	0.175
70	70	360	0.53	0.547	0.547	0.547	0.547	0.542	0.357
140	70	290	0.83	0.806	0.809	0.806	0.808	0.814	0.684
210	70	220	1.01	1.024	1.023	1.022	1.028	1.041	0.986
280	70	150	1.24	1.227	1.232	1.233	1.231	1.527	1.271
430	70	0	1.53	1.655	1.662	1.666	1.672	1.683	1.865

Table 7.5 : Important reactions and associated heats of reaction.

Reaction Number	Reaction	$\Delta H/$	kcal mol ⁻¹
0	$H_2 + O_2 \rightarrow H_2O_2$	H ₁	32.5
1	$OH + H_2 \rightarrow H_2O + H$	H ₂	14.8
2	$H + O_2 \rightarrow OH + O$	H ₃	-16.0
3	$O + H_2 \rightarrow OH + H$	H ₄	-1.8
4	$H + O_2 + M \rightarrow HO_2 + M$	H ₅	47.2
7	$H_2O_2 + M' \rightarrow 2OH + M'$	H ₆	-50.0
8	$H + HO_2 \rightarrow 2OH$	H ₇	39.2
10	$HO_2 + HO_2 \rightarrow H_2O_2 + O_2$	H ₈	42.3
11	$H_2 + HO_2 \rightarrow H_2O_2 + H$	H ₉	-14.7
13	$O + H_2O_2 \rightarrow H_2O + O_2$	H ₁₀	85.0
14	$H + H_2O_2 \rightarrow H_2O + OH$	H ₁₁	68.5
14a	$H + H_2O_2 \rightarrow H_2 + HO_2$	H ₁₂	14.7
15	$OH + H_2O_2 \rightarrow H_2O + HO_2$	H ₁₃	29.3
21	$CH_3-C_6H_4-CH_3 + OH \rightarrow CH_3-C_6H_4-CH_2 + H_2O$	H ₁₄	23.0
23	$CH_3-C_6H_4-CH_3 + O \rightarrow CH_3-C_6H_4-CH_2 + OH$	H ₁₅	6.0
22	$CH_3-C_6H_4-CH_3 + H \rightarrow CH_3-C_6H_4-CH_2 + H_2$	H ₁₆	8.0
24	$CH_3-C_6H_4-CH_3 + HO_2 \rightarrow CH_3-C_6H_4-CH_2 + H_2O_2$	H ₁₇	-6.0
27	$CH_3-C_6H_4-CH_2 + HO_2 \rightarrow CH_3-C_6H_4-CH_2O + OH$	H ₂₅	32.0
28	$CH_3-C_6H_4-CH_2 + HO_2 \rightarrow CH_3-C_6H_4-CH_3 + O_2$	H ₂₆	8.0
29	$CH_3-C_6H_4-CH_2O + O_2 \rightarrow CH_3-C_6H_4-CHO + HO_2$	H ₂₇	0.0
30	$CH_3-C_6H_4-CH_2O \rightarrow CH_3-C_6H_4-CHO + H$	H ₂₈	0.0
31	$CH_3 + H_2 \rightarrow CH_4 + H$	H ₂₉	0.0
32	$CH_3 + O_2 \rightarrow HCHO + OH$	H ₃₀	0.0
33	$CH_3-C_6H_4-CH_3 + O_2 \rightarrow CH_3-C_6H_4-CH_2 + HO_2$	H ₃₁	17.4

activation energies of the reactions involved (Table 7.6) and hence the self heating effects occurring. The magnitude of the self-heating is determined by the composition of the reaction mixture but is typically less than 0.5°C. Self-heating of the reaction mixture creates two effects. Firstly there is a small increase in the value of the calculated rate constants, although this is of very minor importance. The second, and much more important, effect of the self-heating is to increase the total pressure, consequently altering the value for ΔP_{50} , the value of the pressure change when 50% of the additive has been consumed (see Chapter 4). A temperature change of 0.5°C causes an increase in ΔP of 0.33 Torr. Since the values of ΔP_{50} range between 0.3 and 1.8 Torr (Table 4.3) the change in temperature can have a significant effect on ΔP_{50} if it is reached at maximum rate. However, ΔP_{50} is reached well before maximum rate and the change in temperature is usually of the order of 0.1°C which would give an increase in ΔP of ~0.06 Torr. Although this is small it is still important when measuring ΔP and ΔP_{50} .

Following the procedures described in *sections 1* and *2* for the computer program, values of ΔP_{50} are calculated for each mixture used (Tables 7.2 to 7.4).

Section 3 of the computer program utilises the minimisation and optimisation routines to enable the program to calculate the best fit to the observed values of ΔP_{50} by adjusting the chosen rate constants; this is achieved using the *minsq* optimisation routine which is linked upon compilation into the computer program.

The rate constants R_{0-30} , most of which enter the computer program as rate constant ratios (Table 7.6), were employed such that the program can solve the simultaneous equations for [OH], [H], [O] and [HO₂].

Table 7. 6: Important parameters required for the computer program

Computer Ratio (R)	Rate constant	Value	$E_A / \text{kcal mol}^{-1}$
R ₁	k_0	0.00007	50.0
R ₂	k_7	0.0219	47.0
R ₃	k_4 / k_2	13.0	17.8
R ₄	k_{14}	281	-8.0
R ₅	k_{15} / k_1	5.7	-3.0
R ₆	k_{13} / k_1	0.0	-5.0
R ₇	k_{11}	0.00076	20.0
R ₈	k_8	16.6	-17.0
R₉ p-Xylene	k_{21} / k_1	12.6	-3.0
R₉ m-Xylene	k_{21} / k_1	11.8	-3.0
R₉ o-Xylene	k_{21} / k_1	13.3	-3.0
R₁₀ all xylenes	k_{23} / k_3	80.0	-5.0
R ₁₁	k_{22} / k_2	298.0	-8.0
R ₁₂	$k_{24} / (k_{10})^{1/2}$	0.143	15.0
R ₁₄	k_{14a} / k_2	46.0	-5.0
R ₁₅	k_{33}	0.0	0.0
R ₁₆	$k_{37}(k_{10})^{1/2} / k_{27}$	0.0041	0.0
R ₂₃	k_{28} / k_{27}	0.194	0.0
R ₂₄	k_{30} / k_{24}	0.015	0.0
R ₂₅	k_{32} / k_{31}	0.0	40.0
R ₂₆	k_{44}	0.0	-4.0
R ₂₇	OH + HCHO / k_1	0.0	-10.0
R ₂₈	OH + HCHO / k_2	0.0	10.0
R ₂₉	OH + HCHO / $(k_{10})^{1/2}$	0.0	0.0
R ₃₀	RH COEFF IN M TERM	2.0	0.0

All of the rate constant ratios used in the $\text{H}_2 + \text{O}_2$ reaction ($R_{0.8}$ & 14) are known accurately² and on the assumption that the radical, **R**, formed from the radical attack on RH does not reform RH, then the only unknown parameters required to calculate ΔP_{50} are k_{21}/k_1 , k_{22}/k_2 , k_{23}/k_3 and $k_{24}/(k_{10})^{1/2}$.

In principle, all of those values may be varied until the optimal fit between the observed and calculated values of ΔP_{50} are obtained. In practice the optimisation is not sufficiently sensitive to achieve this and past practice has shown that only two rate constant ratios can be optimised.

As O attack is a relatively minor channel for RH removal, then k_{23}/k_3 can be fixed with little loss of accuracy even if the ratio is not known precisely. Later discussion will show that optimisation of k_{21}/k_1 and $k_{24}/(k_{10})^{1/2}$ with k_{22}/k_2 fixed is not an option, so that the two possibilities become

(i) Optimisation of k_{22}/k_2 and $k_{24}/(k_{10})^{1/2}$ with k_{21}/k_1 fixed.

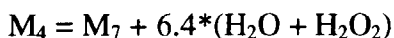
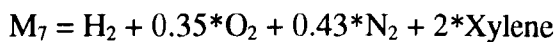
(ii) Optimisation of k_{22}/k_2 and k_{21}/k_1 with $k_{24}/(k_{10})^{1/2}$ fixed.

As k_{21}/k_1 can be calculated from the available literature data with considerable accuracy, the optimisation procedure was used to determine k_{22}/k_2 and $k_{24}/(k_{10})^{1/2}$

7.2.1. The stationary-state analysis.

In summary, the computer program used for the interpretation of the ΔP_{50} values obtained for the addition of each xylene singly to hydrogen + oxygen mixtures, in order to evaluate $k(\text{HO}_2 + \text{Xylene})$ and $k(\text{H} + \text{Xylene})$, was constructed from a stationary state analysis from the reactions shown in (Table 7.1). The rate constant data and concentration terms used by for the program are shown in (Table 7.6).

The third bodies, M_7 and M_4 , present in reactions (7) and (4), respectively, are defined for the computer program as below,



For convenience when solving the steady-state equations, the $[OH]$, $[H]$, $[O]$, $[HO_2]$ and $[H_2O_2]$ are represented by the parameters K, Q, J, G and I respectively (Table 7.1).

The rate equations used by the computer program are shown in Table 7.7.

7.3. Determination of Rate Constant Data.

Normally the main reactions involved in the removal of alkanes are those involving $OH + RH$ and $H + RH$. However, RH can also react with O and, more importantly in the case of aromatic compounds, HO_2 . The reactions with HO_2 are important because the weakness of the C-H bonds in the methyl groups (in the xylenes) due to the electron delocalisation effects leads to a considerable lowering of the activation energy.

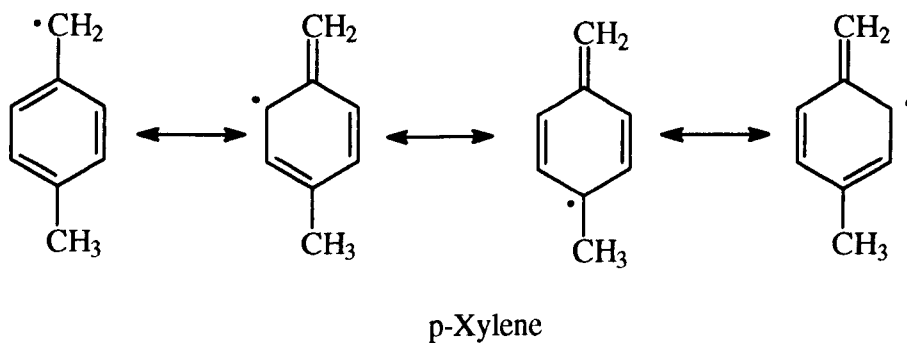
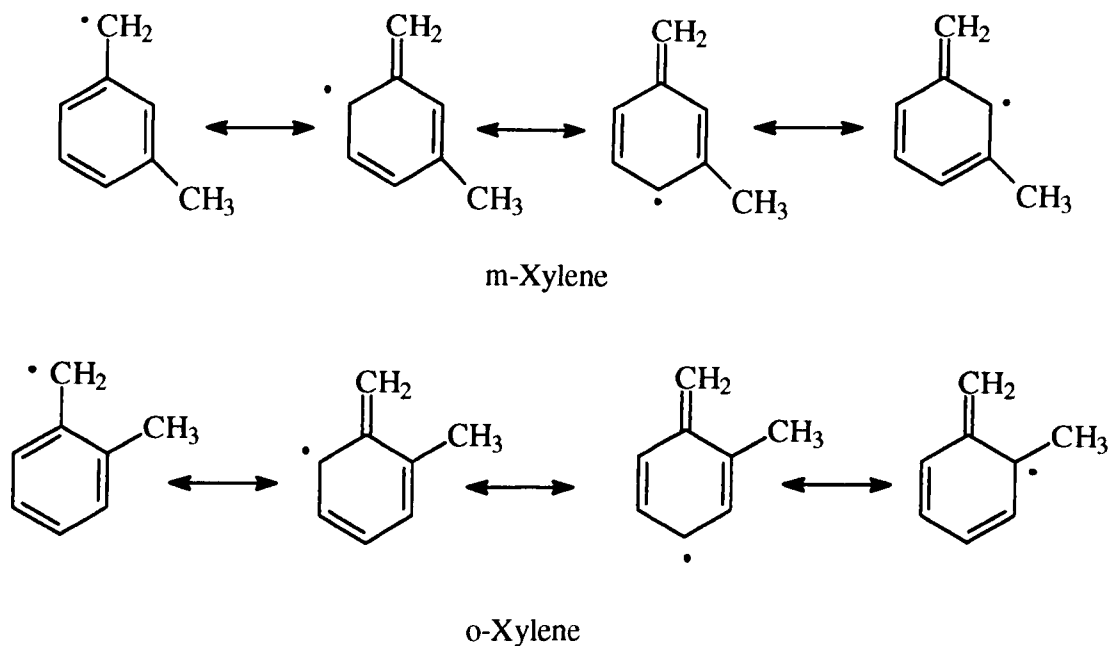


Table 7. 7 : Rate Equations used by the Computer Program.

Array Function	Reaction Rate
F[1] =	$d[\text{H}_2\text{O}_2] / dt = R_1 + G^2 + (A_6 + B_5 + C_5 + E_5)G - \frac{1}{2}A_7I - A_4IJ - A_2IQ - A_{14}IQ - A_5IK$
F[2] =	$d[\text{H}_2\text{O}] / dt = K + A_4IJ + A_2IQ + A_5IK + B_2K + C_2K + E_2K$
F[3] =	$d[\text{XY}] / dt = IN * F_{10} + (B_2K + B_3J + B_4Q + B_5G)F_{10} + (C_2K + C_3J + C_4Q + C_5G) + D_4Q$
F[4] =	$d[\text{ALD}] / dt = (IN + B_2K + B_3J + B_4Q + B_5G)F_{10}$
F[5] =	$d[\text{EPOX}] / dt = (C_2K + C_3J + C_4Q + C_5G)F_1$
F[6] =	$d[\text{RING}] / dt = (C_2K + C_3J + C_4Q + C_5G)(1 - F_1)$
F[7] =	$d[\text{CH}_4] / dt = D_4Q * F_6$
F[8] =	$d[\text{H}_2] / dt = R_1 + K + J + A_6G + D_4Q * F_6 - A_{14}IQ - B_4Q - C_4Q - E_4Q$
F[9] =	$d[\text{O}_2] / dt = R_1 + Q + A_1Q + (IN + B_2K + B_3J + B_4Q + B_5G)(F_9 + F_2F_5 - F_3) - G^2 - A_4IJ + (C_2K + C_3J + C_4Q + C_5G) + D_4Q * F_7 + IN + 2FI + E_2K + E_4Q + E_5G$
F[10] =	$d[\text{HCHO}] / dt = D_4Q * F_7 - FI - E_2K - E_4Q - E_5G$
F[11] =	$d\text{Pressure} / dt = R_1 + A_1Q - \frac{1}{2}A_7I + (IN + B_2K + B_3J + B_4Q + B_5G)(F_2 * F_4)$
F[12] =	$d[\text{CO}] / dt = FI + E_2K + E_4Q + E_5G$



As illustrated earlier, the optimisation procedure has been used to determine k_{22}/k_2 and $k_{24}/(k_{10})^{1/2}$.

7.4. Important Reactions Occurring In The Xylene Oxidation Mechanism

7.4.1. Estimation of R_9 and R_{10} .

Accurately determined experimental rate data are available for k_{21} , the reactions of OH + p-xylene,³⁻⁵ m-xylene^{3,5} and o-xylene^{3,5} (Table 7.8). If a value for $k_1 = 4.5 \cdot 10^8 \text{ l mol}^{-1} \text{ s}^{-1}$ at 753K is taken from the literature⁶ then R_9 (k_{21}/k_1) could be obtained accurately for each xylene such that $R_{9 \text{ p-xylene}} = 12.6$, $R_{9 \text{ m-xylene}} = 11.8$ and $R_{9 \text{ o-xylene}} = 13.2$, at 753K (summarised in Tables 7.6 and 7.9).

Experimental data are also available for k_{23} , the reactions of O with p-xylene^{7,8}, m-xylene^{4,7,8,9} and o-xylene^{7,8}. From the data given in Table 7.8 a value of $k_{23} = 3.0 \cdot 10^9 \text{ l mol}^{-1} \text{ s}^{-1}$ is taken the rate for each xylene at 753K. Consequently, with $k_3 = 3.7 \cdot 10^7 \text{ l}$

Table 7. 8 : Literature search for xylene rate constants

	$k(OH+X \rightarrow P)$		$k(O+X \rightarrow P)$			
o-Xylene	[⁵]5.687	[³]5.947	[⁷]2.393	[⁸]3.040		
m-Xylene	[⁵]4.941	[³]5.291	[⁷]2.984	[⁸]3.976	[⁹]3.779	
p-Xylene	[⁵]5.582	[³]5.688	[⁷]2.417	[⁸]3.053	[⁹]3.363	[⁴]2.417

Units of k are $*10^9 \text{ l mol}^{-1} \text{ s}^{-1}$.

NB: X = Xylene; P = Products (as indicated in literature references.)

Table 7. 9 : Literature xylene rate constants converted into relative rate constants.

	$k_{(OH+X \rightarrow P)}/k_{(OH+H_2)}$		$k_{(O+X \rightarrow P)}/k_{(O+H_2)}$			
o-Xylene	[⁵]12.64	[³]13.22	[⁷]64.68	[⁸]82.16		
m-Xylene	[⁵]10.98	[³]11.77	[⁷]80.65	[⁸]107.45	[⁹]102.14	
p-Xylene	[⁵]12.40	[³]12.64	[⁷]65.32	[⁸]82.51	[⁹]90.89	[⁴]65.23

NB: X = Xylene; P = Products (as indicated in literature references.)

$$k_1 = k_{(OH+H_2)} = 4.5 * 10^8 \text{ l mol}^{-1} \text{ s}^{-1} \quad k_3 = k_{(O+H_2)} = 3.7 * 10^7 \text{ l mol}^{-1} \text{ s}^{-1}.$$

$\text{mol}^{-1} \text{ s}^{-1}$ from the literature⁴ a value of $R_{10} = 80$ can be taken for all three xylenes, (see Table 7.6 and 7.9).

Data are available for p-xylene + H radicals^{4,10} but only at temperatures near to 300K where the mechanism is likely to involve mostly addition. There are currently no data available for the reactions of HO₂ radicals with the xylenes. It is therefore clearly of value to use the experimental data to obtain accurate rate constants for the reactions of H and HO₂ radicals with the xylenes at 753K.

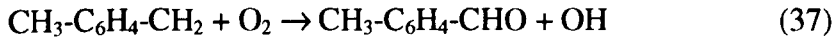
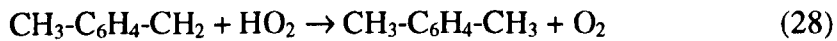
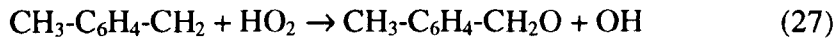
7.4.2. The reactions of methylbenzyl radicals - Estimation of R_{16} and R_{23}

As indicated earlier, it is important to consider the possibility that the methylbenzyl radicals may undergo reactions which regenerate xylene.

The major reaction of the xylene molecules, at temperatures above 500K, is the abstraction of H from the methyl side chain producing methylbenzyl radicals. This is analogous to the reaction of toluene under identical conditions producing benzyl radicals¹¹. As discussed in Chapter 6, the decomposition of neopentylbenzene (NPB) in the presence of oxygen, in a system analogous to that applied to examine the reaction of allyl radicals with HO₂ by Lohdi and Walker¹², was used in order to examine the chemistry of the reactions between HO₂ and benzyl radicals. The findings of Chapter 6 indicate that there is a reaction between HO₂ and benzyl radicals to produce toluene for which a rate constant of $8.4 \times 10^8 \text{ l mol}^{-1} \text{ s}^{-1}$ at 753K has been determined. Since the major products from xylene oxidation are similar in character to those from toluene (see Chapters 2 and 8), being the isomeric-tolualdehydes and toluene from the xylenes compared with benzaldehyde and benzene from toluene and the delocalised nature of

both benzyl and methylbenzyl radicals, then it is also likely that there is a reaction between the methylbenzyl radicals produced from xylene oxidation with HO₂ to reform xylene. The computer program requires appropriate rate expressions for these and other reactions of the methylbenzyl radicals (Table 7.1 reactions 27, 28, 29, 30 and 37) in order to take the resulting regeneration of xylene into account.

A simple mathematical treatment can be applied taking the view that the methylbenzyl reactions are confined to (27),(28) and (37):



It follows that as the rates of reaction $R_{(27)} = k_{27}[\text{CH}_3\text{-C}_6\text{H}_4\text{-CH}_2][\text{HO}_2]$,

$R_{(28)} = k_{28}[\text{CH}_3\text{-C}_6\text{H}_4\text{-CH}_2][\text{HO}_2]$ and $R_{(37)} = k_{37}[\text{CH}_3\text{-C}_6\text{H}_4\text{-CH}_2][\text{O}_2]$ then the fractions of methylbenzyl radicals consumed in the reactions (27), (28) and (37) are given by

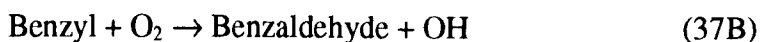
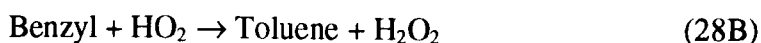
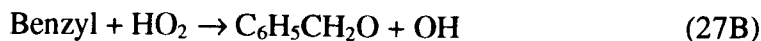
$$F_2 = G / (G + R_{23}G + R_{16}[\text{O}_2]), \quad F_3 = R_{23}G / (G + R_{23}G + R_{16}[\text{O}_2])$$

and $F_9 = R_{16}[\text{O}_2] / (G + R_{23}G + R_{16}[\text{O}_2])$, respectively, where as illustrated in

Table 7.1, $R_{16} = \frac{k_{37}(k_{10})^{1/2}}{k_{27}}$, $R_{23} = \frac{k_{28}}{k_{27}}$ and $G = (k_{10})^{1/2}[\text{HO}_2]$.

It is now important to determine the effect of changes in F_2 , F_3 and F_9 on k_{22}/k_2 and $k_{24}/(k_{10})^{1/2}$ by altering R_{16} and R_{23} .

No values exist for the rate constants for reactions (27), (28) and (37) and as the best approximation, given the similar nature of the species involved, it is proposed to use the experimentally determined values for reactions (27B), (28B) and (37B) for the benzyl radical.



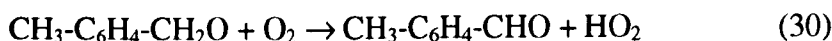
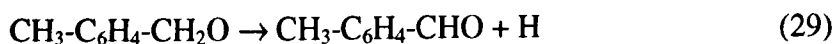
The experimentally determined rate constant ratios from Chapter 6 for the corresponding reactions of the benzyl radicals with HO₂ and O₂ were found to be^{*} :

$$\frac{k_{37}}{k_{28}} = \frac{k_{6.05}}{k_{6.04}} = \frac{k_{37\text{B}}}{k_{28\text{B}}} = 2.37 * 10^{-5} \quad \text{and} \quad \frac{k_{27}}{k_{28}} = \frac{k_{6.03}}{k_{6.04}} = \frac{k_{27\text{B}}}{k_{28\text{B}}} = 5.2 \quad \text{at} \quad 753\text{K}.$$

With $k_{10} = 6.68 * 10^8 \text{ l mol}^{-1} \text{ s}^{-1} = 8.5 * 10^5 \text{ Torr}^{-1} \text{ min}^{-1}$ from the literature⁴ such that $(k_{10})^{1/2} = 924 \text{ Torr}^{-1/2} \text{ min}^{-1/2}$, then $R_{16} = 0.0041 \pm 0.002 \text{ Torr}^{-1/2} \text{ min}^{-1/2}$ and $R_{23} = 0.194 \pm 0.050$ at 753K.

7.4.3. The reactions of CH₃C₆H₄CH₂O radicals - Estimation of R₂₄.

The effects of reactions (29) and (30), which involve CH₃-C₆H₄-CH₂O radicals produced in reaction (27), are investigated because although both produce tolualdehyde, H radicals are produced in reaction (29) and HO₂ radicals in reaction (30).



The fractions of CH₃C₆H₄CH₂O radicals removed by reactions (29) and (30), respectively, are expressed as F₄ and F₅ = 1-F₄, where $F_4 = 1/(1+R_{24}[O_2])$ with $R_{24} = k_{30}/k_{29}$.

* The subscript B is to signify that this reaction involves Benzyl radicals NOT methyl-benzyl radicals.

As indicated earlier, the formation of HO₂ radicals does in principle affect the relative rate of removal of additive and H₂ (effectively ΔP₅₀). By variation of R₂₄ the fraction of HO₂ radicals produced from CH₃C₆H₄CH₂O can be varied from zero to infinity. However, given the use of only 0.05 Torr of xylene, the value of R₂₄ should have little effect on the optimisations. As shown later, this prediction is shown to be true.

7.5. Data Interpretation and Sensitivity Analysis.

The optimised values of $R_{11} = k_{22}/k_2$ and $R_{12} = k_{24}/(k_{10})^{1/2}$ have been obtained from the computer program described above. The fixed values used in the optimisations are shown in Table 7.6. The initial results for each xylene determined from the computer program are given in Table 7.10. Tables 7.2 to 7.4 show the excellent agreement between the observed and calculated values of ΔP₅₀ for addition of 0.05 Torr of each xylene to the H₂ + O₂ mixtures.

Optimisation routines were carried out on the experimental data using predetermined values for R₉, R₁₀, R₁₆, R₂₃ and R₂₄ in order to determine values for R₁₁ and R₁₂. Sensitivity analyses were carried out by variation of a number of the fixed values.

Each of the chosen ratios was varied singularly between 15 and 30% (and up to 100% in some cases) and the values of R₁₁ and R₁₂ were re-optimised and the percentage change from the original optimised values for R₁₁ and R₁₂ recalculated. The findings are discussed below.

Table 7. 10: Results Summary for Xylene Kinetics

p-Xylene		m-Xylene		o-Xylene	
$\frac{k_{24}}{(k_{10})^{1/2}} / \text{Torr}^{-1/2} \text{Min}^{-1/2}$	$\frac{k_{22}}{k_2}$	$\frac{k_{24}}{(k_{10})^{1/2}} / \text{Torr}^{-1/2} \text{Min}^{-1/2}$	$\frac{k_{22}}{k_2}$	$\frac{k_{24}}{(k_{10})^{1/2}} / \text{Torr}^{-1/2} \text{Min}^{-1/2}$	$\frac{k_{22}}{k_2}$
0.143	298	0.151	313	0.180	417
RMS = 5.2		RMS = 3.8		RMS = 3.8	

$R_9 = k_{21}/k_1 = 12.6$ p-xylene, 11.8 m-xylene & 13.2 o-xylene,

$R_{10} = k_{23}/k_3 = 80,$

$R_{16} = 0.0041 \text{ Torr}^{-1/2} \text{ min}^{-1/2}, R_{23} = 0.194$ and $R_{24} = 0.015 \text{ Torr}^{-1}.$

Table 7. 11: Sensitivity analysis for Xylene Kinetics. - Variation in R_9

A) p-xylene

$\frac{k_{21}}{k_1}$	$\frac{k_{24}}{(k_{10})^{1/2}} / \text{Torr}^{-1/2} \text{Min}^{-1/2}$	$\frac{k_{22}}{k_2}$
10.08	0.183 (4.5)	287
12.60	0.143 (5.2)	298
15.12	0.107 (5.9)	309

B) m-xylene

$\frac{k_{21}}{k_1}$	$\frac{k_{24}}{(k_{10})^{1/2}} / \text{Torr}^{-1/2} \text{Min}^{-1/2}$	$\frac{k_{22}}{k_2}$
10.08	0.179 (4.0)	305
11.80	0.151 (3.8)	313
15.12	0.099 (4.1)	329

C) o-xylene

$\frac{k_{21}}{k_1}$	$\frac{k_{24}}{(k_{10})^{1/2}} / \text{Torr}^{-1/2} \text{Min}^{-1/2}$	$\frac{k_{22}}{k_2}$
10.08	0.225 (5.3)	406
13.23	0.180 (3.8)	417
15.12	0.152 (4.1)	426

$R_9 = k_{21}/k_1 = 12.6$ p-xylene, 11.8 m-xylene & 13.2 o-xylene,

$R_{10} = k_{23}/k_3 = 80$,

$R_{16} = 0.0041 \text{ Torr}^{-1/2} \text{ min}^{-1/2}$, $R_{23} = 0.194$ and $R_{24} = 0.015 \text{ Torr}^{-1}$.

7.5.1. Variation of R_9 - OH attack.

Table 7.11 summarises the results from the sensitivity analysis for the variation of R_9 (k_{21}/k_1). Variation of 20% in R_9 was considered sufficient given the precision with which R_9 is known.

Of all of the sensitivity analyses carried out, it is the variation of R_9 which has the greatest effect on R_{11} and particularly R_{12} . However, it is unlikely that the uncertainty in the value of R_9 produces an error of more than 10% in the value of R_{11} for each xylene.

In the case of R_{12} , it is clear that the optimal value is extremely sensitive to the value of R_9 used. In fact an increase of 20% in R_9 is matched almost exactly by a 20% decrease in R_{12} . The accuracy with which R_{12} can be determined, therefore, is very dependant on the reliability of R_9 .

7.5.2. Variation of R_{10} - O attack.

Table 7.12 summarises the sensitivity analysis carried out with variations of R_{10} (k_{23}/k_3) of about 30%. As can be seen R_{11} (H atom attack) is insensitive to the variation in R_{10} , the values of R_{11} changing by only about 2%. However, the values of R_{12} (HO_2 attack) are a little more sensitive with changes in the values of about 12%.

It is difficult to reduce the uncertainty in R_{10} below about 20% and in consequence the error limit placed on R_{12} due to the uncertainty in R_{10} is placed at $\pm 10\%$.

7.5.3. Variation of R_{16} - Methylbenzyl \rightarrow Tolualdehyde.

The value of $R_{16} = \frac{k_{37}(k_{10})^{\frac{1}{2}}}{k_{27}}$ plays a part in determining the fraction of methylbenzyl

radicals that regenerate xylene. No data exist for k_{27} and k_{37} and, as indicated earlier,

Table 7. 12: Sensitivity analysis for Xylene Kinetics. - Variation in R_{10}

A) *p*-xylene

$\frac{k_{23}}{k_3}$	$\frac{k_{24}}{(k_{10})^{1/2}} / \text{Torr}^{-1/2} \text{Min}^{-1/2}$	$\frac{k_{22}}{k_2}$
56	0.161 (4.9)	291
80	0.143 (5.2)	298
104	0.125 (5.6)	305

B) *m*-xylene

$\frac{k_{23}}{k_3}$	$\frac{k_{24}}{(k_{10})^{1/2}} / \text{Torr}^{-1/2} \text{Min}^{-1/2}$	$\frac{k_{22}}{k_2}$
56	0.170 (3.9)	306
80	0.151 (3.8)	313
104	0.133 (3.9)	320

C) *o*-xylene

$\frac{k_{23}}{k_3}$	$\frac{k_{24}}{(k_{10})^{1/2}} / \text{Torr}^{-1/2} \text{Min}^{-1/2}$	$\frac{k_{22}}{k_2}$
56	0.197 (3.7)	411
80	0.180 (3.8)	417
104	0.163 (4.1)	423

$R_9 = k_{21}/k_1 = 12.6$ *p*-xylene, 11.8 *m*-xylene & 13.2 *o*-xylene,

$R_{10} = k_{23}/k_3 = 80$,

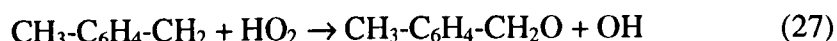
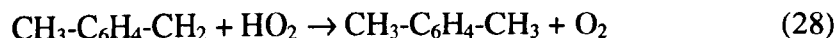
$R_{16} = 0.0041 \text{ Torr}^{-1/2} \text{ min}^{-1/2}$, $R_{23} = 0.194$ and $R_{24} = 0.015 \text{ Torr}^{-1}$.

values for the rate constants are taken as those for the analogous reactions of the benzyl radicals (Chapter 6). With an accurate value for k_{10} from the literature⁴ the recommended value of R_{16} is $0.0041 \text{ Torr}^{-1/2} \text{ min}^{-1/2}$ at 753K

The optimised data are summarised in Table 7.13 for a 50% variation in R_{16} . Although the value of R_{11} is insensitive to the value of R_{16} , R_{12} shows a small inverse dependence (circa 10%). This is consistent with an increase in R_{16} leading to a reduction in the regeneration of the xylenes and hence lower values of the rate constants for attack. Although for the benzyl radical system the analogous value of R_{16} can be determined considerably more accurately than a factor of 50%, it would be unwise to reduce the error limits on R_{11} and R_{12} below those shown in Table 7.13.

7.5.4. Variation of R_{23} - k_{28}/k_{27} .

R_{23} is given by the rate constant ratio k_{28}/k_{27} and also determines the degree of regeneration of xylene.



As indicated earlier, no values of k_{28} and k_{27} are available in the literature. However, use of the value of $k_{27\text{B}}/k_{28\text{B}} = 5.2$ at 753K for the analogous reaction of the benzyl radicals gives $k_{28}/k_{27} = 0.192$.

Sensitivity analysis of the optimisation of k_{22}/k_2 and $k_{24}/(k_{10})^{1/2}$ was carried out with R_{23} varied by a factor of 2 from the optimal value of 0.192. Runs were also carried out with $R_{23} = 0$ which corresponds to a simple case where no xylene is reformed from methylbenzyl radicals. The results are summarised in Table 7.14.

Table 7. 13: Sensitivity analysis for Xylene Kinetics.

$R_{16} / \text{Torr}^{-1/2} \text{ min}^{-1/2}$	$\frac{k_{24}}{(k_{10})^{1/2}} / \text{Torr}^{-1/2} \text{ min}^{-1/2}$			$\frac{k_{22}}{k_2}$		
	p-Xylene	m-Xylene	o-Xylene	p-Xylene	m-Xylene	o-Xylene
0.0082	0.130 (5.3)	0.139 (3.7)	0.167 (3.9)	296	311	412
0.0041	0.143 (5.2)	0.151 (3.8)	0.180 (3.8)	298	313	417
0.0021	0.157 (5.0)	0.166 (3.8)	0.195 (3.7)	295	311	415

$R_9 = k_{21}/k_1 = 12.6$ p-xylene, 11.8 m-xylene & 13.2 o-xylene,

$R_{10} = k_{23}/k_3 = 80$,

$R_{16} = 0.0041 \text{ Torr}^{-1/2} \text{ min}^{-1/2}$, $R_{23} = 0.194$ and $R_{24} = 0.015 \text{ Torr}^{-1}$.

Table 7. 14 : Sensitivity analysis for Xylene Kinetics.

R₂₃	$\frac{k_{24}}{(k_{10})^{1/2}} / \text{Torr}^{-1/2} \text{Min}^{-1/2}$			$\frac{k_{22}}{k_2}$		
	p-Xylene	m-Xylene	o-Xylene	p-Xylene	m-Xylene	o-Xylene
0.400	0.164 (5.1)	0.170 (4.2)	0.199 (3.8)	355	376	496
0.194	0.143 (5.2)	0.151 (3.8)	0.180 (3.8)	298	313	417
0.100	0.133 (5.28)	0.142 (3.7)	0.171 (3.8)	271	286	381
0	0.121 (5.47)	0.132 (3.6)	0.161 (3.9)	245	256	345

R₉ = k₂₁/k₁ = 12.6 p-xylene, 11.8 m-xylene & 13.2 o-xylene,

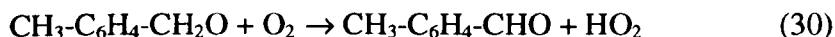
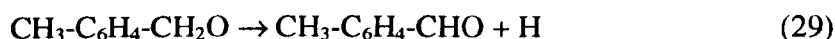
R₁₀ = k₂₃/k₃ = 80,

R₁₆ = 0.0041 Torr^{-1/2} min^{-1/2}, R₂₃ = 0.194 and R₂₄ = 0.015 Torr⁻¹.

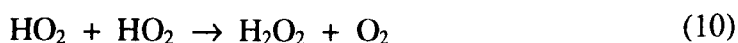
As expected, both the values of both R_{11} and R_{12} rise as the importance of regeneration increases. For each xylene, the optimal values of R_{11} and R_{12} can be regarded as maximum values if R_{23} is reliable. The computer analysis assumes attack at the CH_3 group and a simplified mechanism for the removal of methylbenzyl radicals. In consequence the percentage of regeneration may be over estimated. It is important to note that the values of R_{11} and R_{12} for all xylenes are reduced by only 15% when R_{23} is set to zero. Hence small errors in the percentage of regeneration of xylene will not lead to significant inaccuracy in R_{11} and R_{12} .

7.5.5. Variation of $R_{24} - k_{30}/k_{29}$.

The ratio R_{24} governs the relative importance of the two reactions removing $\text{CH}_3\text{C}_6\text{H}_4\text{CH}_2\text{O}$ radicals.



According to the mechanism a significant number of methylbenzyl radicals are oxidised through the formation of the $\text{CH}_3\text{C}_6\text{H}_4\text{CH}_2\text{O}$ radical. HO_2 radicals are formed in reaction (30) and if formed in significant quantity will perturb the concentration of HO_2 found in the absence of xylene (for example when high pressures of xylene are used). As indicated earlier, this will affect ΔP_{50} because of the competition between reaction (24) and the radical-radical reaction (10).



Given that HO₂ radicals are important in the removal of methylbenzyl radicals, then particularly if a high concentration of xylene is used, the optimal values of R₁₁ and R₁₂ will be sensitive to the value of R₂₄.

The results are summarised in Table 7.15. The value of R₂₄ has been varied over an infinite range with the effect that the CH₃C₆H₄CH₂O radicals are removed uniquely either through H formation or by HO₂ formation. The value of R₂₄=0.015 Torr⁻¹ corresponds to about 50% formation of HO₂ radicals. Table 7.15 shows the optimal values are effectively independent of R₂₄. These conclusions are interesting in a more generic sense in that they confirm that the pressure of xylene used is so low that any change in the HO₂ radical concentration will have a negligible effect on ΔP₅₀.

The optimal values of k_{22}/k_2 and $k_{24}/(k_{10})^{1/2}$ are given in Table 7.16 for each xylene. Error limits are suggested following the sensitivity analyses. It is clear that the optimal values of k_{22}/k_2 are relatively insensitive to the changes in k_{21}/k_1 and k_{23}/k_3 , R₁₆, R₂₃ and R₂₄. The only significant affect is caused by changes in R₂₃, which controls the degree of regeneration of xylene. When R₂₃ is reduced from 0.192 to zero which conforms to no regeneration of xylene, the values of k_{22}/k_2 for each xylene are reduced by about 15%. It may be concluded, as with earlier addition studies, that k_{22}/k_2 can be determined with considerable precision.

The situation with $k_{24}/(k_{10})^{1/2}$ is somewhat different. First, the values are very dependant on the fixed value used for k_{21}/k_1 . Fortunately, as indicated earlier, k_{21}/k_1 is known with considerable accuracy at 753K. The value of $k_{24}/(k_{10})^{1/2}$ is also sensitive to the value of k_{23}/k_3 used (Table 7.12) and to R₁₆, although independent of R₂₄. Further, as expected,

Table 7. 15: Sensitivity analysis for Xylene Kinetics.

	$\frac{k_{24}}{(k_{10})^{1/2}} / \text{Torr}^{-1/2} \text{ min}^{-1/2}$			$\frac{k_{22}}{k_2}$		
R₂₄	p-Xylene	m-Xylene	o-Xylene	p-Xylene	m-Xylene	o-Xylene
1*10 ¹⁰	0.142 (5.1)	0.150 (3.7)	0.179 (3.7)	300	316	412
0.015	0.143 (5.2)	0.151 (3.8)	0.180 (3.8)	298	313	417
0	0.143 (5.2)	0.151 (3.8)	0.180 (3.9)	297	312	414

R₉ = k₂₁/k₁ = 12.6 p-xylene, 11.8 m-xylene & 13.2 o-xylene,

R₁₀ = k₂₃/k₃ = 80,

R₁₆ = 0.0041 Torr^{-1/2} min^{-1/2}, R₂₃ = 0.194 and R₂₄ = 0.015 Torr⁻¹.

Table 7. 16: Summary of the optimal relative rate constants for the xylene kinetic study.

p-Xylene		m-Xylene		o-Xylene	
$k_{24}/(k_{10})^{1/2}$	k_{22}/k_2	$k_{24}/(k_{10})^{1/2}$	k_{22}/k_2	$k_{24}/(k_{10})^{1/2}$	k_{22}/k_2
0.133 ± 0.053	271 ± 40	0.142 ± 0.057	285 ± 43	0.170 ± 0.068	381 ± 57

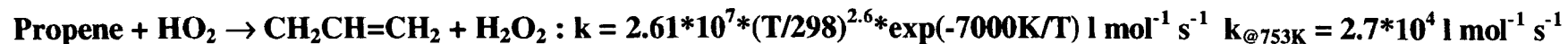
$$R_9 = k_{21}/k_1 = 12.6 \text{ p-xylene, } 11.8 \text{ m-xylene \& } 13.2 \text{ o-xylene,}$$

$$R_{10} = k_{23}/k_3 = 80,$$

$$R_{16} = 0.0041 \text{ Torr}^{-1/2} \text{ min}^{-1/2}, R_{23} = 0.10 \text{ and } R_{24} = 0.015 \text{ Torr}^{-1}.$$

Table 7. 17: Summary of the optimal rate constants for the xylene kinetic study

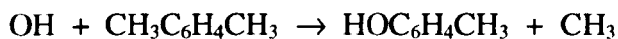
p-Xylene		m-Xylene		o-Xylene	
$k_{24} / \text{l mol}^{-1} \text{ s}^{-1}$	$k_{22} / \text{l mol}^{-1} \text{ s}^{-1}$	$k_{24} / \text{l mol}^{-1} \text{ s}^{-1}$	$k_{22} / \text{l mol}^{-1} \text{ s}^{-1}$	$k_{24} / \text{l mol}^{-1} \text{ s}^{-1}$	$k_{22} / \text{l mol}^{-1} \text{ s}^{-1}$
$9.6 \pm 3.8 \cdot 10^4$	$1.3 \pm 0.2 \cdot 10^9$	$1.03 \pm 0.14 \cdot 10^5$	$1.4 \pm 0.2 \cdot 10^9$	$1.23 \pm 0.49 \cdot 10^5$	$1.8 \pm 0.3 \cdot 10^9$



Tsang W., *J. Phs. Chem.*, 20, 221-247, (1991). - Literature Review.

the values of $k_{24}/(k_{10})^{1/2}$ are affected by the degree of regeneration of xylene. This latter point is the cause of some concern for two reasons.

- (i) The rate constants used to calculate the fraction of methylbenzyl radicals which reform xylene has been equated to that for the analogous reactions of benzyl radicals (Chapter 6).
- (ii) Product analysis for the xylene + H₂ + O₂ system shows that only about 50% of the products can be accounted for. Partly in consequence, the mechanism used for the analysis of the kinetics is oversimplified. Certainly radical attack at the ring has been ignored and formation of cresols through reactions such as



have been ignored.

It is reasonable to assume that these alternative routes to the oxidation chemistry of xylene do not involve regeneration. Given that only 50% of the products can be accounted for, a more suitable choice of R_{23} would be 0.100 (rather than the optimal value from benzyl chemistry) which would reduce the regeneration by a factor of two. This would reduce the optimum values of k_{22}/k_2 and $k_{24}/(k_{10})^{1/2}$ by about 7%. Following these arguments, the recommended values are given in Table 7.17 and correspond to the values given in Table 7.14 for $R_{23} = 0.100$.

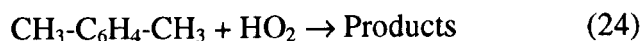
Error limits of $\pm 15\%$ and 40% are placed on the values of k_{22}/k_2 and $k_{24}/(k_{10})^{1/2}$ respectively.

7.6. Summary of the Rate Constants Obtained for the Oxidation of the Xylenes in slow reacting mixtures of Hydrogen and Oxygen.

The values of R_{12} ($k_{24}/(k_{10})^{1/2}$) and R_{11} (k_{22}/k_2) are summarised in **Table 7.16**. These relative rate constants correspond to the overall reaction of the xylene with HO_2 or H to produce products rather than the methylbenzyl radical as implied by reactions (24) and (22) respectively.

Since $k_2 = 9.76 \cdot 10^{10} \exp(-7470\text{K}/T) = 4.8 \cdot 10^6 \text{ l mol}^{-1} \text{ s}^{-1}$ at 753K^6 and $k_{10} = 1.87 \cdot 10^9 \exp(-775\text{K}/T) = 6.68 \cdot 10^8 \text{ l mol}^{-1} \text{ s}^{-1} = 8.5 \cdot 10^5 \text{ Torr}^{-1} \text{ min}^{-1}$, hence $(k_{10})^{1/2} = 923.6 \text{ Torr}^{-1/2} \text{ min}^{-1/2}$ at 753K^4 from the literature, the absolute rate constants can be obtained.

	$k_{24} / \text{l mol}^{-1} \text{ s}^{-1}$	$k_{22} / \text{l mol}^{-1} \text{ s}^{-1}$
p-Xylene	$9.6 \pm 3.8 \cdot 10^4$	$1.3 \pm 0.2 \cdot 10^9$
m-Xylene	$1.03 \pm 0.41 \cdot 10^5$	$1.4 \pm 0.2 \cdot 10^9$
o-Xylene	$1.23 \pm 0.49 \cdot 10^5$	$1.8 \pm 0.3 \cdot 10^9$



Baldwin et al.¹³ obtained rate data for $(\text{H} + \text{Toluene} \rightarrow \text{products})/(\text{H} + \text{O}_2 \rightarrow \text{Products}) = 81.0$ at 753K such that $k(\text{H} + \text{Toluene} \rightarrow \text{Products}) = 3.9 \cdot 10^8 \text{ l mol}^{-1} \text{ s}^{-1}$ at 753K . Other workers^{4,14,15} obtained values for $k(\text{H} + \text{Toluene} \rightarrow \text{Benzyl} + \text{H}_2) = 3.89 \cdot 10^8 \text{ l mol}^{-1} \text{ s}^{-1}$ at 753K .

Wright^{16,17} and Nicovich et al.³ obtained rate data for the reactions between OH radicals and xylene to be approximately twice that for the reaction between OH radicals and toluene. The above results reinforce the original hypothesis of Wright^{16,17} such that the xylenes are at least twice as reactive as toluene to radical attack.

7.7. Specific Reactions of the Xylenes.

The rate constant ratios k_{22}/k_2 and $k_{24}/(k_{10})^{1/2}$ quoted in this chapter correspond to the overall reaction of each xylene with H and HO₂ radicals respectively. It is important to consider the positions available for attack on each xylene by H and HO₂ radicals in order to determine specific rate constants and examine the selectivity of H and HO₂. Examination of the products formed from the oxidation of each xylene (Chapter 8) will enable determination of rate constants for attack at the methyl groups and the ring by H and HO₂ to be determined.

7.8. Thermochemical Aspects.

Although there is a shortage of kinetic data in the literature for the reactions between H and HO₂ with the xylenes at temperatures above 500K it is still possible to compare the relative rate data produced in this study with that for alkanes in order to predict A factors.

Tables 7.18 and 7.19 display values of relative rate constants and heats of reactions for reactions of H and HO₂ with a selection of hydrocarbons at 753K. Figures 7.1 and 7.2 show plots of log₁₀[Rate Constant Ratio (per C-H bond)] against ΔH for H and HO₂ respectively at 753K.

Table 7.18 : Comparisons of heat of reaction (ΔH) with k_{22}/k_2 at 753K

Hydrocarbon	k_{22}/k_2	k_{22}/k_2 per C-H Bond		$\log_{10} k_{22}/k_2$ per C-H Bond	$\Delta H / \text{kJ mol}^{-1}$
CH ₄	12	3		0.477	0
C ₂ H ₆	39	6.5	primary	0.812	-16.7
C ₃ H ₈	125	43	secondary	1.633	-29.2
C ₄ H ₁₀	217	45	secondary	1.653	-29.2
i-C ₄ H ₁₀	223	164	tertiary	2.214	-41.8
neo-C ₅ H ₁₂	52	4.3	primary	0.633	-16.7
(CH ₃) ₂ CHCH(CH ₃) ₂	425	174	tertiary	2.240	-41.8
Toluene	81	27		1.431	-71
p-Xylene	271	45		1.653	-71
m-Xylene	285	47		1.672	-71
o-Xylene	381	63.5		1.802	-71

Table 7.19 : Comparisons of heat of reaction (ΔH) with $k_{24}/(k_{10})^{1/2}$ at 753K

Hydrocarbon	$k_{24}/(k_{10})^{1/2}$	$k_{24}/(k_{10})^{1/2}$ per C-H Bond		$\log_{10} k_{24}/(k_{10})^{1/2}$ per C-H Bond	$\Delta H / \text{kJ mol}^{-1}$
CH ₄	0.020	0.0050		-2.30	58.6
C ₂ H ₆	0.57	0.095		-1.022	41.8
TMB	0.93	0.052		-1.284	41.8
DMB	4.8	1.83	tertiary	0.262	16.7
c-C ₅ H ₁₂	4.8	0.4	secondary	-0.40	29.3
HCHO	18.8	9.4	aldehyde	0.973	-12.5
Toluene					
p-Xylene	3.7	0.62		-0.208	-12.5
m-Xylene	3.9	0.65		-0.187	-12.5
o-Xylene	4.7	0.78		-0.108	-12.5

Figure 7. 1

Plot of $\log_{10} k_{22}/k_2$ (per C-H bond) against ΔH
for $\text{RH} + \text{H} \rightarrow \text{R} + \text{H}_2$ at 753K

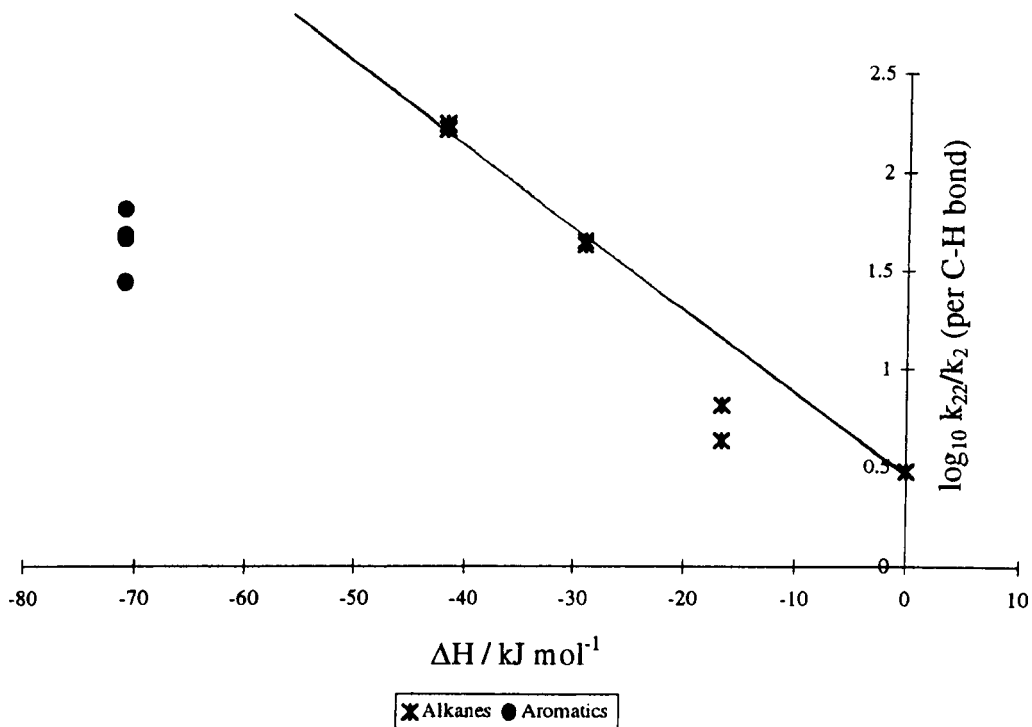
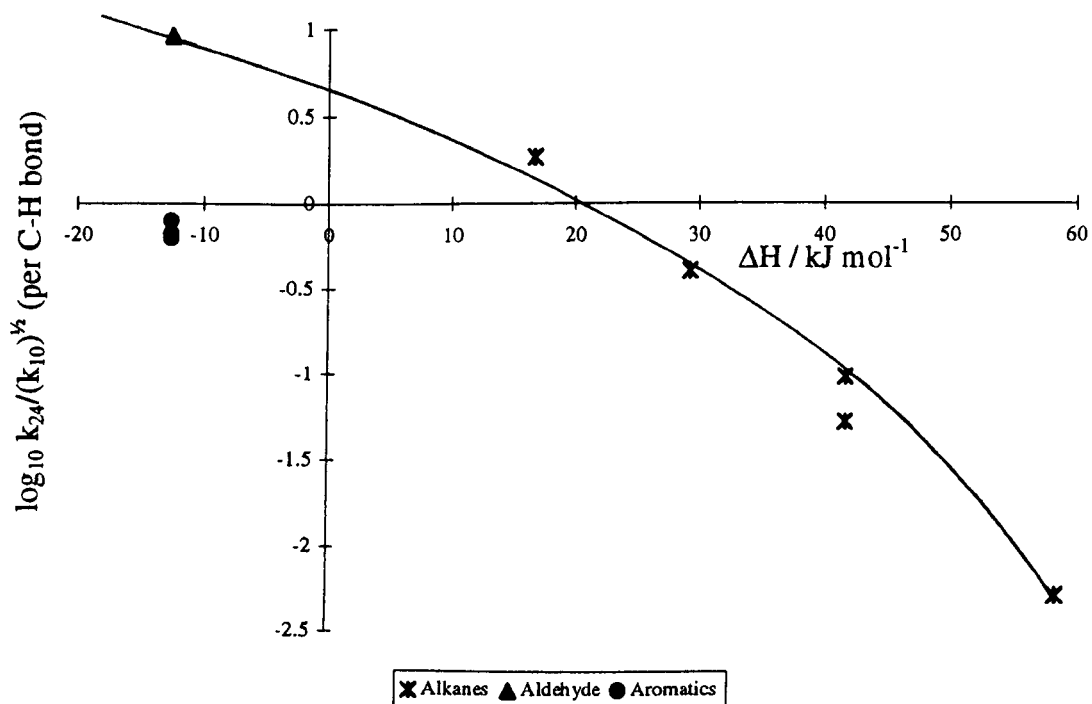


Figure 7. 2

Plot of $\log_{10} k_{24}/(k_{10})^{1/2}$ (per C-H bond) against ΔH
for $\text{RH} + \text{HO}_2 \rightarrow \text{R} + \text{H}_2\text{O}_2$ at 753K



Both plots clearly show that over a narrow range of ΔH , the graph for alkanes is approximately linear. However, the points for the aromatic reactions fall well below the expected values based on the alkane results. The simplest explanation is that for the alkanes (and HCHO) the A factor per C-H bond is approximately constant, but that for the aromatics is an order of magnitude lower.

This reduction in A factor may be a result of the loss of entropy of activation due to the electron delocalisation in the emerging methylbenzyl radical when H atoms are abstracted from the CH₃ side-chain.

This is consistent with the A factor (per C-H bond) for $\text{C}_3\text{H}_6 + \text{O}_2 \rightarrow \text{C}_3\text{H}_5 + \text{HO}_2$ ¹⁸ which is a factor of 10 below that for $\text{HCHO} + \text{O}_2 \rightarrow \text{HCO} + \text{HO}_2$,¹⁹ again due to delocalisation in the allyl radical. Further, thermochemical considerations of the reaction $\text{benzyl} + \text{HO}_2 \rightarrow \text{C}_6\text{H}_5\text{-CH}_3 + \text{OH}$ suggests that the A factor for the reverse reaction is very similar to that for the reaction between $\text{C}_3\text{H}_6 + \text{O}_2$ ^{18,20}.

7.9. References.

- ¹ Baldwin R.R., Hopkins D.E., Norris A.C. and Walker R. W., *Combust. Flame*, **15**, 33, (1970).
- ² Baldwin R.R., Jackson D., Walker R.W. and Webster S.J., *Trans. Faraday. Soc.*, **63**, 1676, (1967).
- ³ Nicovich J.M., Thompson R.L. and Ravishankara A.R., *J. Phys. Chem.* **85**, 2913, (1981).
- ⁴ Baulch D.L., Cobos C.J., Cox R.A., Esser C., Frank P., Just Th., Kerr J.A., Pilling M.J., Troe J., Walker R.W. and Warnatz J., *J. Phys. Chem. Ref. Data.*, **21**, 411, (1992).
- ⁵ Atkinson R., *Chem Rev*, **86**, 69, (1986).
- ⁶ Baulch D.L., Cobos C.J., Cox R.A., Frank P., Hayman G., Just Th., Kerr J.A., Murrells T., Pilling M.J., Troe J., Walker R.W. and Warnatz J., *Comb. Flame*, **98**, 59, (1994).
- ⁷ Cvetanovic R. J., *J. Phys. Chem.Data*, **16**, 261, (1987).
- ⁸ Nicovich J. M., Gump C.A. and Ravishankara A. R., *J. Phys. Chem.*, **86**, 1960, (1982).
- ⁹ Frerichs H., Schliephake V., Tappe M. and Wagner H.G., *Z. Phys. Chem (Neue Folge)*, **165**, 9, (1989).
- ¹⁰ Ackermann L., Hippler H., Pagsberg P., Reihls C. and Troe J. *J. Phys. Chem.*, 5247, **94**, (1990).
- ¹¹ Tully F.P., Ravishankara A.R., Thompson R.L., Nicovich J.M., Shah R.C., Kreutter N.M. and Wine P.H., *J. Phys. Chem.*, **85**, 2262, (1981).
- ¹² Lodhi Z.H. and Walker R.W., *J. Chem. Soc. Faraday Trans.*, **87**, 681, (1991).
- ¹³ Baldwin R.R., Scott M. and Walker R. W., *Twenty-first Symposium (International) on Combustion/The Combustion Institute*, 991, (1986).

- ¹⁴ Hippler H., Reihls C. and Troe J., *Z. Phys. Chem. (Neue Folge)*, **167**, 1, (1990).
- ¹⁵ Rao V.S. and Skinner G.B. *J. Phys. Chem.*, **88**, 4362, (1984).
- ¹⁶ Wright F.J., *J. Phys. Chem.*, **64**, 1944, (1960).
- ¹⁷ Wright F.J., *J. Phys. Chem.*, **66**, 2023, (1962).
- ¹⁸ Stothard N.D. and Walker R.W., *J. Chem. Soc. Faraday Trans.*, **87**, 241, (1991).
- ¹⁹ Baldwin R.R., Fuller A.R., Longthorn D. and Walker R.R., *J. Chem. Soc. Faraday Trans. 1*, **70**, 1257, (1974).
- ²⁰ Walker R.W., "Some Burning Problems in Combustion Chemistry," *Research In Chemical Kinetics, Volume 3*, pp1, Compton R.G. and Hancock G. (editors), © 1995 Elsevier Science B.V., Amsterdam.

Chapter 8.

Discussion of the Analytical Results for the Oxidation of the Xylenes.

8.1. Introduction.

A general overview of the oxidation chemistry of aromatic hydrocarbons such as toluene and xylene was given in Chapter 2; a more detailed account will be given in this chapter with reference to the results discussed in Chapter 5.

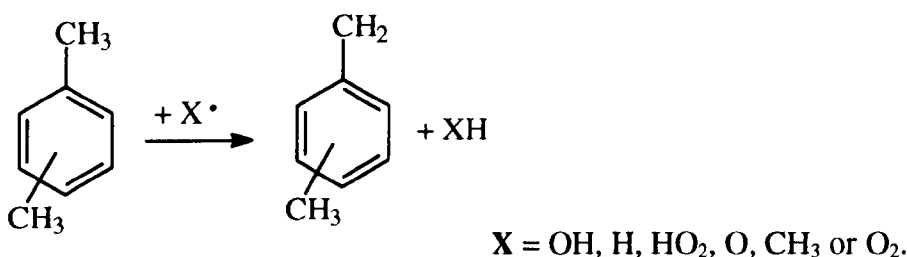
The data illustrated in Chapter 5 show the detectable product yields for the separate addition of each xylene to hydrogen + oxygen mixtures at 753K. In general, the primary products generated from each xylene are as expected by analogy with the oxidation chemistry of toluene¹, where the major initial products were benzaldehyde and benzene. Other research groups have obtained product data from xylene oxidation over a wide temperature range by the use of different techniques. The early quantitative investigation of the oxidation chemistry of the xylenes was carried out by Wright^{2,3}. Subsequent workers⁴⁻⁸ have refined the findings of Wright, identifying numerous products and the changes in the mechanism with variations in temperature. The general consensus is that the overall high temperature oxidation chemistry of the xylenes is similar to that of toluene with o-xylene displaying perhaps two additional distinctive primary products and p-xylene one further distinctive product.

8.2. The Primary Reactions of the Xylenes.

8.2.1. Abstraction of H from the side chain.

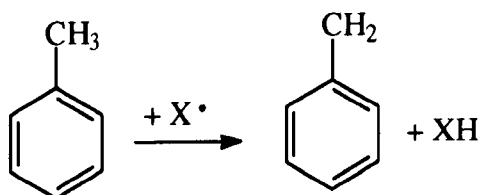
The main reaction of the xylenes appears to be that of abstraction of H from one of the methyl groups producing the methylbenzyl radical (**MeB**), illustrated in Scheme 8.1.

Scheme 8.1



This chemistry is analogous to that of toluene where benzyl radicals are produced and it is not surprising that methylbenzyl and benzyl radicals should have similar reactions.

Scheme 8.2



It is also important to note that in both of the above cases the odd electron will be delocalised into the benzene ring.

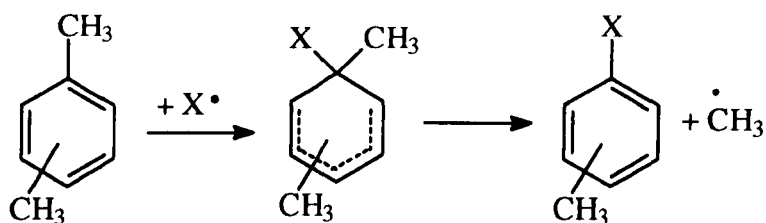
8.2.2. Addition of a radical to the ring.

There are different primary reactions which the xylenes may undergo; the importance of each is dependent upon temperature and conditions. At low temperatures a common

reaction is the addition of the attacking **X** radical to the ring, where **X** can be OH, H or O radicals.

The findings illustrated in Chapter 5, together with those of other workers, indicate that toluene is a major primary product from each xylene. This is probably produced as the result of H atom addition to the ring at the same position as one of the methyl groups, followed by C-C homolysis, as illustrated in Scheme 8.3.

Scheme 8.3



If **X = H** then toluene will be the product and its concentration will increase with an increase in the relative H radical concentration. As observed, the yield of toluene is highest when $[H_2]:[O_2]$ is high so that $[H]$ is high. The relative yield of toluene from each xylene is approximately the same for a given mixture composition (**Figures 5.4, 5.10, and 5.17**). The shape of the profiles and the quantity of toluene produced indicate that Scheme 8.3 is a major reaction pathway for the formation of toluene as a primary product when **X = H**.

Data are available for the formation of benzene from toluene¹ through H atom addition. Consequently, it is possible to estimate a rate constant for the overall process in Scheme 8.3 for the formation of toluene from xylene where H is the attacking radical. If it is assumed that the rate of formation of benzene from toluene¹ ($k_{8.01} = 2.8 \cdot 10^8 \text{ l mol}^{-1} \text{ s}^{-1}$ at 753K) is half that for the formation of toluene from the xylenes, reaction (8.02), since

there are twice the number of positions of attack in xylene as in toluene and the rate of attack is the same for each xylene then $k_{8.02} = 5.6 \cdot 10^8 \text{ l mol}^{-1} \text{ s}^{-1}$ at 753K.

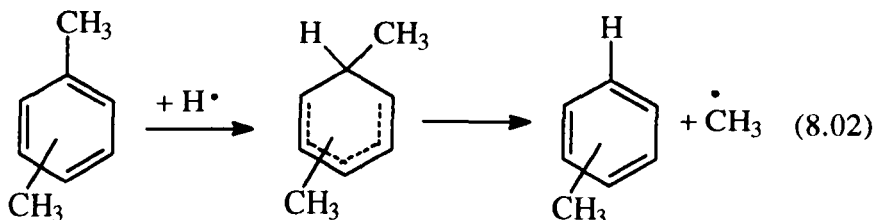
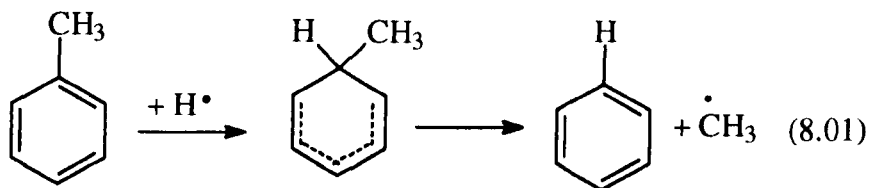


Table 8.1 shows the relative proportion of addition/elimination relative to the overall loss of xylene with respect to H radical attack on each xylene.

Table 8.1

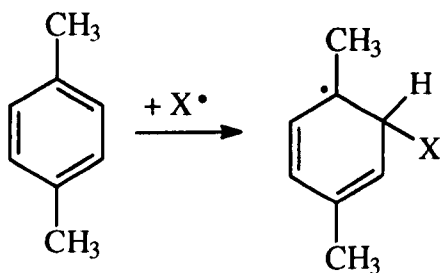
Reaction	$k_{753\text{K}} / \text{l mol}^{-1} \text{ s}^{-1}$
$\text{H} + \text{Xylene} \rightarrow \text{Toluene} + \text{CH}_3$	$5.6 \cdot 10^8$
$\text{H} + \text{p-Xylene} \rightarrow \text{Products}^9$	$1.3 \cdot 10^9$
Percentage of reaction producing Toluene	43%
$\text{H} + \text{m-Xylene} \rightarrow \text{Products}^9$	$1.4 \cdot 10^9$
Percentage of reaction producing Toluene	40%
$\text{H} + \text{o-Xylene} \rightarrow \text{Products}^9$	$1.8 \cdot 10^9$
Percentage of reaction producing Toluene	31%

Chapter 5 shows the actual yields of the important detected products for the oxidation of each xylene. It is clear that only about 50% of the xylene is accounted for as detected products. It is important to note that it is likely that there are products which could not be detected, as discussed later, together with the effect of absorption/adsorption of products on to the glass of the apparatus and sample bulbs used.

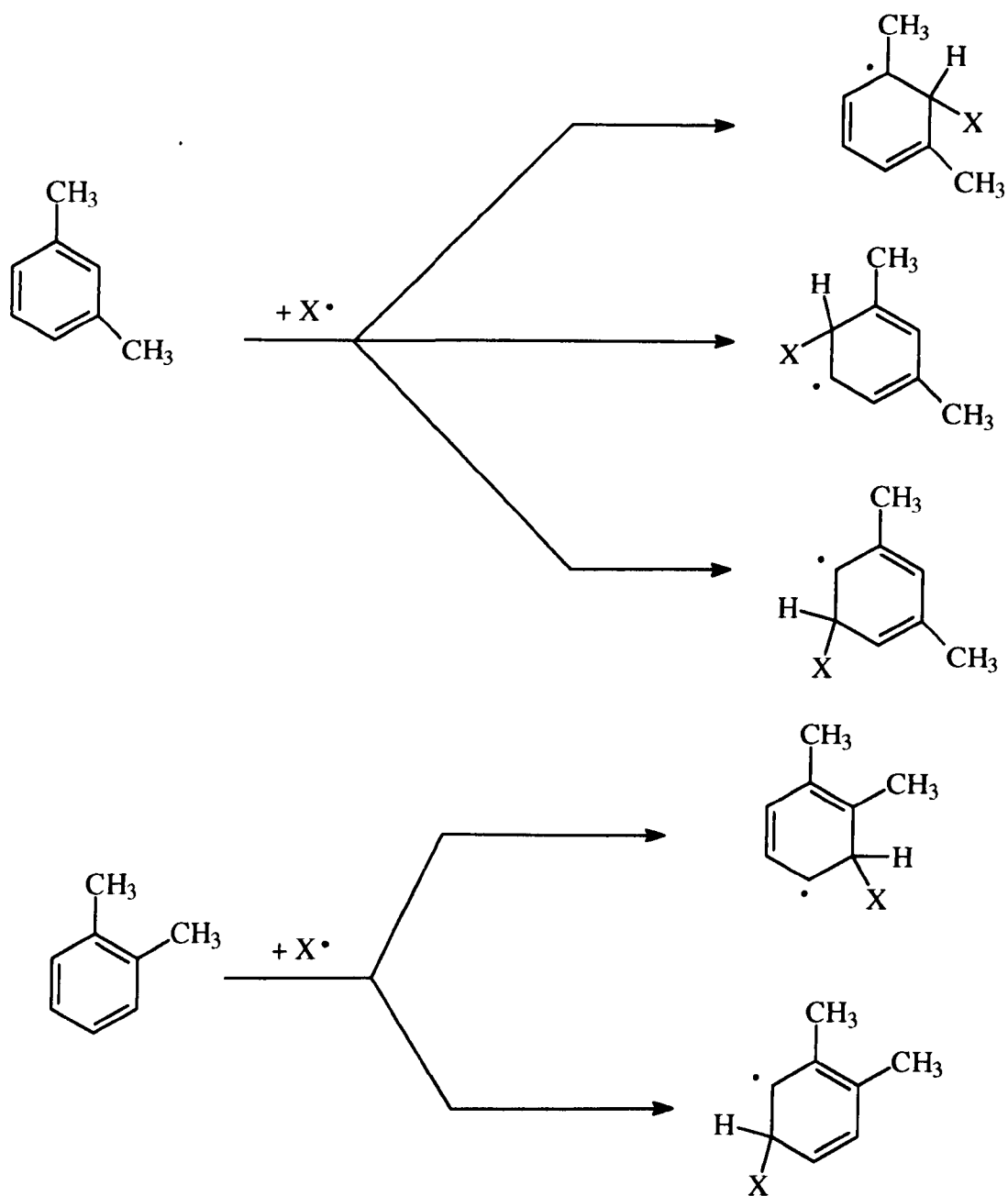
If $X = OH$ then methylphenol may be produced, although no experimental evidence was found in the present study for the formation of the methylphenols. However, the reaction between the chloromethylbenzenes and OH radicals have produced methylphenols at room temperature¹⁰. Consequently the occurrence of such products can not be discounted despite the fact that they have not been detected in this oxidation work.

Further to the displacement of CH_3 , it is also possible for the attacking X radical to add to the ring with the possible outcome of displacing H atoms. Scheme 8.4 illustrates the different positions for addition for each xylene.

Scheme 8.4 : $X = OH$, generally.



Scheme 8.4 continued.



It is clear to see that this type of chemistry is structurally different for each xylene. p-Xylene (**PX**) displays only one position of attack as all the hydrogens are in similar chemical environments; o-xylene displays two different positions for X addition and m-xylene three distinctive positions.

Grovenstein and Mosher¹¹ examined the reactions of O atoms with aromatic hydrocarbons at room temperature and illustrated clearly that the position of the methyl

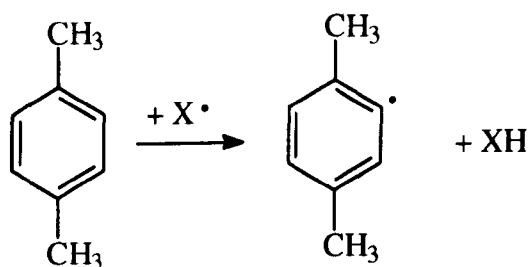
side chain affected the relative attack at the ring; this point was discussed in Chapter 2. If reactions of this nature occurred at 753K there would be a wide array of isomeric products to detect. None were found in this study. Nicovich et al.⁶ showed that electrophilic addition of OH to the ring was a dominant reaction at room temperature.

At temperatures above 500K, however, the importance of addition reactions of this nature decreases significantly relative to the abstraction and displacement routes⁶. As indicated earlier, no evidence of addition products were found in the present study. Consequently, no further discussion will be given.

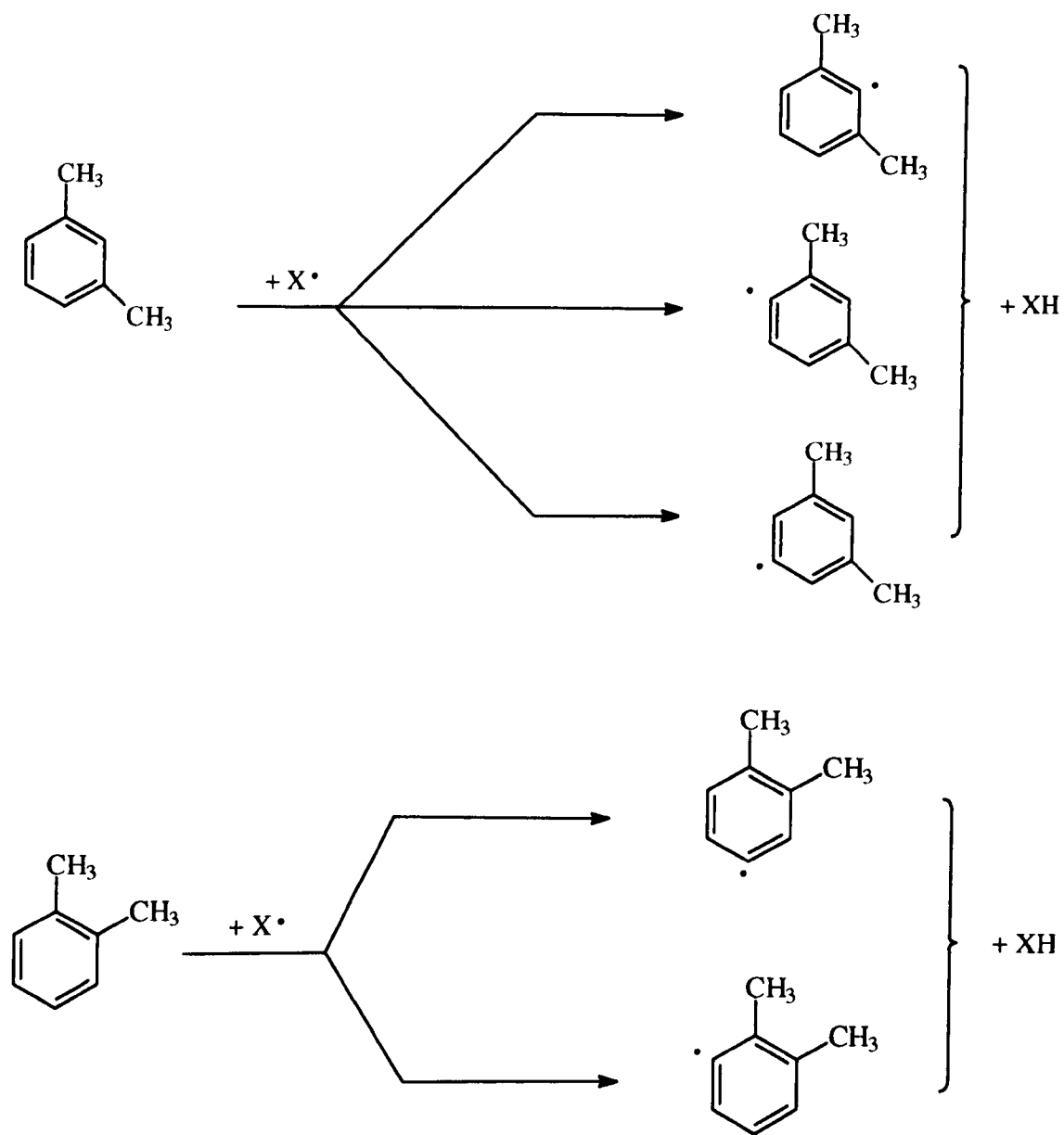
8.2.3. Abstraction of H from the Ring.

Scheme 8.5 illustrates that the position of attack is similar to that for the addition of X described above (Scheme 8.4) and in relation to the number of isomeric radicals produced from each xylene.

Scheme 8.5: X = OH predominantly.

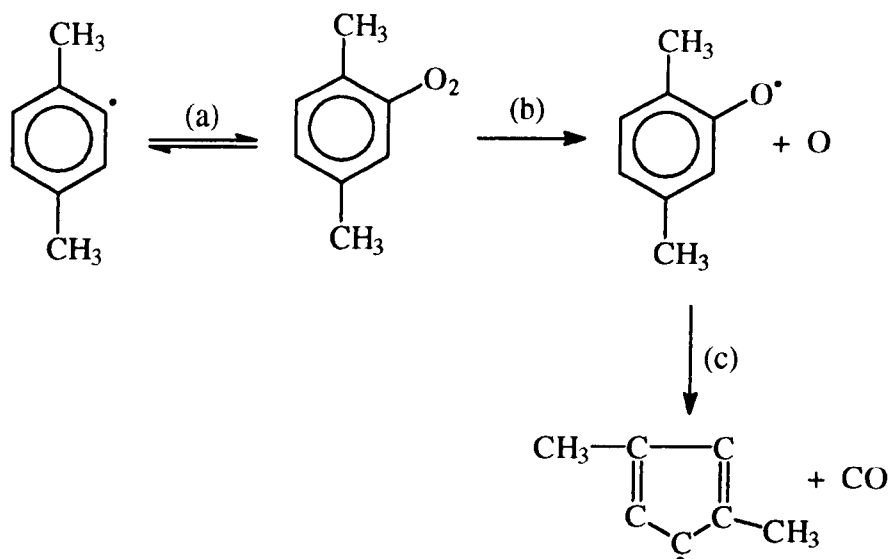


Scheme 8.5 continued.

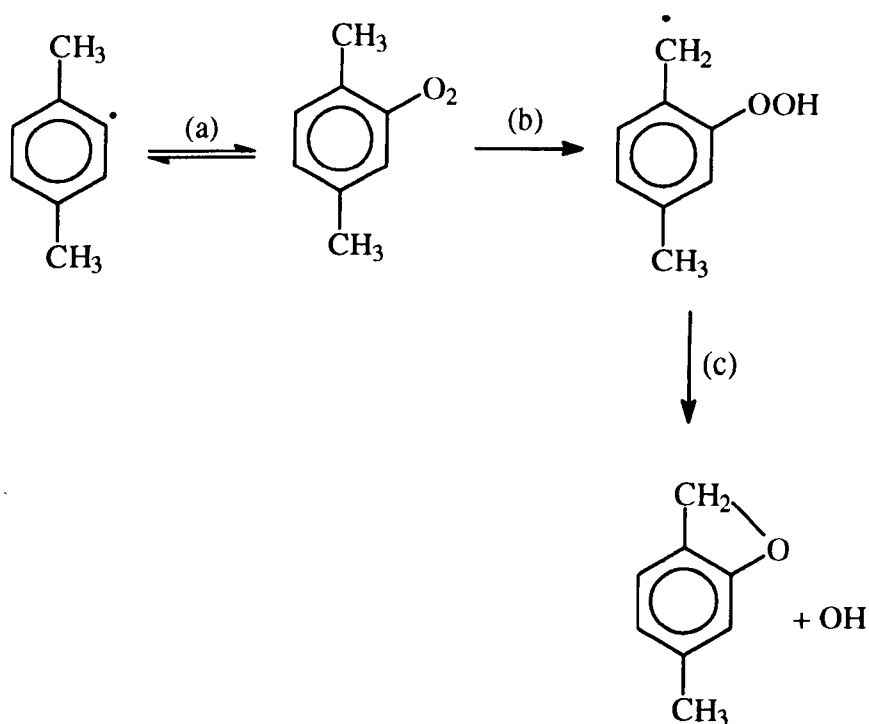


The most likely reaction of the above radicals is addition of molecular oxygen, followed by the formation of CO and cyclic radicals with a ring containing five carbon atoms (Scheme 8.6) or cyclisation with the one of the methyl side chains via QOOH formation to produce a o-heterocycle (Scheme 8.7). The oxidation chemistry is illustrated for the radical formed from p-xylene.

Scheme 8.6



Scheme 8.7



Equilibrium (a) is 'normal' and reaction (b) in both schemes is relatively fast because of the formation of the electron-delocalised phenoxyl or QOOH radical. CO has been found in high yields as an initial product when benzene is added to hydrogen + oxygen mixtures¹ at 753K.

In general the abstraction of H from an aromatic ring is slow even for relatively reactive radicals such as OH. Kinetic data are available for the abstraction of H from benzene. If it is assumed that the rate of abstraction of H from the ring in the xylenes is $\frac{2}{3}$ of the value of the equivalent reaction for benzene then an estimation of a proportion of H abstraction from the ring can be estimated for OH and H as the attacking radicals. Table 8.2 shows data for estimating the percentage of ring attack by OH on *p*-xylene and Table 8.3 shows the data for ring abstraction by H atoms.

Table 8.2

Reaction	$k_{753K} / \text{l mol}^{-1} \text{s}^{-1}$
OH + Benzene \rightarrow Phenyl + H ₂ O ¹²	$7.5 \cdot 10^8$
OH + <i>p</i> -Xylene \rightarrow Products ⁷	$5.7 \cdot 10^9$
Percentage ring H abstraction by OH	8.8%
OH + <i>p</i> -Xylene \rightarrow <i>p</i> -CH ₃ -C ₆ H ₃ CH ₃ + H ₂ O	$5.0 \cdot 10^8$

Table 8.3

H + Benzene → Phenyl + H₂O ¹	1.3*10⁷
H + <i>p</i> -Xylene → Products ⁹	1.3*10 ⁹
Percentage H abstraction by H	0.7%
H + <i>p</i> -Xylene → <i>p</i> -CH ₃ -C ₆ H ₃ CH ₃ + H ₂	9.1*10 ⁶
H + <i>m</i> -Xylene → Products ⁹	1.4*10 ⁹
Percentage H abstraction by H	0.6%
H + <i>m</i> -Xylene → <i>m</i> -CH ₃ -C ₆ H ₃ CH ₃ + H ₂	8.4*10 ⁶
H + <i>o</i> -Xylene → Products ⁹	1.8*10 ⁹
Percentage H abstraction by H	0.5%
H + <i>o</i> -Xylene → <i>o</i> -CH ₃ -C ₆ H ₃ CH ₃ + H ₂	9.0*10 ⁵

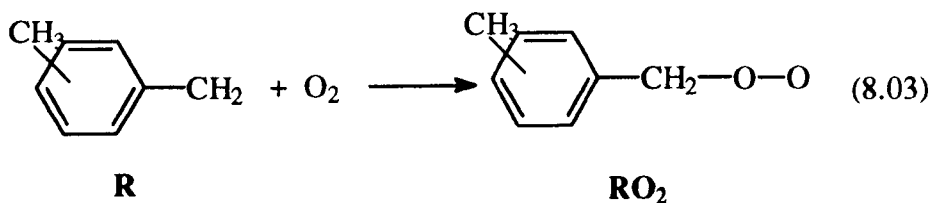
H atom ring abstraction by OH radicals is less than 10% of the overall rate constant and can therefore be considered as having only a minor effect on the overall oxidation chemistry of the xylenes at 753K. H abstraction from the ring by H radicals, being less than 1%, can be considered as very minor relative to the overall rate or reaction. As HO₂ radicals are even more selective than H radicals, abstraction of H from the benzene ring can be considered as negligible. Consequently abstraction from the ring is not considered as a significant reaction in this study at least in the initial stages of oxidation.

As indicated earlier, at temperatures above 500K, the main reactions of the xylenes are those illustrated in Scheme 8.1 and Scheme 8.3. It is these reactions which have been studied as part of the kinetic work in Chapter 7. Since accurate rate constants are known for OH and O as the attacking radicals, it was possible to determine accurate rate constants for H and HO₂ from the experimental work.

8.3. The Reactions of R Radicals.

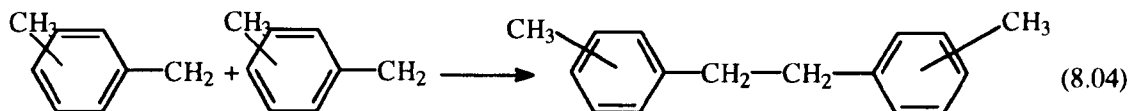
The main R radical is the methylbenzyl radical and the free electron is delocalised around the benzene ring, as in benzyl. Methylbenzyl is fairly inert towards O₂ because the equilibrium $\text{CH}_3\text{-C}_6\text{H}_4\text{-CH}_2 + \text{O}_2 \rightleftharpoons \text{CH}_3\text{-C}_6\text{H}_4\text{-CH}_2\text{OO}$ (8.03) will be well to the left as observed for the benzyl radical and can therefore be consumed to a considerable degree through radical-radical reactions at most temperatures.

Despite the relative inertness of methylbenzyl radicals towards attack by O₂, it is most likely that the main reaction is the formation of the tolualdehydes (and **OXO** from **OTA**), perhaps formed partly in radical-radical processes. This has been shown for the reactions of benzyl radicals where they react with O₂ and HO₂ to produce benzaldehyde as discussed in Chapter 6.

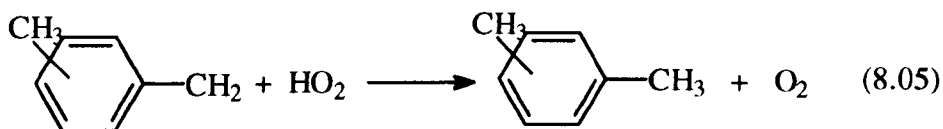


Possible radical-radical reactions of the R radicals include:

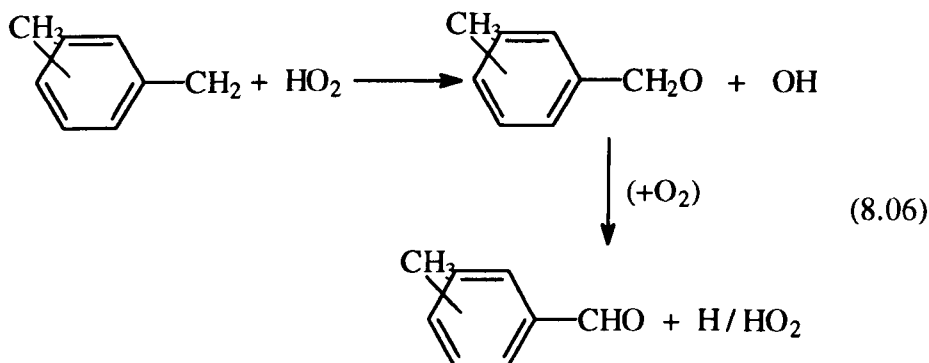
- 1) With another R radical producing di-methylbenzyl.



- 2) With HO₂ reproducing the parent xylene



- 3) With HO₂ producing tolualdehyde.



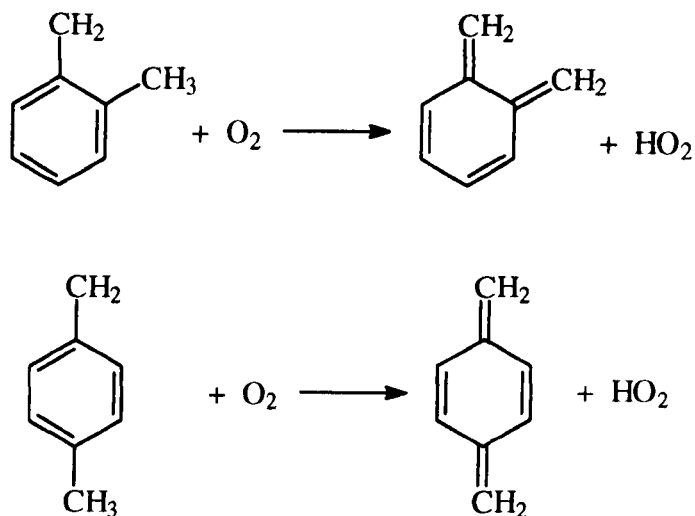
- 4) With CH₃ to produce ethylmethylbenzene.



Reactions (8.04), (8.05), and (8.07) are all termination reactions and reaction (8.06) is a propagation process equivalent to the production of benzaldehyde from benzyl radicals discussed in Chapter 6.

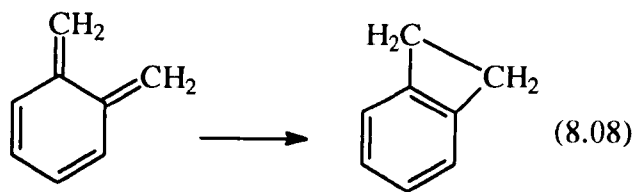
An interesting reaction between *o*-¹³ and *p*-methylbenzyl⁸ radicals and O₂ is the formation of dimethylcyclohexadienes (xylylene). This is not possible for the *m*-methylbenzyl radical.

Scheme 8. 8



The findings of Emdee et al.¹³ showed that *o*-xylylene (5,6-bis(methylene)-1,3-cyclohexadiene a.k.a. 5,6-dimethylene-1,3-cyclohexadiene) was produced from *o*-xylene oxidation; Emdee et al.,⁸ and more recently Eng et al.,¹⁴ also inferred that *p*-xylylene (3,6-dimethylene-cyclohexa-1,4-diene a.k.a. 1,4-cyclohexadiene,3,6-bis(methylene)) could be formed in the oxidation of *p*-xylene. Based upon the activation energies for the formation of alkenes and related compounds from alkyl + O₂ the activation energy for the formation of the xylylenes is likely to be low.

Two subsequent reactions for *o*-xylylene have been suggested by Emdee et al.¹³ At temperatures below about 940K the isomerisation to 1,2-benzocyclobutene may occur¹⁵.



However at temperatures above 1000K, it is suggested that 100% isomerisation to styrene occurs¹⁶.

Emdee et al.⁸ suggested that *p*-phthalaldehyde (benzene-1,4-dicarbaldehyde) was not produced as a result of *p*-tolualdehyde (PTA) oxidation but more likely from subsequent oxidation of *p*-xylylene with O.



Polymerisation of *p*-xylylene was also noted by Errede and Cassidy¹⁷. However, detection of any polymers of this type is not feasible under the experimental conditions used in this study.

Further, it was not possible to examine many of the above reactions directly since the methylbenzylalcohols, phthalaldehydes, 1,2-benzocyclobutene and di-methylbenzyls were not detected. It was not possible to detect even qualitatively dibenzyl because of its involatility since it has a room temperature vapour pressure of only 0.0212 Torr¹⁸. Given the experimental procedure it was not possible to attempt to get a sample of dibenzyl, or the other compounds with similar vapour pressures, into the gas phase without the fear of contamination of the apparatus.

8.4. The Reactions of RO₂ Radicals.

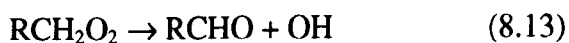
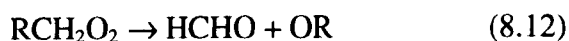
8.4.1. *p*- and *m*-Xylene.

The formation of the RO₂ radical was discussed earlier as the addition of O₂ to the methylbenzyl radical (Section 8.3). Although the main reaction of the RO₂ radical is to decompose to R + O₂ (reaction 8.03). The formation of benzaldehyde from the oxidation of benzyl radicals produced in the decomposition of neopentylbenzene (discussed in Chapter 6) suggests that tolualdehyde formation via RO₂ radicals should occur.

The reactions of the RO₂ radical can also be likened to that of the methylperoxyradical¹⁹ in reaction (8.11):



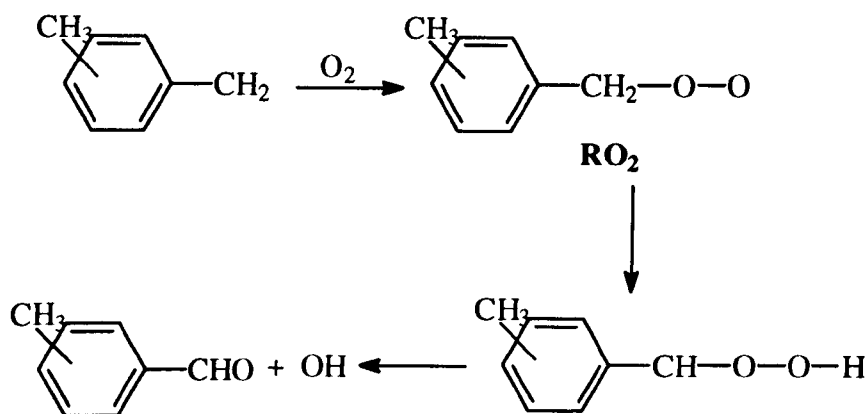
in that it was suggested by Barnard and Hawtin⁴ that, in the case of *p*-xylene being the hydrocarbon, either or both of the overall reactions below might occur (between 733 and 785K) (where R = CH₃C₆H₄).



Barnard and Hawtin⁴ did not detect *p*-tolualdehyde (PTA) and concluded that reaction (8.12) was the major pathway. However they concluded that the lack of detection of PTA may have been due to its high reactivity, particularly as analysis was made relatively late in reaction. Subsequent work⁷ and the findings of this study have given conclusive evidence that the overall reaction (8.13) is indeed a major reaction pathway; Scheme 8.9 below describes the full reaction associated with reaction (8.13). Since HCHO was not measured, no comment can be made on the importance of reaction (8.12).

For p- and m-xylene, the main product from RO_2 is most likely to be tolualdehyde even at temperatures where the $R + O_2 \rightleftharpoons RO_2$ equilibrium is far to the left because in compensation the reaction $RO_2 \rightarrow QOOH$ is fast because of the low C-H bond energy. The occurrence of the $RO_2 \rightarrow QOOH$ reaction has been discussed at length in Chapter 6 with respect to the oxidation of benzyl radicals where the production of QOOH radicals is seen as the major route to the formation of benzaldehyde.

Scheme 8.9

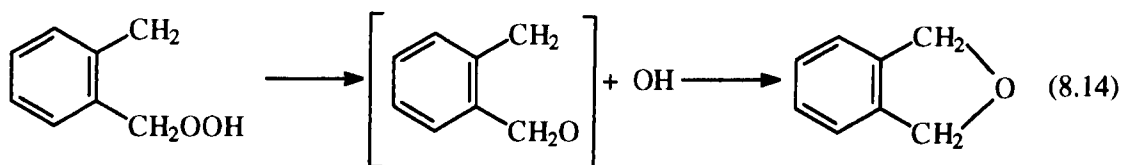


This is consistent with the relatively large quantities of PTA, and MTA from p- and m-xylene (Figures 5.3 and 5.9), respectively. Other possible reactions whereby an o-heterocycle may be produced are unlikely due to excessive strain within the cyclic product particularly if the heterocyclic unit is part of a bridge between the two methyl groups.

8.4.2. o-Xylene.

The RO_2 radical produced from o-xylene oxidation is similar to the ones produced from p- and m-xylene. However, the structure offers the possibility for the formation of two compounds, o-tolualdehyde (OTA) and o-xylene oxide (OXO).

As with most QOOH radicals, the weakest bond in the isomeric product is the O-O bond which breaks to give the ring compound OXO.

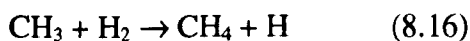
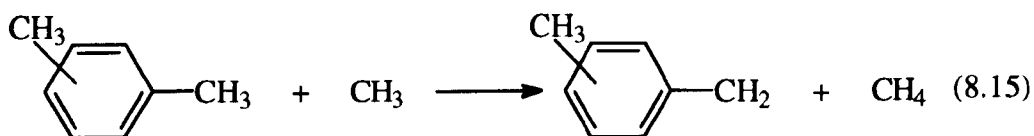


The findings of this study agree with those of Loftus and Satterfield²⁰ who detected appreciable quantities of OXO during their study of the oxidation of o-xylene by air between 455 and 525K.

8.5. Aliphatic Products.

The only quantitatively determined aliphatic product was methane (**Figure 5.7, 5.13 and 5.20**). Trace amounts of ethane and ethene were observed but not of significant quantity to be accurately measured by the gas chromatographic system used.

Methane will be formed in two reactions.

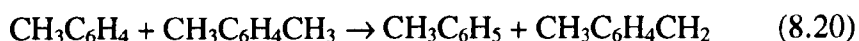


Burr and Strong²¹ were able to determine the relative rate of reactions (8.15) and (8.17) such that $k_{(8.15/8.17)} = 5.3$ between 955 and 980K for all three xylenes. Consequently it is possible to estimate $k_{(8.15/8.16)}$ at 753K. Since $E_A(8.17) - E_A(8.16) = 4 \text{ kJ mol}^{-1}$ [22],[23]

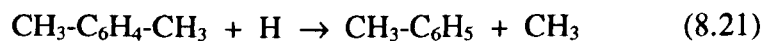
therefore $k_{(8.15 / 8.16)} = 8.5$ between 955 and 980K assuming equal A factors. Since $E_A(8.16) - E_A(8.15) = 6 \text{ kJ mol}^{-1}$ [22],[23] then $k_{(8.15 / 8.16)} = 10.2$ at 753K. Since $k_{8.16} = 9.7 \cdot 10^5 \text{ l mol}^{-1} \text{ s}^{-1}$ at 753K¹² then $k_{(8.15)} = 9.9 \cdot 10^6 \text{ l mol}^{-1} \text{ s}^{-1}$ at 753K. However, given the high concentration of H_2 relative to that of xylene present in this reaction system it most likely that all CH_4 is produced from $\text{CH}_3 + \text{H}_2 \rightarrow \text{CH}_4$.

8.6. Secondary Products.

The secondary products detected were in agreement with those formed initially in the oxidation of toluene under similar conditions¹. The main products were benzaldehyde (Figures 5.5, 5.11 and 5.18) and benzene (Figures 5.6, 5.12 and 5.19) produced in the same manner as the tolualdehydes and toluene discussed earlier in Scheme 8.1, Scheme 8.9 and Scheme 8.3. Toluene was considered to be a secondary product in PX oxidation by Barnard and Hawtin⁴ who suggested that it was formed from the subsequent oxidation of PTA:



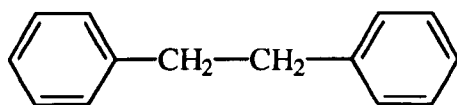
However, this study shows conclusively that under the conditions used toluene is a major primary product, formed as a result of the displacement of a methyl group from the ring by H as described in Scheme 8.3.



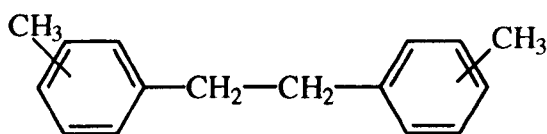
8.7. Other Products.

There are a number of possible products that were not detected using the available analysis techniques. Other workers⁸ have observed styrene, acetylene, cyclopentadiene, vinylacetate as major products. Other minor products that were not detected were phenol, cresols, benzylalcohol, naphthalene and benzofuran.

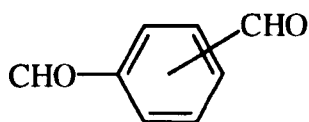
Some other possible aromatic products, common to all three xylenes, which might have been generated as a result of further oxidation are dibenzyl, the di-aldehydes, mentioned earlier, and the ethyltoluenes.



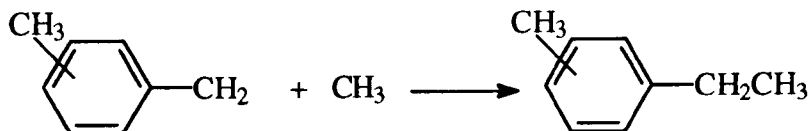
Dibenzyl



Dimethylbenzyl



'Di-aldehyde.'



8.8. References.

- ¹ Baldwin R.R., Scott M. And Walker R. W., *Twenty-first Symposium (International) on Combustion/The Combustion Institute*, 991, (1986).
- ² Wright F.J., *J. Phys. Chem.*, **64**, 1944, (1960).
- ³ Wright F.J., *J. Phys. Chem.*, **66**, 2023, (1962).
- ⁴ Barnard J.A. and Hawtin P., *Comb. Flame*, **5**, 249, (1961).
- ⁵ Barnard J.A. and Sankey B.M., *Comb. Flame.*, **12**, 345, (1968).
- ⁶ Barnard J.A. and Sankey B.M., *Comb. Flame.*, **12**, 353, (1968).
- ⁷ Nicovich J.M., Thompson R.L. and Ravishankara A.R., *J. Phys. Chem.*, **85**, 2913, (1981).
- ⁸ Emdee J.L., Brezinsky K. and Glassman I., *J. Phys. Chem.*, **95**, 1626, (1991).
- ⁹ Ellis C., *Ph.D. Thesis, The University Of Hull*. Chapter 7, (2000).
- ¹⁰ Hulder P. and Louw R., *Rec. Trav. Chim. Pays/Bas.*, **105**, 220, (1986).
- ¹¹ Grovenstein E. Jr., and Mosher A.J., *J. Amer. Chem. Soc.*, **92**, 3810, (1970).
- ¹² Baulch D.L., Cobos C.J., Cox R.A., Esser C., Frank P., Just Th., Kerr J.A., Pilling M.J., Troe J., Walker R.W. and Warnatz J., *J. Phys. Chem. Ref. Data.*, **21**, 411, (1992).
- ¹³ Emdee J.L., Brezinsky K. and Glassman I., *Twenty-Third Symposium (International) on Combustion/The Combustion Society*, 77, (1990).
- ¹⁴ Eng R.A., Fittschen C., Gebert A., Hibomvschi P., Hippler H. and Unterreiner A.-N., Paper presented at *27th International Symposium on Combustion, Boulder, Colorado*, Book of abstracts pp31, (1998).

- ¹⁵ Cava M.P. and Dean A.A., *J. Am. Chem. Soc.*, **81**, 4266, (1959).
- ¹⁶ Chapman O.L., Tsou U.E. and Johnson J.W., *J. Am. Chem. Soc.*, **109**, 553, (1987).
- ¹⁷ Errede L.A. and Cassidy J.P., *J. Phys. Chem.*, **67**, 73, (1963).
- ¹⁸ CRC Handbook of Chemistry and Physics, 51st Edition (1970-1971), The Chemical Rubber Company, pp163.
- ¹⁹ Enikolopyan N.S., *Seventh Symposium (International) on Combustion*, p157, Butterworths: London. (1959).
- ²⁰ Loftus J. and Satterfield C.N., *J. Phys. Chem.*, **69**, 909, (1965).
- ²¹ Burr J.G. and Strong J.D., *J. Am. Chem. Soc.*, **86**, 5065, (1964).
- ²² Kerr J.A. and Parsonage M.J., *Evaluated Kinetics Data on Gas Phase Hydrogen Transfer Reactions of Methyl Radicals*, Butterworths, London, (1976).
- ²³ Kerr J.A. and Moss S.J. (Editors), *CRC Handbook of Bimolecular and Termolecular Gas Reactions*, CRC Press Inc, Boca Raton, Florida, **Volume 1**, 186, (1981).

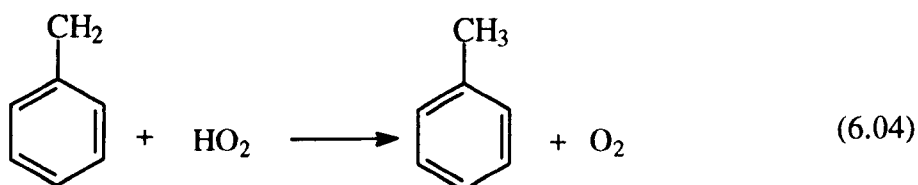
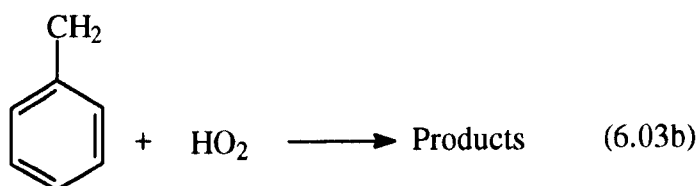
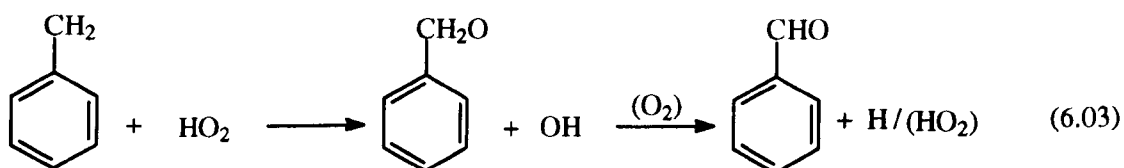
Chapter 9.

Summary and Conclusions[⊕].

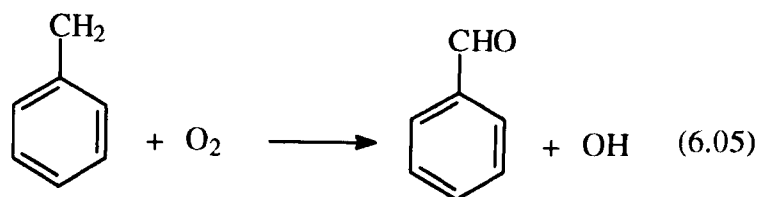
9.1. Decomposition and Oxidation of Neopentylbenzene.

9.1.1. Kinetic Study.

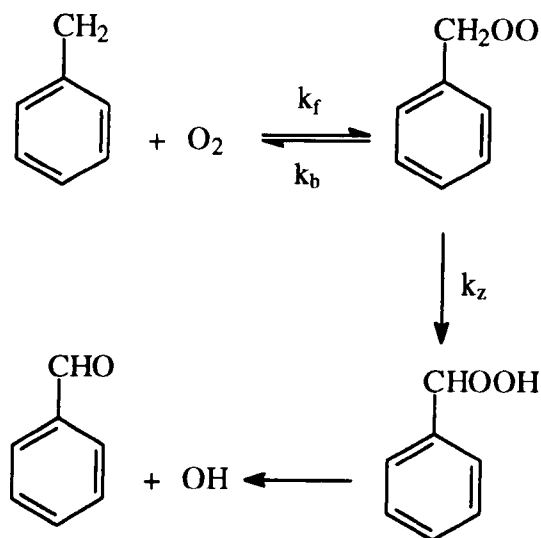
The decomposition of neopentylbenzene (NPB) in the presence of oxygen (and propene) was used to obtain rate data for the reactions of HO₂ with benzyl radicals.



[⊕] All reactions are numbered corresponding to either Chapter 6 for benzyl radicals or Chapter 7 for Xylene oxidation.



Scheme for Reaction (6.05)



Reaction (6.05) is considered to take place via the scheme shown above and no values for the overall rate constant for $k_{6.05}$ are available from the literature. However, values for k_f and k_b were available¹. A reasonable estimation for k_z was also possible, (described in chapter 6) enabling a value for $k_{6.05} = 2.0 \cdot 10^4 \text{ l mol}^{-1} \text{ s}^{-1}$ at 753K to be obtained. Given that $k_{6.07} = 8.3 \cdot 10^4 \text{ l mol}^{-1} \text{ s}^{-1}$ or $105.5 \text{ Torr}^{-1} \text{ min}^{-1}$ at 753K² it was possible to determine $k_{6.04}$ from $(k_{6.05}k_{6.07})/k_{6.04} = 0.0025 \text{ Torr}^{-1} \text{ min}^{-1}$ such that $k_{6.04} = 8.44 \cdot 10^8 \text{ l mol}^{-1} \text{ s}^{-1}$ at 753K. Consequently if $k_{6.03}/k_{6.04} = 5.17$ then $k_{6.03} = 4.36 \cdot 10^9 \text{ l mol}^{-1} \text{ s}^{-1}$ at 753K (summarised in Table 9.1).

Table 9.1 : Summary of Rate Constants for the important reactions of the Benzyl radical with HO₂ at 753K³.

Benzyl + HO₂ → Benzaldehyde + H	k_{3,03}	4.36*10⁹ l mol⁻¹ s⁻¹
Benzyl + HO₂ → Toluene + O₂	k_{6,04}	8.44*10⁸ l mol⁻¹ s⁻¹

One major conclusion is that the rate constant for the reactions of HO₂ with benzyl radicals are similar to those for the corresponding reactions of allyl radicals⁴. Although there is delocalisation of the free electron in the benzyl radical, which is therefore stabilised, there is effectively zero activation energy for reactions (6.03), (6.03b) and (6.04). with an A factor for reaction (6.04) of A_{6,04} = 1.5*10⁹ l mol⁻¹ s⁻¹ at 753K.

9.1.2. Products.

Generally the detected products (Table 9.2) from the decomposition of NPB in the presence of oxygen corresponded to the same products as from the oxidation of toluene⁵ and tetramethylbutane(TMB)⁶ at the same temperature. However, the structural nature of NPB produced an extra detected initial product, that of 2-methyl-1-phenylpropene (MPP). The total detected product yields were less than 100% probably due to the formation of compounds such as dibenzyl, which has a vapour pressure of 0.0212 Torr at 298K and which would condense or absorb on the apparatus rendering detection very difficult.

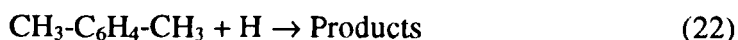
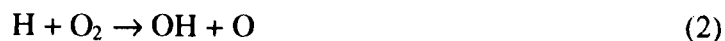
Table 9.2 : Summary of Products produced from the Decomposition of Neopentylbenzene in the Presence of Oxygen³ at 753K.

Benzaldehyde	Toluene	2-Methyl-1-phenylpropene
Ethylbenzene	Benzene	i-Butene
Propene	Ethane	Methane

9.2. The Oxidation Chemistry of the Xylenes.

9.2.1. Kinetics Study.

Arising from the accuracy of the literature data for OH + xylene it was possible to use the computer program to obtain accurate rate data for the reactions between H (22) and HO₂ (24) with the xylenes ($R_{11} = k_{22}/k_2$ and $R_{12} = k_{24}/(k_{10})^{1/2}$).



The results are summarised in Table 9.3 and 9.4.

Table 9.3 : Relative rate constants for xylene kinetics at 753K⁷.

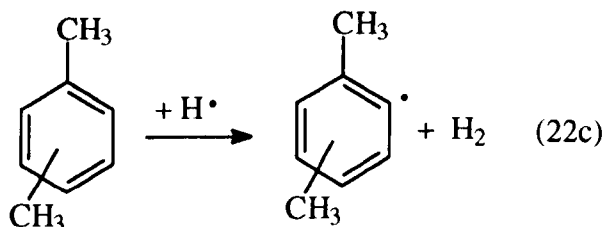
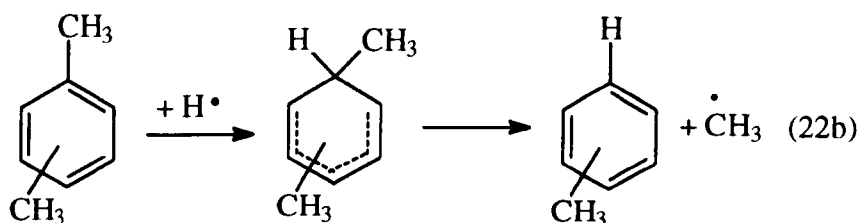
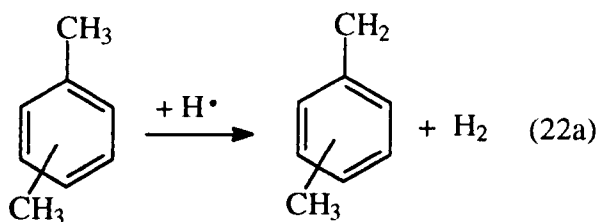
	p-Xylene	m-Xylene	o-Xylene
k_{22}/k_2	271	285	381
$k_{24}/(k_{10})^{1/2} / \text{Torr}^{-1/2} \text{ min}^{-1/2}$	0.133	0.142	0.170

Table 9.4 : Absolute rate constants for xylene and toluene kinetics at 753K⁷.

	p-Xylene	m-Xylene	o-Xylene	Toluene ⁸
$k_{22} / \text{l mol}^{-1} \text{ s}^{-1}$	$1.3 \cdot 10^9$	$1.4 \cdot 10^9$	$1.8 \cdot 10^9$	$3.9 \cdot 10^8$
$k_{24} / \text{l mol}^{-1} \text{ s}^{-1}$	$9.6 \cdot 10^4$	$1.03 \cdot 10^5$	$1.2 \cdot 10^5$	$3.28 \cdot 10^4$

Generally the rate constants for OH, H and HO₂ + xylene are at least twice those for the corresponding reactions for toluene at the same temperature.

For the case of $H + RH$, $k_{(H+xylylene)}$ is approximately 2.5 times higher than $k_{(H+Toluene)}$ (Table 9.4). The value for k_{22} quoted in Table 9.4 corresponds to the overall reaction between each xylene and H atoms. The three obvious pathways are shown below but as discussed in Chapter 8, reaction (22c) contributes only about 0.6% to the value of k_{22} .

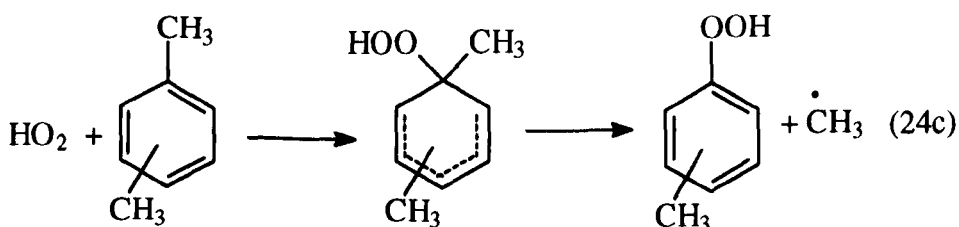
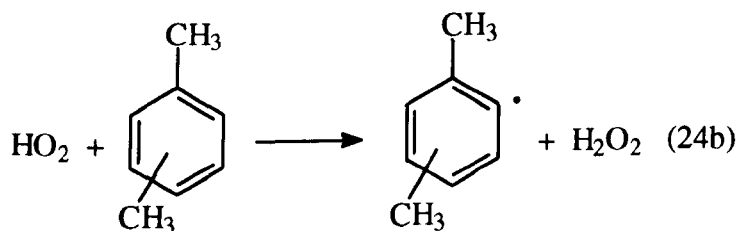


Chapter 8 discussed the position of attack by H and HO₂ radicals on each xylene, and consequently rate constants have been determined for the specific reactions H and HO₂ with each xylene. It is important to note that displacement of CH₃ by H radicals to produce toluene is a significant reaction ($\approx 40\%$) at 753K. All of the data are summarised in Table 9.5. It has been assumed that the rate of attack by H radicals to produce toluene is the same for each xylene.

Table 9.5: Summary of Absolute Rate Constants for H attack on each Xylene⁹.

Specific Rate Constant	Xylene		
	p-Xylene	m-Xylene	o-Xylene
(22a) Methylbenzyl / $l \text{ mol}^{-1} \text{ s}^{-1}$	7.3×10^8	8.3×10^8	1.2×10^9
(22b) Toluene / $l \text{ mol}^{-1} \text{ s}^{-1}$	5.6×10^8		
(22c) $\text{CH}_3\text{-C}_6\text{H}_3\text{-CH}_3$ / $l \text{ mol}^{-1} \text{ s}^{-1}$	9.1×10^6	8.4×10^6	9×10^5

In the case of $\text{HO}_2 + \text{RH}$, $k_{(\text{HO}_2+\text{xylene})}$ is approximately 3 times higher than $k_{(\text{HO}_2+\text{Toluene})}$ (Table 9.4). It is considered that the value for k_{24} corresponds to the abstraction of a H from one of the methyl side chain groups by HO_2 . This conclusion arises from thermochemical considerations as both abstraction from and addition to the ring will be considerably less energetically favourable than the equivalent reaction of H atoms.



The relative reactivity of the xylenes appears to be



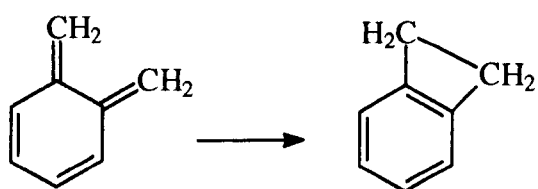
discussed below in section 9.2.2.

9.2.2. Products Study.

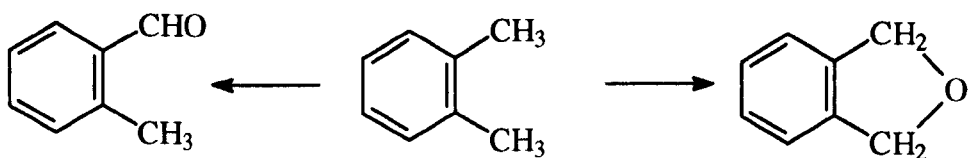
The products study is discussed in Chapter 8. The main conclusion is that the products are in an isomeric sense similar to those for toluene oxidation.

The relative reactivity of the xylenes has been highlighted by Emdee et al.^{10,11} together with some interesting products which were not detected in this work. Xylylene ($\text{CH}_2=\text{C}_6\text{H}_4=\text{CH}_2$) has been shown to be produced from the oxidation of *p*- and *o*-xylene.

Another interesting reaction is that of the isomerisation of *o*-xylylene to 1,2-benzocyclobutene¹².



The production of *o*-xylylene oxide (OXO) was detected in this study in high yields in preference to *o*-tolualdehyde by a factor of up to 5 (figures 5.15 and 5.16).



However, a significant proportion of the products were not detected due to their high molecular mass and low vapour pressure.

9.3. Future Research.

There are a number of avenues open with respect to the study of the oxidation chemistry of the xylenes and benzyl radicals.

9.3.1. Benzyl radicals.

Further study is required in order to obtain rate data above and below 753K for each of the reactions of HO₂ with the benzyl radicals together with more high temperature data for benzyl + O₂. The technique used in this study could also be extended to examine the corresponding reactions for di-methylbenzyl radicals, with modification to the analysis methods in order to prevent the condensation of heavy aromatic products on the apparatus.

9.3.2. Xylene Oxidation.

It is interesting to note the high degree of scarcity of kinetic data for H abstraction reactions by H atoms at temperatures above 500K. Fortunately, simulations show that H abstractions are not key processes in determining oxidation behaviour at high temperatures. Nevertheless the H₂ + O₂ addition system remains the only reliable source of H-atom abstraction data.

Simulations have shown that HO₂ abstractions are important in determining ignition delay times between 800 and 1200K. However, at present all the experimental data available for both abstraction and addition reactions of HO₂ reactions have been determined by the methods discussed in this thesis. It is important that these data are confirmed and the temperature range extended.

9.4. References.

- ¹ Fenter F. F., Noziere B., Caralp F and Lesclaux R., *Int. J. Chem. Kinet.*, **26**, 171, (1994).
- ² Baldwin R. R., Hisham M. W. M. and Walker R. W., *Symp. Int. Combust. Proc.*, **20**, 743, (1985).
- ³ Ellis C., *Ph.D. Thesis, The University Of Hull*. Chapter 6, (2000).
- ⁴ Lodhi Z.H. and Walker R.W., *J. Chem. Soc. Faraday Trans.*, **87**, 2361, (1991).
- ⁵ Baldwin R.R., Scott M. and Walker R. W., *Twenty-first Symposium (International) on Combustion/The Combustion Institute*, 991, (1986).
- ⁶ Atri G.M., Baldwin R.R., Evans G.A. and Walker R.W., *J. Chem. Soc. Faraday Trans I.*, **78**, 366 (1978).
- ⁷ Ellis C., *Ph.D. Thesis, The University Of Hull*. Chapter 7, (2000).
- ⁸ Baulch D.L., Cobos C.J., Cox R.A., Frank P., Hayman G., Just Th., Kerr J.A., Murrells T., Pilling M.J., Troe J., Walker R.W. and Warnatz J., *Comb. Flame*, **98**, 59, (1994).
- ⁹ Ellis C., *Ph.D. Thesis, The University Of Hull*. Chapter 8, (2000).
- ¹⁰ Emdee J.L., Brezinsky K. and Glassman I., *J. Phys. Chem.*, **95**, 1626, (1991).
- ¹¹ Emdee J.L., Brezinsky K. and Glassman I., *Twenty-Third Symposium (International) on Combustion/The Combustion Society*, 77, (1990).
- ¹² Cava M.P. and Dean A.A., *J. Am. Chem. Soc.*, **81**, 4266, (1959).